AUGMENTATION OF STRUCTURAL STABILITY IN MODEL PEPTIDE SYSTEMS THROUGH REDESIGN AND POST-TRANSLATIONAL MODIFICATION.

Alexander James Riemen

A dissertation submitted to the faculty of the University of North Carolina at Chapel Hill in partial fulfillment of the requirements for the degree of Doctor of Philosophy in the Department of Chemistry.

Chapel Hill
2010

Approved by:

Professor Marcey Waters

Professor Garyk Papoian

Professor Gary Pielak

Professor Matthew Redinbo

Professor Linda Spremulli

ABSTRACT

Alexander James Riemen: Augmentation of Structural Stability in Model Peptide Systems Through Redesign and Post-Translational Modifications.
(Under the direction of Marcey L. Waters)

Investigation of the driving forces that dictate protein folding, molecular recognition and biomolecular interactions is paramount for our understanding of complex biological processes. Post-translational modifications of proteins are a key component of cell signaling. Such modifications on the N-terminal tails of histone proteins are known to regulate gene transcription in eukaryotic organisms. Two modifications of particular interest to histone proteins are methylation of lysine and phosphorylation of serine, both which are known to modulate gene transcription. To determine how these modifications affect β-sheet structure, they were investigated in model β-hairpin systems. Small β-hairpin systems allows for the description and quantification of specific interactions which leads to a deeper understanding of the driving forces involved in complex biological processes.

Phosphorylated amino acids were incorporated into a designed β-hairpin peptide to study the effect on β-hairpin structure when the phosphate group is positioned to interact with a tryptophan residue on a neighboring strand. It is shown that phosporylation destabilizes the hairpin structure. The incorporation of two tryptophan residues to form an aromatic pocket that interacts with a lysine or N-methylated lysine was investigated in a β-hairpin peptide system. This tryptophan pocket results in an enhancement in the stability of the β-hairpin. Using a combination of phosphorylation and methylation, we were able to design a β-hairpin peptide in which the stability can be controlled through incorporation of the different

posttranslational modifications. Incorporation of dimethylated lysine results in an increase in hairpin stability, while phosphorylation of serine completely unfolds the hairpin.

A naturally occurring β-hairpin in Ubiquitin was also redesigned to investigate how alternative interactions affect the fold of a natural system. These studies indicate that deletion of Met1 and Val17 from results in a destabilization in hairpin structure by 0.7 kcal/mol.

Initial studies were conducted to determine the necessary requirements to promote favorable tertiary contacts between a β-hairpin α-helix and an for future designed systems. Peptides based on fragments of the GB1 protein that form an α-helix and a β-hairpin in the native protein were modified to promote their prospective secondary structure and were subsequently investigated. However, the experiments conducted yielded ambiguous results.

ACKNOWLEDGEMENTS

I would like to thank Professor Marcey Waters for her guidance, support and mentorship. I greatly appreciated the opportunity she allowed me in pursuing my own research interests.

I would like to thank my committee: Gary Pielak, Garyk Papoian, Matthew Redinbo and Linda Spremulli for their guidance and insight.

Finally, I would like to thank my family and friends both near and far, who have been there throughout my graduate studies.

TABLE OF CONTENTS

LIST OF TABLES

Table Page

LIST OF FIGURES

Figure

LIST OF ABBREVIATIONS

A	Alanine
Ac	aceyl group
AcOH-d4	deuterated acetic acid
Ala	Alanine
Arg	Arginine
Asn	Asparagine
Asp	Aspartic Acid
C	Cysteine
CD	Circular Dichroism
D	Aspartic Acid
D_2O	Dideuterium monoxide
DCM	Dichloromethane
DIPEA	Diisopropylethyl amine
DMF	Dimethylformamide
DMSO	Dimethyl Sulfoxide
d-Pro	d-Proline
DSS	3-(Trimethylsilyl)-1-propanesulfonic acid sodium salt
E	Glutamic Acid
ESI-TOF	Electro Spray Ionization Time of Flight
F	Phenylalanine
Fmoc	N-9-Fluorenylmethyloxycarbonyl
G	Glycine

GdnHCl	Guandinum Hydrochloric Acid
Gln	Glutamine
Glu	Glutamic Acid
Gly	Glycine
HB	Hydrogen Bonded
HBTU	2-(1H-Benzotriazole-1-yl)-1,1,3,3-tetramethyluronium hexafluorophosphate
HOBT	N-hydroxy benzotriazole H2O
HPLC	High Pressure Liquid Chromotography
Hα	peptide backbone α proton
I	Isoleucine
Ile	Isoleucine
K	Lysine
$KPOD_4$	Deuterated potassium phosphate
L	Leucine
Leu	Leucine
Lys	Lysine
M	Methionine
Me	Monomethyl
Me_2	Dimethyl
Me_3	Trimethyl
Met	Methionine
N	Asparagine
NaOAc-d3	Deuterated sodium acetate

nd	not determined
NH2	C-terminal amide
NHB	Non-Hydrogen Bonded
NMR	Nuclear Magnetic Resonance
NOESY	Nuclear Overhauser Effect Spectroscopy
O	Ornithine
Orn	Ornithine
PEG-PAL-PS	Polyethylene glycolaylated phenylalanine ammonia lysase poly styrene
Phe	Phenylalanine
PKA	Protein Kinenase A
PTM	Post Translational Modification
Q	Glutamine
R	Arginine
S	Serine
Ser	Serine
T	Threonine
TFA	Triflouroactetic acid
Thr	Threonine
TIPS	Triisopropyl silane
TOCSY	Totally Correlated Spectroscopy
Trp	Tryptophan
Tyr	Tyrosine
V	Valine

Val	Valine
W	Tryptophan
Y	Tyrosine

CHAPTER I

INTRODUCTION

A. Background and Significance.

Since the famous Anfinsen experiment that demonstrated that the amino acid sequence of a protein can dictate its 3-dimensional structure[1], extensive research has been conducted to understand the driving forces of protein folding and our ability to predict structure and function based on amino acid sequence. The ability to custom tailor proteins for a specific function has utility in a variety of areas including medicine and industry, making protein design an important field of research. Protein design also offers the ultimate test of our understanding of fundamental forces that dictate the structure and function of proteins. Many approaches are being utilized to tackle this complex problem. Examples include computational based approaches, rational design methodologies and iterative library generation also referred to as directed evolution.[2] Many design studies have been performed on smaller peptide systems that folded into a variety of secondary and tertiary structures to determine the importance of local interactions in specific structure formation.[3] These model

---

[1] Sela, M.; Anfinsen, C. B.; Harrington, W. F. *Biochim Biophys Acta* **1957**, *26*, 502-512.

[2] Jackel, C.; Kast, P.; Hilvert, D. *Annual Review of Biophysics* **2008**, *37*, 153-173.

[3] (a) Hill, R. B.; Raleigh, D. P.; Lombardi, A.; Degrado, W. F. *Acc Chem Res* **2000**, *33*, 745-754. (b) Ali, M. H.; Taylor, C. M.; Grigoryan, G.; Allen, K. N.; Imperiali, B.; Keating, A. E. *Structure* **2005**, *13*, 225-234. (c) Dahiyat, B. I.; Mayo, S. L. *Science* **1997**, *278*, 82-87. (d) Dai, Q. H.; Tommos, C.; Fuentes, E. J.; Blomberg, M. R. A.; Dutton, P. L.; Wand, A. J. *J Am Chem Soc* **2002**, *124*, 10952-10953. (e) DeGrado, W. F. *Science* **1997**, *278*, 80-81. (f) Imperiali, B.; Ottesen, J. J. *J Pept Res* **1999**, *54*, 177-184. (g) Kraemer-Pecore, C. M.; Lecomte, J. T. J.; Desjarlais, J. R. *Protein Sci* **2003**, *12*, 2194-2205. (h) Lim, A.; Saderholm,

system studies have lead to general rules for *de novo* design of peptides that fold into desired secondary structure such as α-helices and β-sheets. In fact some of these systems can even be designed to interconvert between different structures depending specific conditions, i.e. pH or temperature.[4] Despite the many advancements in *de novo* protein design, there is still much work to be done before rational protein design becomes a mundane task. The goal of work in this thesis is to study the non-covalent interactions that contribute to structure stability in model peptide systems through rational iterative design. We have focused on further elucidating the factors that contribute to β-hairpin formation in short peptide sequences.

B. β-Hairpins as model systems and their design principles.

General design principles are known in great detail for α-helical structure.[3a,3e,5] Understanding of factors that contribute to β-sheet formation in aqueous solution lag behind that of the α-helix. This is due to the fact that many sequences based on short segments of naturally occurring β-sheets tend to aggregate or are poorly folded in aqueous solution. However, in the early 1990's short peptides (< 20 residues) that fold autonomously into monomeric, antiparallel β-sheet structures in aqueous solution were discovered leading to an explosion of research on this secondary structure.[6] Investigation on peptides that form β-hairpins (where the β-hairpin is considered the smallest isolable unit of a β-sheet) has made considerable progress in defining the factors that contribute to the formation of stable β-sheet

---

M. J.; Makhov, A. M.; Kroll, M.; Yan, Y. B.; Perera, L.; Griffith, J. D.; Erickson, B. W. *Protein Sci* **1998**, *7*, 1545-1554.

[4] Reviewed in Ambroggio, X. I.; Kuhlman, B. *Curr Opin Struct Biol* **2006**, *16*, 525-30.

[5] Reviewed in Micklatcher, C.; Chmielewski, J. *Curr Opin Chem Biol* **1999**, *3*, 724-729.

[6] Reviewed in Gellman, S. H. *Curr Opin Chem Biol* **1998**, *2*, 717-725.

secondary.[6,7] A β-hairpin structure consists of 2 antiparallel β-sheet strands connected though a turn sequence (Figure 1.1).

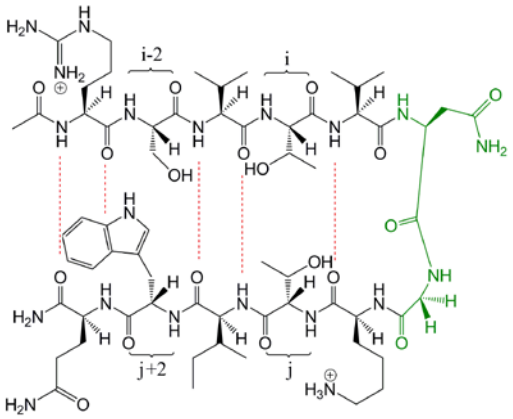

Figure 1.1 Schematic representation of a 12 residue β-hairpin peptide. Hydrogen bonding between strands is shown in red. Key NHB residues are indicated as i, i-2, j and j+2. The Asn-Gly type I' turn sequence is highlighted in green.

Studies on β-hairpin peptides have revealed factors necessary for the formation of a stable hairpin fold which include the turn sequence, side chain-side chain interactions, and individual amino acid β-sheet propensities.[6,8,9] In particular, the proper turn sequence is very important for proper strand alignment and stability, where sequences that forms a Type I' or Type II' are very strong promoters of β-hairpin formation. The Type I' and Type II' conformation is ideal for imbuing a right-handed twist which occurs in the strands composing an antiparrallel β-sheet.[6] Hence, turn sequences that are known to adopt Type I'

[7] (a) Searle, M. S. *Biopolymers* **2004**, *76*, 185-195. (b) Smith, C. K.; Regan, L. *Acc Chem Res* **1997**, *30*, 153-161. (c) Searle, M. S. *J Chem Soc Perkin Trans 2* **2001**, 1011-1020. (d) Waters, M. L. *Biopolymers* **2004**, *76*, 435-445.

[8] Stotz, C. E.; Borchardt, R. T.; Middaugh, C. R.; Siahaan, T. J.; Vander Velde, D.; Topp, E. M. *J Pept Res* **2004**, *63*, 371-382.

[9] Ramirez-Alvarado, M.; Kortemme, T.; Blanco, F. J.; Serrano, L. *Bioorg Med Chem* **1999**, *7*, 93-103.

or II' conformations were used in the designed β-hairpin systems presented throughout this thesis.

Another major contributing factor to hairpin stability is the interaction between side chains on the opposite strands of the β-sheet particular those located in non-hydrogen bonding (NHB) positions (Figure 1.1). These residues tend to have the greatest interaction with each other due to their orientation at these positions, where the side chains are pointed at the opposite cross strand in the antiparallel β-sheet configuration.[10] β-Hairpin studies on these residues have been used to measure interaction energies between side chains with varied non-covalent interactions such as hydrogen bonding[11], salt bridge formation[12,13], π-π[12,14], and cation-π interactions[15,16]. For the aforementioned reasons, we choose these residues to conduct extensive studies on biologically relevant interactions and elucidate additional design principles for β-sheet. It is worth noting that a majority of the hairpin peptides in this thesis are named by the residues in the NHB sites i-2, i, j and j+2 since these are the only residues that vary between systems, with exception to those in chapters 5 and 6.

β-Hairpin peptides are excellent model systems for studying non-covalent interactions that guide protein folding, molecular recognition and biomolecular interactions for multiple

[10] Syud, F. A.; Stanger, H. E.; Gellman, S. H. *J Am Chem Soc* **2001**, *123*, 8667-8677.

[11] Sharman, G. J.; Searle, M. S. *J Am Chem Soc* **1998**, *120*, 5291-5300.

[12] Kiehna, S. E.; Waters, M. L. *Protein Sci* **2003**, *12*, 2657-2667.

[13] Searle, M. S.; Griffiths-Jones, S. R.; Skinner-Smith, H. *J Am Chem Soc* **1999**, *121*, 11615-11620.

[14] Tatko, C. D.; Waters, M. L. *Org Lett* **2004**, *6*, 3969-3972.

[15] Tatko, C. D.; Waters, M. L. *Protein Sci* **2003**, *12*, 2443-2452.

[16] Hughes, R. M.; Waters, M. L. *J Am Chem Soc* **2005**, *127*, 6518-9.

reasons. Their proton NMR spectra are well dispersed making analysis by conventional 1D and 2D NMR techniques possible. Folding of β-hairpin peptides has been shown to be two-state[17], which allows for quantification of free energies, and direct study of individual side chain-side chain interactions.

C. NMR structural characterization of β-Hairpins peptides.

Since NMR β-hairpin characterization is used extensively throughout this thesis, a succinct explanation of the methods used to analyze these structures is warranted (additional details are provided in the experimental section of each chapter). A number of methods are used to both confirm β-haripin structure and quantify β-hairpin stability. Measuring the chemical shift of the Hα residues and comparing them to random coil controls (Figure 1.2a) is commonly used to confirm structure. Relative downfield chemical shifts greater than 0.1 ppm are indicative of β-sheet formation (Figure 1.3a).[18] Another indicator of β-hairpin formation, albeit less frequently used in this thesis, is the chemical shift of the backbone amide protons relative to random coil chemical shift (Figure 1.3b). Extensive downfield shifting is expected at residues participating in hydrogen bonding with cross strand residues when forming an anti parallel β-sheet, i.e. residues in HB positions. Additionally, the splitting pattern of Gly in the Asn-Gly turn sequence is also a good indicator of β-hairpin formation.[19] The Hαs in this Gly residue are diasterotopic and their chemical shifts differ

[17] Streicher, W. W.; Makhatadze, G. I. *J Am Chem Soc* **2006**, *128*, 30-31.

[18] Sharman, G. J.; Griffiths-Jones, S. R.; Jourdan, M.; Searle, M. S. *J Am Chem Soc* **2001**, *123*, 12318-12324.

[19] Griffiths-Jones, S. R.; Maynard, A. J.; Sharman, G. J.; Searle, M. S. *Chem Commun* **1998**, 789-790.

significantly in the β-hairpin conformation. The more well folded the peptide is the greater the splitting, between the two protons (Figure 1.3c).

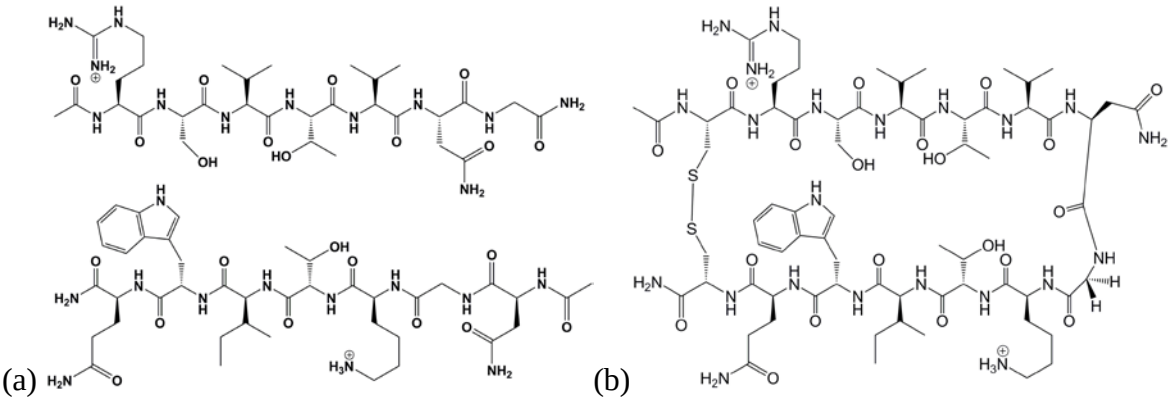

Figure 1.2 Schematic representations of NMR control peptides. (a) Example of unstructured peptides used to obtain random coil chemical shifts. (b) Example of cyclized fully folded control β-hairpin linked through disulfide bond at the termini.

Through the use of a fully folded control peptide (Figure 1.2a) the extent of β-sheet formation can be determined in the terms of fraction folded. Fraction folded represents the relative populations of peptides in β-hairpin conformation verses peptides in an unfolded state. Since interconversion between a folded state and an unfolded state is fast on the NMR time scale, the Hα chemical shifts of represent the average of the distribution between the two populations, therefore allowing for quantification of the fraction folded. The fraction folded can be determined on a per residue basis by comparing the Hα chemical shift to the fully fold chemical shift relative to random coil chemical shift. Overall hairpin stability can then be assessed through averaging of the Hα at the HB positions. The HB sites have been shown to be the most accurate representation of the fraction folded due to minimal interaction with cross strand residues that can influence chemical shifts.[20] Additionally,

[20] Syud, F. A.; Espinosa, J. F.; Gellman, S. H. *J Am Chem Soc* **1999**, *121*, 11577-11578.

comparing the diastereotopic Hα Gly splitting to the fully folded control Gly splitting also allows for an accurate determination of overall fraction folded.[13]

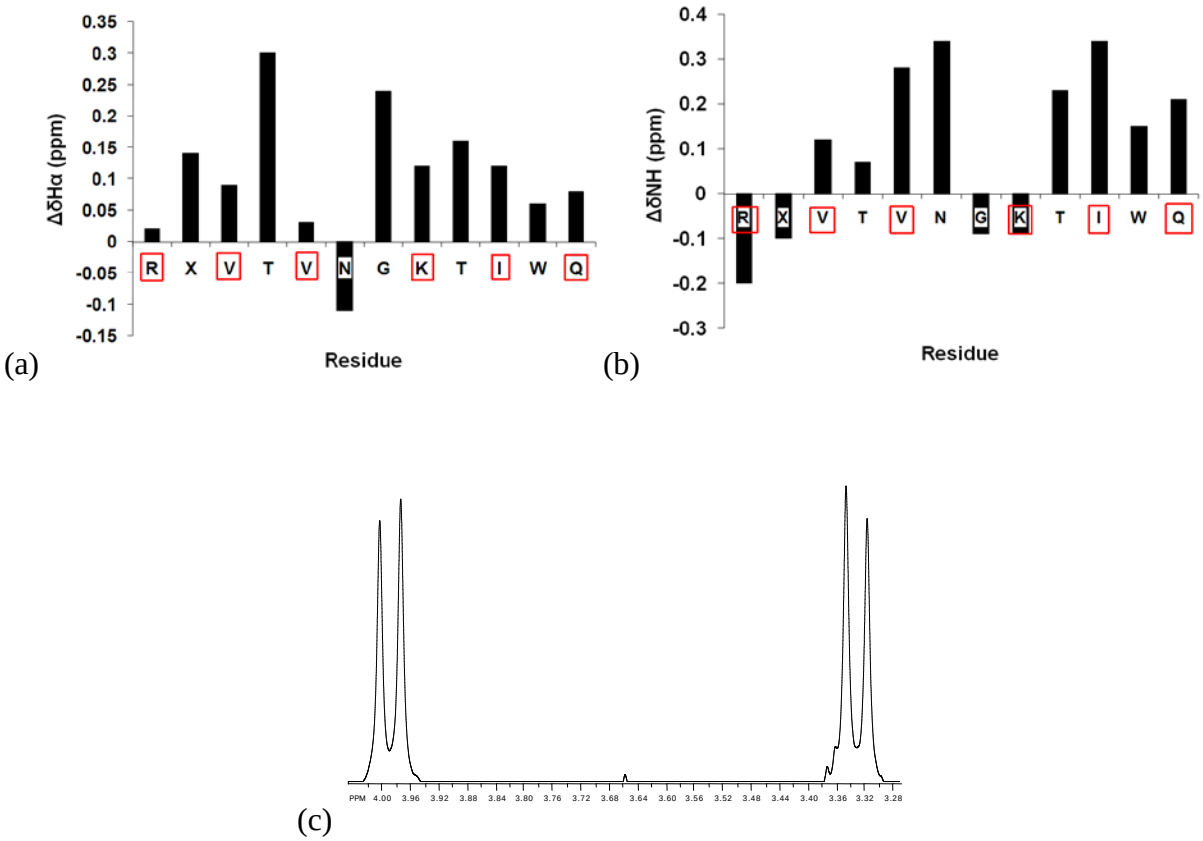

Figure 1.3 (a) Example Hα shifts for a 12 residue β-hairpin peptide (hydrogen bonded residues in red squares). (b) Example backbone amide shifts from a β-hairpin peptide (hydrogen bond residues in red squares). (c) Example Gly splitting from a Type I' Asn-Gly turn in a β-hairpin.

NOEs are another common indicator of β-hairpin structure. They can indicate proximity between residues on opposite strands, confirming the presence of a folded state and also verify correct strand register. However, careful consideration must be taken when interrupting NOE data, because of lack of an NOE can be due to a folded, yet highly dynamic β-hairpin structure. Consequently even well-folded β-hairpins typically display critical NOEs and ROEs but not an overabundance of them in aqueous solution.

D. Post-translational modifications and their importance in chromatin structure.

A majority of the systems discussed throughout this thesis involve the study of the interactions of post-translational modifications (PTMs) in the context of a β-hairpin peptide, thus a brief introduction is warranted. PTMs are defined as any modification that occurs to a peptide or protein after it has been translated by the ribosome. Large numbers of PTMs are known including phosphorylation, methylation, acylation, ubiquitination, and glycoslyation, to name a few. These PTMs are involved in a variety of processes ranging form signaling (acylation and phosphorylation) to targeting (glycosylation) to tagging proteins for degradation (ubiquitination).[21] Of the PTMs studied in this thesis we focused on two important modifications involved in the regulation of chromatin dynamics and gene regulation; phosphorylation and methylation.

In eukaryotic organisms, DNA is compacted into chromatin, which consists of DNA wrapping around an octotmer of histone proteins (H3, H4, H2A, H2B) forming nucleosomes (Figure 1.4). The nucleosome is the fundamental unit of chromatin structure which can be organized into different high order chromatin structures. The unstructured N-terminal peptide tails of histone proteins extend out into solution where they can be covalently modified by a variety of enzymatic processes. The PTMs that occur on these histone tails are involved in the structuring of chromatin in either a heterochromatin structure in which gene transcription is inactivated or a euchromatin structure where genes are actively transcribed.[22] In essence these modifications act as a switching mechanism between and "on" or "off" state of gene transcription. A variety of PTMs are known to occur on these histone tails including

[21] Zhang, Y.; Reinberg, D. *Genes & Development* **2001**, 2343-2360.

[22] Strahl, B. D.; Allis, C. D. *Nature* **2000**, *403*, 41-45.

phosphorylation, acelylation, methylation and ubiquination. These modifications do not appear in isolation of each other, and are thought to work in concert through a complex signaling pathway often referred to as the "histone code".[22] Discussed in more detail in Chapter 4, lysine methylation and serine phosphorylation adjacent to each other on H3 N-terminal histone tail act as a switching mechanism for recruitment of proteins to the chromatin complex that alters it structure.[23] Hence, cross talk between these two modifications control gene transcription through the promotion (lysine methylation) or the disruption (serine phosphorylation) of a protein-protein interaction.

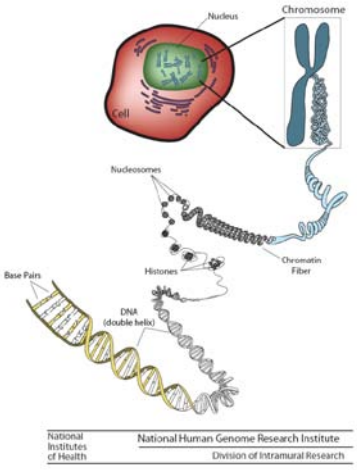

(a)

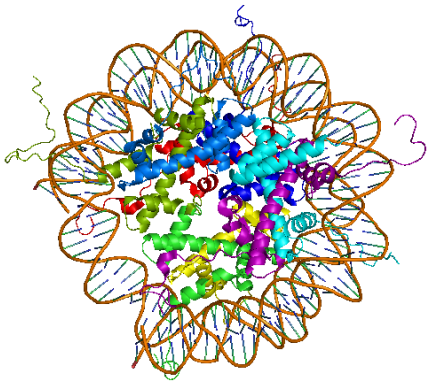

(b)

Figure 1.4 (a) Packing of DNA within the nucleus. (b) Crystal structure of a histone DNA complex (pdb code: 1EQZ).

E. Conclusion.

The aim of the studies presented throughout this text is two fold: (1) to increase our understanding of the driving forces responsible for β-sheet stabilization and (2) to gain insights into the interactions of biologically significant PTMs in model β-hairpin systems.

[23] Fischle, W.; Tseng, B. S.; Dormann, H. L.; Ueberheide, B. M.; Garcia, B. A.; Shabanowitz, J.; Hunt, D. F.; Funabiki, H.; Allis, C. D. *Nature* **2005**, *438*, 1116-22.

Although there has been substantial amount information gained in regards to formation of stable β-hairpins in aqueous solution, our understanding of design principles for β-sheets still lags behind that of the α-helix. Thus, further studies on β-hairpin formation are still relevant. As mentioned earlier, the β-hairpin model system also allows for the isolation and study of specific interactions. This is ideal for quantify a specific interaction utilized by a complex biological system such as the "histone code". The work presented in this thesis will improve our understanding of protein folding and lead to future novel designed systems, as well as provide insights to fundamental forces responsible for effects observed by post translational modification.

CHAPTER II

DESTABLIZATION OF β-HAIRPIN STRUCTURE THROUGH UNFAVORBALE PHOSPHATE INTERACTIONS

(Reproduced, in part with permission from Riemen**,** A.J.; Waters M.L., *JACS.* **2009,** *131*, 14081-14087.)

A. Introduction.

Phosphorylation of proteins is ubiquitious in cellular processes as a regulatory control. It is estimated that about one third of all human proteins are phosphylated.[1] Phosphorylation is a part of intracellular signal transduction pathways that modulate cellular proliferation, macromolecule production, and gene expression.[1] Abnormal phosphorylation can be the cause or the result of many diseases.[1] Currently the most effective method for studying how phosphorylation influences protein structure and function is by comparison of crystal structures of phosphorylated and unphosphorylated proteins.[2] However, not all proteins crystallize easily, such as membrane proteins, thus giving an incomplete picture of how phosphorylation affects the structure and function of proteins. The study of phosphorylated residues on structure in smaller model systems is warranted to obtain a clearer understanding of how this post-translational modification can affect structure.

---

[1] Cohen, P. *Euro J Biochem* 2001, *268,* 5001-5010.

[2] Johnson, L. N.; Lewis, R. J. *Chem Rev* 2001, *101,* 2209-2242.

Recently, a body of information on how phosphorylation influences α-helical structure has emerged from studies in de novo designed α-helical peptides.[3,4,5] Doig and co-workers have shown that phosphoserine strongly stabilizes α-helical peptides when positioned near the N-terminus, or when positioned to make a favorable salt bridge within the helix.[4,5] In a native protein, it has also been shown that phosphorylation of serine and threonine can have a destabilizing effect within α-helix system, particularly with phosphothreonine.[6] In addition, the DeGrado laboratory has used phosphorylation as a molecular switch to promote the self assembly of de novo designed helical bundles.[3]

Numerous studies on peptides that fold into a β-hairpin conformation have led to a thorough understanding of the design elements necessary for β-hairpin formation. However the influence of phosphorylation within model β-sheet systems has not yet been extensively explored. To this end, we designed a series of β-hairpin peptides to gain insights into the effects that phosphorylation can have on a model β-sheet system.

B. β-hairpin destabilization through various phosphorylated amino acids.

i. Significance.

Stabilization or destabilizaion via charge-charge interactions with a phosphorylated residue are to be expected. However, to our knowledge, no one has investigated whether phosphorylation can result in a repulsive interaction with a hydrophobic or aromatic group that could affect peptide structure. Thus, we investigated the destabilizing effect of

[3] Signarvic, R. S.; DeGrado, W. F. *J Mol Biol* 2003, *334*, 1-12.

[4] Andrew, C. D.; Warwicker, J.; Jones, G. R.; Doig, A. J. *Biochemistry* 2002, *41*, 1897-1905.

[5] Errington, N.; Doig, A. J. *Biochemistry* 2005, *44*, 7553-8.

[6] Szilak, L.; Moitra, J.; Krylov, D.; Vinson, C. *Nat Struct Biol* 1997, *4*, 112-4.

phosphorylated amino acids with tryptophan within a designed β-hairpin peptide. The goal of these studies is to help further delineate the range of structural changes that may occur due to phosphorylation particularly in a β-sheet.

ii. Results.

(a) System Design. A set of 12-residue peptides designed to autonomously fold into β-hairpins in aqueous solution was used to investigate the effect of phosphorylation on a side chain-side chain interaction with a cross-strand Trp residue on structure. Features that influence folding include the turn sequence, the β -sheet propensity of the strand residues, and the side chain-side chain interactions.[7] All of the β-hairpins peptides contain the sequence VNGK to promote favorable type I' turn. This turn type has been shown to promote a β-hairpin structure.[8] The **SW-1** peptide system was designed to study the effect of phosphorylation on a modestly folded β-hairpin sequence containing a serine residue in position 2 that is directly cross strand from a tryptophan in position 11 on the non-hydrogen bonded (NHB) face of the hairpin (Figure 2.1a). The NHB face is defined as the face of the peptide displaying side chains from the non-hydrogen bonded residues in a two stranded β-sheet.[9] On the NHB face the side chains of residues are oriented closer to cross strand residue side chains thus giving a larger contribution to hairpin stability through side chain-side chain

[7] Reviewed in Searle, M. S. *J Chem Soc Perkin Trans 2* 2001, 1011-1020.

[8] (a) Hughes, R. M.; Waters, M. L. *J Am Chem Soc* 2005, *127*, 6518-9. (b) Blanco, F. J.; Jimenez, M. A.; Herranz, J.; Rico, M.; Santoro, J.; Nieto, J. L. *J Am Chem Soc* 1993, *115*, 5887-5888. (c) RamirezAlvarado, M.; Blanco, F. J.; Serrano, L. *Nat Struct Biol* 1996, *3*, 604-612. (d) Sharman, G. J.; Searle, M. S. *Chem Commun* 1997, 1955-1956.

[9] Syud, F. A.; Stanger, H. E.; Gellman, S. H. *J Am Chem Soc* 2001, *123*, 8667-8677.

interactions than those residues on the hydrogen bonded (HB) face as discussed in chapter 1.[9] Subsequently, serine was replaced with threonine and tyrosine at position 2 and their phosphorylated analogs to determine the significance of the phosphorylated residue (Figure 2.1b). Unfolded control peptides **1-9** were synthesized in which each peptide consisted of either residues 1-7 composing of the N-terminal arm and turn of the β-hairpin or residues 6-12 consisting of the C-terminal arm and turn (Figure 2.1c). Cyclic peptides **10-14** were synthesized as fully folded controls for each of the β-hairpins. Cyclization was achieved by a disulfide bond between cysteine residues at the N and C-termini of the peptides (Figure 2.1d).

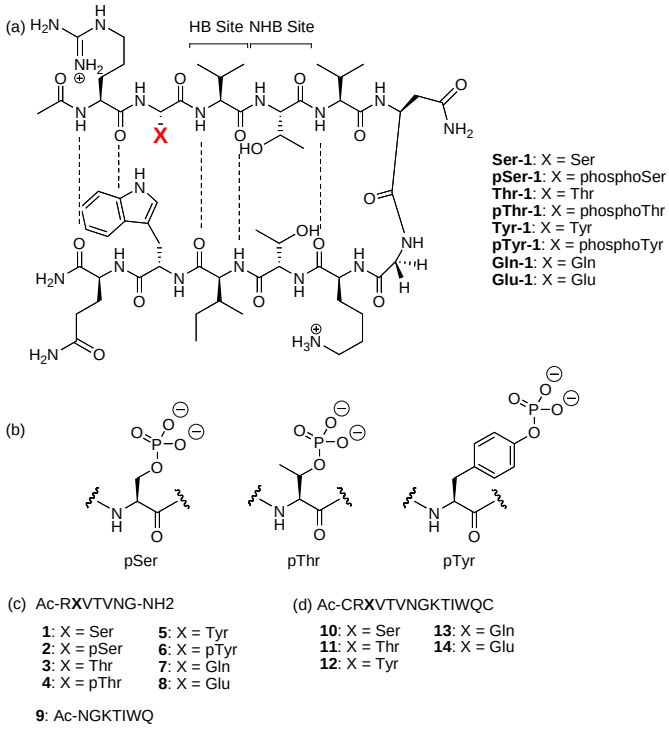

Figure 2.1 (a) Schematic diagram of the designed β-hairpin peptides. Interstrand hydrogen bonding and relative orientation of the side chains are indicated. (b) Structure of the phosphorylated amino acids. (c) Sequences of unstructured control peptides. (d) Sequences of the cyclic control peptides for the fully folded state. The underline residues form a disulfide bond.

(b) SW-1 Peptide Structural Studies. NMR spectroscopy was used to determine to what extent the **SW-1** peptide and the phosphoserine containing peptide **pSW-1** fold into β-hairpin structures. Downfield shifting of ≥ 0.1 ppm of the α-protons (Hα) along the peptide backbone relative to unfolded values indicates β-hairpin structure as previously discussed in chapter 1.[10] **SW-1** was found to have a majority of Hα shifts above 0.1 ppm compared to the unstructured controls, except for the two terminal residues which are typically frayed in β-hairpins and Asn 6 which is located within the turn of the hairpin (Figure 2.2a). This Asn is typically upfield shifted from the unstructured control value due to its conformation in the turn. Downfield shifting of backbone amide hydrogens in HB positions relative to random coil values also indicates β-sheet structure, which is seen for valine 3, valine 5, and isoleucine 10 (Figure 2.2b). NHB residues threonine 4, threonine 9 and tryptophan 11 are also significantly downfield shifted. NOESY data further confirmed that this peptide forms the predicted β-hairpin structure (see Experimental Section).

The **pSW-1** peptide was synthesized with a phosphoserine replacing the serine in **SW-1** and characterized by NMR spectroscopy to study the effect of phosphoserine on the β-hairpin structure. The Hα shifts of **pSW-1** are not as downfield shifted as **SW-1** peptide, many of which are < 0.1 ppm, indicating that incorporation of a phosphoserine causes a destabilization of the β-hairpin structure in this sequence (Figure 2.2a). A decrease in amide backbone shifts is also seen at the hydrogen-bonded positions when compared to **SW-1** (Figure 2.2b). NOESY data of **pSW-1** show no long distance NOEs, indicating little to no β-hairpin structure. The lack of long distance NOE's is indicative of a highly dynamic peptide

[10] Espinosa, J. F.; Munoz, V.; Gellman, S. H. *J Mol Biol* 2001, *306*, 397-402.

which may still sample a β-hairpin conformation but spends most of its time in an unstructured state.

Circular Dichroism (CD) experiments were also performed to confirm that there is a loss of structure with incorporation of phosphoserine (Figure 2.2c). Since the **SW-1** peptide is only modestly folded, there is a large negative signal at 197 nm typical of random coil but there is also shoulder at 215 nm that indicates β-sheet structure. This shoulder at 215 nm for **pSW-1** is not observed and a larger random coil signal at 197 nm is present which is consistent with the NMR data, reinforcing that **pSW-1** has little defined structure.

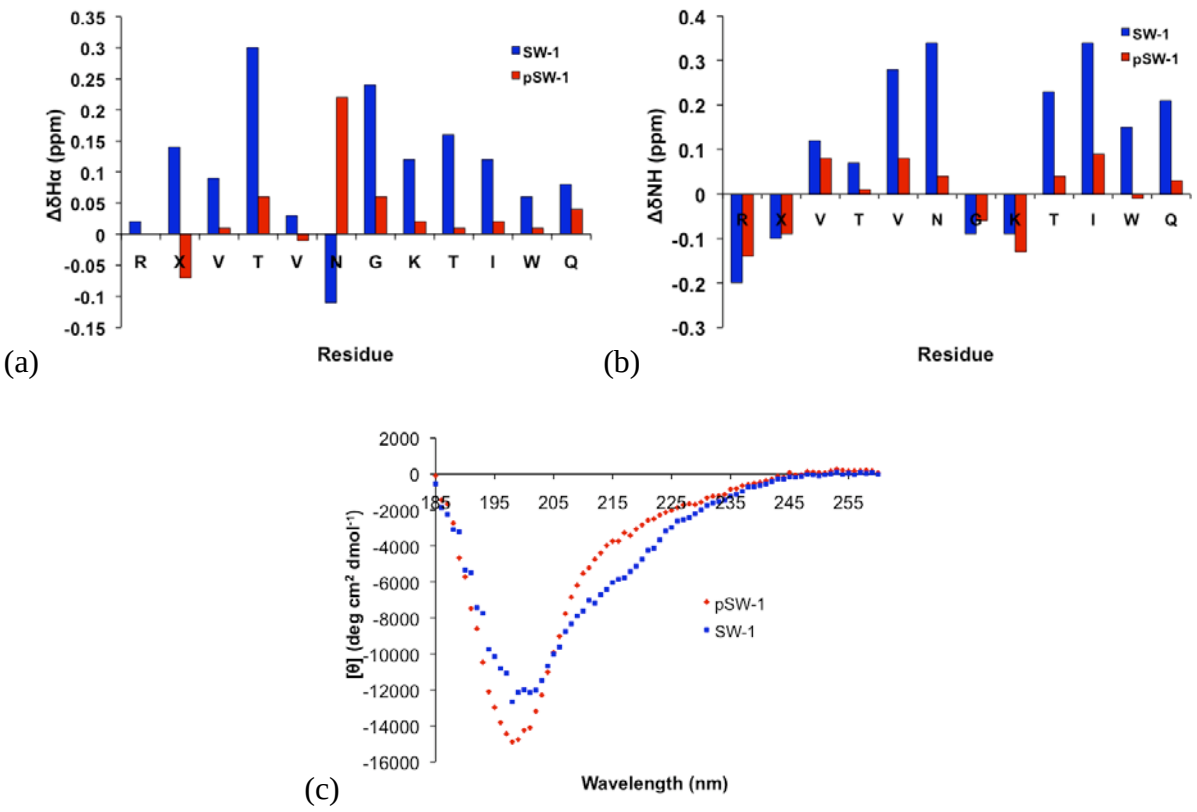

Figure 2.2 (a) Hα chemical shift differences: **SW-1** (blue bars, X = serine) and **pSW-1** (red bars, X = phosphoserine) from random coil peptides in pD 7.0 buffer. The Gly bars reflect the Hα separation in the hairpin. (b) Backbone amide chemical shifts of **SW-1** and **pSW-1**. (c) Circular dichroism spectra comparison of **SW-1** (blue) and **pSW-1** (red) at 25°C in 10 mM sodium phosphate pH 7.0 buffer.

The extent of folding to a β-hairpin by **SW-1** and **pSW-1** peptides was quantified using two methods. The first method utilizes the extent of Hα downfield shifting relative to random coil controls and fully folded control as previously described (see Experimental Section). The second method utilizes the extent of the diastereotopic glycine Hα splitting located in the turn of the hairpin relative to glycine Hα splitting observed in the fully folded control (see Experimental Section). **SW-1** was found to be 40% folded and **pSW-1** only 10% folded using both methods (Table 2.1). The extent of destabilization due to phosphoserine was calculated to be approximately 1.3 kcal/mol. The destabilization that occurs when the phosphoserine is incorporated in this hairpin is believed to result from an unfavorable interaction between the phosphate group and the tryptophan indole ring directly across from it. This destabilization may be caused by repulsion of the negatively charged phosphate and the electron rich indole ring of cross-strand tryptophan, or through steric clash between the large phosphate group and the tryptophan, or a combination of both.

Table 2.1 Fraction folded and ΔG of folding for β-hairpin peptides. Values calculated from data obtained at 25 °C, 50 mM potassium phosphate-*d2*, pD 7.0 (uncorrected), referenced to DSS.

Peptide	Fraction Folded (Gly Splitting)[a]	Fraction Folded (Hα)[b]	ΔG Folding (kcal/mol)	ΔΔG (**pXW-1** – **XW-1**)
SW-1	0.41 (±0.01)	0.40 (±0.04)	0.23 (±0.05)	
pSW-1	0.10 (±0.01)	0.07 (±0.02)	1.53 (±0.05)	1.3
QW-1	0.49 (±0.01)	0.50 (±0.1)	-0.03 (±0.09)	
EW-1	0.39 (±0.01)	0.3 (±0.2)	0.28(±0.09)	0.31
TW-1	0.43 (±0.01)	0.40 (±0.06)	0.2 (±0.1)	
pTW-1	0.21 (±0.01)	0.12 (±0.06)	1.1 (±0.2)	0.9
YW-1	0.88 (±0.02)	0.82 (±0.07)	-0.90(±0.04)	
pYW-1	0.62 (±0.02)	0.5 (±0.3)	0.1 (±0.2)	1.0

(a) Error determined by chemical shift accuracy on NMR spectrometer. (b) Average of the Hα values from Val 3, Val 5, Orn 8, and Ile 10. The standard deviation is in parentheses.

(c) pH Studies. To determine whether the destabilization was caused by electrostatic repulsion of the phosphate group with the electron rich indole ring of tryptophan or a steric clash of the phosphate group with the tryptophan a pH study was performed on **SW-1** and **pSW-1**. By varying the pH and thus the charge on the phosphate group, a change in fraction folded will indicate whether there is an electronic component to the destabilization. A comparison of the fraction folded verses pH for both **SW-1** and **pSW-1** is given in Figure 2.3 It was observed that as the pH increases, the **SW-1** fraction folded is constant, while the **pSW-1** fraction folded decreases. Interestingly, the fraction folded at pH 2.5 and 4.7 is unchanged for **pSW-1,** which correlates to a -1 charge on phosphate, while at pH 7.4 the fraction folded is lower and the phosphate group now has a -2 charge, and a higher fraction folded is observed at pH 1.2 where the phosphate group is uncharged. It appears that as the charge state of the phosphoserine increases, the degree of folding decreases, indicating that the charge of the phosphate is a predominant contributor to the destabilization of the β-hairpin. However, sterics appears to play some role in the destabilization as **pSW-1** is less folded than **SW-1** even in a neutral charge state of the phosphoserine.

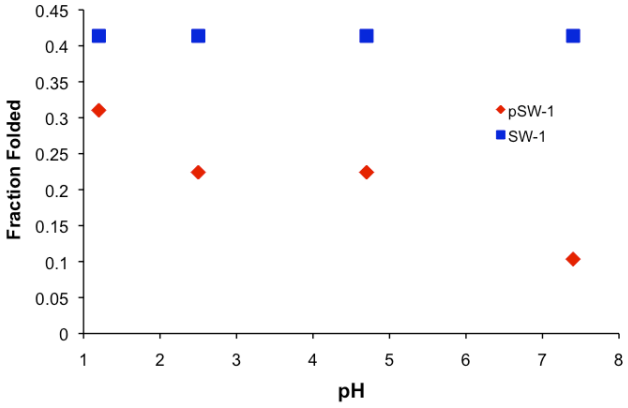

Figure 2.3 pH study of fraction folded of **SW-1** (blue) and **pSW-1** (red). Fraction folded was determined by NMR glycine splitting in buffers with the pD indicated at 20 °C.

(d) Double Mutant Studies. To determine whether the phosphoserine-tryptophan interaction is the major destabilizing interaction, a double-mutant cycle was performed (Figure 2.4).[10] In the double-mutant cycle, both of the interacting residues are mutated individually and together. The single mutants, B and C, disrupt the side-chain-side-chain interaction in A, but may result in other changes that affect the stability of the β-hairpin, such as the β-sheet propensity. The double mutant, D, corrects for all unintended changes that affect the β-hairpin stability. Thus, the sum of the stabilities of peptides A and D minus those of the single mutants, B and C, provides the side-chain-side-chain interaction of phosphoserine and tryptophan. The peptides **SW-1** and **pSV-1** were used as individual mutants and **SV-1** was synthesized as the double mutant. **pSV-1** contains a phosphoserine at position 2 and a valine at position 11 to replace the tryptophan and **SV-1** contains a serine at position 2 and a valine at position 11. The fraction folded and ΔG of folding for all the peptides in the double-mutant cycle are given in Table 2.2 These studies were preformed in a pD 4 buffer solution due to low solubility of **SV-1** and **pSV-1** at pD 7. The interaction of the phosphoserine-tryptophan was calculated to be a destabilization of 0.5 kcal/mol, which is the same as the overall destabilization between **SW-1** and **pSW-1** at pH 4, therefore indicating that this interaction is the direct cause of the destabilization of β-hairpin. Indeed, it is interesting to note that phosphorylation has no impact whatsoever on folding of the **SV-1/pSV-1** peptides, which provides further support that the nature of the destabilization is electronic rather than steric.

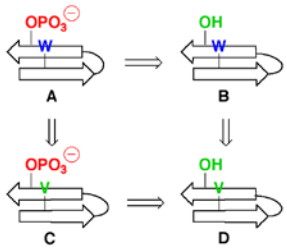

$$\Delta G_A - \Delta G_B - \Delta G_C + \Delta G_D = \Delta\Delta G_{(pX\text{-}W)}$$

Figure 2.4 Double-mutant cycle diagram for interaction between cross-strand phosphoserine and tryptophan. The cross-strand interaction between phosphoserine and tryptophan is determined by subtracting the stability of *B* and *C* from *A* and *D*.

Table 2.2 Double Mutant Cycle Data for **pSW-1** and mutants at pH 4.[a]

	Peptide	Fraction Folded[b]	ΔG_f (kcal/mol)	$\Delta\Delta G_{(pXW)}$ (kcal/mol)
A	**pSW-1**	0.23 (±0.01)	0.74 (±0.05)	
B	**SW-1**	0.41 (±0.01)	0.21 (±0.05)	
C	**pSV-1**	0.22 (±0.02)	0.75 (±0.05)	
D	**SV-1**	0.22 (±0.02)	0.75 (±0.05)	
				0.53

(a) Conditions: 20 °C, 50 mM sodium acetate-*d*, pD 4.0. (b) ΔG of folding was calculated from the fraction folded using equation 3. Error determined by chemical shift accuracy on NMR spectrometer.

(e) EW-1 and QW-1 Peptide Studies. To further investigate the electrostatic destabilization of hairpin, the peptide **EW-1** was study with a glutamic acid at position 2 replacing the phosphoserine. The peptide **QW-1** was used as a neutral analog for direct comparison to **EW-1**. NMR characterization showed that **QW-1** is in fact more stable than **EW-1** at pH 7: **EW-1** is 24% folded while **QW-1** is 50% folded (Figure 2.5a, Table 2.1). Comparison of the CD spectra of **EW-1** and **QW-1** in pH 7 phosphate buffer also indicates that **QW-1** is more folded than **EW-1** (Figure 2.5b). This again shows that placing a negatively charged species cross strand from tryptophan in this hairpin system is destabilizing. A pH study demonstrates that **EW-1** exhibits pH dependence similar to **pSW-1**

(Figure 2.6). At lower pH, **EW-1** becomes more folded, just as with **pSW-1**. In contrast, **QW-1** is independent of pH. Interestingly, when protonated, glutamic acid is more stabilizing than glutamine. The same was not true for **pSW-1** and **SW-1**, which may suggest a greater role for steric repulsion in the case of **pSW-1** than **EW-1**.

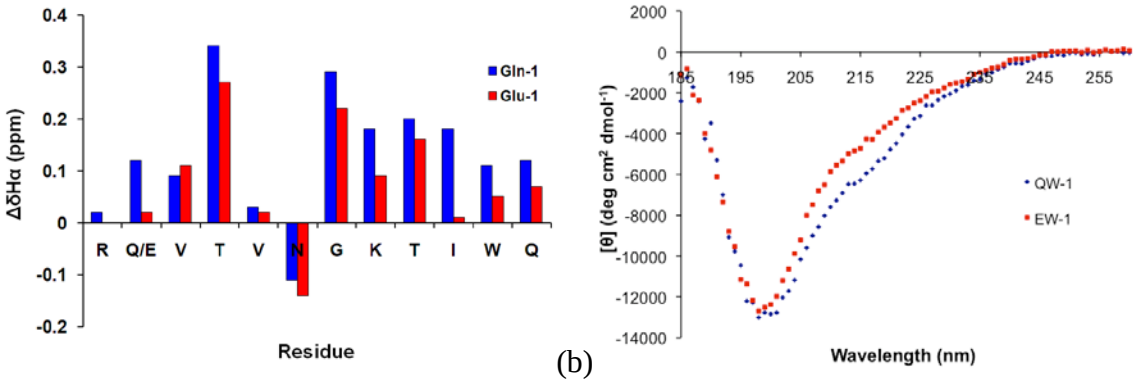

(a) (b)

Figure 2.5 (a) Hα chemical shift differences: **QW-1** (blue bars) and **EW-1** (red bars) from random coil peptides. Values calculated from data obtained at 25 °C, 50 mM potassium phosphate-*d2*, pD 7.0 The Gly bars reflect the Hα separation in the hairpin. (b) Circular dichroism spectra comparison of **SW-1** (blue) and **pSW-1** (Red) at 25°C in 10 mM sodium phosphate pH 7.0 buffer.

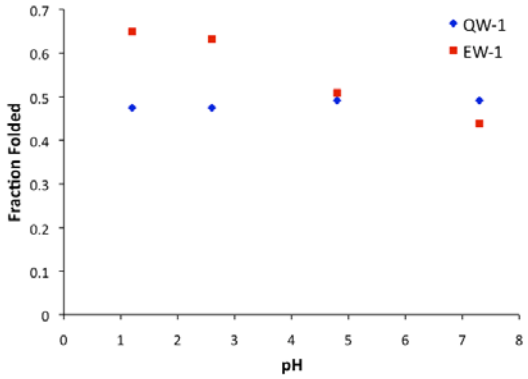

Figure 2.6 pH study of fraction folded of **QW-1** (blue) and **EW-1** (red). Fraction folded was determined by NMR glycine splitting in buffers with the pH indicated at 20 C.

(f) TW-1 Peptide Studies. To determine if phosphothreonine, another commonly phosphorylated amino acid, has the same effect as phosphoserine, the **TW-1** peptide system was designed with the same β-hairpin scaffold as **SW-1**, but with threonine positioned

directly cross strand from tryptophan as in the **SW-1** peptide (Figure 2.1). NMR analysis of the Hα chemical shifts of **TW-1** and **pTW-1** indicate that destabilization occurs when Thr is phosphorylated (Figure 2.7a) to a similar extent as was observed for **SW-1** and **pSW-1**. **TW-1** is about 40% folded while **pTW-1** is only 12% folded, giving a destabilization of approximately 0.9 kcal/mol (Table 2.1). The CD spectra of **TW-1** and **pTW-1** corroborate the NMR data, indicating that **pTW-1** is less stable than **TW-1,** with **TW-1** having a more pronounced shoulder at 215 than **pTW-1** and **pTW-1** having a larger minima at 197 nm (Figure 2.7b).

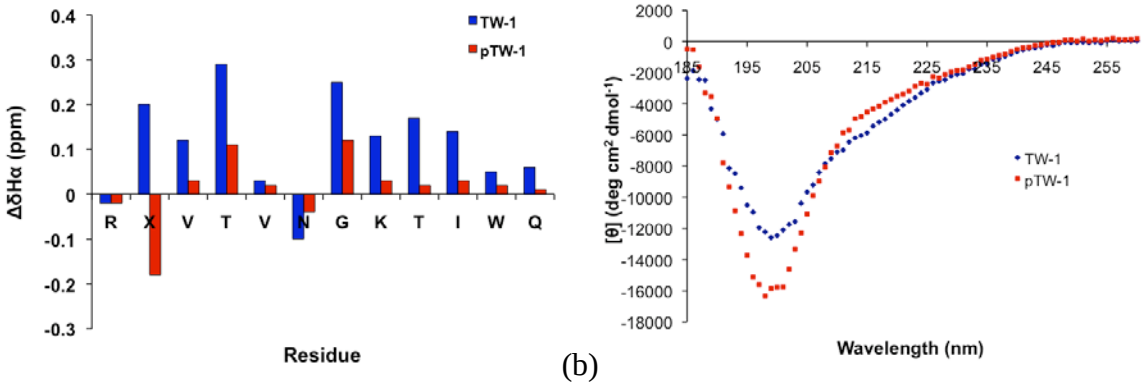

(a) (b)

Figure 2.7 (a) Hα chemical shift differences: **TW-1** (blue bars) and **pTW-1** (red bars) from random coil peptides. Residue X is either threonine (**TW-1)** or phosphothreonine (**pTW-1)**. Values calculated from data obtained at 25 °C, 50 mM potassium phosphate-*d2*, pD 7.0 The Gly bars reflect the Hα separation in the hairpin**.** (b) Circular dichroism spectra comparison of **TW-1** (blue) and **pTW-1** (red) at 25 °C in 10mM sodium phosphate pH 7.0 buffer.

(g) YW-1 Peptide Studies. The effect of tyrosine phosphorylation within the β-hairpin model system was also explored. NMR analysis of **YW-1** indicates that incorporation of the tyrosine cross-strand from the tryptophan stabilizes the hairpin (Figure 2.8a), which is about 82% folded. The incorporation of phosphotyrosine results in a destabilization of 1.0 kcal/mol of the hairpin, which is about 60% folded (Table 2.1). CD spectra confirmed the change in stability between **YW-1** and **pYW-1** showing a strong β-sheet minimum at 215 nm and no

random coil minima at 197 nm for **YW-1** while **pYW-1** has a smaller minimum at 215 nm than **YW-1** and a minimum at 197 nm (Figure 2.8b).

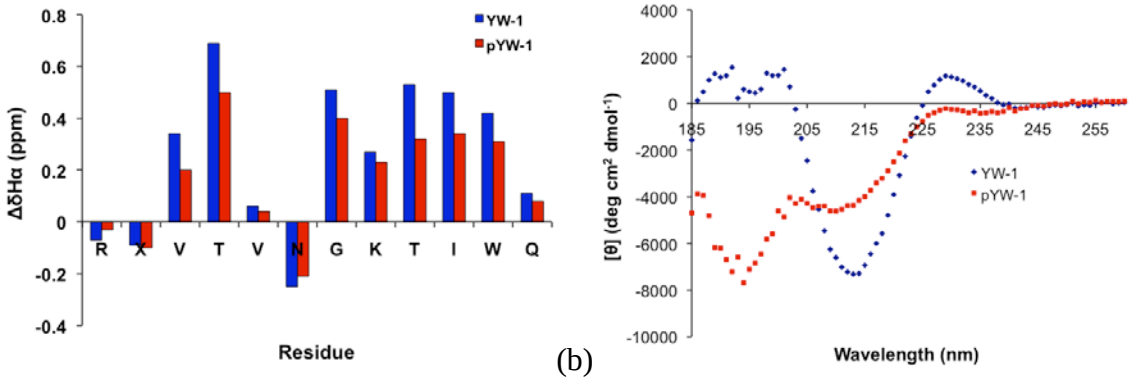

Figure 2.8 (a) Hα chemical shift differences: **YW-1** (blue bars) and **pYW-1-1** (red bars) from random coil peptides. Residue X is either tyrosine (**YW-1)** or phosphotyrosine (**pYW-1)**. Values calculated from data obtained at 25 °C, 50 mM potassium phosphate-*d2*, pD 7.0 The Gly bars reflect the Hα separation in the hairpin. (b) Circular dichroism spectra of **YW-1** (blue) and **pYW-1** (red) at 25°C in 10mM sodium phosphate pH 7.0 buffer.

The larger degree of folding of **YW-1** and **pYW-1** relative to their **SW-1** and **TW-1** analogs is due to a favorable interaction between tyrosine and the tryptophan. It has been previously shown that aromatic groups cross-stand in NHB positions of β-hairpins have a stabilizing effect via edge-face aromatic interactions.[11] NMR characterization of the aromatic region of **YW-1** suggests that Tyr2 interacts with Trp11 in an edge-face interaction as well, with the ortho-proton of Tyr2 directed towards the face of Trp11. The ortho and meta hydrogens on the tyrosine are not equivalent, with one ortho proton significantly upfield shifted (Figure 2.9). The observation of two sets of ortho and meta protons indicates restricted rotation of the aromatic ring of Tyr. In the less folded **pYW-1,** the ortho-proton on

[11] (a)Tatko, C. D.; Waters, M. L. *Protein Sci* 2003, *12*, 2443-2452. (b) Cochran, A. G.; Skelton, N. J.; Starovasnik, M. A. *Proc Nat Acad Sci U.S.A.* 2001, *98*, 5578-5583. (c) Scrutton, N. S.; Raine, A. R. C. *Biochem. J.* 1996, *319*, 1-8.

Tyr is shifted about half as much as in **YW-1**. The lesser extent of aromatic proton shifting is consistent with these residues interacting less in the destabilized hairpin.

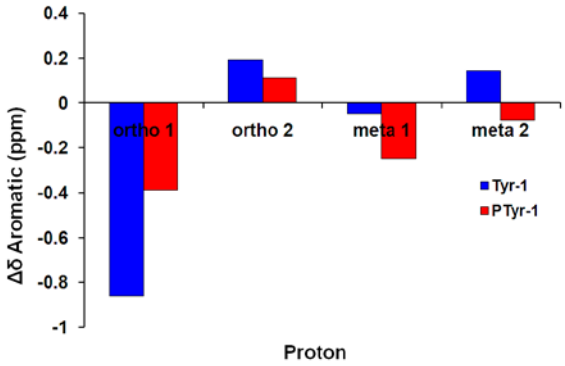

Figure 2.9 Upfield shifting of Tyr protons in **YW-1** and **pYW-1** relative to random coil values determined from control peptides **5** and **6**.

Since the **YW-1** hairpin has a very high stability due to the favorable contacts of the tyrosine, the overall hairpin stability may not be directly destabilized by the interaction of the phosphotyrosine with tryptophan. To address this issue, a double mutant cycle was performed as described in subsection ii(d), where valine replaces tryptophan in the appropriate mutant peptides. As mentioned previously, the double mutant cycle was performed at pH 4 due to solubility limitations of the valine-containing peptides at pH 7. The double mutant study found that the destabilization due to the interaction between phosphotyrosine and tryptophan is approximately 0.4 kcal/mol at pH 4 (Table 2.3). This destabilization is close to the total energy lost upon phosphorylation of Tyr at pH 4 (ie **pYW-1** relative to **YW-1**), which is 0.6 kcal/mol.

Table 2.3 Double mutant Cycle data for **pYW-1** and mutants at pH 4.[a]

	Peptide	Fraction Folded[b]	ΔG_f (kcal mol^{-1})	$\Delta\Delta G_{(pXW)}$ (kcal mol^{-1})
A	**pYW-1**	0.72 (±0.01)	-0.56 (±0.05)	
B	**YW-1**	0.88 (±0.01)	-1.16 (±0.05)	
C	**PTyrV-1**	0.33 (±0.01)	0.42 (±0.05)	
D	**TyrV-1**	0.40 (±0.01)	0.24 (±0.05)	
				0.42

(a) Conditions: 20 °C, 50 mM sodium acetate-*4*, pD 4.0 (uncorrected). (b) ΔG of folding was calculated from the fraction folded using equation 3. Error determined by chemical shift accuracy on NMR spectrometer.

iii. Discussion.

The studies described in this section demonstrate a destabilization of β-hairpin structure upon phosphorylation of a residue (Ser, Thr, Tyr) when it is cross-strand from Trp. A pH dependence was demonstrated, in which protonation of the acidic residue increases the stability of the hairpin, consistent with a repulsive electrostatic interaction. A similar pH dependent destabilization of the folded state was found for Glu across from Trp. In the case of Ser, the same effect is not observed in a control peptide in which Trp is replaced by Val, indicating that the aromatic nature of the cross-strand residue plays a role in the decreased stability of phosporylated peptides. These results are all consistent with a repulsive anion-π interaction as the driving force of for destabilization of the folded state.

Substituting different phosphorylated residues (serine, threonine, tyrosine) in the β-hairpin peptide sequence presented here has a similar destabilizing effect of 0.9 – 1.3 kcal/mol on the β-hairpin structure at pH 7, in which the phosphate is a dianion. This is interesting because tyrosine analog **YW-1** is considerably more stable than **TW-1** and **SW-1**, yet the amount of destabilization caused by incorporation of phosphorylated residue is roughly the same. In contrast, the magnitude of the repulsive Glu-Trp interaction is 0.3

kcal/mol, which is similar to the magnitude of the phosphoSer-Trp interaction at pH 4, in which the phosphate is a mono-anion. It seems that in this hairpin system the phosphate-aromatic interaction is not significantly dependent of the residue that the phosphate group is attached; the charge state has a larger influence on the magnitude of destabilization.

Lawrence and coworkers have designed fluorescent reporter peptides for protein tyrosine kinases that produce a fluorescent signal upon phosphorylation of tyrosine. These tyrosine kinase substrates contain a tyrosine that quenches the fluorophore pyrene in close proximity through an aromatic interaction. Upon phosphorylation of the tyrosine a fluorescent signal is generated due to the disruption of the aromatic interaction, allowing these peptides to act as a fluorescence reporter of tyrosine kinases. It was hypothesized that the charged and bulky phosphate in combination with a less electron rich π system of phosphotyrosine was responsible for the disruption of the tyrosine-pyrene interaction.[12] These fluorescence reporter peptides appear to undergo a similar interaction as is observed in **YW-1** and **pYW-1,** in which the π-π interaction is disrupted by phosphorylation. Indeed it maybe possible to design alternative reporter systems using β-hairpin peptides.

iv. Conclusion.

We have shown that incorporation of phosphorylated residues cross strand from tryptophan in a β-hairpin results in the destabilization of the hairpin structure. The nature of this interaction is primarily a charge-charge repulsion of the negatively charged phosphate group and the electron rich indole ring of tryptophan: a repulsive anion-π interaction. The magnitude of the destabilization is dependent on pH and ranges from 0.4 kcal/mol to approximately 1 kcal/mol. These findings demonstrate a novel mechanism by which

[12] Lawrence, D. S.; Wang, Q. *ChemBioChem* 2007, *8*, 373-378.

phosphorylation may influence protein structure and function. This interaction may also be designed into peptide systems as a means of structure control.

C. Experimental.

i. Synthesis and Purification of Peptides.

Peptides were synthesized by automated solid phase peptide synthesis on an Applied Biosystems Pioneer Peptide Synthesizer using N-9-Fluorenylmethyloxycarbonyl (Fmoc) protected amino acids on a Polyethylene glycolaylated phenylalanine ammonia lysase poly styrene (PEG-PAL-PS) resin. Fmoc-[N]-protected and Benzl-[O]-protected phosphoserine, phosphothreoine, and phosphotyropsin were purchased from AnaSpec. Activation of amino acids was performed with 2-(1H-Benzotriazole-1-yl)-1,1,3,3-tetramethyluronium hexafluorophosphate (HBTU), N-hydroxy benzotriazole H2O (HOBT) in the presence of diisopropylethyl amine (DIPEA) in dimethylformamide (DMF). Peptide deprotection was carried out in 2% 1,8 diazabicyclo[5.4.0]undec-7-ene (DBU), 2% piperidine in DMF for approximately 10 minutes. Extended cycles (75 min) were used for each amino acid coupling step. All control peptides where acetylated at the N-terminus with 5% acetic anhydride, 6% lutidine in DMF for 30 min. Cleavage of the peptide from the resin was performed in 95:2.5:2.5 Trifluoroacetic acid (TFA): Ethanedithiol or Triisopropylsilane (TIPS): water for 3 h. Ethanedithiol was used as a scavenger in for sulfur containing peptides. TFA was evaporated and cleavage products were precipitated with cold ether. The peptide was extracted into water and lyophilized. It was then purified by reverse phase HPLC, using a Vydac C-18 semipreparative column and a gradient of 0 to 100% B over 40 min, where solvent A was 95:5 water:acetonitrile, 0.1% TFA and solvent B was 95:5

actonitrile:water, 0.1% TFA. After purification the peptide was lyophilized to powder and identified with ESI-TOF mass spectroscopy.

ii. Cyclization of peptides.

Cyclic control peptides were cyclized by oxidizing the cysteine residues at the ends of the peptide via stirring in a 10 mM phosphate buffer (pH 7.5) in 1% Dimethyl sulfoxide (DMSO) solution for 9 to 12 hours. The solution was lyophilized to a powder and purified with HPLC using the method described above.

iii. CD Spectroscopy.

CD spectroscopy was performed on an Aviv 62DS Circular Dichroism Spectrophotometer. Spectra were collected from 260 nm to 185 nm at 25°C, 1 sec scanning.

iv. NMR Spectroscopy.

NMR samples were made to a concentration of 1 mM in dideuterium monoxide (D_2O) buffered to pD 4.0 (uncorrected) with 50 mM deuterated sodium acetate (NaOAc-d3), 24 mM deuterated acetic acid (AcOH-d4), 0.5 mM 3-(Trimethylsilyl)-1-propanesulfonic acid sodium salt (DSS), or pD 7.0 (uncorrected) with 50 mM deuterated potassium phosphate ($KPOD_4$), 0.5 mM DSS. Samples were analyzed on a Varian Inova 600-MHz instrument. One dimensional spectra were collected by using 32-K data points and between 8 to 128 scans using 1.5 sec presaturation. Two dimensional total correlation spectroscopy (TOCSY) and nuclear Overhauser spectroscopy (NOESY) experiments were carried out using the pulse sequences from the chempack software. Scans in the TOCSY experiments were taken 16 to 32 in the first dimension and 64 to 128 in the second dimension. Scans in the NOESY experiments were taken 32 to 64 in the first dimension and 128 to 512 in the second dimension with mixing times of 200 to 500 msec. All spectra were analyzed using standard

window functions (sinbell and gaussian with shifting). Presaturation was used to suppress the water resonance. Assignments were made by using standard methods as described by Wüthrich.[13] All experiments were run at 298 K (Hα shift) or 293.15K (double mutant and pH studies).

v. Determination of Fraction Folded.

To determine the unfolded chemical shifts, 7-mers were synthesized as unstructured controls and cyclic peptides were synthesized for fully folded. The chemical shifts for residues in the strand and one turn residue were obtained from each 7-mer peptide. The chemical shifts of the fully folded state were taken from the cyclic peptides. The fraction folded on a per residue bases was determined from Equation 1.

$$\text{Fraction Folded} = [\delta\text{obs} - \delta 0]/[\,\delta 100 - \delta 0], \qquad [1]$$

where δobs is the observed Hα chemical shift, δ100 is the Hα chemical shift of the cyclic peptides, and δ0 is the Hα chemical shift of the unfolded 7-mers. The overall fraction folded for the entire peptide was obtained by averaging the fraction folded of resides Val 3, Lys 8, and Ile 10. These residues are in hydrogen bonded positions have been shown to be the most reliable in determining fraction folded.[14] The overall fraction fold was also determined using the extent of Hα glycine splitting observed in the turn residue Gly10 given in Equation 2.

$$\text{Fraction Folded} = [\Delta\delta_{\text{Gly Obs}}]/[\,\Delta\delta_{\text{Gly 100}}], \qquad [2]$$

where $\Delta\delta_{\text{Gly Obs}}$ is the difference in the glycine Hα chemical shifts of the observed, and $\Delta\delta_{\text{Gly 100}}$ is the difference in the glycine Hα chemical shifts of the cyclic peptides. The ΔG of

[13] Wüthrich, K. *NMR of Proteins and Nucleic Acids*; Wiley: New York, 1986.

[14] Syud, F. A.; Espinosa, J. F.; Gellman, S. H. *J Am Chem Soc* 1999, *121*, 11577-11578.

folding at 298 K for the peptides was calculated using Equation 3 where *f* is the fraction folded.

$$\Delta G = -RT \ln (f/(1-f)), \quad [3]$$

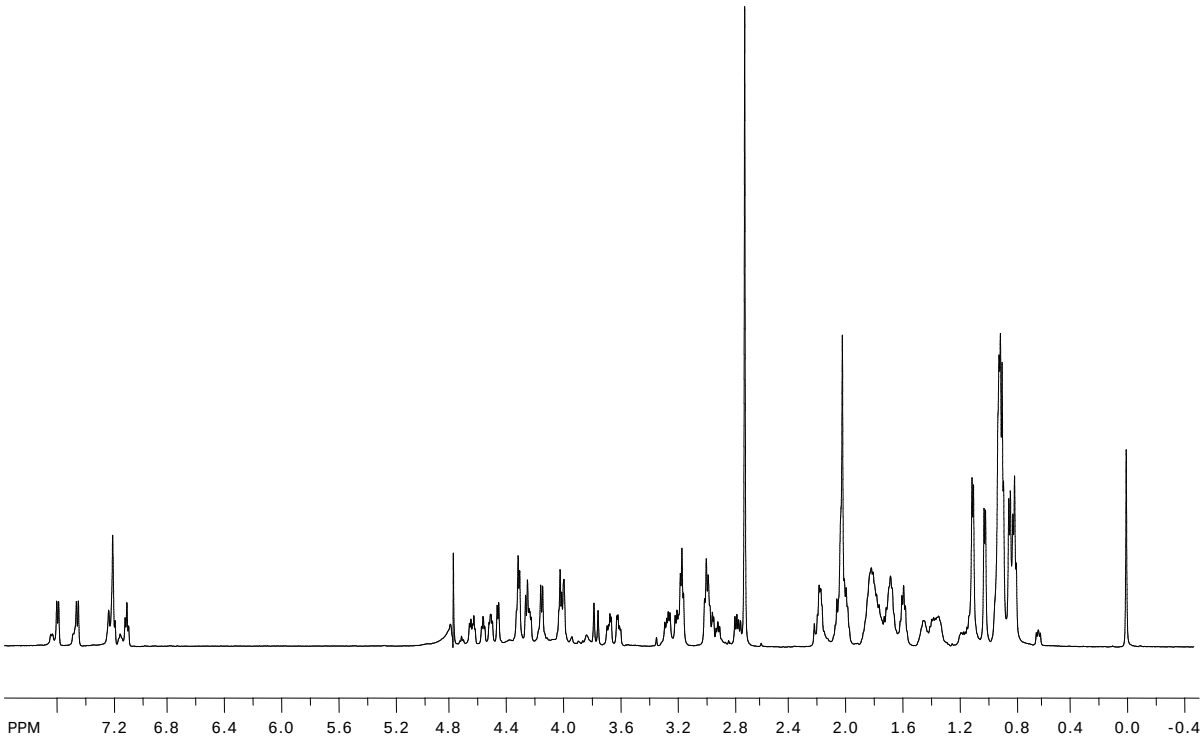

Figure 2.10 [1]HNMR of Peptide **SW-1:** Ac-Arg-Ser-Val-Thr-Val-Asn-Gly-Lys-Thr-Ile-Trp-Gln-NH2

Table 2.4 Proton Chemical Shift Assignments for Peptide **SW-1** at pH 7**.**

Residue	α	β	γ	δ	ε	Amide
R	4.34	1.8	1.6	3.14		8.12
S	4.64	3.65				8.37
V	4.16	2	0.87			8.4
T	4.67	4.02	1.09			8.37
V	4.32	2.01	0.86			8.56
N	4.58	2.93	2.66			9.02
G	4.02,3.78					8.48
K	4.52	1.8	1.72	1.69	2.95	8.06
T	4.47	4	0.97			8.48
I	4.27	1.79	N/A	0.81		8.56
W	4.73	3.2,3.24	H5 7.12, H2/6 7.21, H7 7.47,H4 7.59			8.4
Q	4.25	1.8	2.14			8.27

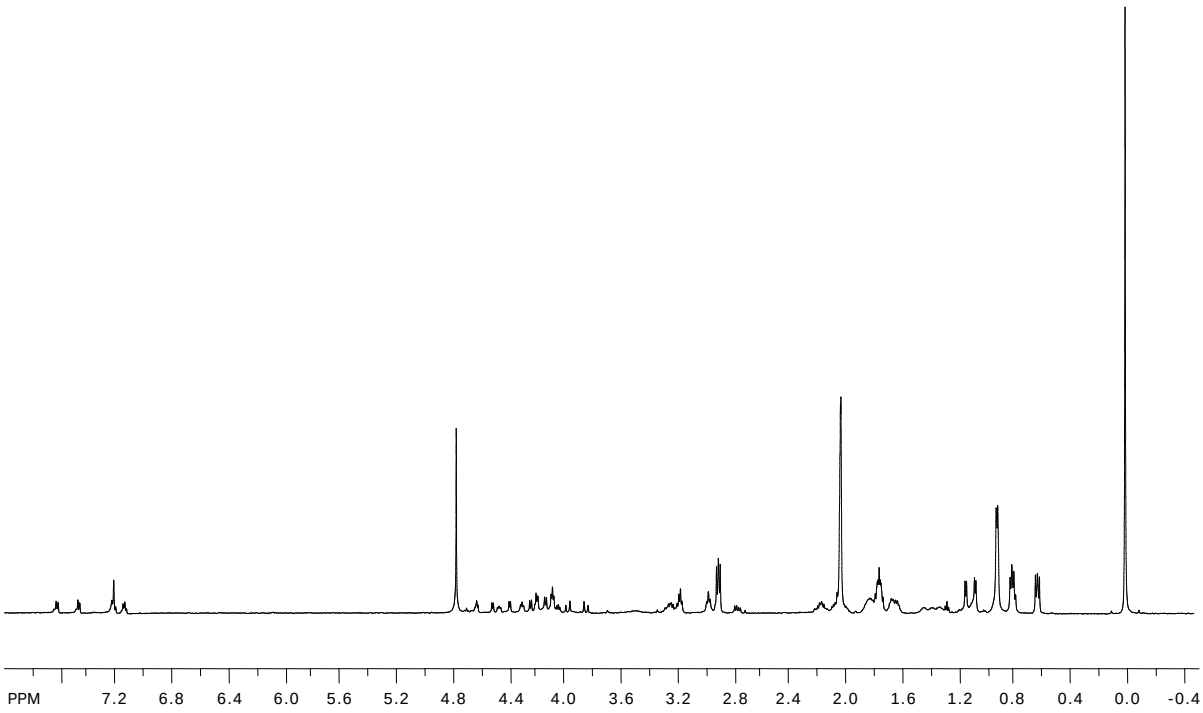

Figure 2.11 [1]HNMR of Peptide **pSW-1:** Ac-Arg-Ser(PO_3)-Val-Thr-Val-Asn-Gly-Lys-Thr-Ile-Trp-Gln-NH2

Table 2.5 Proton Chemical Shift Assignments for Peptide **pSW-1** at pH 7**.**

Residue	α	β	γ	δ	ε	Amide
R	4.32	1.8	1.66	3.19		8.22
S-PO3	4.52	4.02				8.6
V	4.23	2.1	0.93			8.22
T	4.42	4.1	1.15			8.3
V	4.13	2.05	0.92			8.39
N	4.66	2.89,2.78				8.73
G	3.95,3.89					8.39
K	4.42	1.79	1.42	1.72	2.97	8.02
T	4.32	4.06	1.07			8.29
I	4.17	1.8	N/A	0.8		8.31
W	4.68	3.25	H6 7.14,H5 7.24,H2 7.28,H4 7.48,H7 7.63			8.24
Q	4.21	1.81	2.13			8.09

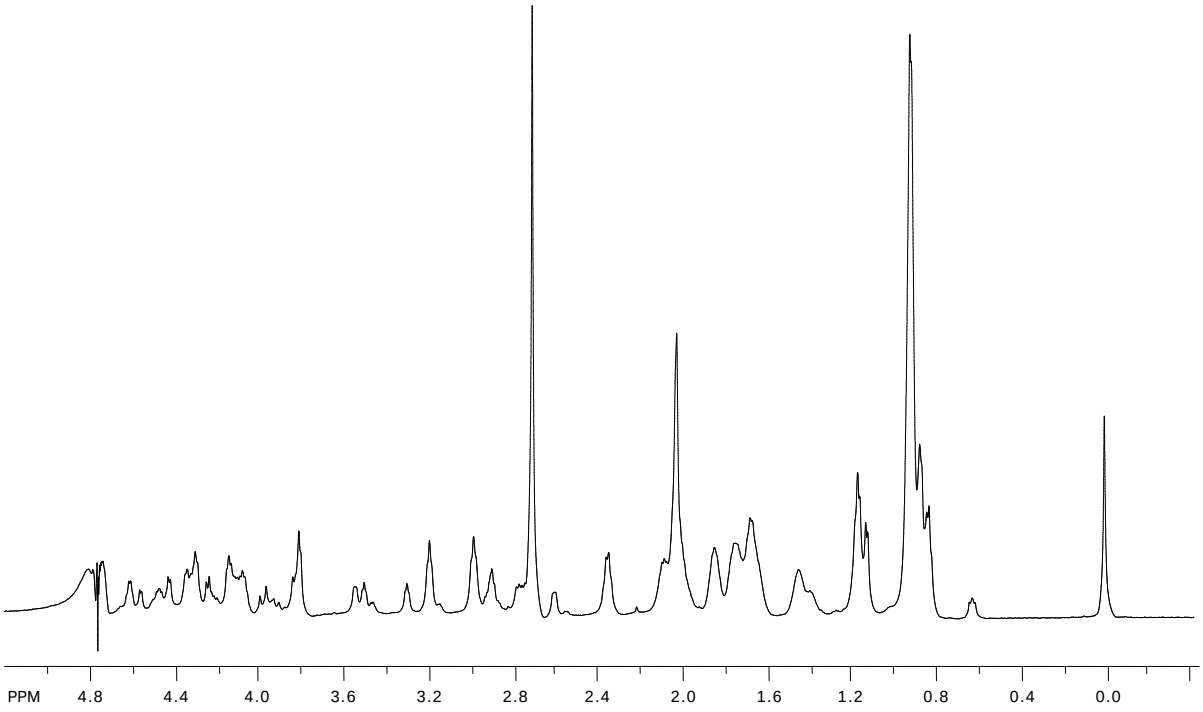

Figure 2.12 [1]HNMR of Peptide **SV-1:** Ac-Arg-Ser-Val-Thr-Val-Asn-Gly-Lys-Thr-Ile-Val-Gln-NH2

Table 2.6 Proton Chemical Shift Assignments for Peptide **SV-1.**

Residue	α	β	γ	δ	ε
R	4.35	1.77	1.68	3.2	
S	4.63	3.82			
V	4.32	2.01	0.91		
T	4.45	4.1	1.17		
V	4.15	2.04	0.91		
N	4.63	2.81/2.78			
G	3.99/3.86				
K	4.49	1.78	1.43	1.75	3
T	4.58	4.07	1.12		
I	4.25	1.85	1.46	1.19/0.86	
V	4.14	2.04	0.093		
Q	4.34	2.01	2.36		

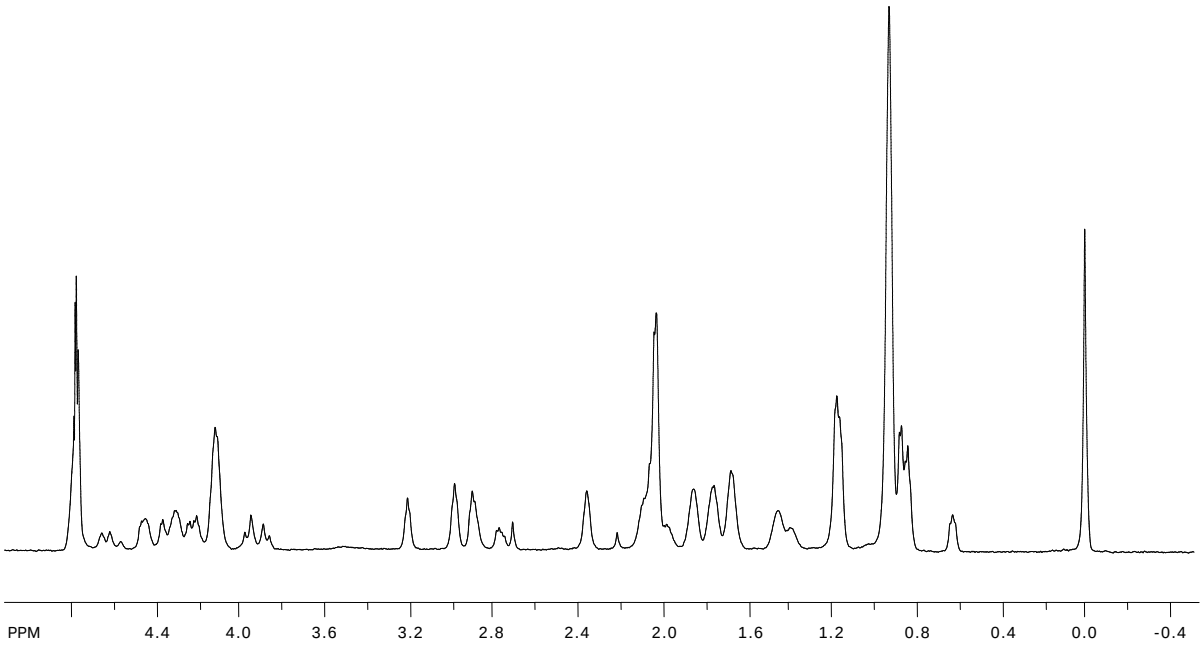

Figure 2.13 ^{1}HNMR of Peptide **pSV-1:** Ac-Arg-Ser(PO_3)-Val-Thr-Val-Asn-Gly-Lys-Thr-Ile-Val-Gln-NH2

Table 2.7 Proton Chemical Shift Assignments for Peptide **pSV-1.**

Residue	α	β	γ	δ	ε
R	4.34	1.79	1.72	3.22	
S-PO3	4.63	4.13			
V	4.25	2.1	0.99		
T	4.48	4.13	1.16		
V	4.15	2.06	0.93		
N	4.67	2.84, 2.80			
G	3.99, 3.86				
K	4.45	1.81	1.43	1.75	3
T	4.38	4.13	1.18		
I	4.23	1.86	1.47	0.88	
V	4.25	2.1	0.99		
Q	4.32	1.99	2.37		

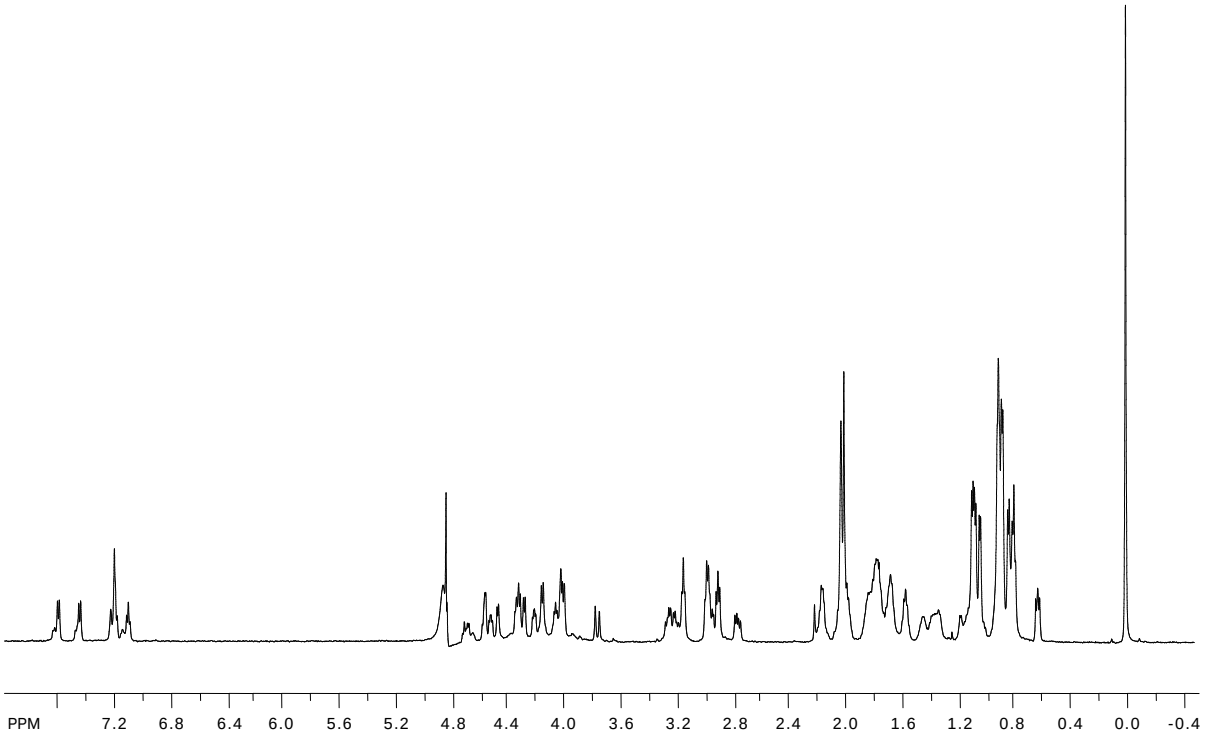

Figure 2.14 [1]HNMR of Peptide **TW-1:** Ac-Arg-Thr-Val-Thr-Val-Asn-Gly-Lys-Thr-Ile-Trp-Gln-NH2

Table 2.8 Proton Chemical Shift Assignments for Peptide **TW-1.**

Residue	α	β	γ	δ	ε
R	4.35	1.77	1.6	3.17	
T	4.58	4.07	1.08		
V	4.33	2.03	0.89		
T	4.67	4.03	1.1		
V	4.16	2.01	0.92		
N	4.58	2.96,2.78			
G	4.03,3.78				
K	4.53	1.81	1.42	1.76	2.99
T	4.48	4.03	1.04		
I	4.29	1.84	1.1	0.84	
W	4.72	3.25	H5 7.11, H6,2 7.20, H7 7.46, H4 7.60		
Q	4.23	1.8	2.18		

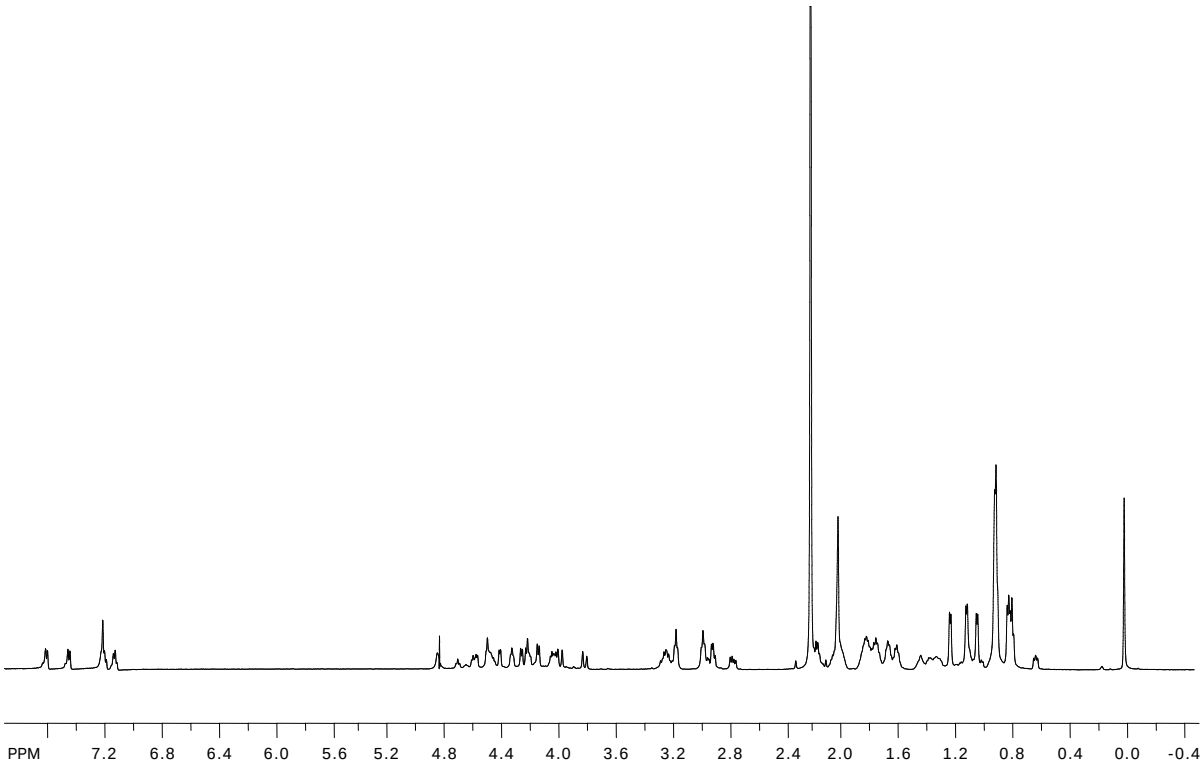

Figure 2.15 ^{1}HNMR of Peptide **pTW-1:** Ac-Arg-Thr(PO_3)-Val-Thr-Val-Asn-Gly-Lys-Thr-Ile-Trp-Gln-NH2

Table 2.9 Proton Chemical Shift Assignments for Peptide **pTW-1** at pH 7**.**

Residue	α	β	γ	δ	ε
R	4.32	1.76	1.64	3.18	
T-PO3	4.33	4.29	1.23		
V	4.23	2.09	0.9		
T	4.46	4.07	1.13		
V	4.14	2.03	0.9		
N	4.64	2.90,2.78			
G	3.96,3.84				
K	4.43	1.76	1.41	1.67	2.97
T	4.33	4.04	1.04		
I	4.18	1.81	1.1	0.8	
W	4.69	3.25	H6 7.14,H5 7.21,H2 7.28, H7 7.47,H47.64		
Q	4.18	1.81	2.16,1.98		

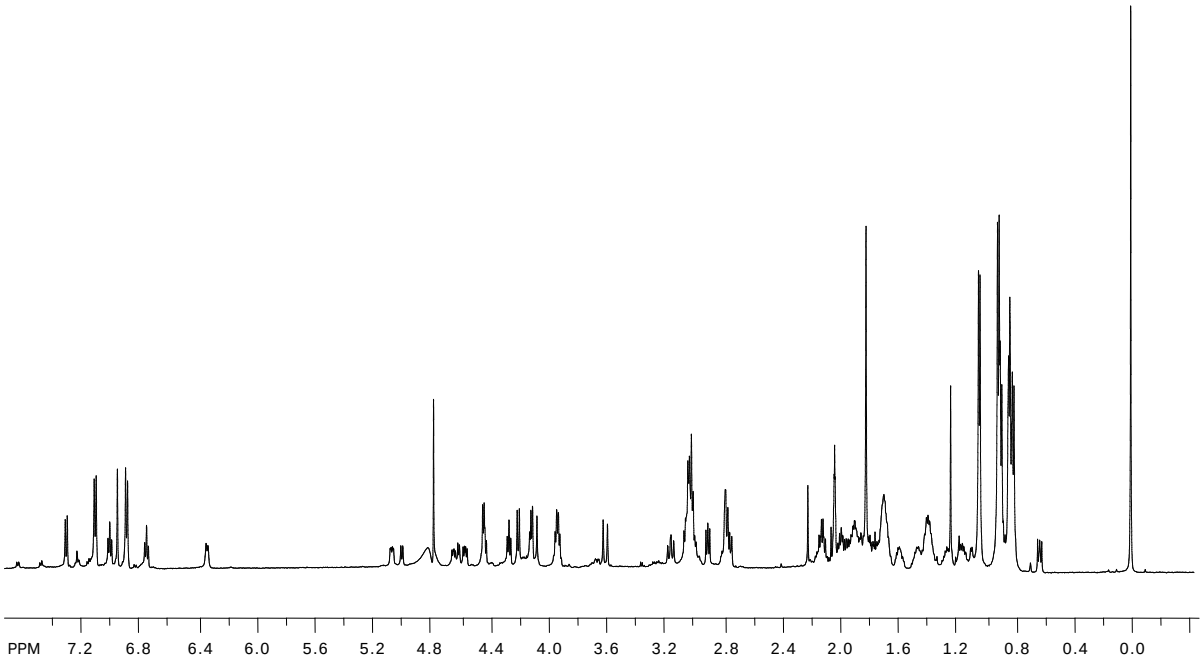

Figure 2.16 [1]HNMR of Peptide **YW:** Ac-Arg-Tyr-Val-Thr-Val-Asn-Gly-Lys-Thr-Ile-Trp-Gln-NH2

Table 2.10 Proton Chemical Shift Assignments for Peptide **YW.**

Tyr-1	α	β	γ	δ	ε
R	4.1	1.6	1.37	3.02	
Y	4.57	3.08,2.99	[H2,6] 6.73, 7.30, [H3,5] 6.25, 6.94		
V	4.46	2	0.81		
T	5.03	3.92	1.04		
V	4.21	1.94	0.89		
N	4.44	3.05,2.76			
G	4.10,3.59				
K	4.67	1.83	1.43	1.75	3.02
T	4.84	3.92	1.05		
I	4.65	1.89	1.16	0.9	
W	5.09	2.75	H5,6 6.91, H2 6.96, H4 7.13, H7 7.24		
Q	4.28	1.9	2.1		

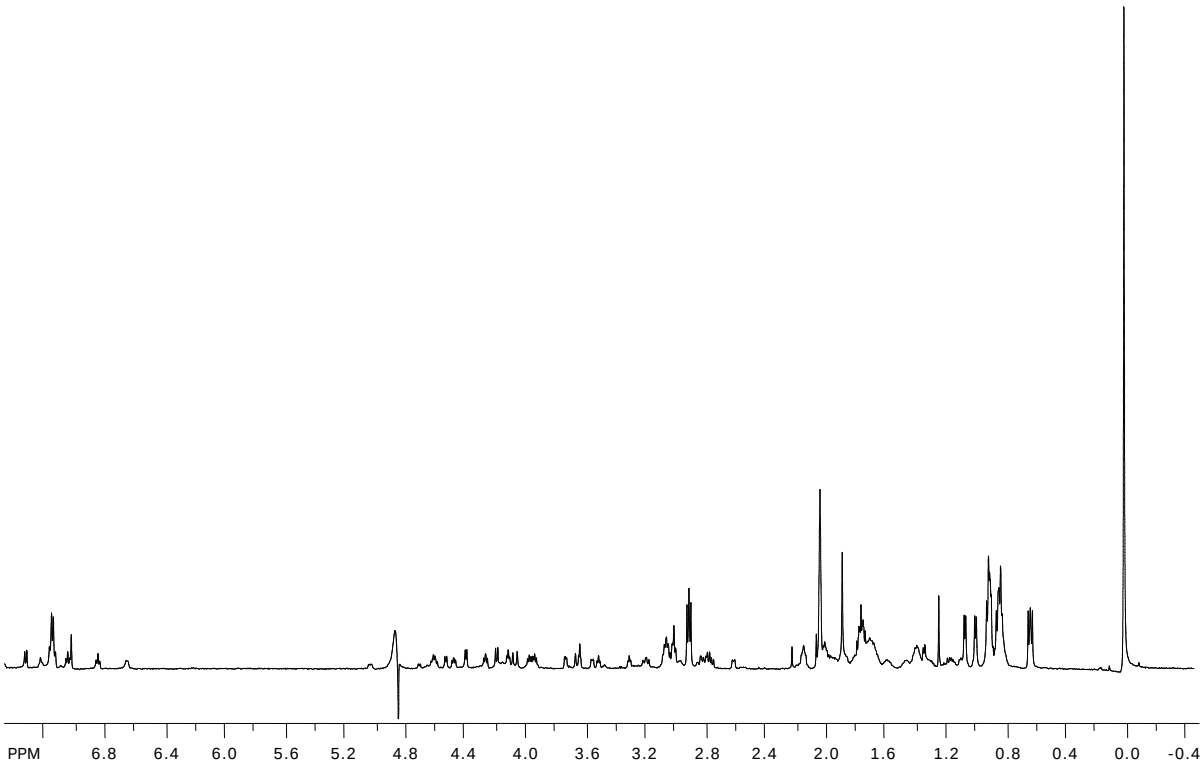

Figure 2.17 ^{1}HNMR of Peptide **pYW-1:** Ac-Arg-Tyr(PO_3)-Val-Thr-Val-Asn-Gly-Lys-Thr-Ile-Trp-Gln-NH2

Table 2.11 Proton Chemical Shift Assignments for Peptide **pYW-1** at pH 7**.**

pYW	α	β	γ	δ	ε
R	4.13	1.59	1.35	3.06	
Y-PO3	4.63	3.1	[H2,6] 6.83, 7.06 [H3,5] 6.89,7.33		
V	4.37	2.02	0.85		
T	4.89	3.99	1.09		
V	4.2	1.96	0.91		
N	4.51	3.00,2.78			
G	4.07,3.67				
K	4.63	1.81	1.43	1.76	3.04
T	4.63	3.93	0.95		
I	4.49	1.87	n/a	0.88	
W	4.98	2.74	H5 7.01, H6,2 7.16,H7 7.48,H4 7.65		
Q	4.25	1.96,1.75	2.14		

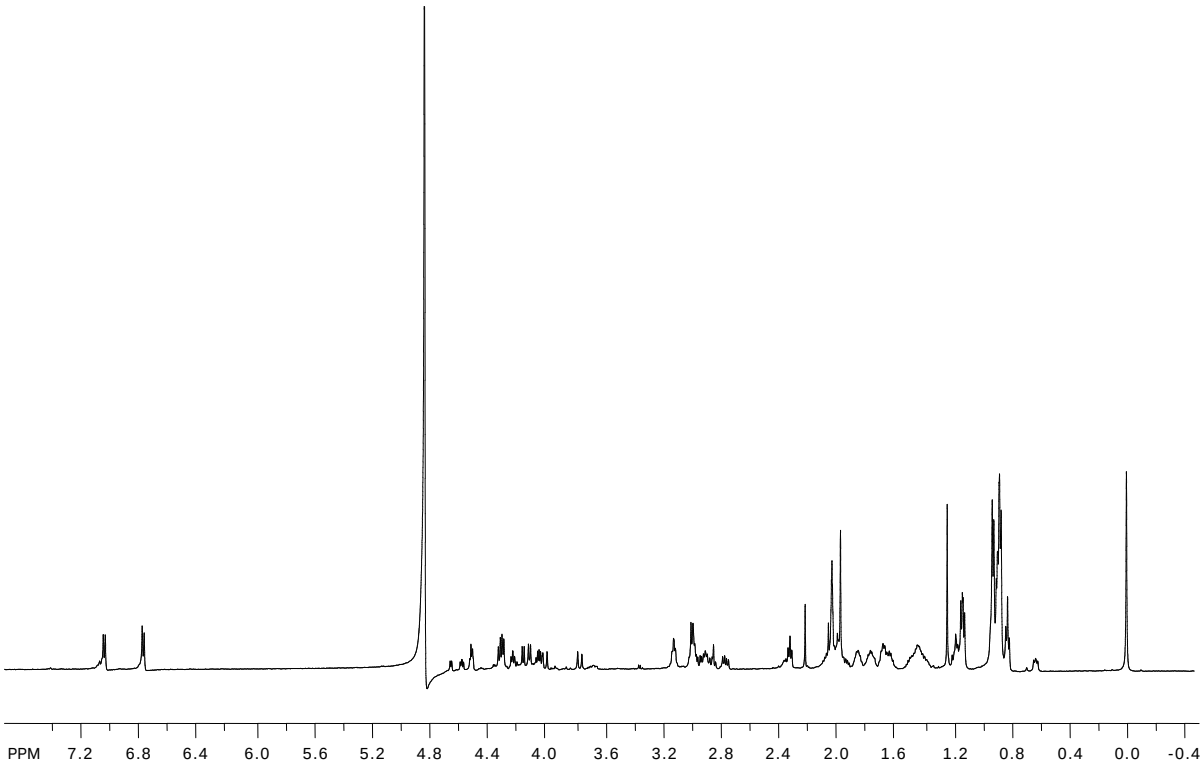

Figure 2.18 [1]HNMR of Peptide **YV-1:** Ac-Arg-Tyr-Val-Thr-Val-Asn-Gly-Lys-Thr-Ile-Val-Gln-NH2

Table 2.12 Proton Chemical Shift Assignments for Peptide **YV-1.**

Residue	α	β	γ	δ	ε
R	4.24	1.64	1.47	3.12	
Y	4.86	2.86	[H2,6] 7.05	[H3,5] 6.83	
V	4.17	2.02	0.92		
T	4.67	4.07	1.14		
V	4.13	1.99	0.89		
N	4.59	2.95,2.77			
G	3.78, 4.01				
K	4.52	1.81	1.43	1.74	3
T	4.52	4.05	1.14		
I	4.33	1.87	1.18	0.88	
V	4.23	1.89	0.87		
Q	4.3	1.94	2.02,2.33		

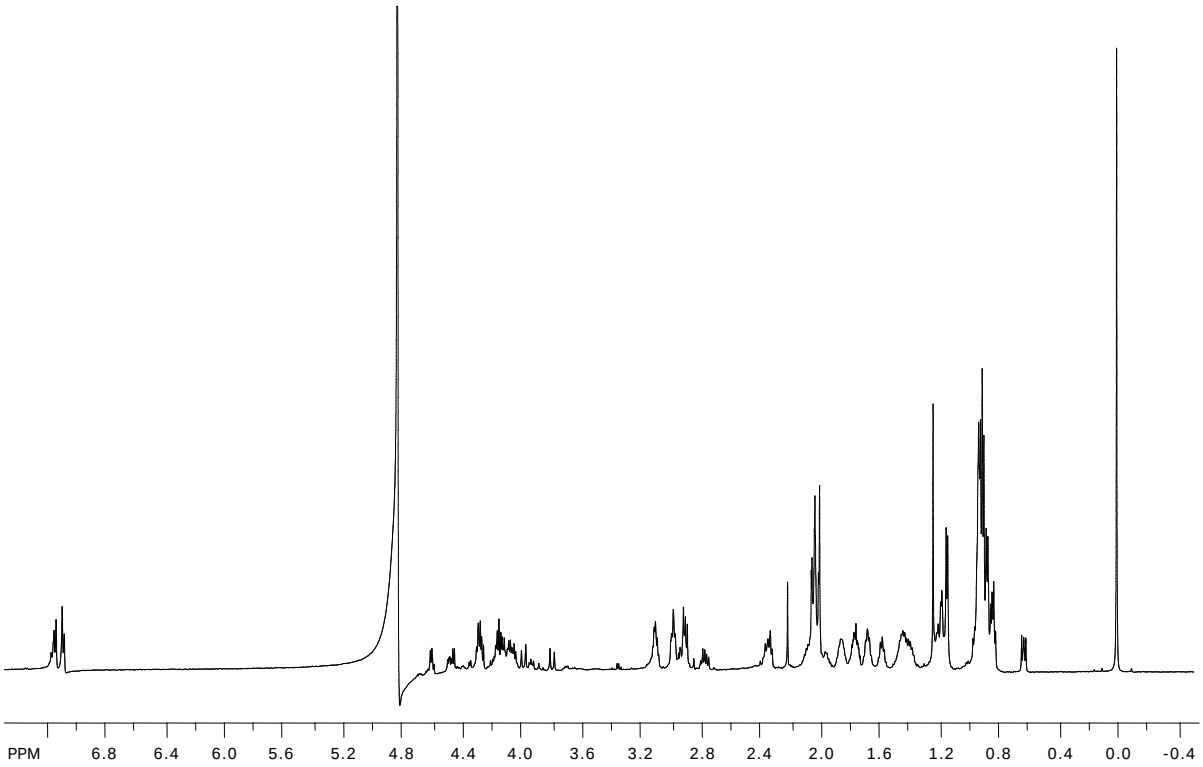

Figure 2.19 ^{1}HNMR of Peptide **pYV-1:** Ac-Arg-Tyr(PO_3)-Val-Thr-Val-Asn-Gly-Lys-Thr-Ile-Val-Gln-NH2

Table 2.13 Proton Chemical Shift Assignments for Peptide **pYV-1.**

Residue	α	β	γ	δ	ε
R	4.18	1.62	1.42	3.12	
Y-PO3	4.8	3.12,2.91	7.16,7.11		
V	4.16	2.03	0.93		
T	4.63	4.1	1.15		
V	4.11	2.03	0.93		
N	4.63	2.93,2.78			
G	3.81, 4.00				
K	4.5	1.79	1.41	1.75	2.98
T	4.48	4.08	1.15		
I	4.3	1.87	1.18	0.88	
V	4.21		0.91		
Q	4.3	1.96	2.35		

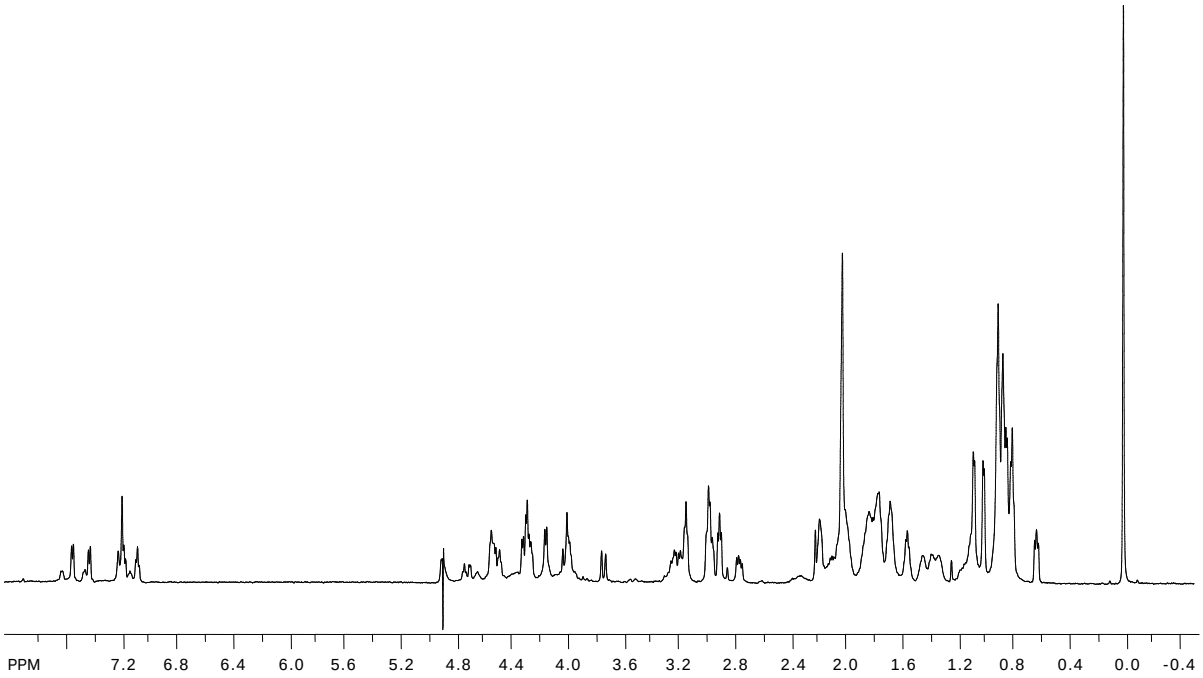

Figure 2.20 [1]HNMR of Peptide **QW-1:** Ac-Arg-Gln-Val-Thr-Val-Asn-Gly-Lys-Thr-Ile-Trp-Gln-NH2

Table 2.14 Proton Chemical Shift Assignments for Peptide **QW-1.**

Residue	α	β	γ	δ	ε
R	4.29	1.74	1.59	3.16	
Q	4.5	1.85	2.06		
V	4.28	2.01	0.85		
T	4.72	4.02	1.09		
V	4.17	1.99	0.91		
N	4.58	2.96, 2.78			
G	4.05, 3.76				
K	4.58	1.82	1.42	1.77	2.98
T	4.51	3.99	0.99		
I	4.33	1.86	1.07	0.85	
W	4.78	3.21	H5 7.09, H2,6 7.21, H7 7.46, H4 7.56		
Q	4.29	1.82	2.2		

Table 2.15 Proton Chemical Shift Assignments for Peptide **EW-1.**

Residue	α	β	γ	δ	ε
R	4.25	1.72	1.57	3.14	
E	4.4	1.89	2.14		
V	4.26	2.03	0.86		
T	4.65	4.08	1.14		
V	4.15	2.01	0.88		
N	4.53	2.66,2.82			
G	4.01,3.79				
K	4.49	1.82	1.42	1.77	2.94
T	4.47	4.03	1.05		
I	4.16	1.79	N/A	0.87	
W	4.72	3.23	H4 7.59,H7 7.58,H5 7.15,H2 7.30,H6 7.22		
Q	4.29	1.79	2.18		

Table 2.16 Proton Chemical Shift Assignments for Peptide **cyclic SW.**

Residue	α	β	γ	δ	ε
C	4.93	3.35,3.16			
R	4.59	1.85,1.61	1.5	3.16	
S	4.73	2.96			
V	4.21	1.91	0.89		
T	5.09	3.86	0.99		
V	4.44	1.97	0.83		
N	4.38	3.09,2.77			
G	4.12,3.54				
K	4.68	1.84	1.44	1.73	3.01
T	4.75	3.88	0.89		
I	4.49	1.88	1.38,1.16,0.8	0.88	
W	5.02	3.13	H5 7.19, H7 7.44,H2 7.39,H5 7.03,H6 7.17		
Q	4.61	2.10,1.87	2.23		
C	4.93	3.35,3.16			

Table 2.17 Proton Chemical Shift Assignments for Peptide **cyclic TW.**

Residue	α	β	γ	δ	ε
C	4.95	3.05, 2.90			
R	4.63	1.61	1.43	3.13	
T	4.95	3.8	0.7		
V	4.47	1.96	0.8		
T	5.12	3.86	0.99		
V	4.21	1.89	0.88		
N	4.38	2.75, 3.08			
G	3.54, 4.11				
K	4.7	1.83	1.43	1.78	3.02
T	4.8	3.91	0.96		
I	4.57	1.89	1.11	0.86	
W	5.01	3.14, 3.10	H5 7.00, H6 7.14, H2 7.17, H7 7.40,H4 7.44		
Q	4.63	1.84	2.19		
C	5.12	2.94, 2.15			

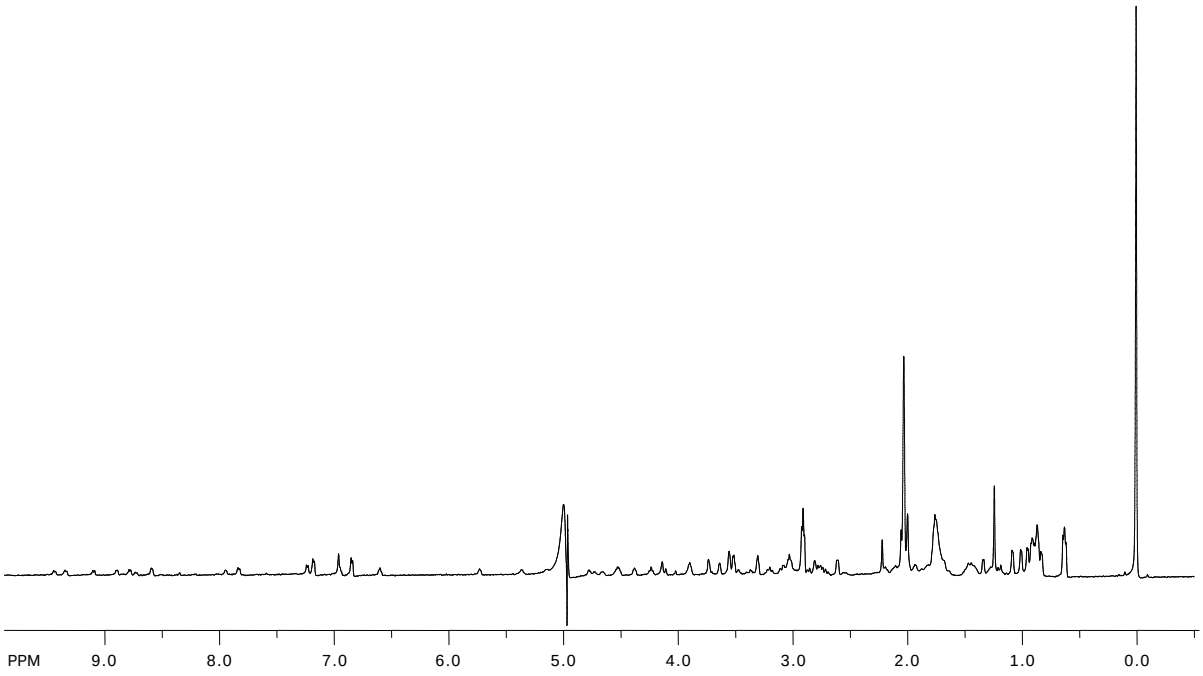

Figure 2.21 [1]HNMR of Peptide **cyclic YW:** Ac-Cys-Arg-Tyr-Val-Thr-Val-Asn-Gly-Lys-Thr-Ile-Trp-Gln-Tyr-NH2

Table 2.18 Proton Chemical Shift Assignments for Peptide **cyclic YW.**

Residue	α	β	γ	δ	ε
C	4.76	2.89,2.75			
R	4.17	1.76	1.41	3.02	
Y	4.67	3.18,2.85	[H3,5]	[2,6] 6.61,7.25	
V	4.5	2.09	0.81		
T	4.98	3.87	1.04		
V	4.22	1.91	0.89		
N	4.36	2.74,3.07			
G	4.10,3.52				
K	4.76	1.83	1.43	1.76	3.02
T	5.13	3.87	0.98		
I	4.76	1.9		0.93	
W	5.33	2.76			
Q	4.52	1.73,1.97	2.12		
C	4.93	2.64,1.46			

Table 2.19 Proton Chemical Shift Assignments for Peptide **Ac-RSVTVNG-NH2.**

Residue	α	β	γ	δ	Amide
R	4.32	1.82,1.77	1.66	3.21	8.32
S	4.5	3.85			8.47
V	4.13	2.08	0.94		8.28
T	4.37	4.16	1.18		8.3
V	4.23	2.12	0.93		8.28
N	4.69	2.85,277			8.68
G	3.9				8.57

Table 2.20 Proton Chemical Shift Assignments for Peptide **Ac-RS(PO_3)VTVNG-NH2.**

Residue	α	β	γ	δ	Amide
R	4.32	1.83	1.69	3.21	8.36
S-PO3	4.59	4.15			8.69
V	4.14	2.09	0.93		8.14
T	4.36	4.16	1.2		8.29
V	4.22	2.11	0.93		8.31
N	4.44	4.68	2.79		8.69
G	3.82	3.91,3.89			8.45

Table 2.21 Proton Chemical Shift Assignments for Peptide **Ac-RTVTVNG-NH2.**

Residue	α	β	γ	δ	ε
R	4.37	1.78	1.66	3.21	
T	4.38	4.15	1.19		
V	4.21	2.08	0.93		
T	4.38	4.15	1.19		
V	4.13	2.07	0.92		
N	4.68	2.78			
G	3.9				

Table 2.22 Proton Chemical Shift Assignments for **Ac-RT(PO_3)VTVNG-NH2.**

Residue	α	β	γ	δ	ε
R	4.34	1.79	1.68	3.2	
T-PO3	4.51	4.42	1.3		
V	4.2	2.08	0.93		
T	4.35	4.14	1.17		
V	4.12	2.05	0.93		
N	4.68	2.8			
G	3.89				

Table 2.23 Proton Chemical Shift Assignments for **Ac-RYVTVNG-NH2.**

Resiude	α	β	γ	δ	ε
R	4.17	1.62	1.45	3.11	
Y	4.66	3.07,2.87	[H2,6] 7.11	[H3,5] 6.80	
V	4.12	2.06	0.93		
T	4.34	4.15	1.19		
V	4.15	2.01	0.9		
N	4.69	2.85,2.76			
G	3.85				

Table 2.24 Proton Chemical Shift Assignments for **Ac-RY(PO_3)VTVNG-NH2.**

Residue	α	β	γ	δ	ε
R	4.16	1.59	1.44	3.14	
Y-PO3	4.73	3.20,2.96	[H2,6] 7.22	[H3,5] 7.14	
V	4.17	2.04	0.93		
T	4.39	4.19	1.23		
V	4.16	2.04	0.95		
N	4.72	2.96,2.79			
G	3.91				

Table 2.25 Proton Chemical Shift Assignments for **Ac-RQVTVNG-NH2.**

Residue	α	β	γ	δ	ε
R	4.27	1.76	1.63	3.2	
Q	4.38	2.05	2.35		
V	4.19	2.05	0.94		
T	4.38	4.14	1.19		
V	4.14	2.08	0.94		
N	4.69	2.76			
G	3.9				

Table 2.26 Proton Chemical Shift Assignments for **Ac-REVTVNG-NH2.**

Residue	α	β	γ	δ	ε
R	4.25	1.74	1.63	3.19	
E	4.38	2.02	2.39		
V	4.15	2.06	0.93		
T	4.38	4.14	1.17		
V	4.13	2.06	0.92		
N	4.67	2.77			
G	3.89				

Table 2.27 Proton Chemical Shift Assignments for **Ac-NGKTIWQ-NH2.**

Residue	α	β	γ	δ	ε	Amide
N	4.68	2.81				8.46
G	3.94					8.57
K	4.4	1.84,1.78	1.4	1.67	2.97	8.15
T	4.31	4.09	1.1			8.25
I	4.15	1.79	1.32,1.10	0.81		8.22
W	4.67	3.26	H6/H2 7.24, H47.65,H7 7.49, H5 7.16			8.25
Q	4.17	2.01,1.81	2.17			8.06

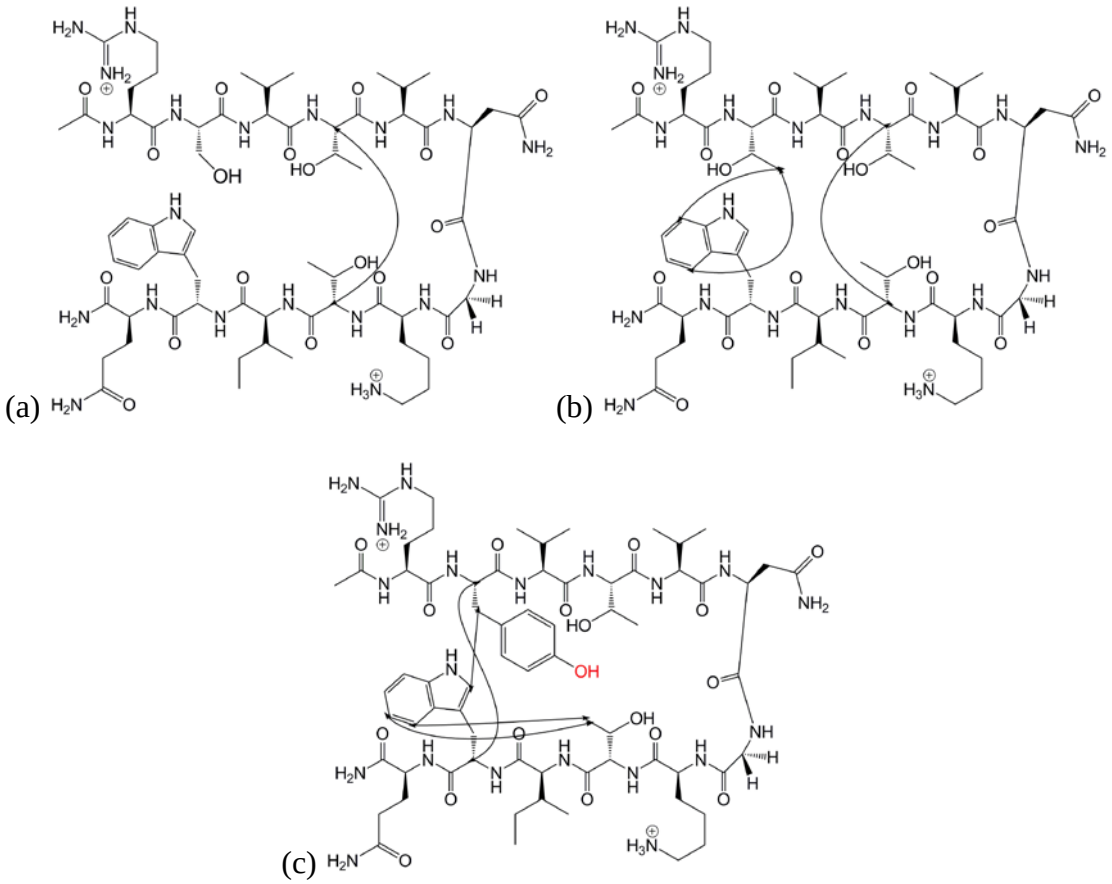

Figure 2.28 Observed NOEs for (a) **SW**, (b) **TW,** (c) **YW** and **pYW** where the red hydroxyl group is phosphorylated in **pYW**.

Table 2.22 NOEs observed in Peptides **SW, TW, YW, and pYW** at 298 K.

SW

Residue	**Proton**	**Residue**	**Proton**
Thr 4	α	Thr 9	α

TW

Residue	**Proton**	**Residue**	**Proton**
Thr 2	γ	Trp 11	Ar 4
Thr 2	γ	Trp 11	Ar 7
Thr 4	α	Thr 9	α

YW and pYW

Residue	**Proton**	**Residue**	**Proton**
Tyr 2	α	Trp 11	α
Tyr 2	β	Trp 11	Ar 2
Thr 9	γ	Trp 11	Ar 4
Thr 9	γ	Trp 11	Ar 5

CHAPTER III

STABILIZATION OF β-HAIRPIN STRUCTURE THROUGH A TRYPTOPHAN POCKET

(Reproduced, in part with permission from Riemen**,** A.J.; Waters M.L., *Biochemistry.* **2009,** *48*, 1525-1531.)

A. Trytophan pocket interaction with Lysine and Methylated Lysine

i. Background and Significance

Methylation of lysine residues in histone proteins is a posttranslational modification that is involved in the regulation of chromatin condensation and gene expression.[1] The modified methylated lysine residues at specific locations of the histone tails results in recruitment of various chromatin remodeling proteins.[1,2,3] Recent crystallographic data has shown that proteins involved in chromatin remodeling, including chromodomains, PHD domains, and Tudor domains, recognize and bind trimethylated lysine of histone tails with an aromatic cage made up of three or four aromatic rings.[2,3] The stabilizing forces between the methylated lysine and its aromatic binding pocket are driven by cation-π and van der waals interactions (Figure 3.1).[2,3,4] In each case, at least two of the aromatic residues reside within a

---

[1] Martin, C.; Zhang, Y. *Nat Rev Mol Cell Biol* **2005**, *6*, 838-849.

[2] Jacobs, S. A.; Khorasanizadeh, S. *Science* **2002**, *295*, 2080-2083.

[3] Li, H. T.; Ilin, S.; Wang, W. K.; Duncan, E. M.; Wysocka, J.; Allis, C. D.; Patel, D. J. *Nature* **2006**, *442*, 91-95.

[4] Hughes, R. M.; Wiggins, K. R.; Khorasanizadeh, S.; Waters, M. L. *Proc Nat Acad Sci U.S.A.* **2007**, *104*, 11184-11188.

β-sheet, forming a cleft. This interesting structural feature may be amenable to designed peptide systems that form a β-hairpin containing an aromatic cleft for intramolecular binding of lysine or methylated lysine, thus mimicking the aromatic pocket of the chromodomain and PHD domains.

Previous work in model β-hairpin systems has shown that lysine and N-methylated lysine packs against a tryptophan positioned diagonally cross strand in a cation-π interaction (Figure 3.1c), simulating the interaction between trimethylated lysine (KMe3) and one of the aromatic residues in the β-sheet of the HP1 chromodomain or the BPTF PHD domain.[5,6,7] Methylation of lysine in this hairpin greatly increases the hairpin stability due to an enhanced interaction with Trp.[6,8] Moreover, comparison of KMe3 to its neutral analog in which nitrogen is replaced by carbon results in loss of the interaction with Trp in the peptide model system as well as loss of the binding to the aromatic pocket in the HP1 chromodomain.[4] The goal of this project was to further investigate the interaction between methylated lysine and aromatic binding pockets. We designed a β-hairpin that contains an aromatic pocket similar to one observed in chromatin remodeling proteins (Figure 3.1a and b) that results in a highly stable β-hairpin containing a lysine positioned to interact with an aromatic pocket.

[5] Tatko, C. D.; Waters, M. L. *J Am Chem Soc* **2004**, *126*, 2028-2034.

[6] Hughes, R. M.; Waters, M. L. *J Am Chem Soc* **2005**, *127*, 6518-9.

[7] Hughes, R. M.; Benshoff, M. L.; Waters, M. L. *Chem Eur J* **2007**, *13*, 5753-5764.

[8] Hughes, R. M.; Kiehna, S. E.; Waters, M. L. *Biopolymers* **2005**, *80*, 497-497.

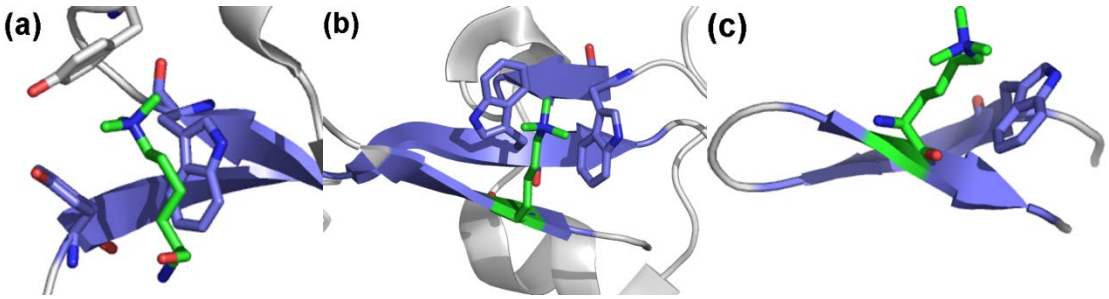

Figure 3.1. (a) Structure of the aromatic binding pocket of the HP1 chromodomain bound to a histone peptide containing trimethyllysine (green); β-sheet structure is shown in blue (pdb: 1KNE). (b) Structure of the aromatic binding pocket of the domain bound to a histone peptide containing trimethyllysine (green); β-sheet structure is shown in blue (pdb: 3GL6). (c) NMR structure of the β-hairpin peptide WKMe3 indicating the cation-pi interaction between Trp and trimethyllysine (green); β-sheet structure is shown in blue.[7]

ii. Results and Discussion.

a.) Peptide Design. The Trp pocket series of peptides were synthesized to investigate the effects of placing lysine and its varying methylation states cross-strand from a ditryptophan cleft on a β-hairpin. The sequence Ac-RWVWVNGOKMe$_n$ILQ-NH2, where n = 0 - 3, was used to create an aromatic pocket on the non-hydrogen bonded (NHB) face of the peptide with which KMe$_n$ can interact. This sequence was adapted from previously designed β-hairpins used to study cation-π interactions between lysine and tryptophan.[5,6] This design assumes an interdigitated arrangement of side chains 2, 4, 9, and 11 resulting from the twist in the β-sheet as has been shown in related peptide sequences.[7,9] Thus residue 9 is oriented to pack between the two tryptophan side chains at positions 2 and 4, whereas residue 11 packs against the outer face of Trp2. Residues Asn6 and Gly7 were included to facilitate a type I' turn which have been shown to be favorable in β-hairpin formation.[10] Cyclic peptides were

[9] Cochran, A. G.; Skelton, N. J.; Starovasnik, M. A. *Proc Nat Acad Sci U.S.A.* **2001**, *98*, 5578-5583.

[10] (a) RamirezAlvarado, M.; Blanco, F. J.; Serrano, L. *Nat Struct Biol* **1996**, *3*, 604-612. (b) Blanco, F. J.; Jimenez, M. A.; Herranz, J.; Rico, M.; Santoro, J.; Nieto, J. L. *J Am Chem Soc* **1993**, *115*, 5887-5888. (c) Sharman, G. J.; Searle, M. S. *Chem Commun* **1997**, 1955-1956.

synthesized as fully folded controls for each of the Trp Pocket series β-hairpins. Cyclization was achieved by a disulfide bond between cysteine residues at the N and C-termini of the peptides. Unfolded control peptides consisting of either the N-terminal arm or the C-terminal arm were used to obtain random coil chemical shifts.

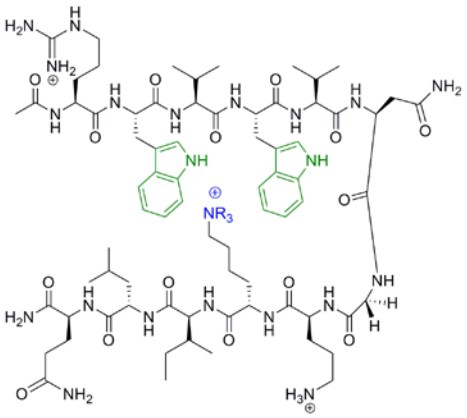

Figure 3.2. Trp pocket series of peptides containing Trp at positions 2 and 4 and Lys (**WWKL)**, mono- (**WWKmeL)**, di- (**WWKme2L)**, or trimethyl (**WWKme3L)** Lys at position 9 (R = H or Me, accordingly).

b.) Structure determination and characterization. NMR and CD were used to probe the interaction between the ditryptophan pocket and lysine in its various methylated forms. As discussed in chapter 1, downfield shifting of ≥ 0.1 ppm of the Hα protons along the peptide backbone relative to unfolded values indicates a β-sheet conformation.[11] All of the Trp Pocket series exhibited highly folded β-hairpin structure (Figure 3.3a). Residues KMe_n 9 and Leu 11 exhibit upfield shifting of Hα from the unfolded control due to the electron shielding caused by their proximity to the aromatic indole rings of the tryptophans directly cross strand from these residues. The Asn 6 Hα is shifted upfield because this residue adopts a turn conformation in the β-hairpin. Minimal shifting of Gln12 Hα is due to fraying of the terminus. Analysis of backbone amide chemical shift from random coil in the hydrogen

[11] Sharman, G. J.; Griffiths-Jones, S. R.; Jourdan, M.; Searle, M. S. *J Am Chem Soc* **2001**, *123*, 12318-12324.

bonded positions (Arg 1, Val 3, Val 5, Ile 10, Qln 12) also confirmed β-hairpin formation with large downfield chemical shift for these residues (Figure 3.3b). A typical large downfield shift was also observed of Asn 6 which confirms the formation of the turn structure. CD spectra for all Trp pocket peptides further confirm the formation of β-sheet structure with a characteristic minimum at 215 nm (Figure 3.3c).

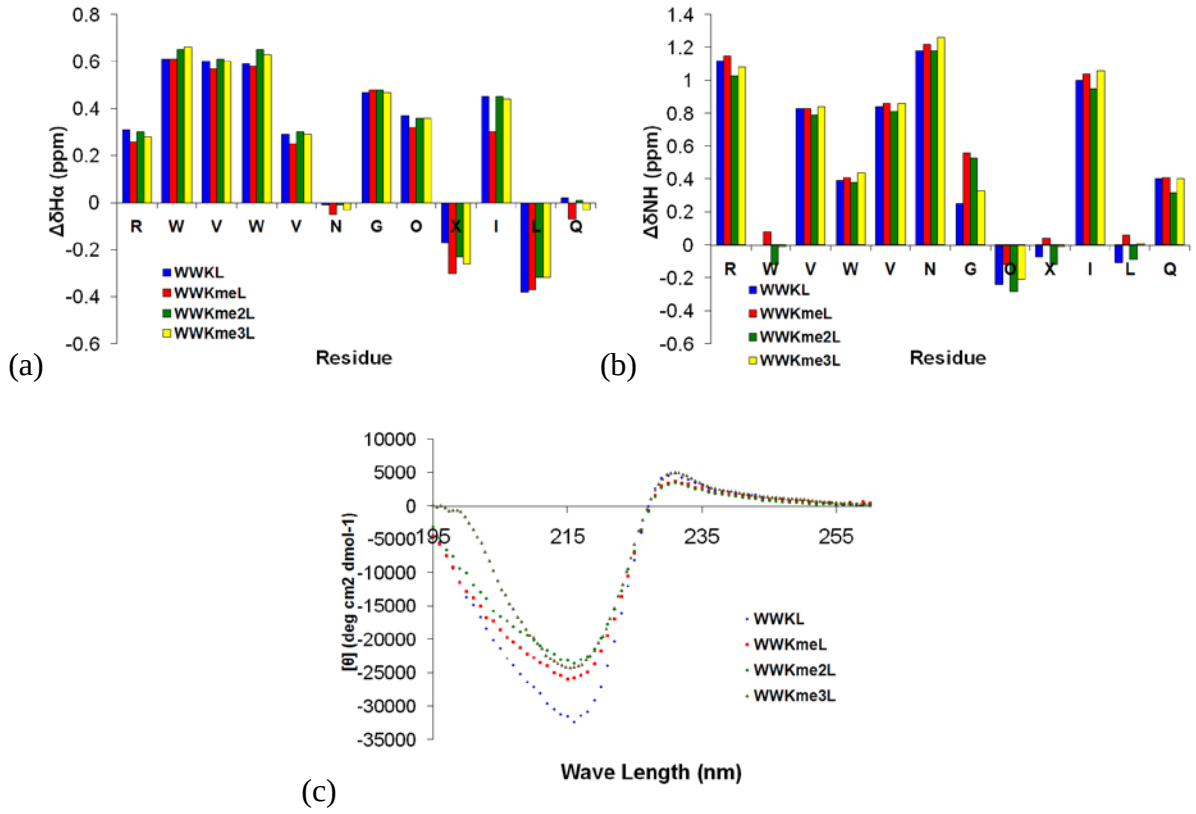

Figure 3.3. (a) Trp pocket peptides Hα chemical shift differences from random coil controls. The Gly bars reflect the Hα separation in the hairpin. (b.) Trp pocket peptides backbone amide chemical shift differences from random coil control. Conditions: 293 K, 50 mM sodium acetate-d_4, pH 4.0 (uncorrected), referenced to DSS. (c) Far-UV CD spectra of Trp pocket peptides. Conditions: 10 mM sodium phosphate buffer pH 7.0 at 298 K.

The extent of folding to a β-hairpin by the Trp pocket series of peptides was quantified using two methods described in Chapter 1 and the experimental section. Both Hα shifting method and glycine splitting method showed that all of the peptides in the Trp Pocket series

are ≥ 90% folded. However due to error associated with a small change in chemical shift at this range in folding, it is difficult to determine which of the series is the most well folded (Table 3.1).

Table 3.1. Fraction folded for Trp pocket series peptides. Conditions: 293 K, 50 mM sodium acetate-d_4, pH 4.0 (uncorrected), referenced to DSS.

Peptides	Fraction Folded (Gly)[a]	Fraction Folded (Hα)[b]
WWKL	≥ 0.99 (±0.02)	0.96 (±0.09)
WWKmeL	≥ 0.99 (±0.02)	0.9 (±0.1)
WWKme2L	0.97 (±0.02)	0.98 (±0.01)
WWKme3L	≥ 0.99 (±0.02)	0.94 (±0.03)

(a) Error determined by chemical shift accuracy on NMR spectrometer. (b) Average of the Hα values from Val3, Val5, Orn8, and Ile10. The standard deviation is in parentheses.

Direct interaction between the lysine side chain and tryptophan pocket was also determined by NMR. The chemical shift of the side chain protons are affected by the surrounding environment, in particular the ring current effects arising from nearby aromatic rings, the degree of upfield shifting of the lysine side chain protons in this peptide series relative to the unfolded control is indicative of interaction of the lysine with the tryptophan pocket (Figure 3.3). All of the hairpins show extensive upfield shifting indicating that the lysine residues are in close proximity to the face of the indole rings. The γ, δ and ε methylene groups of the lysine are shifted the greatest extent. An increase in upfield shifting upon methylation of the lysine is observed, indicating that the methyl groups are helping the lysine pack into the tryptophan pocket. This has been observed in other reported β-hairpins.[6,7] However in the Trp Pocket peptides the upfield shifting is more dramatic with the additional tryptophan side chain.

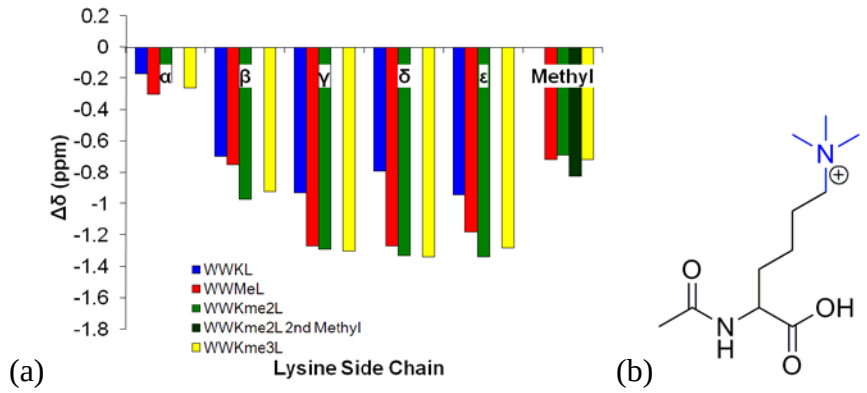

Figure 3.4. (a)Side-chain chemical shifts of lysine and methylated states of the Trp pocket series relative to random coil values. Conditions: 293 K, 50 mM sodium acetate-d_4, pH 4.0 (uncorrected), referenced to DSS. (b) Lysine side chain protons (R = H or Me, accordingly).

NOEs were obtained for the Trp Pocket series to confirm that these β-hairpins are forming in the correct register and to investigate how the lysine and its methylated analogs interact with the two tryptophans on the opposite strand. NOEs were observed between the Hα of Trp2 and Leu11, and between the Hα of Trp4 and Lys9 for all of the peptides in the Trp Pocket series indicating that a β-hairpin is forming in the correct register. The number of NOEs between the NHB residues increases as the number of methyl groups on the lysine increases indicating that as methylation of the lysine is increased a more rigid β-hairpin is formed (Figure 3.4). Interestingly, two unique methyl groups are observed for dimethyllysine in **WWKme2L**. NOEs indicate that they are oriented towards specific tryptophan indole rings suggesting that KMe2 has a rigid orientation within the tryptophan pocket (Figure 3.4c).

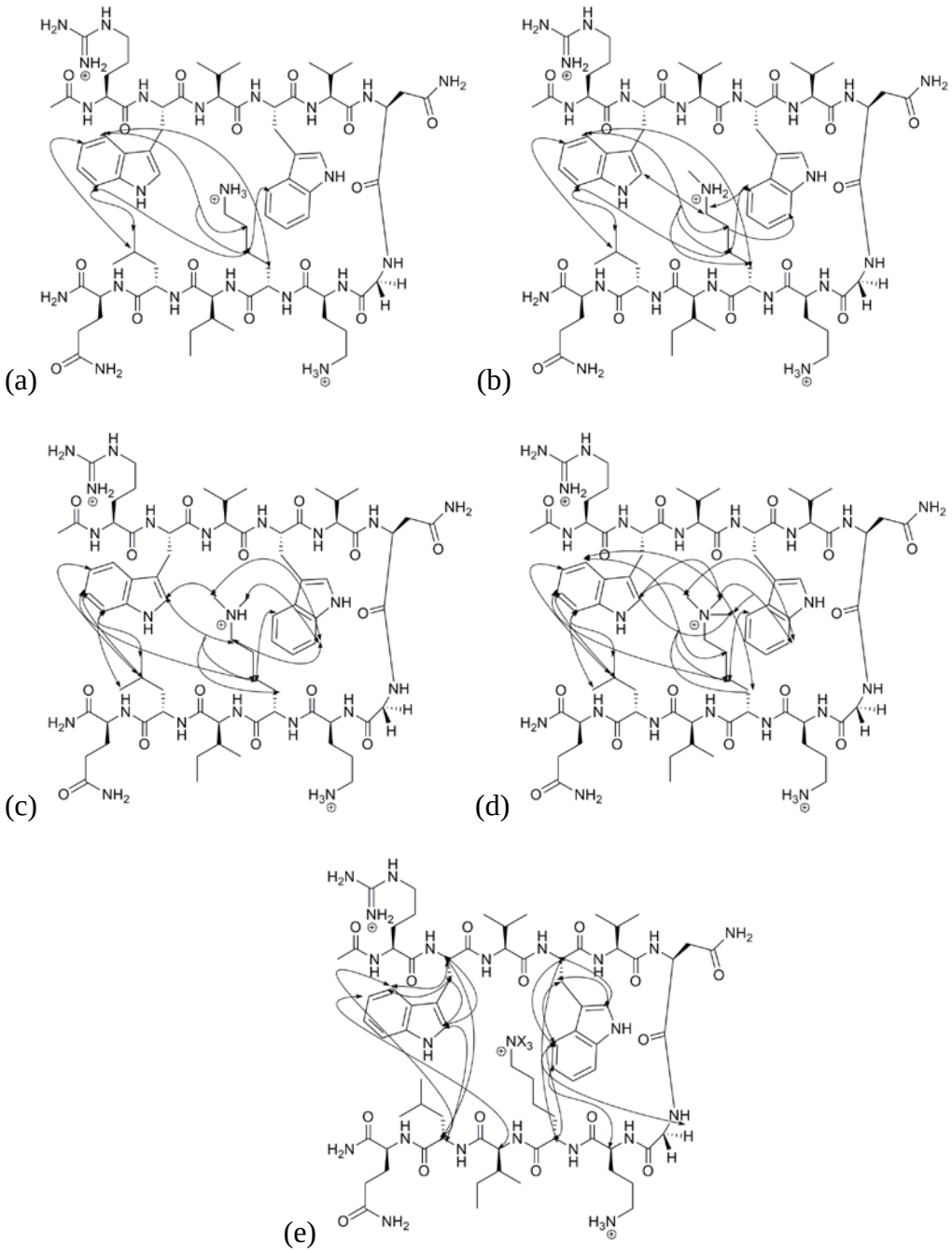

Figure 3.5. NOEs of side-chain side-chain interactions between cross strand residues on the NHB face in (a) **WWKL**, (b) **WWKmeL**, (c) **WWKme2L**, and (d) **WWKme3L.** (e) NOEs observed for all Trp Pocket peptides where X = H for lysine, X=CH_3, H,H for monomethylated lysine, X=CH_3, CH_3, H for dimethylated lysine, and X = CH_3 for trimethylated lysine.

c.) Thermal Denaturation Studies. To determine the thermodynamic parameters for folding of the Trp pocket series of peptides, thermal denaturations were performed by following the change in Gly splitting with temperature. A plot of the fraction folded versus temperature is given in Figure 3.6. Surprisingly, all of the hairpins are well folded even at 350 K showing that these peptides are very thermally stable. Nonetheless, folding is still fast on the NMR timescale. **WWKMe3L** is the most thermally stable of all the variants and is still ~94% folded at 350 K. This hairpin also experiences some slight cold denaturation which is indicative of some contribution of a hydrophobic driving force.[12] **WWKMe2L** is the next most thermally stable hairpin and also exhibits slight cold denaturation. Cold denaturation is not observed for **WWKMeL** or **WWKL**.

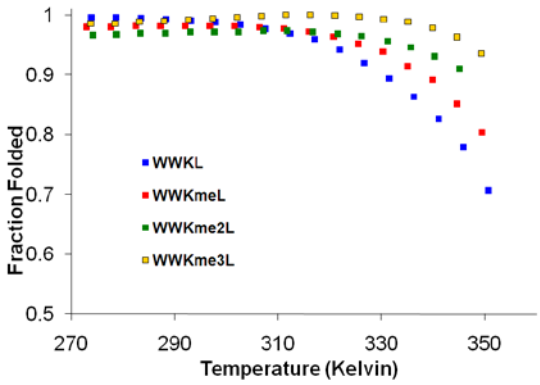

Figure 3.6. Thermal Denaturation of Trp pocket Series**.** Fraction folded was calculated from extent of Gly splitting. Conditions: 50 mM sodium acetate-d_4, pH 4.0 (uncorrected), referenced to DSS.

Thermodynamic parameters for folding were obtained for **WWKMeL** and **WWKL** by nonlinear fitting of the data using equation 3 (see Experimental Section) and are given in Table 3.2. Since **WWKme2L** and **WWKme3L** are well folded even at high temperatures we were unable to fit the thermal denaturation data. **WWKL** has a highly favorable enthalpic component for folding but also has a fairly high entropic penalty for folding as compared to

[12] Hughes, R. M.; Waters, M. L. *J Am Chem Soc* **2006**, *128*, 12735-12742.

the previously reported **WK** peptide, which has only a single Trp-Lys interaction.[5] **WWKMeL** has a weaker enthalpic driving force for folding than **WWKL** but also has smaller entropic penalty. The same trend was observed in the **WKMe$_n$** series of peptides reported previously.[6,7] The reduced enthalpic driving force upon methylation has been explained by the distribution of positive charge on the methylated lysine over a larger surface area, whereas the decreased entropic penalty resulting from Lys methylation has been attributed to the increased hydrophobicity of the methylated Lys, which results in an decreased entropic penalty when it is removed from aqueous solution upon folding.

Table 3.2. Thermodynamic Parameters for Folding at 298 K for **WWKL** and **WWKMeL** peptides. Error in parentheses determined from fit of plot. Conditions: 50 mM sodium acetate-d_4, pH 4.0 (uncorrected), referenced to DSS.

Peptide	ΔH° kcal/mol	ΔS° cal/mol K	ΔCp° cal/mol K
WWKL	-10.9 (±0.8)	-28 (±3)	-100 (±21)
WWKMeL	-2.8 (±0.2)	-1.6 (±0.7)	-311 (±8)

d.) Chemical Denaturation of WWKme3L. Since **WWKme3L** peptide is so thermally stable, chemical denaturation experiments were also performed on this peptide. Initially tryptophan fluorescence was monitored at varying concentrations of GdnHCl, however no appreciable change was observed in this system. Far-UV CD analysis revealed that little change was occurring in the global structure of the peptide even in 6 M GdnHCl (see Experimental Section). The structure of **WWKme3L** appears to be resistant to chemical denaturation at high concentrations of GdnHCl, so we performed a thermal denaturation monitored by CD in the presence of a chemical denaturant (Figure 3.7a). Due to error

generated by increasing absorbance in the β-sheet region of the CD spectra (210-215 nm) as the concentration of GdnHCl is increased, we switched to using urea as a denaturant. The co-chemical thermal denaturation experiment revealed a loss of β-sheet structure as the temperature was increased (Figure 3.7). This experiment further demonstrates how structurally stable **WWKme3L** peptide truly is, requiring both a chemical denaturant and high temperatures to observe unfolding.

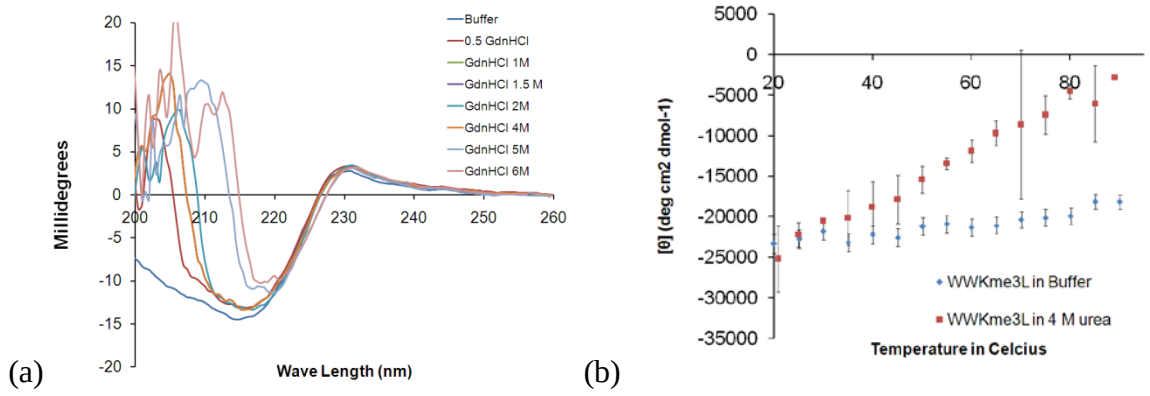

Figure 3.7. (**a)** Far-UV CD spectra of **WWKme3L** in pH 7.0 buffer with varying concentrations of GdnHCl at 25°C. **(b)**Thermal Melt of **WWKme3L** monitored at 215 nm by CD. Error bars obtained through treatment of the raw data though a smoothing function provided in the Pistar software. Conditions: 10 mM sodium phosphate buffer pH 7.0 in the presence of 4M Urea (red) or with no denaturant (blue). The characteristic minimum for β-sheet CD spectra was observed at 215 nm wavelength for the **WWKme3L** peptide.

e.) Contributions of Trp2 and Trp4. Because tryptophan has the most favorable β-sheet propensity of any of the twenty natural amino acids[13], the enhanced stability of the tryptophan pocket hairpins relative to those with a single tryptophan cannot solely be attributed to increased favorable side chain-side chain interactions. To assess whether the interaction of lysine 9 with tryptophans at both position 2 and 4 was significantly contributing to the high stability of the Trp Pocket peptides, individual double mutant cycles

[13] Cochran, A. G.; Tong, R. T.; Starovasnik, M. A.; Park, E. J.; McDowell, R. S.; Theaker, J. E.; Skelton, N. J. *J Am Chem Soc* **2001**, *123*, 625-632.

were performed.[14,15] Double mutant cycles isolate the interaction energy of two residues by mutating each individual residue, but also accounting for unintended changes to stability by comparison to the double mutant, yielding the ΔG for the interaction of interest. For the interaction between lateral cross strand residues, tryptotphan 4 was replaced with alanine and lysine 9 was replaced with serine.[16] The cross-stand Trp4-Lys9 interaction was calculated to be -1.1 kcal/mol. For the diagonal lysine-tryptophan interaction, tryptophan 2 was replaced with alanine and lysine 9 with serine. The diagonal interaction was also determined to be -1.0 kcal/mol. Because WWKL is so stable, there is an inherently large error in calculating its free energy of folding (ie, 99% folded results in a stability of -2.67 kcal/mol, whereas 96% folded gives -1.85 kcal/mol). Thus, the absolute values from the double mutant cycles are not meaningful. Nonetheless, because the error in the energetic stability of **WWKL** is common to both double mutant cycles, the relative energies of the lateral and diagonal Trp-Lys interactions are meaningful. These results indicate that the interaction energy is equivalent despite differences in geometry.

Table 3.3. Fraction folded and ΔG values of single and double mutants. Conditions 293 K, 50 mM sodium acetate-d_4, pH 4.0 (uncorrected), referenced to DSS.

Peptide	Fraction Folded (Gly)	ΔG (kcal/mol)	ΔΔG (kcal/mol)
WWKL	0.96[a] ± 0.09	-1.85	
AWKL	0.54 ± 0.01	-0.09	
WWSL	0.74 ± 0.01	-0.61	
AWSL	0.64± 0.01	0.07	-1.1 ± 0.8 (W2-K9)
WAKL	0.37± 0.01	0.31	
WASL	0.27± 0.02	0.58	-1.0 ± 0.8 (W4-K9)

(a) The fraction folded for this peptide was determined from the Hα chemical shifts.

[14] Tatko, C. D.; Waters, M. L. *Protein Sci* **2003**, *12*, 2443-2452.

[15] Tatko, C. D.; Waters, M. L. *Org Lett* **2004**, *6*, 3969-3972.

[16] Espinosa, J. F.; Munoz, V.; Gellman, S. H. *J Mol Biol* **2001**, *306*, 397-402.

iii. Conclusion

We have utilized a binding motif found in a native protein-protein interaction to design an extremely well folded β-hairpin. This system exploits the high β-sheet propensity of Trp in conjunction with favorable and selective cation-π interactions between Trp and Lys or methylated Lys to give the most thermally stable designed hairpin peptides currently reported. The interaction between the lysine and the tryptophan pocket is comparable to previously reported tryptophan-lysine and N-methylated lysine interactions in β-hairpins and a similar trend is observed with an increased stability as N-methylation is increased.[6,7] The high stability of the **WWKL** β-hairpin peptides may be amenable to other applications such as peptide antibiotics where highly structured β-hairpin peptides are required that are usually cyclized to stabilize hairpin formation.[17]

B. Tryptophan pocket variant with alanine and glycine

i. Introduction

As discussed in section A we have shown that introduction of tryptophan cleft motif greatly increases β-hairpin stability structure through enhanced interaction with cross-strand lysine and methylated lysine. Since the tryptophan cleft motif design was based on proteins that bind to methylated lysine residues in histone proteins, we sought to investigate the potential of tryptophan pocket peptides to bind methyl ammonium species intermolecularly. Not only will receptors for methylated lysine further our understanding of this important intermolecular interaction, but will provide invaluable tools for further study of the complex "histone code". Antibodies currently exist for the detection of site specific lysine

[17] Lai, J. R.; Huck, B. R.; Weisblum, B.; Gellman, S. H. *Biochemistry* **2002**, *41*, 12835-12842.

methylation, but are influenced by neighboring posttranslational modifications.[18] Other draw backs to the use of antibodies are they are only useful for *in vitro* detection, they are sensitive to freeze-thaw cycles, and they take a significant amount of time to generate. A peptide receptor system is an attractive strategy for methylated lysine recognition because peptides are easily synthesized. They also have a wide variety of functionality that can exceed canonical amino acids and the design elements for structured systems are becoming more accessible.

To allow for interaction of non-covalently linked quaternary amines the Trp pocket sequence was redesigned with either alanine or glycine at position 9 (Figure 3.8a). By replacing the lysine residue that interacts with the cross strand tryptophan cleft with residue that is too short to fill the aromatic cleft we hope to create a suitable binding pocket similar to what is observed in methyl-lysine binding proteins. It is expected that incorporation of alanine and glycine at position 9 will result in a less stable hairpin structure due to low β-sheet propensity of these residues as well as loss of favorable side chain-side chain and may even unfold the hairpin completely. It is also possible that the hairpin structure will reconstitute when bound to a quaternary amines. Therefore, the structures of redesigned trp pocket peptides, **WWAL** and **WWGL,** were investigated with or without the presence of methyl ammonium species.

[18] Kouzarides, T. *Cell* **2007**, *128*, 693-705.

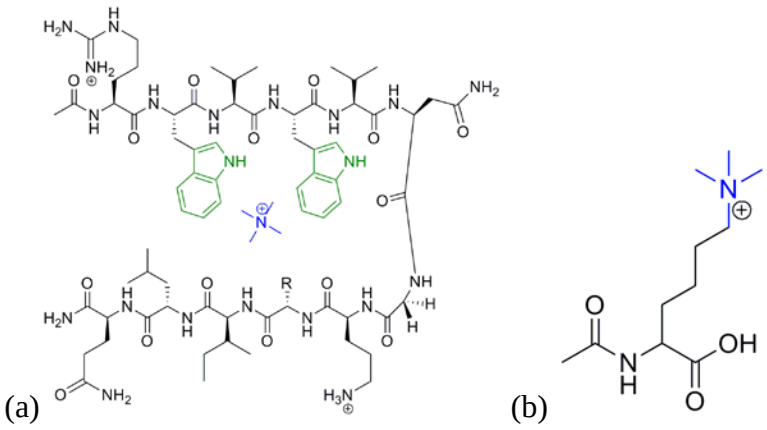

Figure 3.8. (a) Variant tryptophan pocket peptides WWAL and WWGL (R = Me or H, accordingly). Tetramethyl ammonium is shown in blue predicted to bind between the two tryptophans. (**b)** Aceylated trimethyl lysine.

ii. Results and Discussion.

a.) Binding studies with Tetramethyl ammonium and Trimethylated Lysine. To assess if **WWAL** or **WWGL** could bind quaternary amines, NMR binding experiments were attempted. NMR spectra of 1mM **WWAL** in the presence of 1 mM or 10 mM tetramethyl ammionium iodide $(CH_3)_4NI$ were compared to control spectra of either 1mM **WWAL** or 1mM $(CH_3)_4NI$. If the **WWAL** peptide is binding to $(CH_3)_4NI$ through a tryptophan cleft, upfield chemical shifting of methyl groups of $(CH_3)_4NI$ are expected. It is also possible that binding could cause conformational changes in the peptide structure resulting in perturbation of chemical shifts in the peptide. However no discernable alterations in the chemical shifts were observed in **WWAL** or $(CH_3)_4NI$ when mixed in a 1:1 or 1:10 ratio indicating that no binding was occurring. A similar NMR binding experiment with **WWGL** was conducted with $(CH_3)_4NI$ but yielded the same results.

We next tested Ac-Kme3 (Figure 3.8b) as a potential ligand for the tryptophan cleft in the **WWAL** peptide. Ac-Kme3 acts as a better model ligand for a modified histone tail and the additional alkyl chain may provide more favorable contacts to induce a binding event

with the peptide. NMR binding experiment with 1mM **WWAL** and 1mM Ac-Kme3 yielded no detectable change in the chemical shifts of either compounds, again indicating no binding was occurring. It became evident that binding using this design was not feasible, possibly due to the formation of peptide structures with non-optimal geometry of the tryptophan residues for external interactions. Further NMR characterization of these peptides was warranted to investigate what, if any, structures they are forming.

b.) NMR structure characterization of WWAL and WWGL. Analysis of the Hα shifts from random coil indicated that **WWAL** was forming a β-hairpin structure with significant downfield shifting for residues composing β-sheet segments, with the exception Alanine 9 and Leu 11 (Figure 3.9a). Upfield shifting of these residues is expected due to electronic shielding from the cross strand tryptophans as was seen in the Trp pocket peptides in section A. Amide backbone chemical shifts of **WWAL** further confirmed hairpin formation with significant downfield shifting of the hydrogen bonded residues (Arg 1, Val 3, Val 5, Ile 10, Gln 12) and a large downfield shift of Asn 6 indicating type I' turn formation (Figure 3.9b).

Analysis of Hα chemical shifts for **WWGL** revealed a pattern that did fit with the predicted β-sheet structure (Figure 3.9a). Most of the residues had minimal Hα downfield shifting with the exception of Trp 2, Trp 4, and Asn 6. Downfield shifting of the Hα of Asn 6 is a good indication that a type I' turn is not forming because this hydrogen is typically upfield shifted in the turn and is seen in all the previously examined trp pocket peptides. However a large glycine splitting is observed in Gly 7 which indicates that some structure is forming. We speculate that some alternative loop structure is forming in WWGL that is not β-hairpin like.

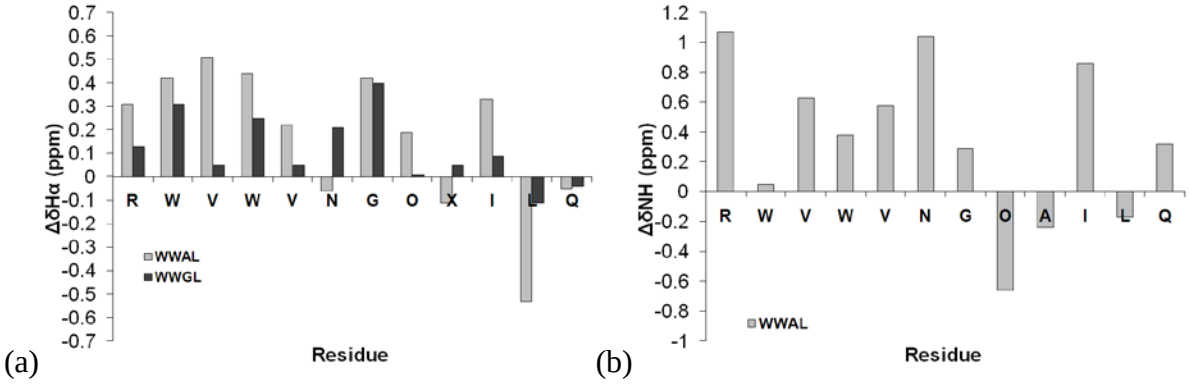

Figure 3.9 (a) Hα chemical shift differences from random coil controls for WWAL (Light Gray) where residue X = Ala, and WWGL (Dark Gray) where residue X = Gly. The Gly bars reflect the Hα separation of the two diastereotopic Hα of Gly in the hairpin. (b) Backbone amide shift differences from random coil control for WWAL. Conditions 293 K, 50 mM sodium acetate-d_4, pH 4.0 (uncorrected), referenced to DSS.

Quantification of fraction folded for **WWAL** using the methods described in the experimental showed that **WWAL** was approximately 85% folded with good agreement between glycine splitting and Hα shifts (Table 3.4). We also attempted to fit Hα shift data to determine fraction folded for **WWGL** (Table 3.4) which indicated low hairpin formation as predicted form general downfield shift of the Hαs. Since this sequence does not appear to form a β-hairpin structure as indicated by Hα shifts and did not bind to external quaternary amines, no further analysis of this structure was conducted.

Table 3.4 Fraction folded for **WWAL** and **WWGL**. Conditions: 293 K, 50 mM sodium acetate-d_4, pH 4.0 (uncorrected), referenced to DSS.

Peptides	Fraction Folded (Gly)[a]	Fraction Folded (Hα) [b]
WWAL	0.89 (±0.02)	0.85 (±0.03)
WWGL	N/A	0.12 (±0.08)[c]

(a) Error determined by chemical shift accuracy on NMR spectrometer. (b) Average of the Hα values from Val3, Val5, Orn8, and Ile10. The standard deviation is in parentheses. (c) Determined using cyclic WWAL as fully folded control.

NOEs were obtained for **WWAL** to garner information about its β-hairpin structure (Figure 3.10). Back bone-back bone and side chain-back bone NOEs (Figure 3.10b) are very similar to what was observed in the trp pocket peptides of section A indicating that the same general β-hairpin conformation was forming. Side chain-side chain NOEs between the methyl side chain of Ala 9 and the indole ring of Trp 4 and Trp 2 were observed (Figure 3.10a). These NOE's along with a significant upfield shift of the methyl hydrogens of Ala 9 from random coil (Δ -0.83 ppm) suggest that this methyl group is packing against the cross strand tryptophans.

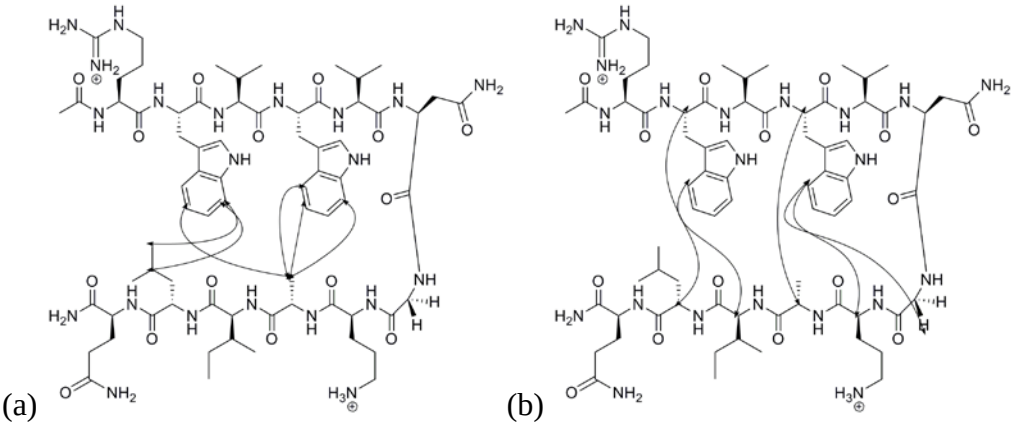

Figure 3.10 (a) NOEs of cross strand side chain-side chain interaction for **WWAL**. (b) NOEs cross strand Backbone-backbone and sidechain-backbone interactions of **WWAL**.

c.) Thermal denaturation study. To determine the thermodynamic parameters for folding of the **WWAL** peptide, thermal denaturations were performed by following the change in Gly splitting with temperature. A plot of the fraction folded versus temperature is given in Figure 3.11. As expected from initial fraction folded data the **WWAL** peptide is less thermally stable than the previous Trp pocket peptides. Alanine has a low β-sheet propensity so it is expected that it will destabilize the hairpin fold relative to amino acid with higher sheet propensity. Ala 9 is also much shorter than lysine and as seen with the NOE data,

makes a few number of favorable contacts with the cross strand tryptophan thus making the hairpin less thermally stable as well.

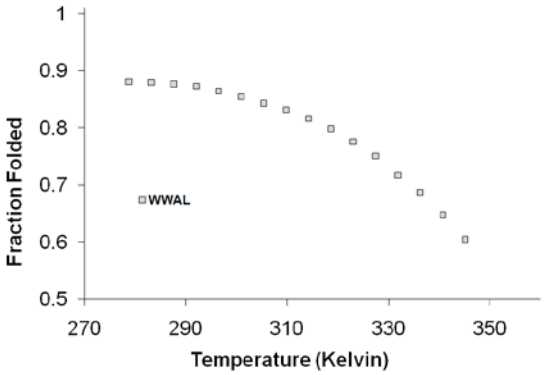

Figure 3.11. Thermal Denaturation of **WWAL.** Fraction folded was calculated from extent of Gly splitting. Conditions: 50 mM sodium acetate-d_4, pH 4.0 (uncorrected), referenced to DSS.

Thermodynamic parameters for folding were obtained for **WWAL** by nonlinear fitting of the data using equation 3 (see Experimental Section) and are compared to **WWKL** in Table 3.5. The Ala substitution results in shift in driving forces for hairpin formation when compared with **WWKL**. The **WWAL** hairpin has more favorable entropic component and a more negative $\Delta Cp°$ than **WWKL** consistent with an increase in hydrophobic clustering during folding. There is also a significant lose in an enthalpic driving force which can be contributed to the loss of a favorable cation-π interaction. In all the thermal dynamic parameters indicate that there is a significantly weaker driving force for folding.

Table 3.5. Comparison of Thermodynamic Parameters for Folding at 298 K for **WWKL** and **WWAL** peptides. Error in parentheses determined from fit of plot. Conditions: 50 mM sodium acetate-d_4, pH 4.0 (uncorrected), referenced to DSS.

Peptide	ΔH° kcal/mol	ΔS° cal/mol K	ΔCp° cal/mol K
WWKL	-10.9 (±0.8)	-28 (±3)	-100 (±21)
WWAL	-2.78 (±0.03)	-5.6 (±0.1)	-146 (±2)

iii. Conclusion

Although the redesigned **WWAL** and **WWGL** peptides did not show any interaction with quaternary ammoniums, some interesting β-hairpin design features of the Trp pocket sequence were elucidated. A stark contrast between the structures formed with a singular substitution at position 9 is observed. The **WWAL** hairpin is well folded in solution but with a different geometry of tryptophan packing to accommodate Ala 9 when compared to **WWKL.** However by removing a single methyl unit at this position there is a complete loss of β-hairpin formation as was seen with **WWGL**. It seems that placing a flexible Gly residue at position 9 disrupts the nucleation of the hairpin fold, potentially by making alternative structures more accessible, such as larger loop like configuration or a turn type that doesn't promote β-sheet. The information obtained from this study is significant in furthering our understanding secondary structure design and will undoubtedly be useful with future β-hairpin design.

C. Alternative tryptophan pocket peptides.

i. Introduction.

Since the WWKL peptide was highly stabilized and WWAL peptide was well folded in solution we wanted to further explore the robustness of this peptide sequence. Thus a variety of alternative sequences where investigated keeping with the design model of aromatic cleft motif with interaction to a cationic species.

(a) Arginine interaction with the Tryptophan pocket. Arginine is another cationic residue that is often observed in protein structures and protein-protein interactions, packing favorably with aromatic residues.[19] Previous studies have shown that a favorable cation-pi interaction is observed between a cross strand diagonal cross strand tryptophan-arginine pair in a β-hairpin peptide.[12,14] This hairpin was more stable than its tryptophan-lysine counter part. Thus it is likely that replacing the lysine residue in the WWKL peptide with an arginine will result in a more stabilized β-hairpin structure through enhanced interaction between the guanidinium group and the aromatic tryptophan cleft. To study this interaction the sequence Ac-RWVWVNGKRILQ-NH2 was designed with Arg at position 9 which is oriented to interact with cross strand tryptophan cleft (Figure 3.12a).

(b) Alternative residues at position 11. The leucine at position 11 in the Trp pocket peptides packs against tryptophan at position 2 through favorable van der Waals and hydrophobic interactions. We sought to vary the residue at position 11 to probe the effect on hairpin formation with residues that have alternative cross strand interactions with Trp 2. The

[19] (a) Burley, S. K.; Petsko, G. A. *Febs Lett* **1986**, *203*, 139-143. (b) Flocco, M. M.; Mowbray, S. L. *J Mol Biol* **1994**, *235*, 709-717. (c) Mitchell, J. B. O.; Nandi, C. L.; Mcdonald, I. K.; Thornton, J. M.; Price, S. L. *J Mol Biol* **1994**, *239*, 315-331. (d) Gallivan, J. P.; Dougherty, D. A. *Proc Nat Acad Sci U.S.A.* **1999**, *96*, 9459-9464. (e) Devos, A. M.; Ultsch, M.; Kossiakoff, A. A. *Science* **1992**, *255*, 306-312.

peptide **WWKK** was designed with the sequence Ac-RWVWVNGOKIKQ-NH2 with a lysine at position 11 to investigate the effect of the addition of another potential cation-π interaction with Trp 2 (Figure 3.12b). The peptide **WWKW** was designed with the sequence Ac-RWVWVNGKKIWQ-NH2 to introduce a π-π interaction between the side chains of residues 2 and 11 (Figure 3.12c).

(c) Design of Tryptophan-Phenylalanine pocket hairpin. Of the known aromatic cage regions that bind methylated lysine only one or two tryptophan residues form these binding pockets, with the rest of sides consisting of phenylalanine or tyrosine.[20] Tryptophan residues are also rare compared to other aromatic amino acids found in proteins. Thus we wanted to explore the effect of replacing one of the Trp residues with Phe on the stability of the β-hairpin as well as the interaction with Lys 9 with the new Trp-Phe aromatic cleft. The peptide **WFKL** was designed with the sequence Ac-RWVFVNGOKILQ-NH2 for this purpose with Phe at position 4 (Figure 3.12d).

(d) Design of Alternative Tryptophan cleft. In the Trp pocket design, the two Trp residues are on the N-terminal strand of the β-hairpin, being one residue apart in sequence to orient the side chains on the NHB face. This creates an aromatic cleft in which a lysine or methylated lysine sits, and is similar to what is seen in methyl lysine binding proteins of histone tails. However, in these methyl lysine recognition domains, the residues that compose the aromatic cage are typically further apart in sequence space usually occurring on an adjacent β-strand (Figure 3.1b). To investigate the interaction of lysine and trimethylated lysine in a hairpin peptide that more closely emulates this binding cleft we designed the

[20] Adams-Cioaba, M. A.; Min, J. R. *Biochem Cell Biol* **2009**, *87*, 93-105.

GWK$_x$W peptide with the sequence : Ac-RGVWVNGKK$_x$IWQ-NH2 where x = me$_0$ or me$_3$ (Figure 3.12e).

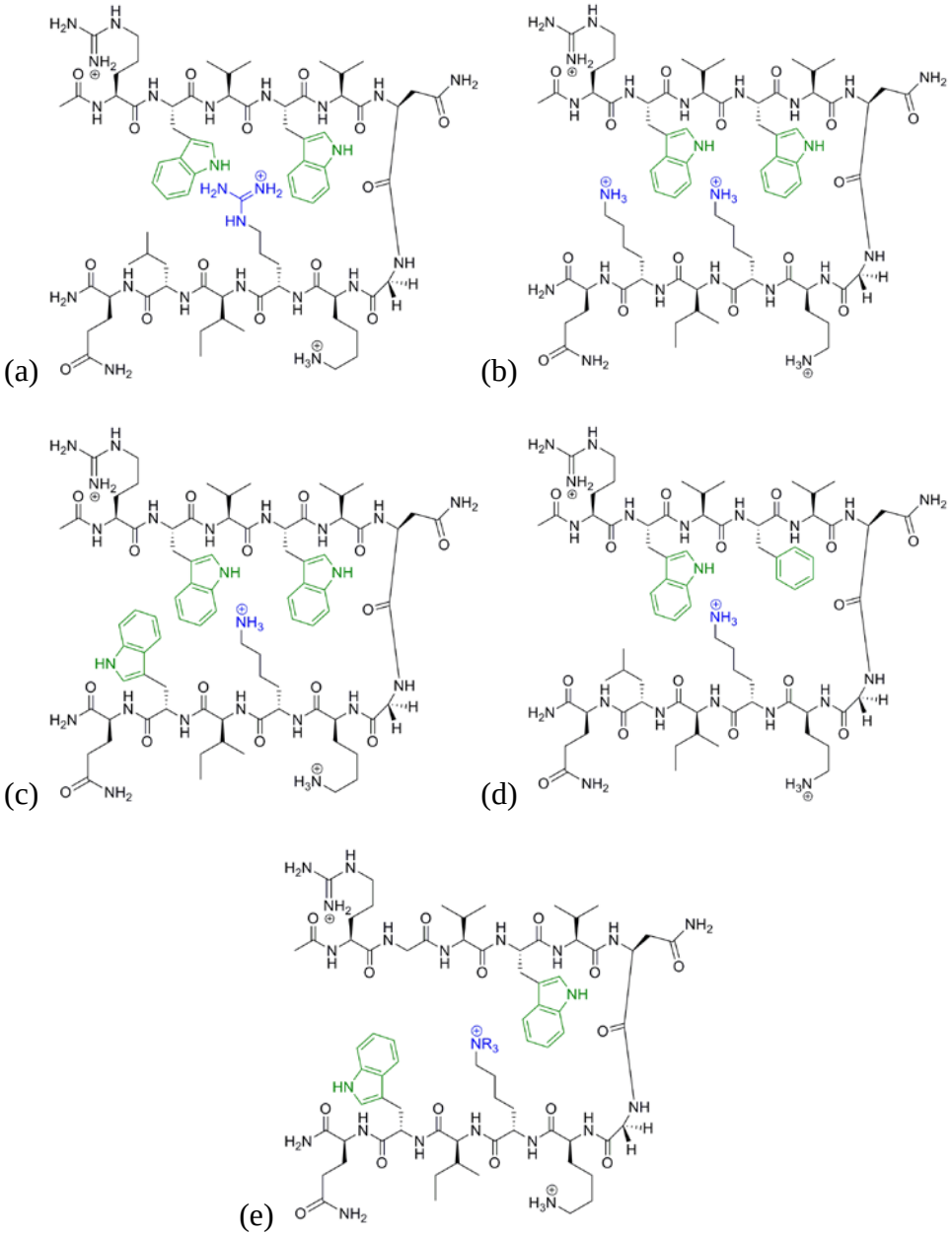

Figure 3.12. (a) **WWRL** hairpin containing arginine at position 9. (b) **WWKK** hairpin containing a lysine at position 11. (c) **WWKW** hairpin containing a tryptophan at position 11. (d) **WFKL** hairpin containing a phenylalanine at position 4. (e) **GWKG** series of peptides containing glycine at position 2, tryptophans at positions 4 and 11, and lysine or trimethylysine at position 9 (R = H or Me, accordingly).

ii. Results and Discussion.

(a) Studies on WWRL hairpin. The **WWRL** peptide was synthesized and characterized by NMR to study the effect of an alternative cationic residue in the Trp pocket sequence. Analysis of downfield chemical shifting of the Hα revealed a very similar shifting pattern as **WWKL** (Figure 3.13a). A large downfield chemical shift is observed for all residues in the β-strands except for Arg 9 and Leu 11. These residues are upfield shifted due to electronic shielding from the cross strand tryptophans. Comparison of amide backbone chemical shifts between **WWRL** and **WWKL** also shows a similar hydrogen bonding pattern, with large downfield shifts at residues Arg 1, Val 3, Val 5, Ile 10, and Gln 12 (Figure 3.13b)**.** A large downfield shift is also observed for Asn 6, which is expected for this residue in a type I' turn conformation. Taken together, the NMR chemical shift data of back bone protons for **WWRL** is consistent with the same degree of β-hairpin formation in the same register as **WWKL.** Hairpin formation is further confirmed by non sequential NOEs observed between side chain-back bone, side chain-side chain and back bone-back bone in **WWRL (**Figure 3.13c, d)**.**

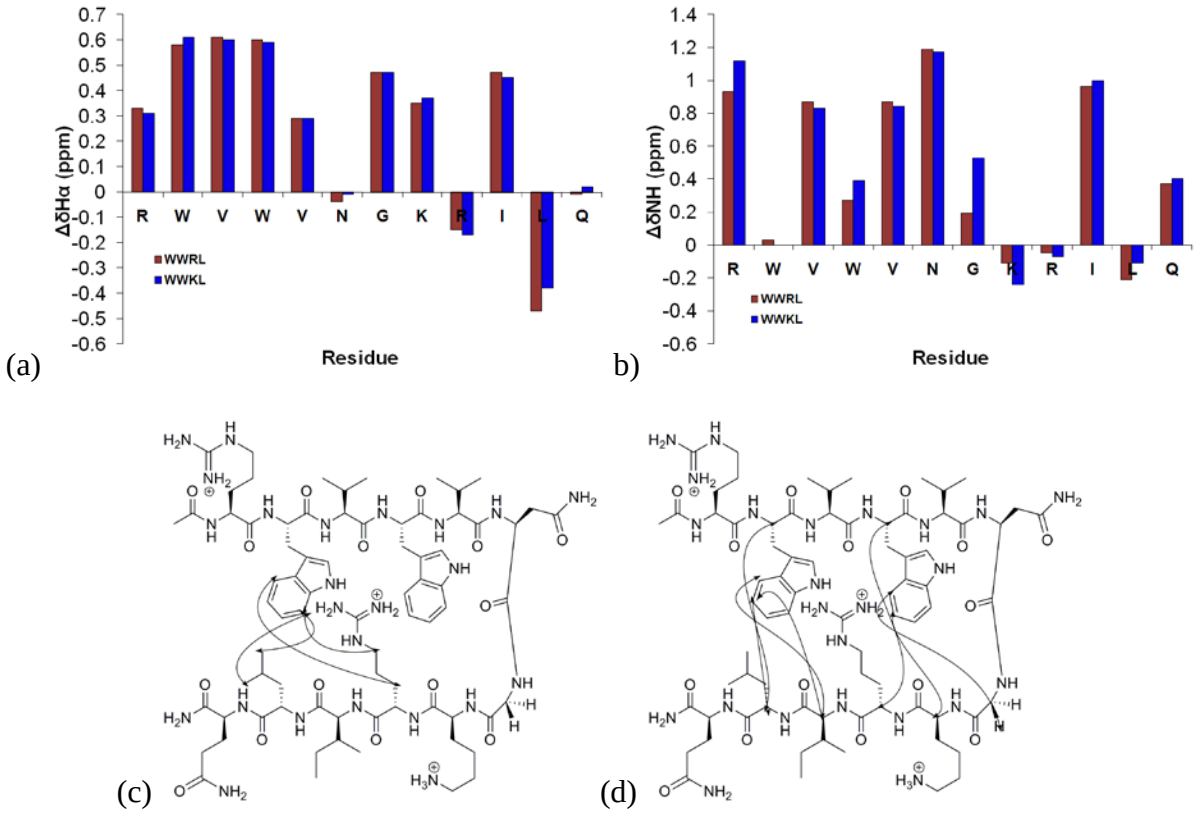

Figure 3.13. (a) **WWRL** (purple) and **WWKL** (blue) peptide Hα chemical shift differences from random coil controls. The Gly bars reflect the Hα separation in the hairpin. (b) **WWRL** (purple) and **WWKL** (blue) peptides backbone amide chemical shift differences from random coil control. (c) NOEs of cross strand side chain-side chain interaction for **WWRL**. (d) NOEs cross strand Backbone-backbone and sidechain-backbone interactions of **WWRL**. Conditions: 293 K, 50 mM sodium acetate-d_4, pH 4.0 (uncorrected), referenced to DSS.

Quantification of fraction folded for **WWRL** using the methods described in the Experimental section show that **WWRL** is approximately 94% folded with good agreement between glycine splitting and Hα shifts (Table 3.6) which is comparable to what is seen with **WWKL** (96% folded).

Table 3.6. Fraction folded for Alternative Trp Pocket peptides. Conditions: 293 K, 50 mM sodium acetate-d_4, pH 4.0 (uncorrected), referenced to DSS.

Peptides	Fraction Folded (Gly)[a]	Fraction Folded (Hα)[b]
WWKL	≥ 0.99 (±0.02)	0.96 (±0.09)
WWRL	0.97 (±0.02)	0.94 (±0.03)
WWKK	0.93 (±0.02)	0.89 (±0.03)
WWKW	≥ 0.99 (±0.02)	≥ 0.99 (±0.06)
WFKL	0.91 (±0.02)	0.85 (±0.09)
GWKW	0.54 (±0.02)	0.50 (±0.10)
GWKme3W	0.60 (±0.02)	0.54 (±0.10)

(a) Error determined by chemical shift accuracy on NMR spectrometer. (b) Average of the Hα values from Val3, Val5, Orn8, and Ile10. The standard deviation is in parentheses.

Interaction between the Arg 9 and the tryptophan cleft was also observed via the degree of upfield shifting of the Arg side chain from random coil (Figure 3.14). When compared to Lys 9 of **WWKL** there is a distinction between the extent of upfield shifting between side chain residues. This is an indication of different packing geometries between the Arg and the tryptophan cleft as compared to Lys. NOE data shows a distinct cross peaks between the β and δ methlenes of Arg 9 and the indole ring Trp 2, but no side chains cross peaks are observed with Trp 4 (Figure 3.13c). In a similar hairpin system where a Glu was at position 4, Arg 9 was shown to be packing in parallel stacking conformation with the indole ring of Trp 2 commonly seen in protein crystal structures.[14] It is possible that Arg 9 in **WWRL** is primarily stacking in a similar conformation with Trp 2, and any interaction with Trp 4 is more dynamic.

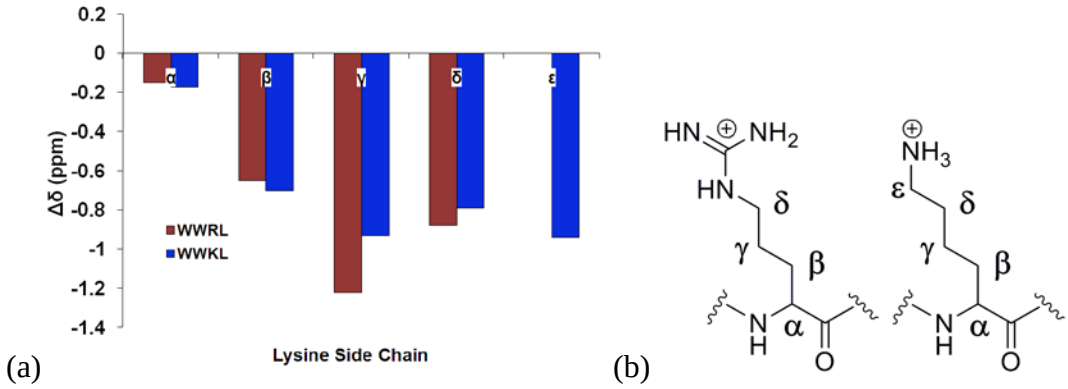

Figure 3.14. (a) Comparison of residue 9 side-chain chemical shifts for **WWRL** (purple) and **WWKL** (blue) relative to random coil values. Conditions: 293 K, 50 mM sodium acetate-d_4, pH 4.0 (uncorrected), referenced to DSS. (b) Lysine and Arginine side chain protons.

To gain thermodynamic information about the folding of **WWRL**, thermal denturations were preformed by following the change in Gly splitting with temperature (see Figure 3.46 in the Experimental Seciton). Slight cold denaturation is observed in **WWRL** similar to what was seen in the methylated Trp pocket peptides discussed in section A. Cold denaturation is an indication of some degree of hydrophobic driving force in structure folding.[12] Non-linear fitting of fraction folded verses temperature data of **WWRL** using equation 3 (see Experimental Section) yield thermal dynamic parameters for ΔH°, ΔS°, and ΔCp° for folding (Table 3.7). The incorporation of Arg at position 9 has significantly decreased enthalpic component to folding when compared to lysine. This is consistent with less favorable contact observed with Arginine and the Trp pocket. However the entropic penalty for **WWRL** folding is practically zero whereas in **WWKL** it is substantial (-28 cal/mol K). This increase in favorable entropy may be explained by arginines ability to interact a variety of conformations within the tryptophan pocket whereas lysine can only fit distinctly in a few well defined conformations. Since the guanidinium group of arginine has a lower penalty for desolvation in water than the amine of lysine, it is conceivable that the guanidinium group of arginine will fit in larger number of conformations within the hydrophobic tryptophan pocket

whereas the amine will remain solvated and must orient lysine amine outside the pocket. Also arginine's interactions with aromatic groups can make van-der waals contacts through the delocalized-π system of the guanidium, and more electrostatic cation-π contacts, increasing potential interactions between two aromatic groups. Indeed, it seems that the folding of **WWRL** is due to more of a hydrophobic collapse with a more negative ΔCp° than **WWKL.** It appears as though arginine is making more non-specific interaction in the tryptophan cleft making the folding of **WWRL** more hydrophobic in nature, as opposed to **WWKL.** However, this loss in cation-π specificity slightly decreases the overall stability of the hairpin fold when compared to **WWKL.**

Table 3.7. Comparison of Thermodynamic Parameters for Folding at 298 K for Alternative Trp Pocket peptides. Error in parentheses determined from fit of plot. Conditions: 50 mM sodium acetate-d_4, pH 4.0 (uncorrected), referenced to DSS.

Peptide	ΔH° kcal/mol	ΔS° cal/mol K	ΔCp° cal/mol K
WWKL	-10.9 (±0.8)	-28 (±3)	-100 (±21)
WWRL	-2.3 (±0.2)	-0.7 (±0.7)	-330 (±11)
WWKK	-6.6 (±0.2)	-17.4 (±0.4)	-111 (±4)
WFKL	-4.21 (±0.06)	-9.9 (±0.2)	-141 (±3)

(b) Studies on WWKK and WWKW. The peptides **WWKK** and **WWKW** were synthesized and characterized by NMR to study the effects on the Trp pocket hairpin formation with alternative residues at position 11. This position can influence the orientation of Trp 2 and may have an impact on the aromatic pocket. Analysis of the change Hα shifting from random coil values shows well folded hairpins for both **WWKK** and **WWKW** (Table

3.6)**.** Large downfield shifting is seen in all the expected residues composing the β-strands in both peptides (Figure 3.15a). Analysis of the amide backbone chemical shift difference from random coil also indicates well folded β-hairpin formation in the proper register (Figure 3.15). When compared with backbone chemical shifts of **WWKL** both **WWKK** and **WWKW** show the same shifting pattern with the exception of residues Arg 1 and Qln 12 in the **WWKW** peptide. There is a decreased chemical shift in Arg 1 and an increase for Qln 12 suggesting the termini residues in **WWKW** are now in an alternate conformation. The upfield chemical shifting in Arg 1 is likely due to electronic shield from the cross strand indole ring of Trp 11 but may also be due to a non-β sheet orientation.

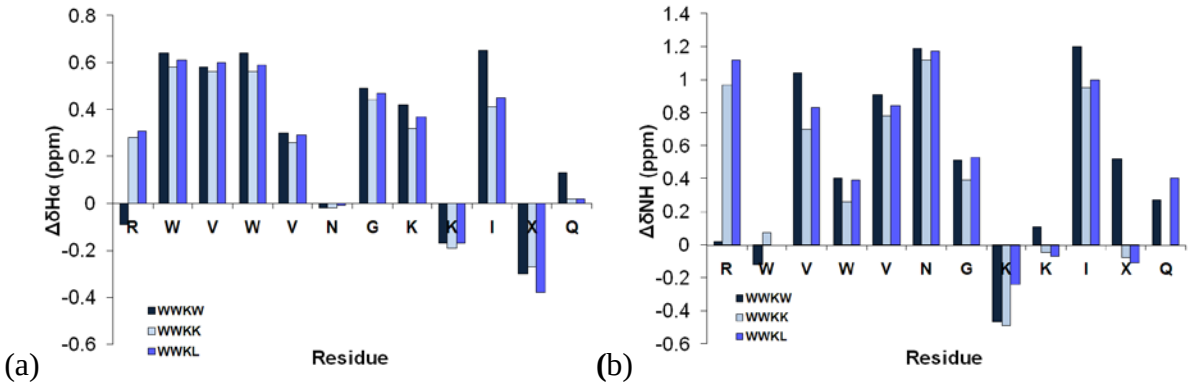

(a) (b)

Figure 3.15. (a) **WWKW (**light blue) and **WWKK** (dark blue) peptides Hα chemical shift differences from random coil controls. The Gly bars reflect the Hα separation in the hairpin. (b) **WWKW** and **WWKK** peptides backbone amide chemical shift differences from random coil control. Conditions: 293 K, 50 mM sodium acetate-d_4, pH 4.0 (uncorrected), referenced to DSS.

Observed cross strand NOEs for **WWKK** and **WWKW** confirmed proper β-hairpin formation (Figure 3.16). Interestingly NOEs between the β-methylene of Arg 1 and the indole ring of Trp 11 are observed, giving more support for twisted Arg 1 backbone conformation. The backbone chemical shift data also suggests different degrees of β-hairpin formation between the peptides where **WWKW** is the most well folded, **WWKL** is the next most folded, and **WWKK** being the least well folded of the peptides. Quantification of

fraction folded using the methods described in the experimental agrees with this observation where **WWKW** is at least 99% folded, **WWKL** is 96% folded, and **WWKK** is 90% folded with good agreement between glycine splitting and Hα shifts (Table 3.6). This trend is consistent with the relative β-sheet propensities of Trp, Leu and Lys.

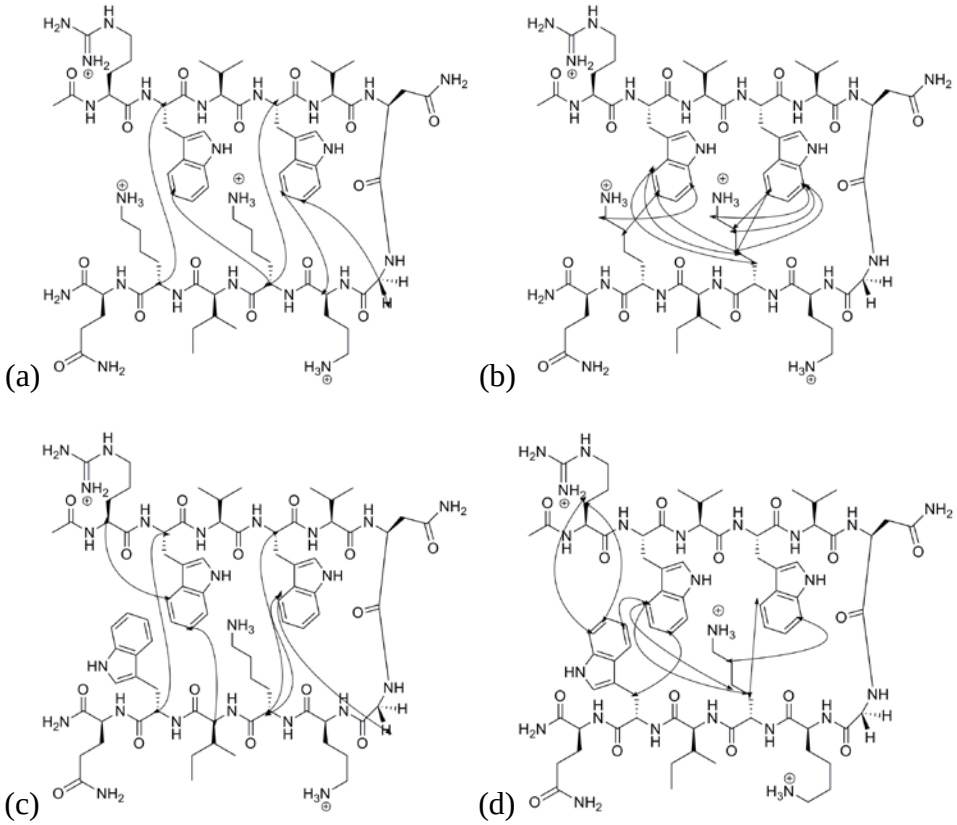

Figure 3.16. (a) NOEs cross strand Backbone-backbone and sidechain-backbone interactions of **WWKK**. (b) NOEs of cross strand side chain-side chain interaction for **WWKK**. (c) NOEs cross strand Backbone-backbone and sidechain-backbone interactions of **WWKW**. (b) NOEs of cross strand side chain-side chain interaction for **WWKW**.

Interaction between the Lys 9 in **WWKK** and **WWKW** and the tryptophan cleft was also observed via the degree of upfield shifting of the Lys side chain from random coil (Figure 3.17). When comparing the Lys 9 upfield shifting between **WWKK**, **WWKW**, and **WWKL**, the largest degree of upfield shifting is observed for **WWKK**, followed by **WWKW,** and least of all **WWKL**. A similar upfield shifting pattern is seen between

WWKW and **WWKL** with the γ, δ, and ε methylenes being the most upfield shifted with relatively little difference between the methylenes. This suggests that the tryptophan cleft on the N-terminal strand is relatively similar between the peptides. However in **WWKW**, the upfield shifting of these methylenes is slightly larger than **WWKL**. This result is consistent with the observation that **WWKW** is more folded; therefore the lysine-tryptophan cleft interaction is increased. Both Lys 9 and Lys 11 in **WWKK** interact with cross strand tryptophans and undergo a large upfield chemical. Lys 9 experiences the largest amount of upfield shifting, resulting from interaction with both Trp 2 and Trp 4. Interestingly the δ methylene of Lys 9 in **WWKK** is the most upfield shifted when compared to all of methylenes for Lys 9 in **WWKW** and **WWKL**. This upfield shifting pattern for Lys 9 in **WWKK** suggests a change in the tryptophan cleft lysine interaction. Upfield shifting of residue Lys 11 in **WWKK** is most pronounced in the γ and δ methylene group which is likely due to the respective orientations of Trp 2 and Lys 11 where the ε-methylene is not oriented into the π-cloud of Trp 2. It is evident that altering the residue at position 11 is effecting the interaction between the tryptophan cleft and lysine.

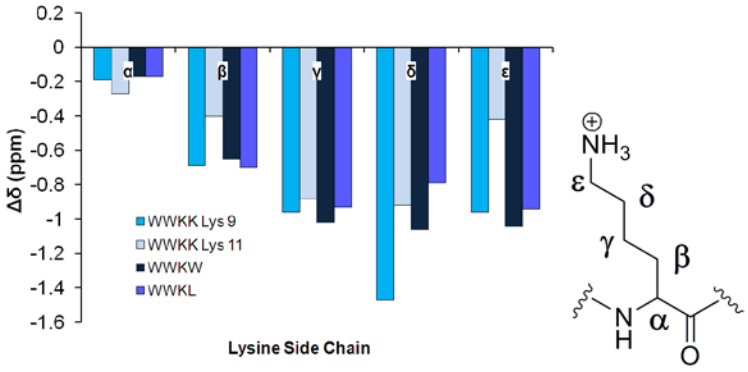

Figure 3.17 Comparison of lysine side-chain chemical shifts for **WWKK , WWKW** and **WWKL** (true blue) relative to random coil values. Conditions: 293 K, 50 mM sodium acetate-d_4, pH 4.0 (uncorrected), referenced to DSS.

To gain thermodynamic information about the folding of **WWKK** and **WWKW**, thermal denturations were preformed by following the change in Gly splitting with temperature (Table 3.7). Comparison of thermal denaturation plots of **WWKK** and **WWKW** indicate not only a difference in stability but also a difference in driving forces for folding (see Figure 3.46 in Experimental Section). Similarly to what is observed in previously discussed **WWKme2L, WWKme3L,** and **WWRL** peptides, **WWKW** experiences cold denaturation, which is evidence for a major hydrophobic component in folding. The degree of hairpin stability is also comparable to well folded **WWKme2L**, and **WWKme3L** where **WWKW** is still approximately 90% folded even at 80°C**.** Not surprisingly, the **WWKK** is less stable than **WWKL** and **WWKW** and exhibits the greatest extent of denaturation. Thermodynamic parameters for folding were obtained for **WWKK** by nonlinear fitting of the data using equation 3(see Experimental Section) and are given in Table 3.7. We were unable to obtain a fit for **WWKW** due to its high stability. Comparing the energetics of folding between **WWKL** and **WWKK** reveal little difference in the driving forces between these two systems where the ratio between $\Delta H°$ and $\Delta S°$ is relatively the same albeit the ΔG of folding for **WWKK** is less. This result suggests that the lysine at position 11 is only stabilizing the hairpin through non-specific hydrophobic packing against tryptophan 2 like leucine, which corroborates with upfield shifting data of the lysine side chain. If an additional specific cation-π interaction were occurring, the enthalpy of the system would be more favorable.

Increased stability of the **WWKW** hairpin over **WWKL** is due to a combination of factors. Tryptophan has a higher beta sheet propensity than leucine. Tryptophan also has a larger hydrophobic surface area than leucine so there is a strong drive for hydrophobic clustering and likely explains the observed cold denaturation. Tryptophan can also undergo

π-π interactions with the cross-strand tryptophan. The aromatic protons are significantly upfield shifted of Trp 11, indicating a favorable edge-face π-π interaction. This is reminiscent of the tryptophan packing observed in the highly stable Trpzip β-hairpin peptide design by Cochran and co-workers where the NHB face contained tryptophans at positions 2, 4, 9 and 11.[9] It is likely that Trp 2 and Trp 11 of **WWKW** are oriented in the same manner as Trpzip for these positions. Indeed, it may be possible to create an even more stable trp pocket than **WWKme3L** by replacing leucine 11 with tryptophan.

(c) NMR characterization of WFKL. The **WFKL** peptide was synthesized and characterized by NMR to study the implications of incorporating an alternative aromatic residue into the trp pocket sequence. Analysis of downfield chemical shifting of the Hα revealed a very similar shifting pattern as **WWKL** (Figure 3.18a). A notable difference between the Hα shifting of the two peptides is observed at Lys 9 wherein this residue is upfield shifted in **WWKL** and only slightly downfield shifted in **WFKL**. This is an indication that Phe 4 is not packing against this Hα of lysine 9 as well as Trp 4. Analysis of the backbone amide shifting from random coil indicates a β-hairpin formation with correct hydrogen bonding pattern indicated by large downfield shifting of residues Val 3, Val 5, Asn 6, Ile 10, Gln 12 (Figure 3.18b). Comparison of amide shifting to **WFKL** and **WWKL** suggests some alteration in backbone formation between the two hairpins.

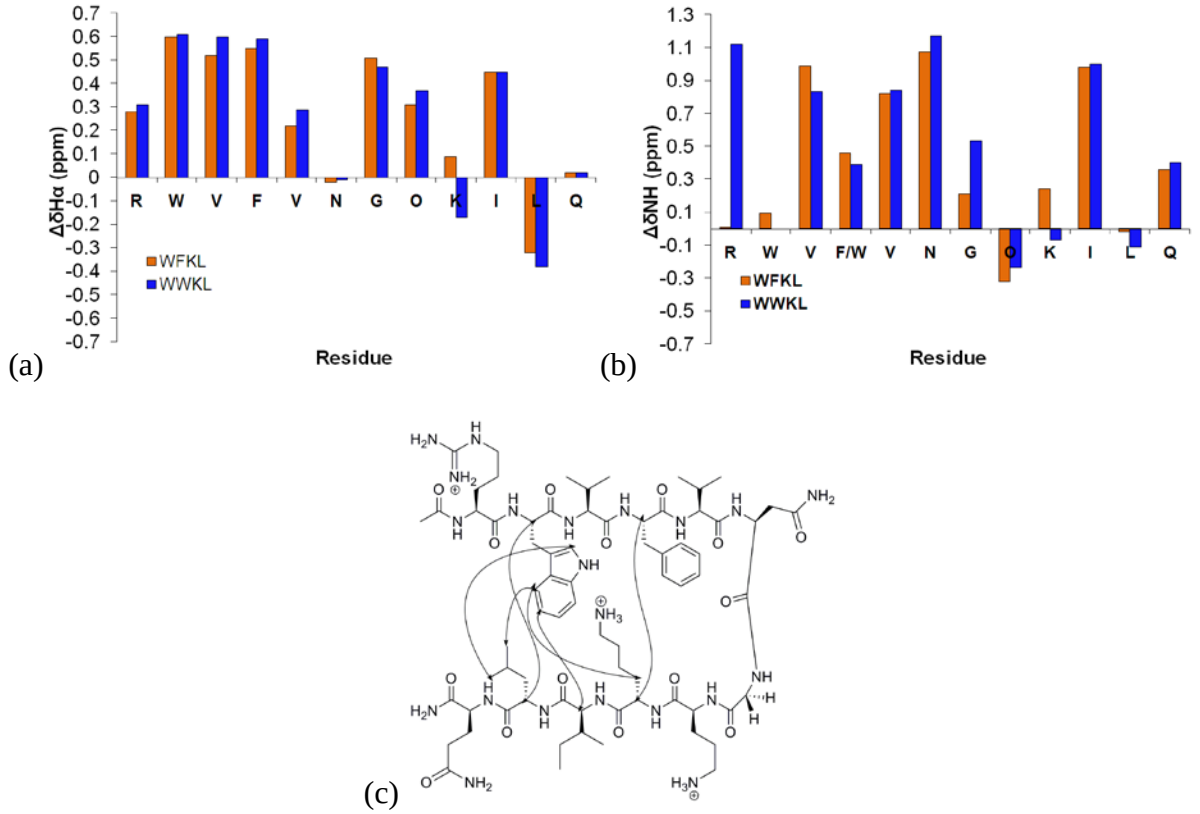

Figure 3.18. (a) **WFKL** peptide Hα chemical shift differences from random coil controls. The Gly bars reflect the Hα separation in the hairpin. (b) **WFKL** peptides backbone amide chemical shift differences from random coil control. (c) NOEs cross strand interactions of **WFKL**. Conditions: 293 K, 50 mM sodium acetate-d_4, pH 4.0 (uncorrected), referenced to DSS.

Hairpin formation was further confirmed by non sequential NOEs observed between side chain-back bone, side chain-side chain and back bone-back bone in **WFKL (**Figure 3.18c)**.** Few NOEs were identified between cross-strand residues particularly between Phe 4 and the cross strand Lys 9, Orn 8, and Gly 7 typically seen for the Trp pocket peptides. This possibly indicates a more dynamic hairpin specifically at residue 4. Quantification of fraction folded for **WFKL** using the methods described in the experimental showed that **WFKL** was approximately 91% folded by glycine splitting and 85% by Hα shifts (Table 3.6) indicating that **WFKL** is not as well folded as **WWKL** (96% folded).

Interaction between Lys 9 and the aromatic cleft was observed via upfield shifting from random coil of the lysine side chain. Comparison of Lys 9 upfield shifting data between **WWKL** and **WFKL** shows a significant difference in interaction between the two peptides (Figure 3.19). It appears that Lys 9 is primarily packing against Trp 2 and has little or no interaction with Phe 4 indicated by the sequential increase in upfield shifting along the side chain towards the terminal amine. This pattern is observed in previously reported peptides designed to study the cation-π between Trp 2 and Lys 9 [7,14].

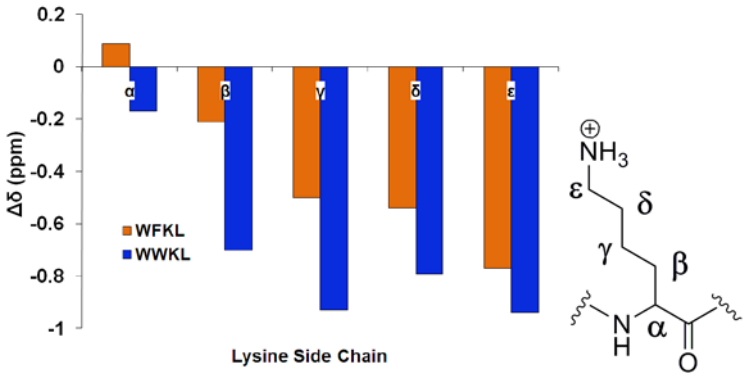

Figure 3.19. Comparison of lysine side-chain chemical shifts for **WFKL** (orange) and **WWKL** (blue) relative to random coil values. Conditions: 293 K, 50 mM sodium acetate-d_4, pH 4.0 (uncorrected), referenced to DSS.

To gain thermodynamic information about the folding of **WFKL**, a thermal denturation was preformed by following the change in Gly splitting with temperature (Figure 3.46). **WFKL** is less thermal dynamically stable **WWKL** and exhibits a higher degree of unfolding at higher temperatures. Non-linear fitting of the fraction folded verses temperature using equation 3 (see Experimental Section) revealed favorable enthalphic component and a unfavorable entropic component for folding similar to what is seen with **WWKL** albeit with a less favorable ΔG° for folding (Table 3.7).

It is apparent that replacing Trp 4 with Phe results in a less stable hairpin system. This is possiblely due to a poorer cation-π interaction between Phe and Lys which, has been observed in other hairpin systems.[14] It is also likely at position 4 phenylalanine cannot adopt an orientation that packs favorably with Lys 9, resulting in a less stable hairpin. Another factor is the lower β-sheet propensity phenylalanine compared to tryptophan. Nonetheless this phenylalanine substitution still results in highly stable β-hairpin compared to other non-trp pocket hairpin designs.

(d) NMR Characterization of GWKW series. The peptides **GWKW** and **GWKme3W** were synthesized and characterized to investigate alternative orientations of favorable tryptophan clefts in a β-hairpin sequence. In these peptides, the two Trp residues are in different strands in the i and j+2 positions, with Lys at position j. Analysis of downfield chemical shifting of the Hα protons indicate β-haripin formation with residues in the β-strand region exhibiting downfield shifting ≥ 0.1 ppm from random coil for both **GWKW** and **GWKme3W** (Figure 3.20a) albeit not to the extent of the previously discussed Trp pocket peptides. Calculation of fraction folded using the methods described in the experimental section revealed that **GWKW** is approximately 50% folded in solution while **GWKme3W** is closer to 60% folded (Table 3.6). This is consistent with an increase in hairpin stability seen peptides containing trimethylated lysine-tryptophan interactions as discussed in section A.

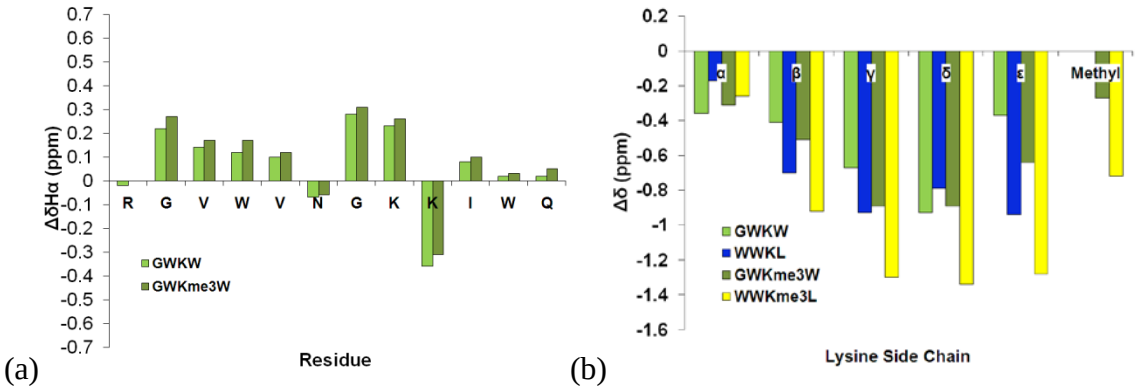

Figure 3.20. (a) **GWKW** (light green) and **GWKme3W** (dark green) peptides Hα chemical shift differences from random coil controls. The Gly bars reflect the Hα separation in the hairpin. (b) Comparison of lysine chemical shifts **GWKW, WWKL**(blue), **GWKme3W**, and **WWKme3** (yellow) relative to random coil values. Conditions: 293 K, 50 mM sodium acetate-d_4, pH 4.0 (uncorrected), referenced to DSS.

Analysis of Lys 9 interaction with the new tryptophan cleft through upfield shifting of the lysine side chain protons showed a more favorable interaction was occurring when Lys 9 is trimethylated (Figure 3.20). However, the upfield shifting observed by Lys 9 and trimethylated Lys 9 is substantial less than what is observed for **WWKL** and **WWKme3L** with the exception of δ methylene where **GWKW's** lys is greater than **WWKL's** lys**.** It is apparent that the GWKW design produces a less stable β-hairpin with a less favorable interaction between lys and the two tryptophans. Since trimethylation of Lys 9 only slightly increased its stability, no further characterization was performed on this design.

iii. Conclusion.

The survey conducted on the malleability of the Trp pocket sequence in β-hairpin formation has given us valuable insights into highly stabilized β-hairpin design. Changing the cationic residue at position 9 still results in a highly stabilized hairpin, but alters the nature of the interaction between residue 9 and the tryptophan cleft as was seen in **WWRL.** Changing the residue at position 11 also affect the degree of stability in the Trp pocket sequence by

varying the interaction between Trp 2 and residue 11 as is seen with the peptides **WWKW** and **WWKK**. Replacement of Leu 11 with Trp increases hairpin stability substantially and is the most stable unmodified natural sequence (i.e. no methylated lysine). Incorporating Lys at position 11 decreases overall hairpin stability and the data gathered does not support a substantial cation-π interaction between Lys 11 and Trp 2 as was initially intended. Replacement of Trp 4 with Phe decreases the hairpin stability as demonstrated in **WFKL** indicates that tryptophan is the most optimized residue for creating a stable hairpin system with an aromatic pocket that interacts with a cross strand lysine residue. The most stabilizing lysine or methylated lysine – tryptophan cleft interaction is achieved when the tryptophans are located at position 2 and 4 as was seen from the analysis of the **GWKW** series. Although not a complete survey of all potential variations in aromatic pocket design, the studies presented here are a good start for future de novo designed systems that are highly stabilized in water.

D. Experimental.

i. Synthesis and Purification of peptides.

Peptides were synthesized by automated solid phase peptide synthesis on an Applied Biosystems Pioneer Peptide Synthesizer using Fmoc protected amino acids on a PEG-PAL-PS resin. Mono and dimethylated Fmoc-protected lysine were purchased from AnaSpec. Activation of amino acids was performed with HBTU, HOBT in the presence of DIPEA in DMF. Deprotections were carried out in 2% DBU , 2% piperdine in DMF for approximately 10 min. Extended cycles (75 min) were used for each amino acid coupling step. All peptides where acetylated at the N-terminus with 5% acetic anhydride, 6% lutidine in DMF for 30 min. Cleavage of the peptide from the resin was performed in 95:2.5:2.5 TFA: Ethanedithiol

or Triisopropylsilane (TIPS): water for 3 h. Ethanedithiol was used as a scavenger for sulfur containing peptides. TFA was evaporated and cleavage products were precipitated with cold ether. The peptide was extracted into water and lyophilized. It was then purified by reverse phase HPLC, using a Vydac C-18 semipreparative column and a gradient of 0 to 100% B over 40 min, where solvent A was 95:5 water:acetonitrile, 0.1% TFA and solvent B was 95:5 actonitrile:water, 0.1% TFA. After purification the peptide was lyophilized to powder and identified with ESI-TOF mass spectroscopy.

ii. Cyclization of cyclic peptides.

Cyclic control peptides were cyclized by oxidizing the cysteine residues at the ends of the peptide by stirring in a 10 mM phosphate buffer (pH 7.5) in 1% DMSO solution for 9 to 12 hours. The solution was lyophilized to a powder and purified with HPLC using previously described method.

iii. Methylation of dimethyl lysine.

Peptides containing dimethyl lysine were methylated to trimethyl lysine on resin by reacting with 8 µl 1,3,4,6,7,8-Hexahydro-1-methyl-2H-pyrimide [1,2-9-] pyrimidine and 62 µl brought up to 5 ml in DMF. Reaction mixture was agitated by nitrogen bubbling under a vented septum for 5 h. Resin was washed with DMF 3x and then washed with 3x dichloromethane.

iv. NMR Spectroscopy.

NMR samples were made to a concentration of 1 mM in D_2O buffered to pD 4.0 (uncorrected) with 50 mM NaOAc-d3, 24 mM AcOH-d4, 0.5 mM DSS. Samples were analyzed on a Varian Inova 600-MHz instrument. One dimensional spectra were collected by using 32-K data points and between 8 to 128 scans using 1.5 sec presaturation. Two

dimensional total correlation spectroscopy (TOCSY) and nuclear overhauser spectroscopy (NOESY) experiments were carried out using the pulse sequences from the chempack software. Scans in the TOCSY experiments were taken 16 to 32 in the first dimension and 64 to 128 in the second dimension. Scans in the NOESY experiments were taken 32 to 64 in the first dimension and 128 to 512 in the second dimension with mixing times of 200 to 500 msec. All spectra were analyzed using standard window functions (sinbell and Gaussian with shifting). Presaturation was used to suppress the water resonance. Assignments were made by using standard methods as described by Wüthrich.[21] All experiments were run at 298.15 K.

[21] Wüthrich, K. *NMR of Proteins and Nucleic Acids*; Wiley: New York, 1986.

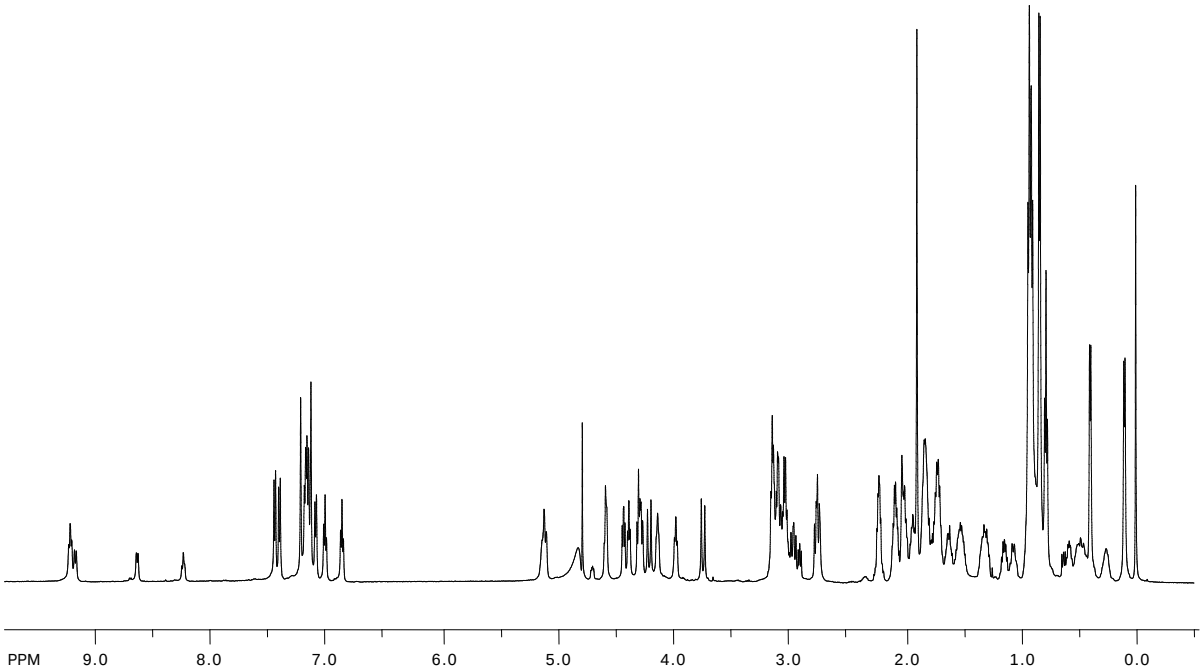

Figure 3.21 ^{1}HNMR of Peptide **WWKL:** Ac-Arg-Trp-Val-Trp-Val-Asn-Gly-Orn-Lys-Ile-Leu-Gln-NH2

Table 3.8 Proton Chemical Shift Assignments for Peptide **WWKL.**

Residue	α	β	γ	δ	ε	Amide
R	4.4	1.53	1.66	3.16		8.06
W	5.12	2.76	7.13,7.08,6.84,7.21,7.43			8.29
V	4.29	1.94	0.92			9.22
W	5.16	3.11	7.16,7.21,7.00,7.39			8.68
V	4.6	2.1	0.9			9.23
N	4.45	2.77/3.13				9.62
G	3.75,4.22					8.8
O	4.72	1.81	1.77	3.06		7.89
K	4.14	1.07	0.49	0.9/0.26	2.05	8.26
I	4.59	1.85	1.15/1.34	0.84		9.25
L	4	1.29	0.58	0.39/0.099		8.26
Q	4.32	2.02	2.24			8.73

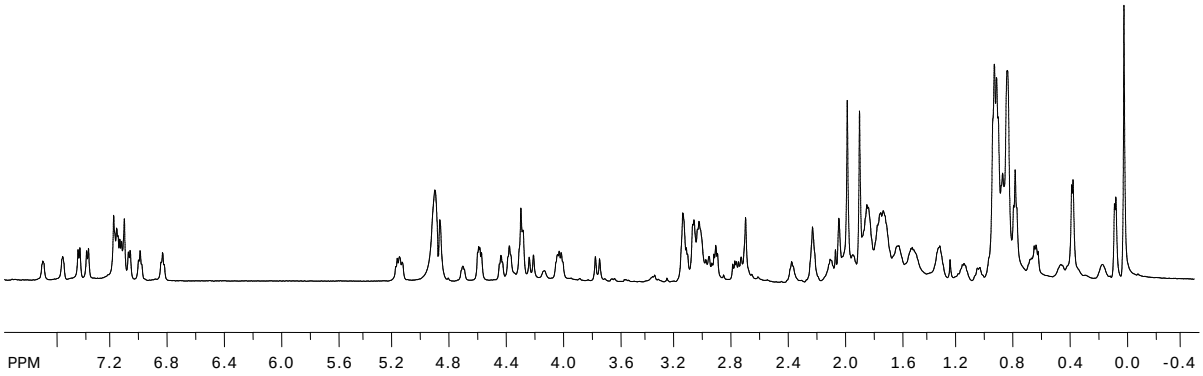

Figure 3.22 ^{1}HNMR of Peptide **WWKmeL:** Ac-Arg-Trp-Val-Trp-Val-Asn-Gly-Orn-Lys(Me)-Ile-Leu-Gln-NH2

Table 3.9 Proton Chemical Shift Assignments for Peptide **WWKmeL.**

Residue	α	β	γ	δ	ε	Amide
R	4.35	1.56	1.65	3.11		8.09
W	5.12	2.95/2.82	7.16,7.09,6.84,7.20,7.41			
V	4.25	1.9	0.9			9.22
W	5.15	3.05	7.19,7.14,6.99,7.20,7.35			
V	4.57	2.05	0.83			9.25
N	4.41	2.74/3.08				9.67
G	4.23,3.75					8.83
O	4.69	1.79	1.73	3.01		8.01
					1.83 CH3 =	
Kme	4.04	1	0.15	0.43	1.98	8.37
I	4.54	1.81	1.12	0.79		9.28
L	4	1.28	0.64	0.35/0.038		8.42
Q	4.27	1.97	2.23			8.73

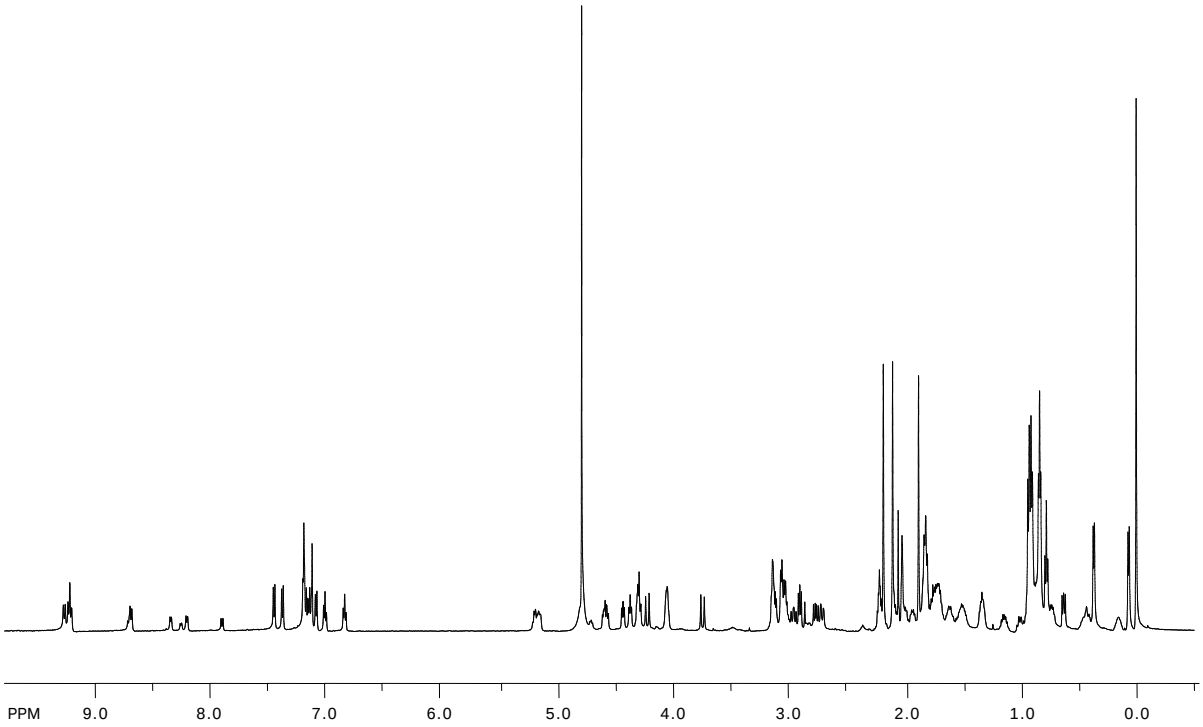

Figure 3.23 ^{1}HNMR of Peptide **WWKme2L:** Ac-Arg-Trp-Val-Trp-Val-Asn-Gly-Orn-Lys(Me2)-Ile-Leu-Gln-NH2

Table 3.10 Proton Chemical Shift Assignments for Peptide **WWKme2L.**

Residue	α	β	γ	δ	ε	Amide
R	4.39	1.52	1.66	3.15		7.97
W	5.16	2.97,2.71		7.10,7.06,6.80,7.40		8.17
V	4.3	1.98	0.92			9.18
W	5.22	3.07		7.17,7.13,6.97,7.33		8.67
V	4.61	2.09	0.87			9.2
N	4.45	2.78, 3.13				9.63
G	3.75,4.23					8.8
O	4.72	1.82	1.79	3.03		7.84
Kme2	4.07	0.98	0.11	0.36	1.78 $(CH3)_2$= 2.18, 2.05	8.22
I	4.59	1.84	1.15	0.82		9.23
L	4.07	1.34	0.95/0.74	0.37/0.062		8.3
Q	4.31	1.82,1.99	2.22			8.67

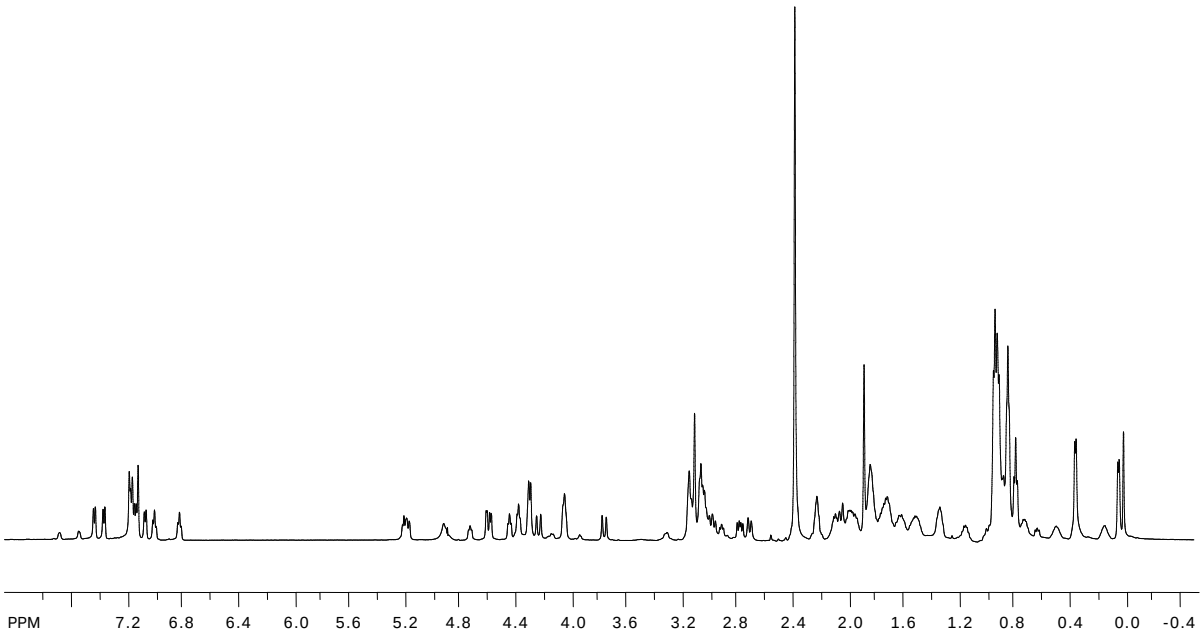

Figure 3.24 ^{1}HNMR of Peptide **WWKme3L:** Ac-Arg-Trp-Val-Trp-Val-Asn-Gly-Orn-Lys(Me3)-Ile-Leu-Gln-NH2

Table 3.11 Proton Chemical Shift Assignments for Peptide **WWKme3L.**

Residue	α	β	γ	δ	ε	Amide
R	4.37	1.53	1.63	3.14		8.02
W	5.17	2.95/2.66		7.16,7.08,6.83,7.45		8.28
V	4.6	2.08	0.86			9.23
W	5.14	3.21		7.13,7.02,7.38		8.73
V	4.29	1.8	0.92			9.25
N	4.43	3.76,3.21				9.71
G	4.22,3.75					8.88
O	4.72	1.8	1.76	3.03		7.92
Kme3	4.07	0.92	0.13	0.45,0.32	2.02 , $(CH3)_3$ = 2.38	8.32
I	4.58	1.83	NA	0.82		9.31
L	4.07	1.31	0.48	0.024,0.033		8.38
Q	4.28	1.96	2.21			8.73

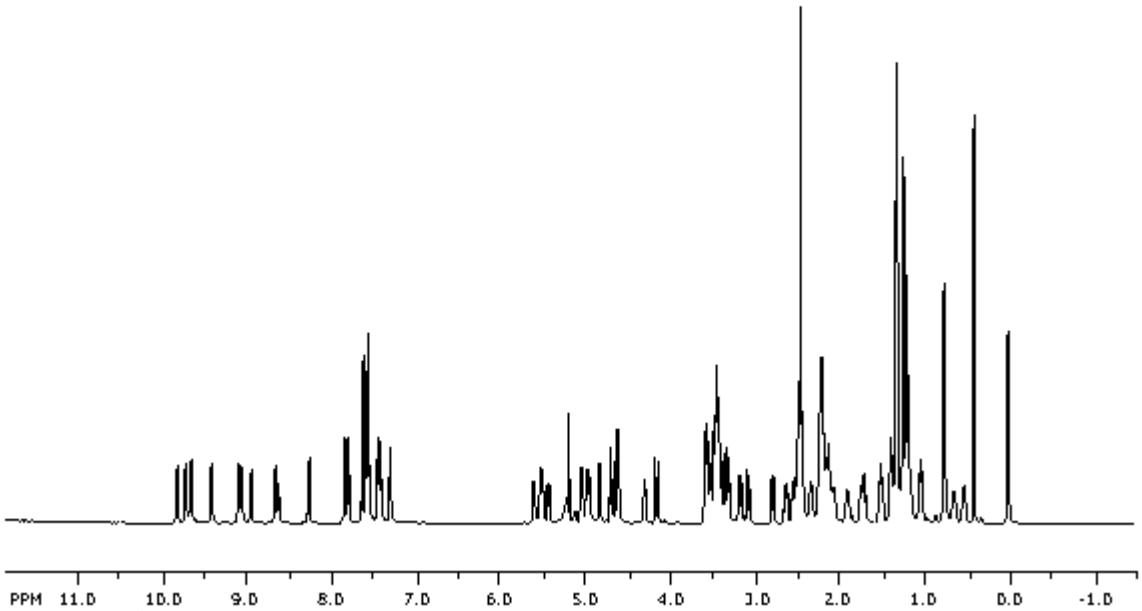

Figure 3.25 ^{1}HNMR of Peptide **cyclic WWKL:** Ac-Cys-Arg-Trp-Val-Trp-Val-Asn-Gly-Orn-Lys-Ile-Leu-Gln-Cys-NH2

Table 3.12 Proton Chemical Shift Assignments for Peptide **cyclic WWKL.**

Residue	α	β	γ	δ	ε
C	5.11	3.05,2.68			
R	4.59	1.79	1.5	3.18	
W	5.04	2.91		7.16,7.03,6.88,7.24,7.43	
V	4.27	1.91	0.92		
W	5.14	3.08		7.15,7.20,7.00,7.20	
V	4.64	2.08	0.83		
N	4.42	2.76/3.14			
G	4.23,3.76				
O	4.72	1.82			
K	4.22	0.98	0.63	0.25	2.06
I	4.67	1.82	1.1	0.83	
L	3.91	1.29	0.76/0.35	0.12,-0.40	
Q	4.55	1.81	2.07		
C	5.22	2.39,2.97			

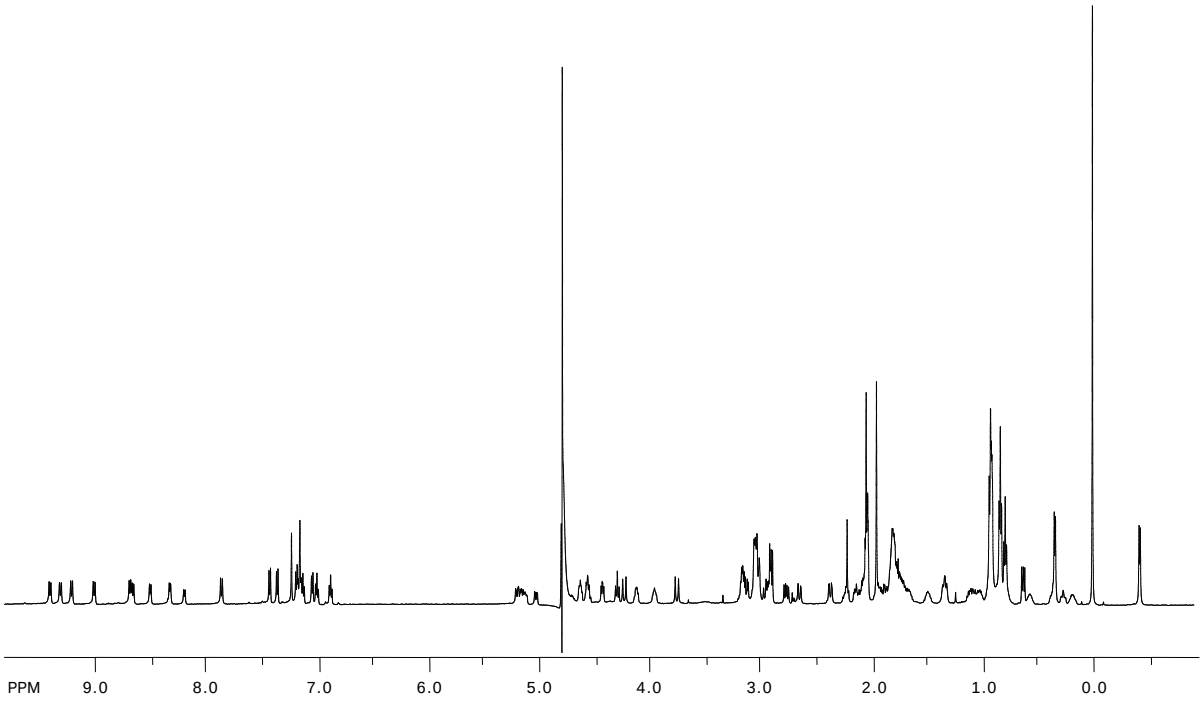

Figure 3.26 [1]HNMR of Peptide **cyclic WWKmeL:** Ac-Cys-Arg-Trp-Val-Trp-Val-Asn-Gly-Orn-Lys(Me)-Ile-Leu-Qln-Cys-NH2

Table 3.13 Proton Chemical Shift Assignments for Peptide **cyclic WWKmeL.**

Residue	α	β	γ	δ	ε
C	5.11	3.00,2.62			
R	4.54	1.46	1.78	3.14	
W	5.01	2.9	7.13,7.03,6.8		
V	4.27	1.9	0.88		
W	5.13	3.02	7.20,7.15,6.9		
V	4.64	2.06	0.82		
N	4.41	2.74/3.10			
G	4.20,3.72				
O	4.68	1.78	1.78	3	
Kme	4.11	1.02	0.54	0.32/0.16	1.8, CH3 = 1.94
I	4.6	1.78	1.08	0.82	
L	3.93	1.32	0.74	0.26,-0.44	
Q	4.53	1.77	2.06		
C	5.19	2.92,2.34			

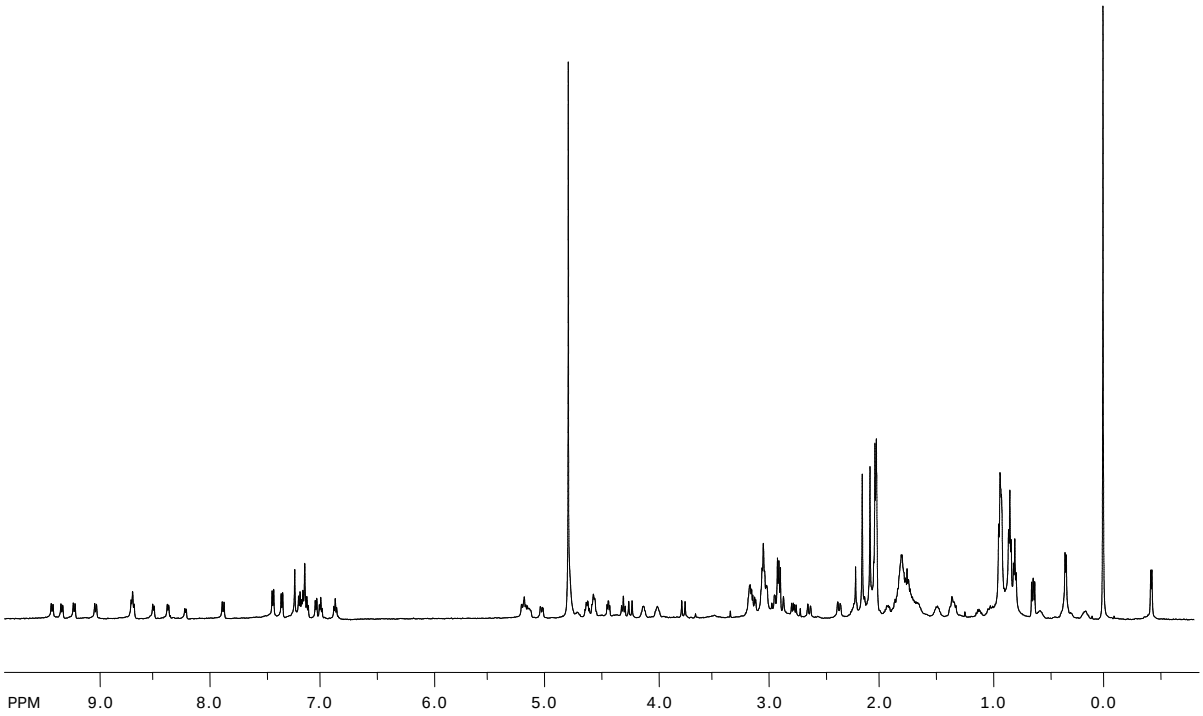

Figure 3.27 ^{1}HNMR of Peptide **cyclic WWKme2L:** Ac-Cys-Arg-Trp-Val-Trp-Val-Asn-Gly-Orn-Lys(Me2)-Ile-Leu-Gln-Cys-NH2

Table 3.14 Proton Chemical Shift Assignments for Peptide **cyclic WWKme2L.**

Residue	α	β	γ	δ	ε
C	5.14	3.04,2.64			
R	4.59	1.48	1.78	3.15	
W	5.03	2.91		6.87,7.06,7.14,7.42,7.25	
V	4.3	1.94	0.92		
W	5.14	3.06		7.00,7.17,7.35,7.22	
V	4.62	2.07	0.83		
N	4.42	2.77, 3.11			
G	3.74,4.23				
O	4.73	1.78	NA	3.04	
					1.82, $(CH3)_2$
Kme2	4.11	0.98	0.56	0.15	= 2.04, 2.16
I	4.62	1.8	1.1	0.83	
L	3.98	1.33	0.76	0.35,-0.44	
Q	4.56	1.81	2.04		
C	5.19	3.00,2.36			

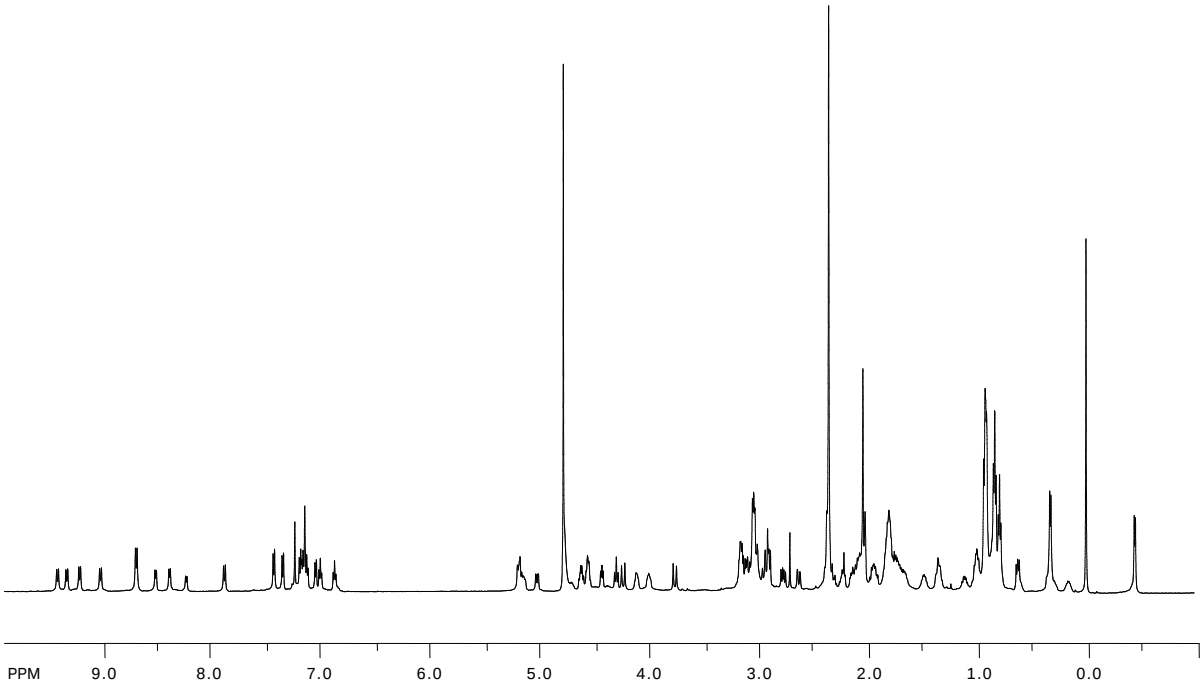

Figure 3.28 [1]HNMR of Peptide **cyclic WWKme3L:** Ac-Cys-Arg-Trp-Val-Trp-Val-Asn-Gly-Orn-Lys(Me3)-Ile-Leu-Qln-Cys-NH2

Table 3.15 Proton Chemical Shift Assignments for Peptide **cyclic WWKme3L.**

Residue	α	β	γ	δ	ε
C	5.15	2.63,3.06			
R	4.57	1.8	1.67	3.17	
W	5.03	2.91		7.18,7.06,6.89,7.25,7.45	
V	4.31	1.94	0.92		
W	5.21	3.01		7.21,7.25,7.17,7.37	
V	4.64	2.07	0.87		
N	4.43	3.14/2.77			
G	4.24,3.76				
O	4.73	1.84	1.73	3.04	
Kme3	4.13	1.95	1.00,0.62	0.31,0.17	2.1, $(CH3)_3$= 2.36
I	4.62	1.81	1.12	0.84	
L	3.99	1.37	0.77	0.34,-0.45	
Q	4.56	1.80/2.13	2.23		
C	5.21	3.01,2.36			

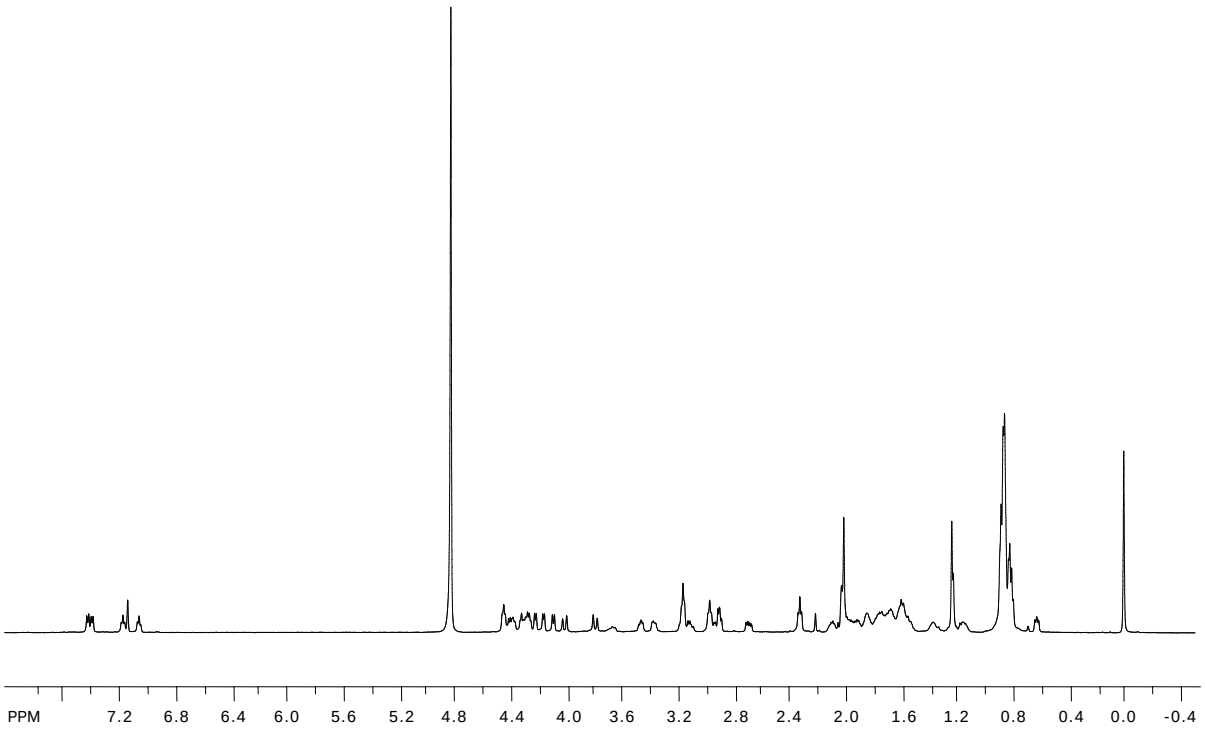

Figure 3.29 ^{1}HNMR of Peptide **AWSL:** Ac-Arg-Ala-Val-Trp-Val-Asn-Gly-Orn-Ser-Ile-Leu-Gln-NH2

Table 3.16 Proton Chemical Shift Assignments for Peptide **AWSL.**

Residue	α	β	γ	δ	ε
R	4.24	1.73	1.63	3.14	
A	4.39	1.25			
V	4.16	2.01	0.84		
W	4.83	3.12			
V	4.07	1.9	0.84		
N	4.43	2.92,2.69			
G	3.98, 3.76				
O	4.43	1.82	1.68	2.97	
S	4.32	3.41			
I	4.21	1.83	1.17	0.84	
L	4.37	1.55		0.84	
Q	4.26	1.94	2.31		

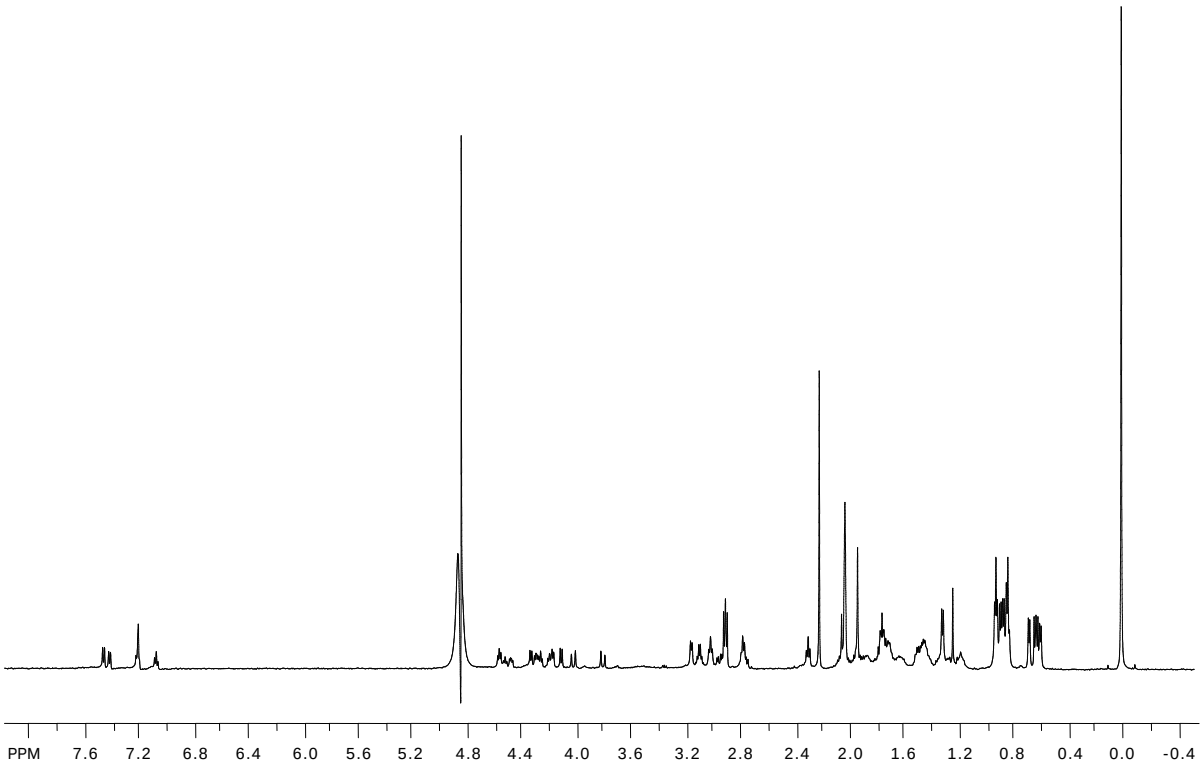

Figure 3.30 ^{1}HNMR of Peptide **WAKL:** Ac-Arg-Trp-Val-Ala-Val-Asn-Gly-Orn-Lys-Ile-Leu-Gln-NH2

Table 3.17 Proton Chemical Shift Assignments for Peptide **WAKL.**

Residue	α	β	γ	δ	ε
R	4.27	1.63	1.45	3.08	
W	4.9	3.16		7.13,7.27,7.46,7.49	
V	4.16	1.94	0.84		
A	4.56	1.31			
V	4.1	2	0.91		
N	4.64	2.94,2.76			
G	4.01,3.81				
O	4.49	1.83	1.72	3.02	
K	4.52	1.69	1.31	1.46	2.76
I	4.33	N/A	N/A	0.87	
L	4.18	1.42	1.16	0.64	
Q	4.29	1.92	2.3		

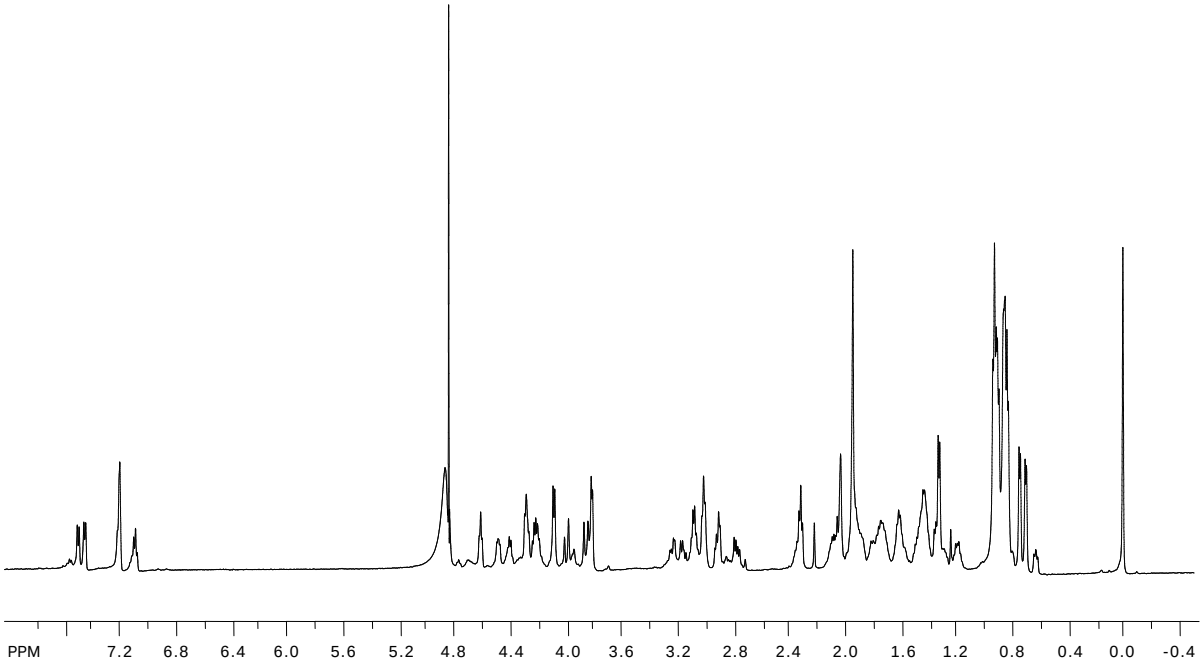

Figure 3.31 ^{1}HNMR of Peptide **WASL:** Ac-Arg-Trp-Val-Trp-Val-Asn-Gly-Orn-Lys-Ile-Leu-Gln-NH2

Table 3.18 Proton Chemical Shift Assignments for Peptide **WASL.**

Residue	α	β	γ	δ	ε
R	4.24	1.57	1.46	3.08	
W	4.76	3.16		7.12,7.22,7.48,7.52	
V	4.09	1.99	0.89		
A	4.4	1.32			
V	4.09	1.99	0.89		
N	4.62	2.8			
G	3.99,3.92				
O	4.48				
S	4.62	3.82			
I	4.31	1.9	0.89		
L	4.21	1.43	1.34	0.74	
Q	4.29	1.94	2.36		

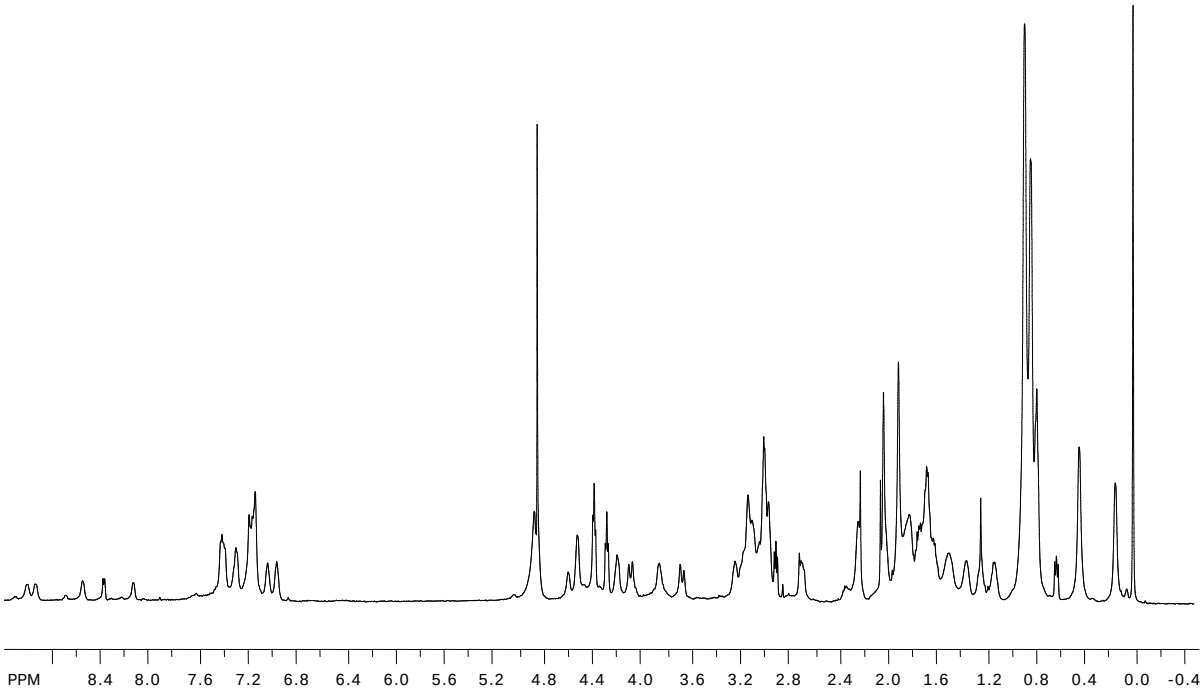

Figure 3.32 ^{1}HNMR of Peptide **WWSL:** Ac-Arg-Trp-Val-Trp-Val-Asn-Gly-Orn-Ser-Ile-Leu-Gln-NH2

Table 3.19 Proton Chemical Shift Assignments for Peptide **WWSL.**

Residue	α	β	γ	δ	ε
R	4.38	1.68	1.56	3.13	
W	4.92	2.96		6.96,7.18,7.22,7.43	
V	4.46	2.01	0.85		
W	5	3.1		7.05,7.22,7.36	
V	4.17	1.89	0.87		
N	4.38	2.68,2.96			
G	4.08,3.67				
O	4.52	1.71	1.68	3	
S	4.59	3.21,3.13			
I	4.52	1.84	1.09	0.82	
L	3.85	1.24	0.42	0.15	
Q	4.28	1.86	2.26		

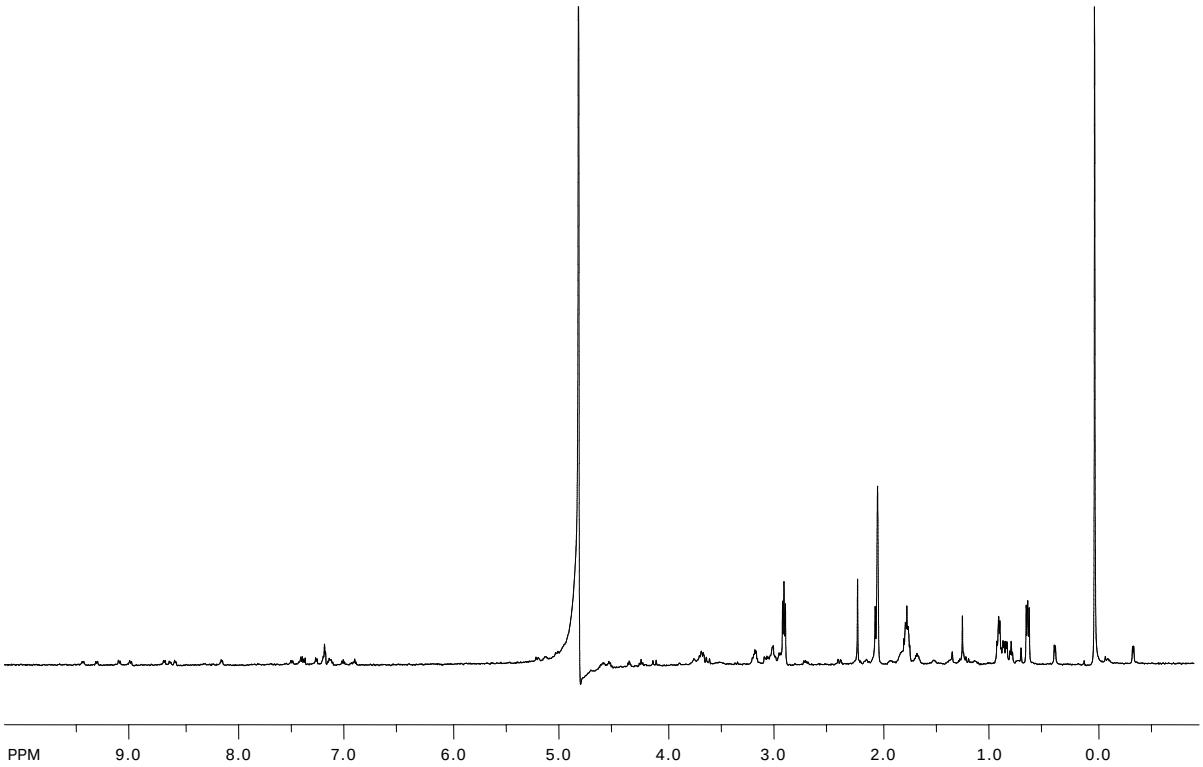

Figure 3.33 ^{1}HNMR of Peptide **cyclic WWSL:** Ac-Cys-Arg-Trp-Val-Trp-Val-Asn-Gly-Orn-Ser-Ile-Leu-Gln-Cys-NH2

Table 3.20 Proton Chemical Shift Assignments for Peptide **cyclic WWSL.**

Residue	α	β	γ	δ	ε
C	5.2	2.98,2.40			
R	4.61	1.78	1.51	3.18	
W	5.15	3.09		6.93,7.20,7.43,7.49	
V	4.61	2.06	0.88		
W	5.04	2.91		7.02,7.14,7.39,7.39	
V	4.25	1.89	0.91		
N	4.36	3.08,2.70			
G	4.13,3.62				
O	4.56	1.77	1.67	3.02	
S	4.77	3.03,3.18			
I	4.61	1.79		0.82	
L	3.75	1.23	0.38	-0.094,-0.37	
Q	4.54	1.79	2.20,207		
C	4.98	2.95			

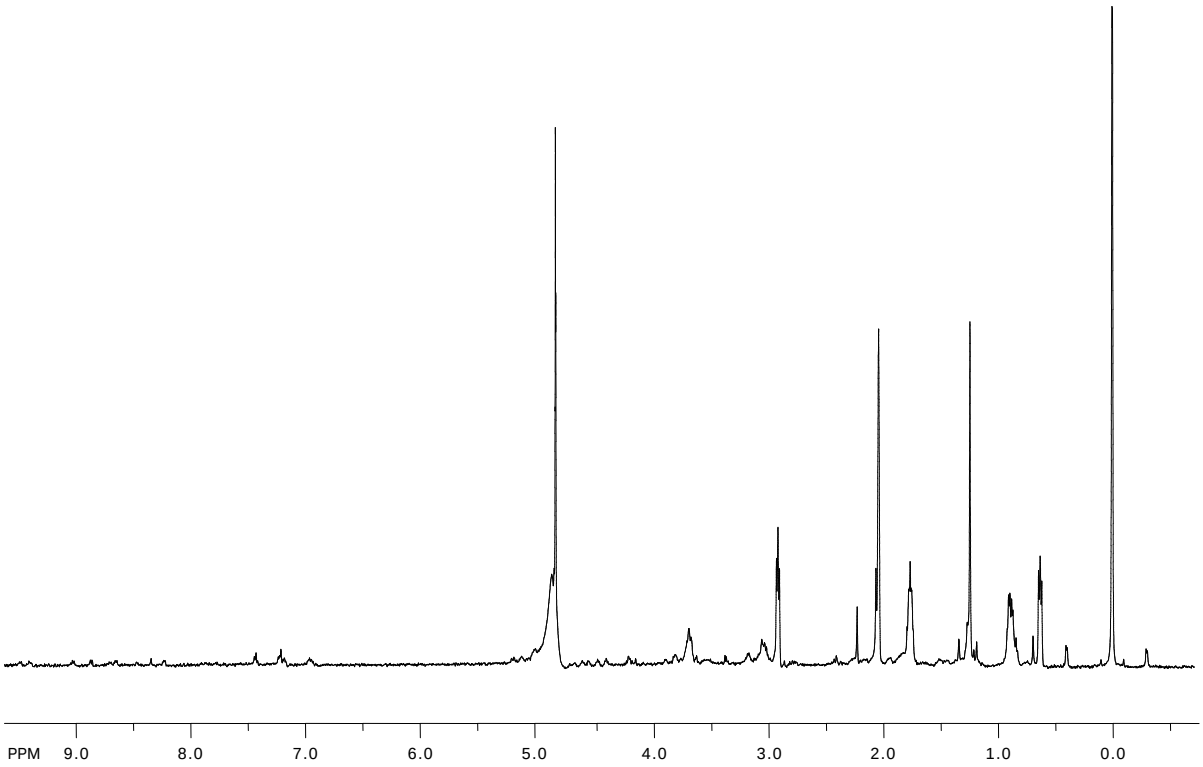

Figure 3.34 [1]HNMR of Peptide **cyclic WASL:** Ac-Cys-Arg-Trp-Val-Ala-Val-Asn-Gly-Orn-Ser-Ile-Leu-Gln-Cys-NH2

Table 3.21 Proton Chemical Shift Assignments for Peptide **cyclic WASL.**

Residue	α	β	γ	δ	ε
C	5.03	2.98			
R	4.6	1.8	1.49	3.15	
W	5.03	2.98		6.97,7.21,7.23,7.43,7.87	
V	4.47	1.99	0.88		
A	5.03	1.26			
V	4.19	1.93	0.89		
N	4.38	2.75,3.10			
G	4.21,3.88				
O	4.69	1.83	1.7	3.04	
S	5.13	3.80,3.68			
I	4.66	1.87		0.89	
L	3.79	1.25	0.38	-0.058,-0.30	
Q	4.54	1.83	2.23,2.06		
C	5.02	2,98,2.40			

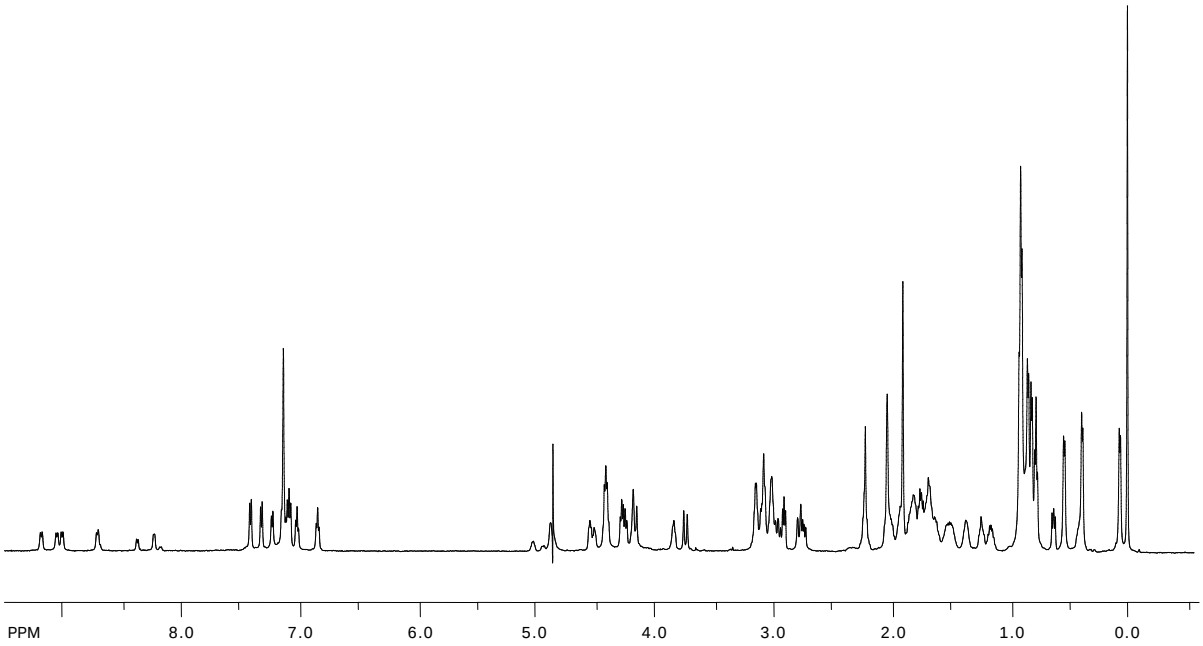

Figure 3.35 ^{1}HNMR of Peptide **WWAL:** Ac-Arg-Trp-Val-Trp-Val-Asn-Gly-Orn-Ala-Ile-Leu-Gln-NH2

Table 3.22 Proton Chemical Shift Assignments for Peptide **WWAL.**

Residue	α	β	γ	δ	ε	Amine
R	4.4	1.63	1.52	3.11		8.01
W	4.93	2.95/2.76				8.34
V	4.51	2.02	0.86			9.02
W	5.01	3.06				8.67
V	4.22	1.92	0.89			8.97
N	4.4	2.73,3.08				9.49
G	4.16,3.74					8.56
O	4.53	1.77	1.69	3		7.71
A	4.18	0.52				8.15
I	4.42	1.77	1.15	0.79		9.13
L	3.84	1.23	0.84	0.39,0.051		8.2
Q	4.27	1.98,1.84	2.21			8.67

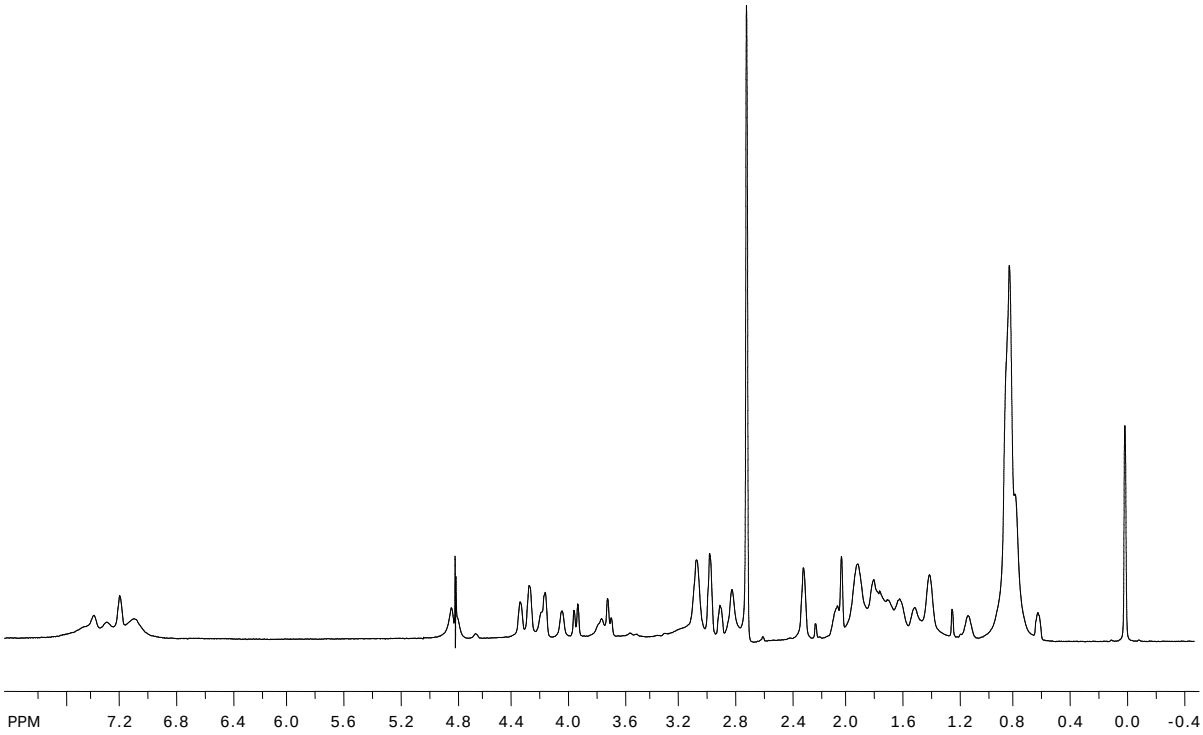

Figure 3.36 [1]HNMR of Peptide **WWGL:** Ac-Arg-Trp-Val-Trp-Val-Asn-Gly-Orn-Gly-Ile-Leu-Gln-NH2

Table 3.23 Proton Chemical Shift Assignments for Peptide **WWGL.**

Residue	α	β	γ	δ	ε
R	4.22	1.62	1.42	3.08	
W	4.82	3.08			
V	4.05	1.96	0.83		
W	4.82	3.08			
V	4.05	1.96	0.83		
N	4.67	2.82			
G	3.93,3.53				
O	4.35	1.74	1.67	2.98	
G	3.71,3.76				
I	4.18	1.81	1.17	0.86	
L	4.26	1.51		0.77	
Q	4.28	1.94,2.11	2.31		

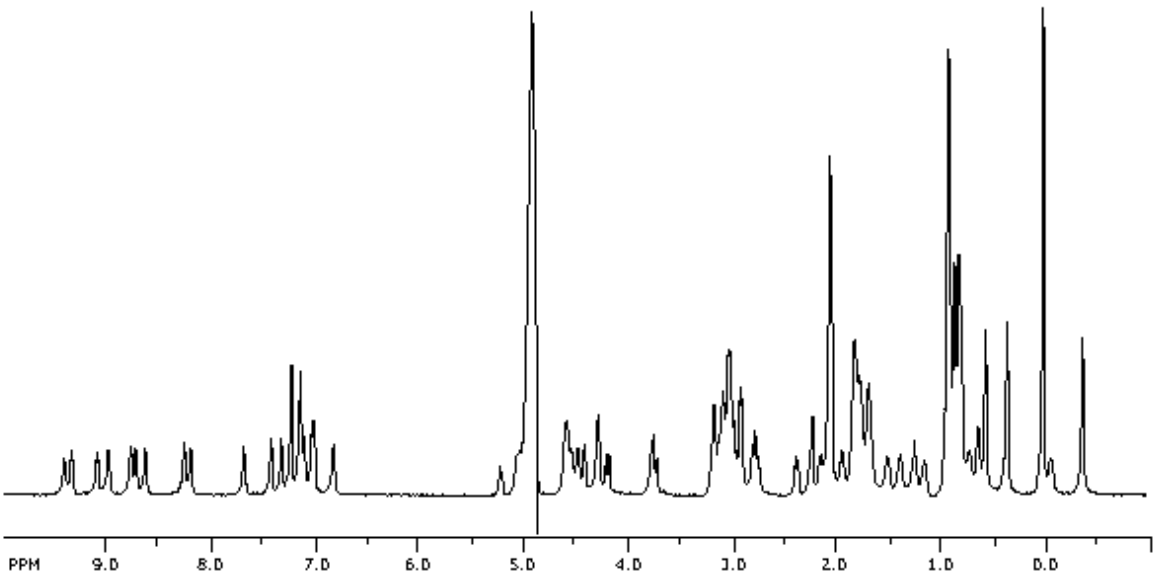

Figure 3.37 [1]HNMR of Peptide **cyclic WWAL:** Ac-Cys-Arg-Trp-Val-Trp-Val-Asn-Gly-Orn-Ala-Ile-Leu-Gln-Cys-NH2

Table 3.24 Proton Chemical Shift Assignments for Peptide **cyclic WWAL.**

Residue	α	β	γ	δ	ε
C	4.95	2.99,2.79			
R	4.6	1.81	1.66	3.15	
W	5.05	2.91			
V	4.57	2.06	0.88		
W	5.09	3.08			
V	4.27	1.93	0.92		
N	4.43	3.12,2.76			
G	4.18,3.76				
O	4.57	1.77	1.7	3.02	
A	4.27	0.57			
I	4.47	1.77	1.13	0.81	
L	3.78	1.24	0.35	-0.37	-0.073
Q	4.53	1.83,2.13	2.22		
C	5.22	2.97,2.41			

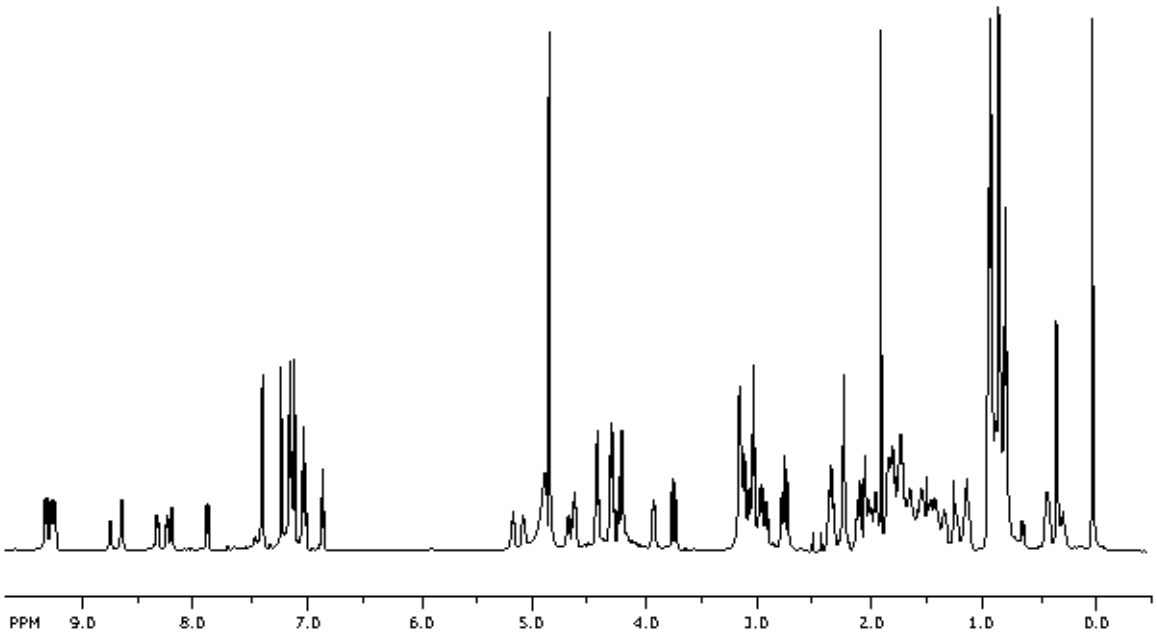

Figure 3.38 [1]HNMR of Peptide **WWRL:** Ac-Arg-Trp-Val-Trp-Val-Asn-Gly-Lys-Arg-Ile-Leu-Gln-NH2

Table 3.25 Proton Chemical Shift Assignments for Peptide **WWRL.**

Residue	α	β	γ	δ	ε	Amine
R	4.42	1.71	1.59	3.12		7.87
W	5.09	2.95,2.81				8.32
V	4.61	2.08	0.85			9.26
W	5.17	3.07				8.56
V	4.29	2.01	0.92			9.26
N	4.42	3.13,2.77				9.64
G	4.22,3.75					8.79
K	4.68	1.75	1.42	1.75	3.03	8.01
R	4.21	1.13,0.77	0.41,0.26	2.33		8.32
I	4.62	1.82	1.09	0.83		9.26
L	3.92	1.21	0.79	0.39,0.0037		8.2
Q	4.31	1.83	2.2			8.74

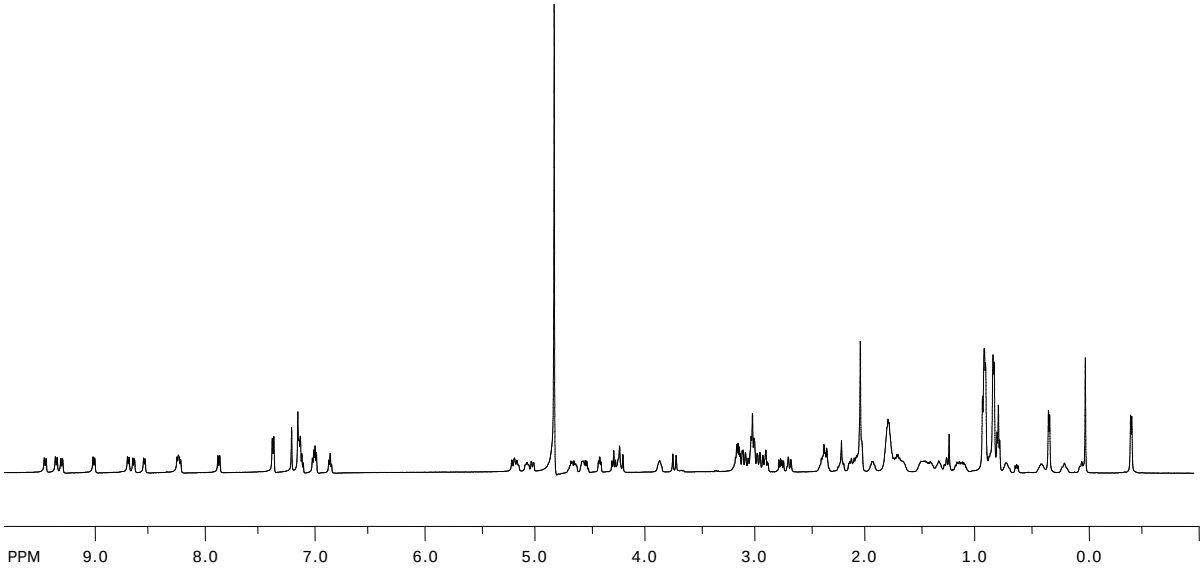

Figure 3.39 [1]HNMR of Peptide **cyclic WWRL:** Ac-Cys-Arg-Trp-Val-Trp-Val-Asn-Gly-Orn-Lys-Ile-Arg-Gln-Cys-NH2

Table 3.26 Proton Chemical Shift Assignments for Peptide **cyclic WWRL.**

Residue	α	β	γ	δ	ε
C	5.02	2.93			
R	4.58	1.78	1.5	3.16	
W	5.07	2.99,2.70			
V	4.65	2.1	0.86		
W	5.17	3.08			
V	4.3	1.95	0.93		
N	4.41	2.76, 3.13			
G	4.23,3.75				
K	4.69	1.78	1.43	1.78	3.03
R	4.23	1.15, 0.86	0.19,0.39	2.4	
I	4.68	1.81		0.83	
L	3.88	1.26	0.73,0.33	0.028,-0.42	
Q	4.55	1.8	2.06,2.15		
C	5.21	2.96,2.36			

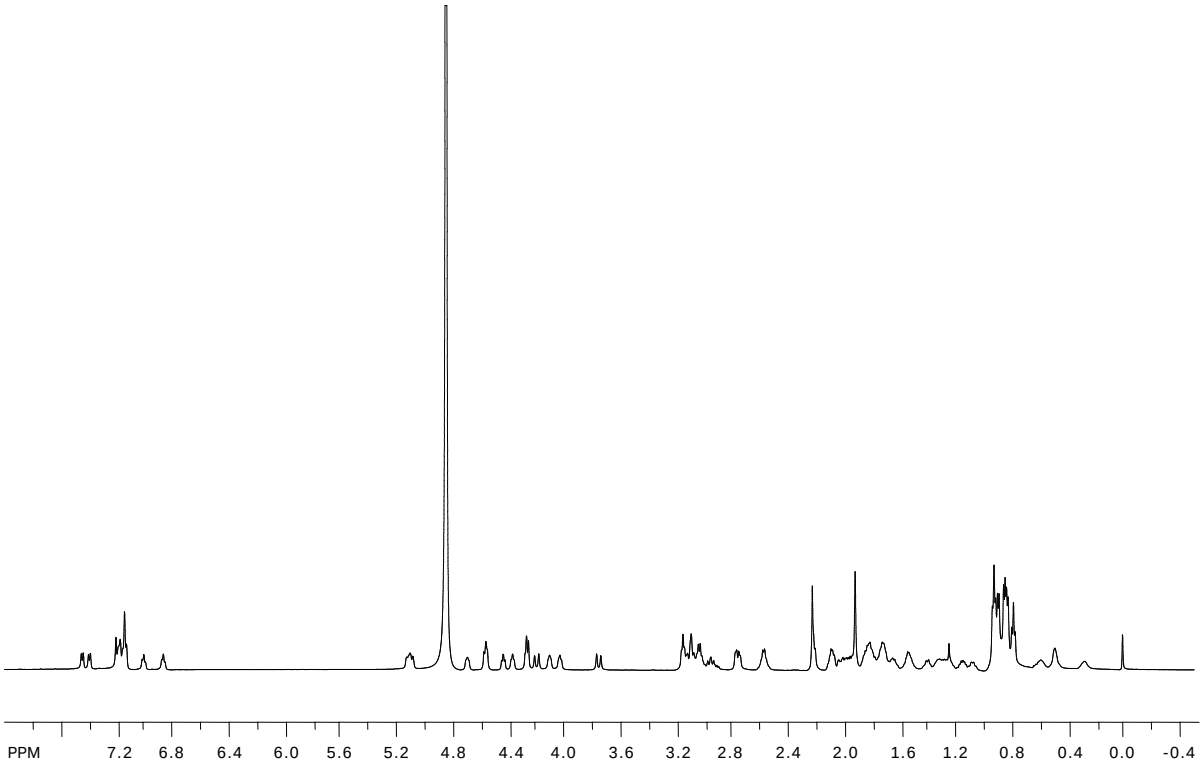

Figure 3.40 [1]HNMR of Peptide **WWKK:** Ac-Arg-Trp-Val-Trp-Val-Asn-Gly-Orn-Lys-Ile-Lys-Gln-NH2

Table 3.27 Proton Chemical Shift Assignments for Peptide **WWKK.**

Residue	α	β	γ	δ	ε	Amide
R	4.37	1.54	1.67	3.15		7.91
W	5.09	2.95,2.76		6.89, 7.15,7.18,7.43		8.36
V	4.56	2.07	0.85			9.09
						8.55
W	5.13	3.06		7.02, 7.18, 7.20, 7.40		
V	4.26	1.94	0.92			9.17
N	4.44	2.76/3.08				9.57
G	3.75/4.19					8.66
O	4.69	1.8	1.77	3.03		7.69
K	4.11	1.07	0.49	0.29	2.03	8.31
I	4.57	1.84	1.11	0.84		9.17
K	4.03	1.36	0.57	0.84	2.57	8.39
Q	4.32	2.02	2.24			8.47

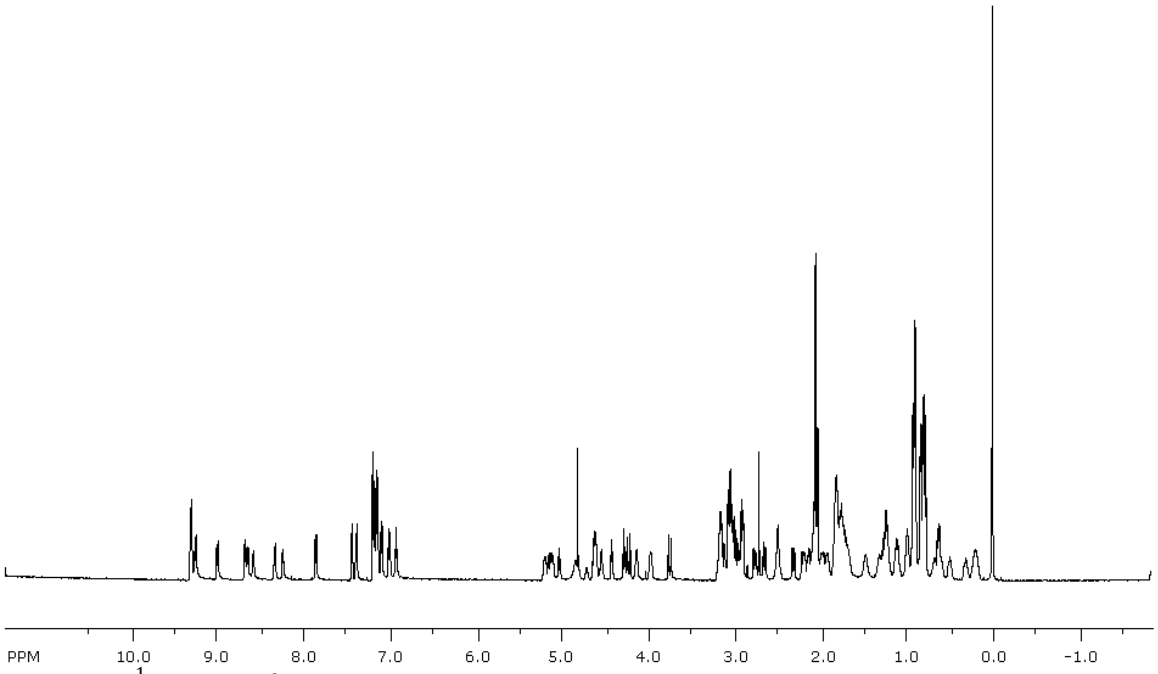

Figure 3.41 [1]HNMR of Peptide **cyclic WWKK:** Ac-Cys-Arg-Trp-Val-Trp-Val-Asn-Gly-Orn-Lys-Ile-Lys-Qln-Cys-NH2

Table 3.28 Proton Chemical Shift Assignments for Peptide **cyclic WWKK.**

Residue	α	β	γ	δ	ε
C	5.03	2.95			
R	4.61	1.8	1.77	3.16	
W	5.21	2.98,2.66			
V	4.63	2.06	0.81		
W	5.12	3.05			
V	4.28	2.07	0.9		
N	4.43	3.12,2.75			
G	3.75,4.22				
O	4.74	1.75	1.75	3.03	
K	4.13	1	0.59	0.23	2.07
I	4.6	1.78	1.22	0.85	
K	3.98	1.23	0.67	0.46,0.19	2.48
Q	4.56	1.76,1.97	2.14		
C	5.16	2.91,2.30			

Table 3.29 Proton Chemical Shift Assignments for Peptide **WWKW.**

Residue	α	β	γ	δ	ε	Amide
R	4	1.58, 1.36	1.18	3.04		6.96
W	5.15	3.06, 2.71	7.03, H2 7.22, 7.39 H4 7.48			8.17
V	4.58	2.03	0.81			9.43
W	5.21	3.06	7.09, 7.27, 7.36			8.69
V	4.3	1.97	0.94			9.3
N	4.44	3.13, 2.78				9.64
G	4.25, 3.76					8.78
K	4.68	1.79	1.43	3.05		7.89
K	4.11	1.07	0.37	0.58,0.20	1.92, 6.99	8.17
I	4.78	1.88		0.9		9.39
W	4.35	2.82, 2.16	H 7.16,H6 6.84, H5 6.23, H4 5.14			8.78
Q	4.28	1.60,1.83	2.07			8.33

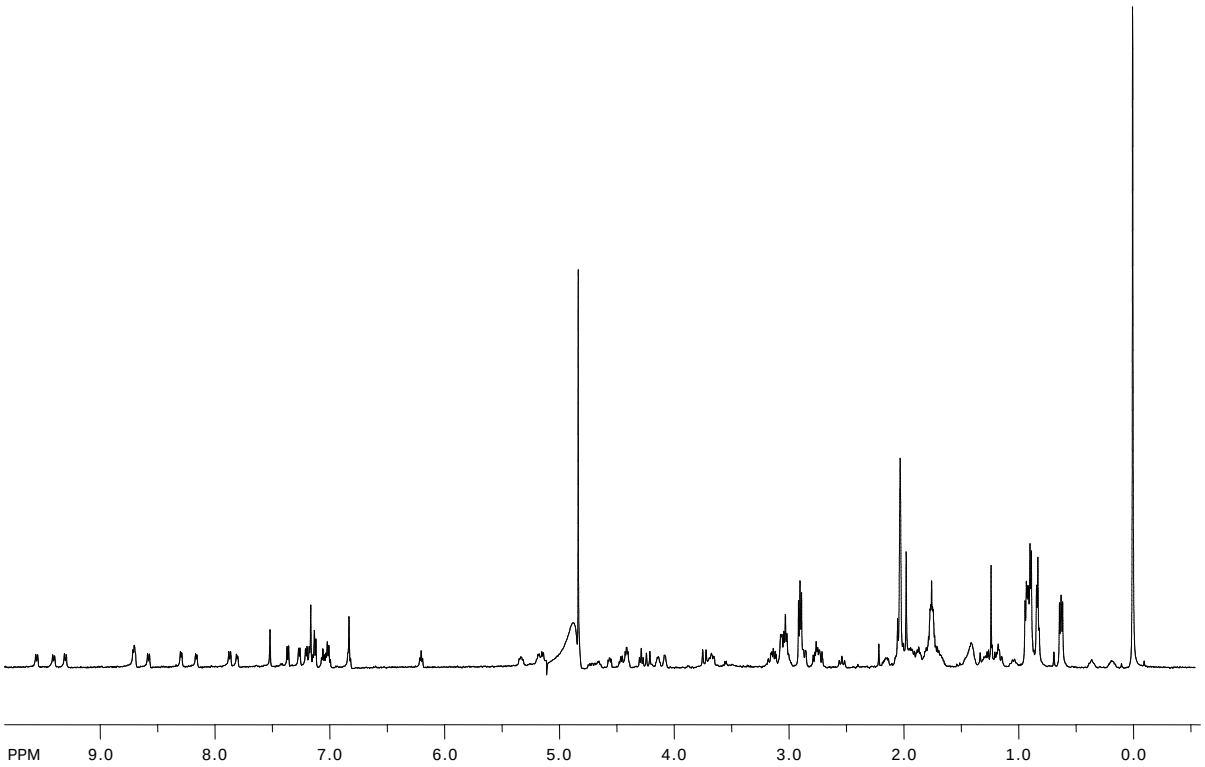

Figure 3.43 [1]HNMR of Peptide **cyclic WWKW:** Ac-Cys-Arg-Trp-Val-Trp-Val-Asn-Gly-Orn-Lys-Ile-Trp-Gln-Cys-NH2

Table 3.30 Proton Chemical Shift Assignments for Peptide **cyclic WWKW.**

Residue	α	β	γ	δ	ε
C	nd	nd			
R	4.1	1.77	nd	3.03	
W	nd	nd	nd		
V	4.57	2.01	0.86		
W	nd	nd			
V	4.29	1.96	0.93		
N	4.34	3.14,2.78			
G	4.24, 3.75				
K	4.69	1.79	1.44	3.05	
K	4.15	1.04	0.63	0.36,0.19	1.88
I	4.76	1.87		0.88	
W	nd	nd	nd		
Q	4.48	1.68,1.96	2.09		
C	nd	nd			

Table 3.31 Proton Chemical Shift Assignments for Peptide **WFKL.**

Residue	α	β	γ	δ	ε	Amide
R	4.38	1.66	1.53	3.14		8.05
W	5.12	3.01				8.32
V	4.53	2.08	0.85			9.08
F	5.2	2.94				8.69
V	4.23	1.91	0.93			8.91
N	4.42	2.76,3.06				9.57
G	4.17,3.66					8.57
O	4.66	1.83	1.78	3.04		7.81
K	4.4	1.56	0.92	1.15	2.22, 7.13	8.57
I	4.59	1.86	1.16	0.86		9.23
L	4.06	1.35	0.7	0.46,0.20		8.35
Q	4.32	1.85	2.14,2.02			8.69

Table 3.32 Proton Chemical Shift Assignments for Peptide **cyclic WFKL.**

Residue	α	β	γ	δ	ε
C	5.05	2.91			
R	4.59	1.79	1.49	3.16	
W	5.13	2.78,3.04			
V	4.62	2.11	0.86		
F	5.28	2.88			
V	4.24	1.9	0.91		
N	4.4	2.76,3.11			
G	4.19, 3.63				
O	4.7	1.84	1.75	3.03	
K	4.5	1.59	1.36,1.21	1.04,0.88	2.19
I	4.76	1.84	1.34,1.19	0.85	
L	3.92	1.33	0.78,0.38	0.13,-0.40	
Q	4.57	1.79	2.09		
C	5.21	2.97,2.38			

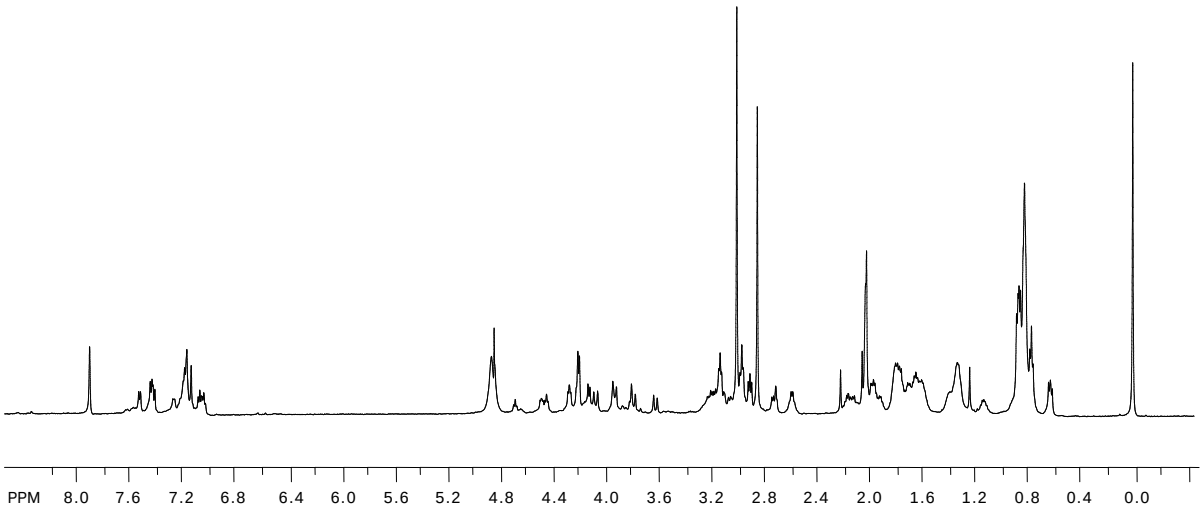

Figure 3.43 ^{1}HNMR of Peptide **GWKW:** Ac-Arg-Gly-Val-Trp-Val-Asn-Gly-Orn-Lys-Ile-Trp-Gln-NH2

Table 3.33 Proton Chemical Shift Assignments for Peptide **GWKW.**

Residue	α	β	γ	δ	ε
R	4.27	1.77	1.61	3.11	
G	3.92,3.70				
V	4.2	1.91	0.81		
W	4.84	3.07			
V	4.11	1.9	0.86		
N	4.45	2.96,2.72			
G	4.06,3.78				
K	4.49	1.73	1.37	1.69	2.96
K	3.92	1.33	0.71	0.78	2.59
I	4.21	1.8		0.81	
W	4.68	3.18			
Q	4.19	1.79	2.13		

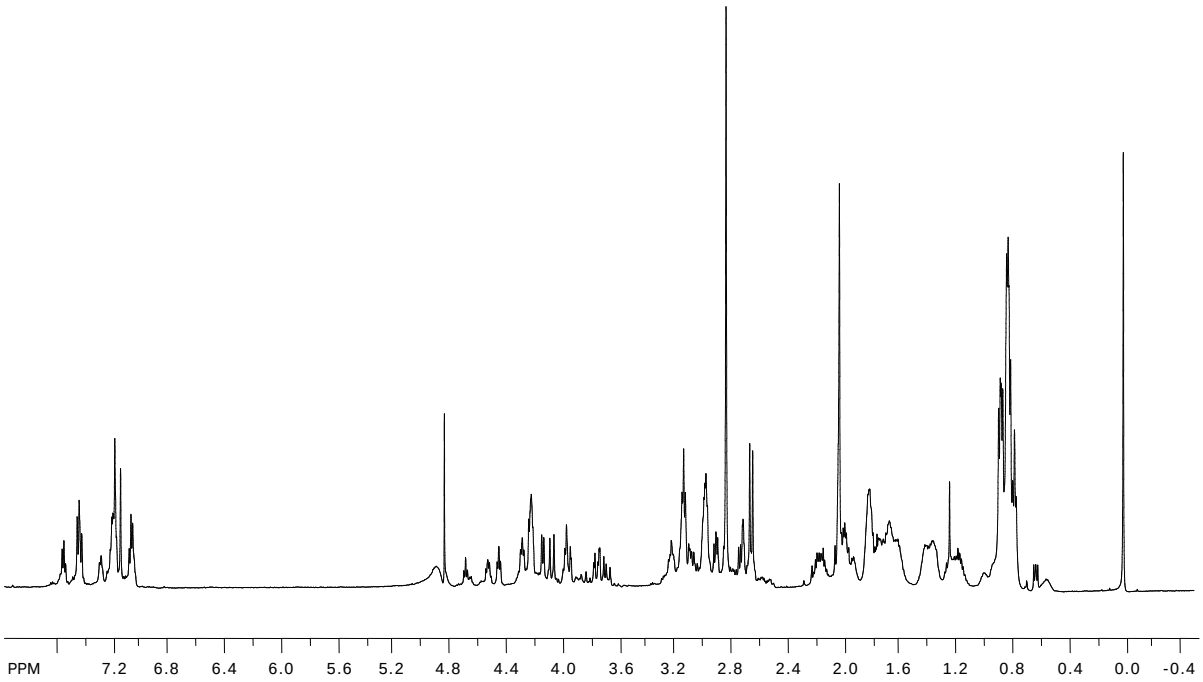

Figure 3.44 ^{1}HNMR of Peptide **GWKme3W:** Ac-Arg-Gly-Val-Trp-Val-Asn-Gly-Lys-Lys(Me3)-Ile-Trp-Gln-NH2

Table 3.34 Proton Chemical Shift Assignments for Peptide **GWKme3W.**

Residue	α	β	γ	δ	ε
R	4.29	1.76	1.63	3.14	
G	3.97,3.70				
V	4.23	2	0.87		
W	4.89	3.08			
V	4.13	1.93	0.87		
N	4.46	2.98,2.73			
G	4.07,3.76				
K	4.52	1.71	1.39	1.71	2.98
Kme3	3.97	1.41,1.23	0.54	0.77,0.99	2.66
I	4.23	1.82	1.35,1.17	0.83	
W	4.69	3.2			
Q	4.22	1.81	2.15		

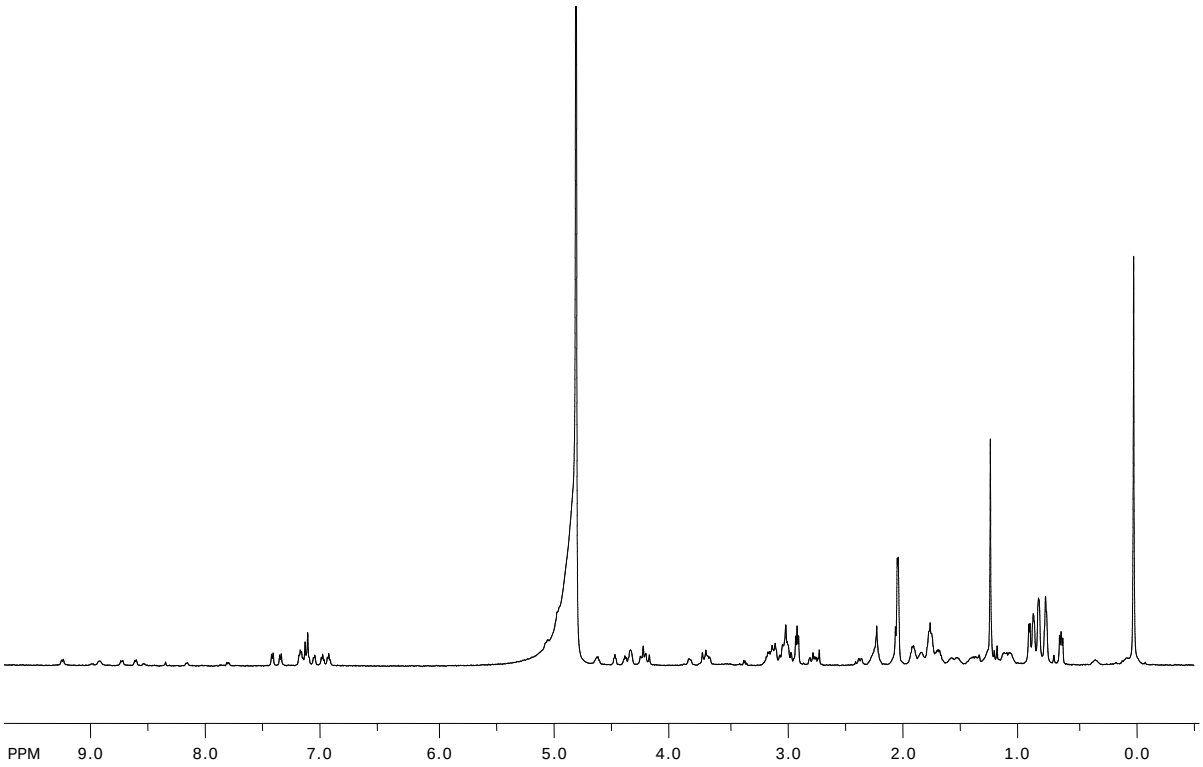

Figure 3.45 ^{1}HNMR of Peptide **cyclic GWKW:** Ac-Cys-Arg-Gly-Val-Trp-Val-Asn-Gly-Lys-Lys-Ile-Trp-Gln-Cys-NH2

Table 3.35 Proton Chemical Shift Assignments for Peptide **cyclic GWKW.**

Residue	α	β	γ	δ	ε
C					
R	4.51	1.8	1.58	3.17	
G	4.21,3.88				
V	4.36	nd	0.81		
W	4.99	3			
V	4.25	1.92	0.9		
N	4.42	3.11,2.75			
G	4.21,3.70				
K	4.64	1.76	1.4	1.71	3.01
K	3.85	1.1	0.35	0.034	2.26
I	4.36	1.88		0.81	
W	4.92	3			
Q	4.63	1.91	2.22		
C					

Table 3.36 Proton Chemical Shift Assignments for Peptide **Ac-RWVWVNG-NH2.**

Residue	α	β	γ	δ	ε	Amine
R	4.09	1.58	1.35	3.03		6.94
W	4.51	3.04		7.25,7.39,7.22,7.02,7.61		8.29
V	4	1.85	0.8			8.39
W	4.57	3.15		7.25,7.39,7.22,7.02,7.61		8.29
V	4	1.85	0.8			8.39
N	4.46	2.73/2.64				8.45
G	3.94					8.27

Table 3.37 Proton Chemical Shift Assignments for Peptide **Ac-RAVWVNG-NH2.**

Residue	α	β	γ	δ	ε
R	4.22	1.73	1.67	3.15	
A	4.26	1.27			
V	3.99	1.94	0.84		
W	4.68	3.24		7.15,7.21,7.48,7.63	
V	4.04	2.01	0.9		
N	4.49	2.80,2.68			
G	3.86				

Table 3.38 Proton Chemical Shift Assignments for Peptide **Ac-RWVAVNG-NH2.**

Residue	α	β	γ	δ	ε
R	4.16	1.59	1.41	3.07	
W	4.69	3.24		7.14,7.22,7.48,7.59	
V	3.94	1.9	0.83		
A	4.16	1.33			
V	4.03	2.06	0.92		
N	4.67	2.76			
G	3.87				

Table 3.39 Proton Chemical Shift Assignments for Peptide **Ac-NGOSILQ-NH2.**

Residue	α	β	γ	δ	ε
N	4.7	2.81			
G	3.96				
O	4.43	1.86	1.72	3.02	
S	4.5	3.86			
I	4.19	1.9	1.45,1.20	0.9	
L	4.36	1.64		0.9	
Q	4.29	1.99	2.37		

Table 3.40 Proton Chemical Shift Assignments for Peptide **Ac-RWVFVNG-NH2.**

Residue	α	β	γ	δ	ε	Amine
R	4.1	1.58	1.36	3.04		8.04
W	4.52	3.15				8.23
V	4.01	1.89	0.86			8.09
F	4.65	3.1				8.23
V	4.01	1.89	0.86			8.09
N	4.44	2.75,2.62				8.5
G	3.94					8.36

Table 3.41 Proton Chemical Shift Assignments for Peptide **Ac-NGORILQ-NH2.**

Residue	α	β	γ	δ	ε	Amine
N	4.68	2.81				8.5
G	3.93					8.6
O	4.33	1.84	1.43	1.7	2.99	8.12
R	4.36	1.78	1.63	3.21		8.37
I	4.15	1.87	1.48,1.20	0.9		8.3
L	4.39	1.62	0.92			8.41
Q	4.32	1.99	2.38			8.37

Table 3.42 Proton Chemical Shift Assignments for Peptide **Ac-NGOKIKQ-NH2.**

Residue	α	β	γ	δ	ε	Amine
N	4.69	2.81				8.47
G	3.95					8.59
O	4.37	1.87	1.76	3.02		8.18
K	4.3	1.76	1.45		1.76	8.36
I	4.16	1.86	1.21,1.46	0.91		8.22
K	4.3	1.76	1.45	1.76	2.99	8.47
Q	4.3	2.01	2.39			8.47

Table 3.43 Proton Chemical Shift Assignments for Peptide **Ac-NGOKIWQ-NH2.**

Residue	α	β	γ	δ	ε	Amine
N	4.66	2.81				8.46
G	3.91					8.56
O	4.26	1.61	1.31		2.86	8.36
K	4.28	1.72	1.39	1.64	2.96	8.06
I	4.13	1.8	1.39	1.16	0.85	8.19
W	4.65	3.27				8.26
Q	4.15					8.06

Table 3.44 Proton Chemical Shift Assignments for Peptide **Ac-RGVWVNG-NH2.**

Residue	α	β	γ	δ	ε
R	4.29	1.85	1.64	3.18	
G	3.87				
V	4.06	1.99	0.83		
W	4.72	3.24			
V	4.01	1.94	0.83		
N	4.52	2.81,2.66			
G	3.87				

Table 3.45 Proton Chemical Shift Assignments for Peptide **Ac-NGKKIWQ-NH2.**

Residue	α	β	γ	δ	ε
N	4.67	2.8			
G	3.93				
K	4.26	1.61	1.32	1.61	2.88
K	4.28	1.74	1.38	1.71	2.96
I	4.13	1.81	Nd	0.86	
W	4.66	3.27			
Q	4.17	1.79	2.15		

Table 3.46 NOEs observed in Peptides **WWKL,** and **WWKmeL** at 298K.

WWKL				WWKmeL			
Residue	**Proton**	**Residue**	**Proton**	**Residue**	**Proton**	**Residue**	**Proton**
Trp 2	Ar 4	Lys 9	β	Trp 2	α	Leu 11	α
Trp 2	Ar 4	Lys 9	γ	Trp 2	Ar 4	Lys 9	β
Trp 2	Ar 4	Lys 9	δ	Trp 2	Ar 4	Lys 9	γ
Trp 2	α	Leu 11	α	Trp 2	Ar 4	Lys 9	δ
Trp 2	Ar 5	Leu 11	γ	Trp 2	Ar 5	Leu 11	γ
Trp 2	Ar 7	Lys 9	γ	Trp 2	Ar 7	Leu 11	δ
Trp 2	Ar 7	Leu 11	δ	Trp 2	Ar 2	Lys 9	ε
Trp 2	Ar NH	Leu 11	δ	Trp 4	Ar 4	Lys 9	ε
Trp 4	Ar 4	Lys 9	γ	Trp 4	Ar 7	Lys 9	δ
Trp 4	α	Lys 9	α	Trp 4	Ar 4	Lys 9	γ
Trp 4	Ar 4	Leu 11	α	Trp 4	α	Leu 11	α
Trp 4	Ar 5	Ile 10	α	Trp 4	Ar 4	Leu 11	α
Trp 4	Ar 2	Leu 11	α	Trp 4	Ar 5	Ile 10	α
Trp 4	Ar 4	Gly 7	α	Trp 4	Ar 2	Leu 11	α
Trp 4	Ar 5	Orn 8	α	Trp 4	Ar 4	Gly 7	α
Trp 4	Ar NH	Lys 9	δ	Trp 4	Ar 5	Orn 8	α
Asn 6	NH	Gly 7	NH				

Table 3.47 NOEs observed in Peptides **WWKme2L, and WWKme3L** at 298K.

WWKme2L NOE				WWKme3L NOE			
Residue	**Proton**	**Residue**	**Proton**	**Residue**	**Proton**	**Residue**	**Proton**
Trp 2	α	Leu 11	α	Trp 2	α	Leu 11	α
Trp 2	Ar 4	Leu 11	γ	Trp 2	Ar 4	Lys 9	β
Trp 2	Ar 5	Leu 11	γ	Trp 2	Ar 4	Lys 9	δ
Trp 2	Ar 6	Leu 11	δ	Trp 2	Ar 5	Leu 11	γ
Trp 2	Ar 6	Lys 9	γ	Trp 2	Ar 6	Lys 9	γ
Trp 2	Ar 7	Leu 11	δ	Trp 2	Ar 6	Leu 11	γ
Trp 2	Ar 2	Lys 9	β	Trp 2	Ar 7	Leu 11	δ
Trp 2	Ar 2	Lys 9	γ	Trp 2	Ar 2	Lys 9	CH3
Trp 2	Ar 2	Lys 9	ε	Trp 2	Ar 4	Lys 9	β
Trp 2	Ar 2	Lys 9	CH3 1	Trp 2	Ar 4	Lys 9	γ
Trp 2	α	Leu 11	α	Trp 2	Ar 4	Lys 9	δ
Trp 4	Ar 4	Lys 9	γ	Trp 4	Ar 4	Lys 9	γ
Trp 4	Ar 7	Lys 9	ε	Trp 4	Ar 7	Lys 9	CH3
Trp 4	Ar 7	Lys 9	CH3 2	Trp 2	Ar 4	Leu 11	α
Trp 4	Ar 7	Lys 9	CH3 1	Trp 2	Ar 5	Ile 10	α
Trp 4	Ar 4	Leu 11	α	Trp 2	Ar 2	Leu 11	α
Trp 4	Ar 5	Ile 10	α	Trp 4	Ar 4	Gly 7	α
Trp 4	Ar 2	Leu 11	α	Trp 4	Ar 5	Orn 8	α
Trp 4	Ar 4	Gly 7	α				
Trp 4	Ar 5	Orn 8	α				

Table 3.48 NOEs observed in Peptides **WWAL** and **WWRL** at 298K.

WWAL				WWRL			
Residue	**Proton**	**Residue**	**Proton**	**Residue**	**Proton**	**Residue**	**Proton**
Trp 2	α	Leu 11	α	Trp 2	α	Leu 11	α
Trp 2	Ar 5	Ala 9	β	Trp 2	Ar 2	Arg 1	α
Trp 2	Ar 5	Ile 10	α	Trp 2	Ar 4	Arg 9	β
Trp 2	Ar 2	Ala 9	β	Trp 2	Ar 4	Ile 10	α
Trp 2	Ar 4	Leu 11	δ	Trp 2	Ar 4	Leu 11	α
Trp 2	Ar 7	Leu 11	γ	Trp 2	Ar 5	Ile 10	α
Trp 4	α	Ala 9	α	Trp 2	Ar 6	Leu 11	δ
Trp 4	Ar 5	Orn 8	α	Trp 2	Ar 7	Leu 11	δ
Trp 4	Ar 5	Ala 9	β	Trp 2	Ar 7	Arg 9	δ
Trp 4	Ar 6	Gly 7	α	Trp 4	α	Arg 9	α
Trp 4	Ar 6	Ala 9	β	Trp 4	Ar 4	Arg 9	α
				Trp 4	Ar 4	Gly 7	α
				Trp 4	Ar 5	Orn 8	α

Table 3.49 NOEs observed in Peptides **WFKL,** and **WWKK** at 298K.

WFKL				WWKK			
Residue	**Proton**	**Residue**	**Proton**	**Residue**	**Proton**	**Residue**	**Proton**
Trp 2	α	Leu 11	α	Trp 2	α	Leu 11	α
Trp 2	Ar 4	Leu 11	δ	Trp 2	Ar 5	Lys 9	α
Trp 2	Ar 2	Leu 11	δ	Trp 2	Ar 5	Lys 11	δ
Trp 2	Ar 5	Ile 10	α	Trp 2	Ar 5	Lys 9	γ
Trp 2	Ar 4	Lys 9	β	Trp 2	Ar 4	Lys 9	γ
Trp 4	α	Lys 9	α	Trp 2	Ar 4	Lys 9	β
				Trp 2	Ar 7	Lys 11	ε
				Trp 4	α	Lys 9	α
				Trp 4	Ar 5	Orn 8	α
				Trp 4	Ar 5	Lys 9	γ
				Trp 4	Ar 5	Lys 9	δ
				Trp 4	Ar 6	Gly 7	α
				Trp 4	Ar 7	Lys 9	ε
				Trp 4	Ar 7	Lys 9	γ
				Trp 4	Ar 7	Lys 9	δ

Table 3.50 NOEs observed in Peptides **WWKW** at 298K.

Residue	**Proton**	**Residue**	**Proton**
Trp 2	α	Trp 11	α
Trp 2	Ar 4	Arg 1	α
Trp 2	Ar 4	Lys 9	γ
Trp 2	Ar 4	Lys 9	β
Trp 2	Ar 4	Trp 11	Ar 5
Trp 2	Ar 6	Trp 11	α
Trp 2	Ar 6	Trp 11	β
Trp 4	α	Lys 9	α
Trp 4	Ar 4	Gly 8	α
Trp 4	Ar 4	Lys 9	α
Trp 4	Ar 4	Lys 9	β
Trp 4	Ar 7	Lys 9	δ
Trp 11	Ar 6	Arg 1	β
Trp 11	Ar 7	Arg 1	β

v. Determination of fraction folded.

To determine the unfolded chemical shifts, 7-mers were synthesized as unstructured controls and cyclic peptides were synthesized for fully folded. The chemical shifts for residues in the strand and one turn residue were obtained from each 7-mer peptide. The chemical shifts of the fully folded state were taken from the cyclic peptides. The fraction folded on a per residue bases was determined from equation 1.

$$\text{Fraction Folded} = [\delta\text{obs} - \delta 0]/[\,\delta 100 - \delta 0], \qquad [1]$$

where δobs is the observed Hα chemical shift, δ100 is the Hα chemical shift of the cyclic peptides, and δ0 is the Hα chemical shift of the unfolded 7-mers. The overall fraction folded for the entire peptide was obtained by averaging the fraction folded of resides Val3, Val5, Orn8, and Ile10. These residues are in hydrogen bonded positions have been shown to be the most reliable in determining fraction folded. The overall fraction fold was also determined using the extent of Hα glycine splitting observed in the turn residue Gly10 given in equation 2.

$$\text{Fraction Folded} = [\Delta\delta_{\text{Gly Obs}}]/[\,\Delta\delta_{\text{Gly 100}}], \qquad [2]$$

where $\Delta\delta_{\text{Gly Obs}}$ is the difference in the glycine Hα chemical shifts of the observed, and $\Delta\delta_{\text{Gly 100}}$ is the difference in the glycine Hα chemical shifts of the cyclic peptides.

vi. Determination of thermodynamic parameters.

Variable temperature NMR was used in order to determine the thermodynamic parameters of the peptide folding. A temperature range of 275 to 351 K was explored in five-degree increments using a Varian Inova 600-MHz spectrometer. Temperature calibration was performed with ethylene glycol and methanol standards by using standard macros in Varian software. The change in glycine chemical shift difference was followed with temperature.

The fraction folded of the peptide was plotted against temperature, and the curve was fitted by using the following Equation 3[22]:

$$\text{Fraction folded} = (\exp[x / RT])/ (1 + \exp[x / RT]) \quad [3]$$

Where

$$x = (T[\Delta S_{298}° + \Delta Cp° \ln\{T / 298\}] - [\Delta H_{298}° + \Delta Cp°\{T-298\}])$$

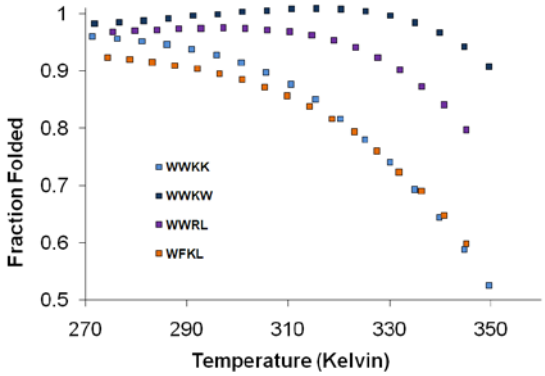

Figure 3.46. Thermal Denaturation of Alternative Trp Pocket peptides**.** Fraction folded was calculated from extent of Gly splitting. Conditions: 50 mM sodium acetate-d_4, pH 4.0 (uncorrected), referenced to DSS.

[22] Maynard, A. J.; Sharman, G. J.; Searle, M. S. *J Am Chem Soc* **1998**, *120*, 1996-2007

Table 3.52 Temperature Dependence of the Fraction Folded from Glycine Chemical Shift Data for the Trp pocket series**.**

WWKL:		WWKmeL:		WWKme2L:		WWKme3L:	
Temp (K)	Fraction folded	Temp (K)	Fraction folded	Temp (K)	Fraction folded	Temp (K)	Fraction folded
273.91	0.996	272.97	0.980	274.18	0.966	273.8	0.985
278.71	0.996	277.75	0.980	278.75	0.967	278.5	0.985
283.51	0.995	282.53	0.982	283.37	0.969	283.2	0.989
288.31	0.993	287.31	0.981	288.24	0.969	288.0	0.990
293.12	0.990	292.09	0.981	293.03	0.971	292.7	0.992
297.92	0.988	296.87	0.981	297.72	0.971	297.4	0.994
302.72	0.984	301.65	0.981	302.32	0.971	302.1	0.996
307.52	0.977	306.43	0.979	307.21	0.973	306.8	0.998
312.32	0.969	311.21	0.977	311.8	0.973	311.6	1.000
317.12	0.960	315.99	0.972	316.7	0.971	316.3	1.000
321.92	0.942	320.77	0.964	321.53	0.968	321.0	0.999
326.72	0.920	325.55	0.952	326.19	0.964	325.7	0.997
331.52	0.894	330.33	0.939	331.2	0.956	330.5	0.993
336.32	0.863	335.12	0.915	335.68	0.946	335.2	0.989
341.12	0.827	339.90	0.891	340.29	0.931	339.9	0.978
345.92	0.779	344.68	0.851	345.16	0.910	344.6	0.963
350.72	0.706	349.46	0.803			349.3	0.935

Table 3.53 Temperature Dependence of the Fraction Folded from Glycine Chemical Shift Data for the Trp pocket Variants**.**

WWAL:		WWRL:		WWKK:		WWKW:	
Temp (K)	Fraction folded	Temp (K)	Fraction folded	Temp (K)	Fraction folded	Temp (K)	Fraction folded
274.43	0.878	275.44	0.968	271.40	0.960	271.82	0.982
278.85	0.880	279.80	0.970	276.30	0.956	276.68	0.984
283.28	0.880	284.16	0.971	281.19	0.951	281.55	0.987
287.70	0.877	288.52	0.973	286.08	0.945	286.42	0.991
292.12	0.872	292.88	0.974	290.98	0.937	291.28	0.996
296.55	0.864	297.24	0.975	295.87	0.928	296.15	0.998
300.97	0.854	301.60	0.974	300.77	0.914	301.02	1.003
305.39	0.843	305.96	0.971	305.66	0.897	305.89	1.005
309.82	0.831	310.32	0.968	310.55	0.877	310.75	1.008
314.24	0.816	314.68	0.962	315.45	0.850	315.62	1.009
318.66	0.798	319.03	0.953	320.34	0.816	320.49	1.008
323.09	0.776	323.39	0.941	325.24	0.780	325.35	1.004
327.51	0.751	327.75	0.923	330.13	0.741	330.22	0.996
331.93	0.717	332.11	0.901	335.02	0.693	335.09	0.984
336.36	0.687	336.47	0.873	339.92	0.644	339.95	0.966
340.78	0.648	340.83	0.841	344.81	0.588	344.82	0.941
345.20	0.605	345.19	0.797	349.71	0.525	349.69	0.907

WFKL:

Temp (K)	Fraction folded
274.42	0.923
278.85	0.920
283.28	0.915
287.70	0.909
292.13	0.903
296.55	0.895
300.98	0.885
305.40	0.871
309.83	0.856
314.25	0.838
318.68	0.816
323.11	0.794
327.53	0.760
331.96	0.723
336.38	0.690
340.81	0.648
345.23	0.598

vii. CD Spectroscopy.

CD spectroscopy was performed on an Applied photophysics Pistar-180 Circular Dichroism spectrophotometer. Spectra were collected at 215nm from 20°C to 90°C with 1 sec scanning. A CD comparison of **WWKme3L** in 10mM sodium phosphate buffer pH 7.0 and in the presence of 4M urea was made to insure that **WWKme3L** was still well folded before a co-chemical thermal melt was preformed as discussed in section A.ii.d (Figure 3.37).

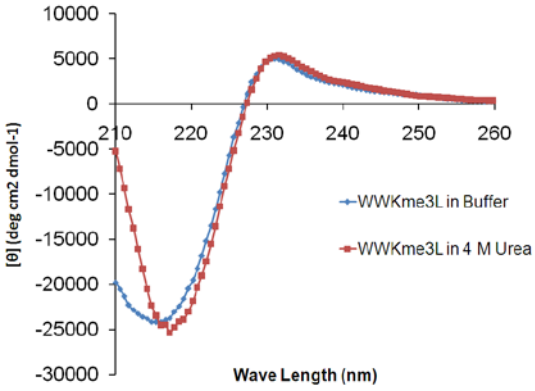

Figure 3.47 Comparison of CD spectra of **WWKme3L** in 10mM sodium phosphate buffer pH 7.0 and in 4 M Urea at 25°C.

CHAPTER IV

DESIGN OF SWITCH β-HAIRPIN PEPTIDES CONTROLLED BY POST-TRANSLATIONAL MODIFICATIONS

A. Background and Significance.

In biology, many cellular processes are regulated using chemical modification to proteins resulting in activation or deactivation of a specific function. Gene regulation can be controlled by modification to the histone proteins that package DNA. Currently there is extensive work on understanding how and what modifications to histone proteins affect gene transcription often referred to as the "Histone Code".[1] Not only do these modifications effect cell differentiation, it is becoming prevalent that altered histone modifications profiles are present in diseases.[2] In fact, misregulation of histone modifications is involved in malaria[3], mental disorders[4], and is being extensively studied in cancers[2]. Increased understanding of the histone code will not only further our understanding of fundamental biological processes but also lead to cures for a variety of diseases.

---

[1] Strahl, B. D.; Allis, C. D. *Nature* **2000**, *403*, 41-45.

[2] Lennartsson, A.; Ekwall, K. *Biochim Biophys Acta, Gen Subj* **2009**, *1790*, 863-868.

[3] Ralph, S. A.; Scherf, A. *Curr Opin Microbiol* **2005**, *8*, 434-440.

[4] (a) Waggoner, D. *Semin Pediatr Neurol* **2007**, *14*, 7-14. (b) Peedicayil, J. *Indian J Med Res* **2007**, *126*, 105-11.

Two prevalent modifications to the N-terminal tail of the H3 histone protein known to effect gene transcription are phosphorylation of serine 10 and methylation of lysine 9.[5] Methylation of lysine 9 of the H3 histone is known to induce binding to heterochromatin protein 1 (HP 1) which results in a restructuring of the chromatin structure that inhibits gene transcription.[6] The methylated lysine binds to an aromatic cage in HP 1 which only binds to di and trimethylated lysine.[7] This binding is largely driven by cation-π interactions between methylated lysine and the aromatic cage.[8] Work from the Allis laboratory has shown that HP 1 chromodomain is expelled from the from the histone complex when serine 10 of histone 3 is phosphorylated thus allowing for transcription to resume.[5] The phosphorylation of serine 10 on histone 3 disrupts a favorable hydrogen bond with a glutamic acid residue in the bind groove of HP 1 and results in a charge-charge repulsion.[5] More recently, characterization of Chp1 Chromodomain, another methylated lysine 9 recognition domain that utilizes an aromatic binding pocket, has shown that phosphorylation of serine 10 strongly reduces Chp1 binding affinity to the histone 3 tail.[9] A non-histone protein, Dam1 kinetochore protein also utilizes a similar cross-talk strategy using methylation of lysine and phosphorylation serine

---

[5] Fischle, W.; Tseng, B. S.; Dormann, H. L.; Ueberheide, B. M.; Garcia, B. A.; Shabanowitz, J.; Hunt, D. F.; Funabiki, H.; Allis, C. D. *Nature* **2005**, *438*, 1116-22.

[6] (a) Lachner, M.; O'Carroll, N.; Rea, S.; Mechtler, K.; Jenuwein, T. *Nature* **2001**, *410*, 116-120. (b) Nakayam, J.; Rice, J. C.; Strahl, B. D.; Allis, C. D.; Grewal, S. I. S. *Science* **2001**, *292*, 110-113. (c) Bannister, A. J.; Zegerman, P.; Partridge, J. F.; Miska, E. A.; Thomas, J. O.; Allshire, R. C.; Kouzarides, T. *Nature* **2001**, *410*, 120-124. (d) Nielsen, S. J.; Schneider, R.; Bauer, U. M.; Bannister, A. J.; Morrison, A.; O'Carroll, D.; Firestein, R.; Cleary, M.; Jenuwein, T.; Herrera, R. E.; Kouzarides, T. *Nature* **2001**, *412*, 561-565.

[7] Jacobs, S. A.; Khorasanizadeh, S. *Science* **2002**, *295*, 2080-2083.

[8] Hughes, R. M.; Wiggins, K. R.; Khorasanizadeh, S.; Waters, M. L. *Proc Nat Acad Sci U.S.A.* **2007**, *104*, 11184-11188.

[9] Schalch, T.; Job, G.; Noffsinger, V. J.; Shanker, S.; Kuscu, C.; Joshua-Tor, L.; Partridge, J. F. *Molecular Cell* **2009**, *34*, 36-46.

where methylation of Lys233 inhibits phosphorylation of nearby residues.[10] Phosphorylation of Dam1 is an important modification during chromosome segregation, thus methylation is acting as a switch to inhibit chromosome segregation. Using phosphorylation and methylation we sought to design a molecular switch peptide to investigate the effect of these modifications in a model system.

Many conformational switches peptides have been designed for a plethora of reasons. These peptides can be used as models for extremely complex structural transitions found in nature. Peptides that change conformational states have been designed to study protein misfolding diseases such as Alzheimer's and Parkinson's disease.[11,12,13] Other switch peptides have been designed as sensors in which a conformational change due to a stimulus results in a fluorescence signal.[12,14] Still others have been developed as novel self-assembling

[10] Zhang, K.; Lin, W. C.; Latham, J. A.; Riefler, G. M.; Schumacher, J. M.; Chan, C.; Tatchell, K.; Hawke, D. H.; Kobayashi, R.; Dent, S. Y. R. *Cell* **2005**, *122*, 723-734.

[11] Skwarczynski, M.; Kiso, Y. *Curr. Med. Chem.* **2007**, *14*, 2813-2823.

[12] Pagel, K.; Koksch, B. *Curr Opin Chem Biol* **2008**, *12*, 730-9.

[13] (a) Mutter, M.; Chandravarkar, A.; Boyat, C.; Lopez, J.; Dos Santos, S.; Mandal, B.; Mimna, R.; Murat, K.; Patiny, L.; Saucede, L.; Tuchscherer, G. *Angewandte Chemie-International Edition* **2004**, *43*, 4172-4178. (b) Taniguchi, A.; Skwarczynski, M.; Sohma, Y.; Okada, T.; Ikeda, K.; Prakash, H.; Mukai, H.; Hayashi, Y.; Kimura, T.; Hirota, S.; Matsuzaki, K.; Kiso, Y. *ChemBioChem* **2008**, *9*, 3055-3065. (c) Camus, M. S.; Dos Santos, S.; Chandravarkar, A.; Mandal, B.; Schmid, A. W.; Tuchscherer, G.; Mutter, M.; Lashuel, H. A. *ChemBioChem* **2008**, *9*, 2104-2112. (d) Mimna, R.; Camus, M. S.; Schmid, A.; Tuchscherer, G.; Lashuel, H. A.; Mutter, M. *Angew Chem Int Ed Engl* **2007**, *46*, 2681-4.

[14] (a) Balakrishnan, S.; Zondlo, N. J. *J Am Chem Soc* **2006**, *128*, 5590-5591. (b) Wang, Q.; Cahill, S. M.; Blumenstein, M.; Lawrence, D. S. *J Am Chem Soc* **2006**, *128*, 1808-1809. (c) Torrado, A.; Imperiali, B. *J. Org. Chem.* **1996**, *61*, 8940-8948. (d) Shults, M. D.; Pearce, D. A.; Imperiali, B. *J Am Chem Soc* **2003**, *125*, 10591-10597. (e) Walkup, G. K.; Imperiali, B. *J Am Chem Soc* **1997**, *119*, 3443-3450.

materials.[12,15,16] A variety of methods have been employed to induce a structural transition in switch peptides such as pH, temperature, metal binding, and chemical modification.[12] To this end, we sought to develop a hairpin switch system utilizing post-translational modifications (PTMs) to control the extent of β-hairpin formation through design elements elucidated in studies discussed in Chapters 2 and 3. Ideally this system would be moderately folded in an unmodified state, become well folded when a key lysine residue is methylated, and poorly folded when a key serine residue is phosphorylated.

B. Design towards ideal switch system.

i. WQKS Hairpin System.

The initial hairpin designed used in the development of a peptide in which PTMs modulate folding was based on previous report systems used to study the interaction cation-π interactions.[17] Thus, the peptide **WQKS** was used with key design features that we believed would alter the hairpin stability when specific PTMs are incorporated (Figure 4.1). The sequence orients a tryptophan in position 2 to interact with lysine at position 9 which as previously discussed results in a favorable cation-π interaction that helps to stabilize the hairpin fold. More importantly, when the side chain amine of lysine at position 9 is methylated, a more stable hairpin is produced through increased favorable interactions between the lysine side chain and indole ring of tryptophan.[18,19] We wanted to utilize this

[15] Kuhnle, H.; Borner, H. G. *Angew Chem Int Ed Engl* **2009**, *48*, 6431-4.

[16] Pochan, D. J.; Schneider, J. P.; Kretsinger, J.; Ozbas, B.; Rajagopal, K.; Haines, L. *J Am Chem Soc* **2003**, *125*, 11802-11803.

[17] Tatko, C. D.; Waters, M. L. *Protein Sci* **2003**, *12*, 2443-2452.

[18] Hughes, R. M.; Waters, M. L. *J Am Chem Soc* **2005**, *127*, 6518-9.

[19] Hughes, R. M.; Benshoff, M. L.; Waters, M. L. *Chem Eur J* **2007**, *13*, 5753-5764.

favorable interaction to increase the stability of our system when this key lysine is methylated. Serine 11 is also positioned directly cross strand from Trp 2 which, when phosphorylated, should decrease the overall hairpin stability due to an unfavorable interaction between the phosphate group and the indole ring of the tryptophan as was previously discussed in Chapter 2.[20]

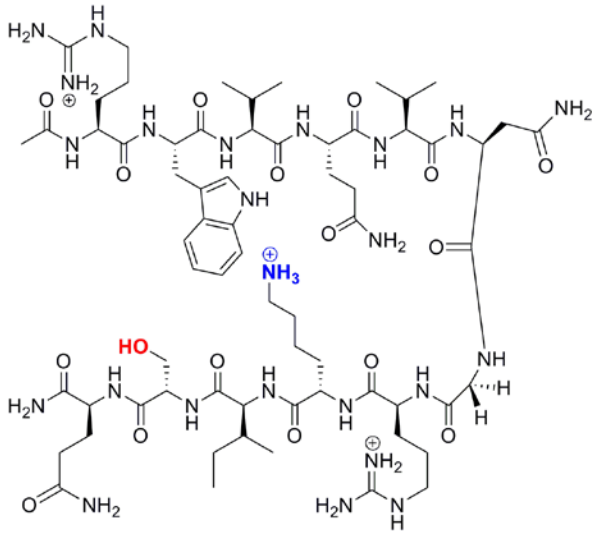

Figure 4.1 Schematic representation of **WQKS** series of peptides. The ammonium group of Lysine at position 2 in blue is dimethylated in **WQK(Me_2)S** and **WQK(Me_2)S(PO_3)** peptides. The hydroxyl group of serine at position 4 in red is phosphorylated in **WQKS(PO_3)** and **WQK(Me2)S(PO3)** peptides.

A series of five peptides where synthesized to investigate the effect of incorporating phosphoserine and dimethyl lysine on hairpin stability using the **WQKS** system. One dimensional NMR spectra where taken to assess β-hairpin formation of these peptides. The unmodified **WQKS** contains no residues with PTM's, **WQKS(PO_3)** contains phosphoserine at position 11, **WQK(Me_2)S** contains dimethyl lysine at position 9, and **WQK(Me_2)S(PO_3)** contains both PTMs. A cyclic control peptide **(cyclic WQKS)** was also synthesized as a

[20] Riemen, A. J.; Waters, M. L. *J Am Chem Soc* **2009**, *131*, 14081-14087.

100% folded control with the sequence Ac-CRWVQVNGOKISQC-NH2, in which the two terminal cystiene residues are linked via a disulfide bond.

Using the difference of proton splitting of Gly 7 for each of **WQKS** peptides, a fraction fold of hairpin formation was determined (Table 4.1). This method for the fraction folded calculation is described in the experimental section. Analysis of the fraction folded data revealed that the unmodified **WQKS** was rather poorly folded around 20%. The phosphorylated analog **WQKS(PO_3)** as predicted was less stable than **WQKS,** being roughly 16% folded. This is calculated as a destabilization of 0.15 Kcal/mol by the difference in ΔG of folding for **WQKS** and **WQKS(PO_3)**. The methylated analog **WQK(Me_2)S** was substantially more stable than its unmodified counter part, being approximately 40% folded. This is calculated as a 0.55 Kcal/mol increase in stability upon dimethylation of lysine 9. The double modified **WQK(Me_2)S(PO_3)** is 34% which is a 0.40 kcal/mol increase in stability over the unmodified **WQKS**. Interestingly, it appears that the effects of PTMs are additive in relationship to hairpin formation in this system, where methylation of lysine 9 added stability of -0.55 kcal/mol is diminished by phosphorylation of serine 11 by 0.15 kcal/mol to give a stablization of -0.40 kcal/mol in the double modified peptide (Table 4.1).

Table 4.1 NMR characteratization for **WQKS** β-hairpin peptides. Values calculated from data obtained at 20 °C, 50 mM potassium phosphate-*d2*, pD 4.0 (uncorrected), referenced to DSS.

Peptide	Observed Gly Splitting of Hα (ppm)[a]	Fraction Folded (Gly Splitting)[a]	ΔG Folding (kcal/mol)	ΔΔG (**WQKS(x)-WQKS)**
WQKS	0.10 (±0.01)	0.20 (±0.01)	0.80 (±0.03)	
WQKS(PO_3)	0.08 (±0.01)	0.16 (±0.01)	0.96 (±0.03)	0.15 (±0.04)
WQK(Me_2)S	0.20 (±0.01)	0.40 (±0.01)	0.24 (±0.03)	-0.55 (±0.04)
WQK(Me_2)S(PO_3)	0.17 (±0.01)	0.34 (±0.01)	0.39 (±0.03)	-0.40 (±0.04)
cyclic WQKS	0.50 (±0.01)	1.00 (±0.01)	-	-

(a) Error determined by chemical shift accuracy on NMR spectrometer.

Although the results of **WQKS** series are intriguing, the initial stability of the unmodified **WQKS** is far too low for any practical application, and the uncertainty in hairpin population in this region is high. Thus no further characterization of this system was preformed. Nonetheless the information gained from this design was promising, in that manipulation of hairpin formation using methylation of lysine and phosphorylation of serine is feasible.

ii. KSWQ Hairpin System.

The next β-hairpin design to investigate the effects of incorporating multiple PTMs on hairpin stability was the **KSWQ** system (Figure 4.2.). We sought to improve initial hairpin stability by positioning the key Trp residue on the non-hydrogen bonding (NHB) face closer to the turn region of the hairpin. Stabilizing residues closer to the turn sequence have been shown to increase overall stability by further enforcing β-sheet formation at the nucleating turn sequence.[21] To keep the favorable lysine-tryptophan interaction intact through position 2 – position 9 diagonal, lysine was positioned at residue 2 and tryptophan at position 9. Thus Trp 9 is close to the VNGO turn sequence while positioned to interact with lysine and dimethyl lysine at position 2. Serine was positioned at residue 4 so it is still oriented directly cross strand from tryptophan. An added feature of this design is the potential to use Protein Kinase A (PKA) to enzymatically phosphorylated the sequence, since PKA recognizes the sequence RKXS for phosphorylation at Ser 4.

[21] (a) Searle, M. S. *J Chem Soc, Perkin Trans 2* **2001**, 1011-1020. (b) Espinosa, J. F.; Munoz, V.; Gellman, S. H. *J Mol Biol* **2001**, *306*, 397-402. (c) Kiehna, S. E.; Waters, M. L. *Protein Sci* **2003**, *12*, 2657-2667.

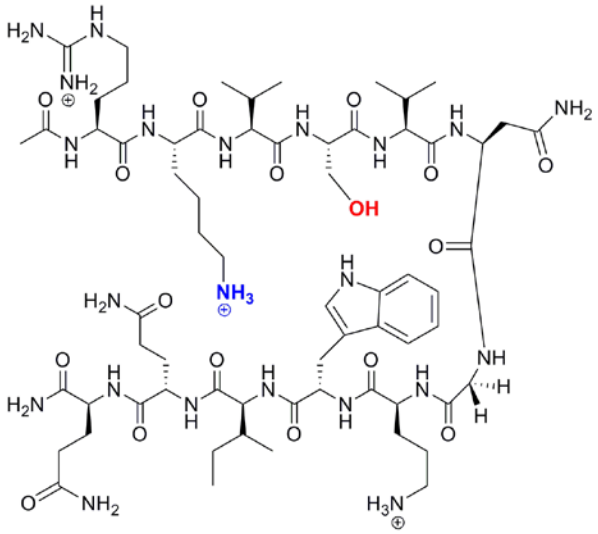

Figure 4.2 Schematic representation of **KSWQ** series of peptides. The ammonium group of Lysine at position 2 in blue is dimethylated in **K(Me_2)SWQ** and **K(Me_2)S(PO_3)WQ** peptides. The hydroxyl group of serine at position 4 in red is phosphorylated in **KS(PO_3)WQ** and **K(Me2)S(PO3)WQ** peptides.

The **KSWQ** series of peptides was synthesized and characterized by NMR. A cyclic **KSWQ** peptide was synthesized as fully folded controls for the **KSWQ** series β-hairpins. Cyclization was achieved by a disulfide bond between cysteine residues at the N and C-termini of the peptides. Unfolded control peptides consisting of either the N-terminal arm or the C-terminal arm were used to obtain random coil chemical shifts. β-sheet formation was first examined for each of **KSWQ** variants by the extent of Hα shifting from random coil (Figure 4.3). As discussed in Chapter 1, downfield shifting of≥ 0.1 ppm of the Hα protons along the peptide backbone relative to unfolded values indicates a β-sheet conformation.[22] Downfield shifting of the Hα protons showed that the peptides **KSWQ,** and **K(Me_2)SWQ** form β-hairpins with a majority of the backbone protons above 0.1 ppm. A larger extent of downfield shifting is observed for **K(Me_2)SWQ,** indicating a high degree of β-hairpin

[22] Sharman, G. J.; Griffiths-Jones, S. R.; Jourdan, M.; Searle, M. S. *J Am Chem Soc* **2001**, *123*, 12318-12324.

formation for the methylated lysine modification. The peptide **KS(PO_3)WQ** yielded no downfield shifting greater than 0.1 ppm with the exception of Trp 9. Incorporation of phosphoserine in this sequence results in a relatively unfolded peptide with little evidence for β-hairpin structure formation. The peptide **K(Me_2)S(PO_3)WQ** displays some downfield shifting above 0.1 ppm indicating that when both modifications are present there is still some hairpin formation albeit to a lesser extent than the unmodified **KSWQ**. Upfield shifting at Val 5 is observed for all peptides in the **KSWQ** series. This is likely due to electronic shielding of the indole ring of the cross strand Trp 9. The indole ring of Trp 9 may also be electronically shielding Ser 4, resulting in low downfield shifting in **KSWQ, K(Me_2)SWQ,** and **K(Me_2)S(PO_3)WQ**.

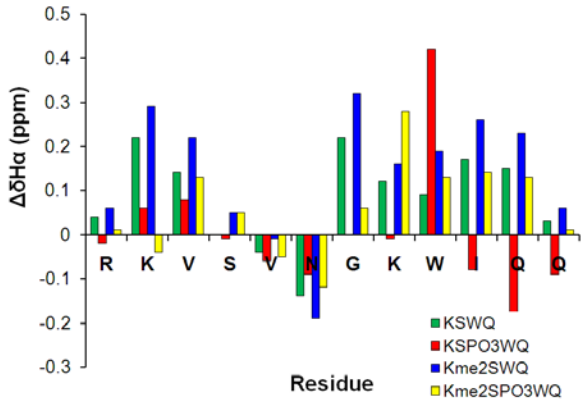

Figure 4.3 Hα chemical shift differences from random coil controls. The Gly bars reflect the Hα separation in the hairpin. Conditions: 293 K, 50 mM potassium phosphate in pD 4.0 buffer (uncorrected), referenced to DSS.

Quantification of the fraction folded was determined using both methods described in the experimental section for the **KSWQ** peptides (Table 4.2). The unmodified **KSWQ** peptide was estimated to be approximately 34% folded, with good agreement between Hα and Gly

splitting method of fraction folded determination. The phosphorylated **KS(PO_3)WQ** peptide is unfolded according to Gly splitting and approximately 10% folded by Hα. Discrepancy between fraction folded for this peptide is likely due to the close proximity of the phosphate group to the Gly in the turn, altering the Gly splitting. Using the estimated fraction folded from the Hα calculation, it seems that phosphorylation is causing 0.5 kcal/mol destabilization in hairpin structure for **KSWQ** sequence. The methylated **K(Me_2)SWQ** peptide is approximately 50% folded with good agreement between both α shifting and Gly splitting. This is a 0.4 kcal/mol stablization in hairpin structure when lysine is dimethylated at position 2. The double modified **K(Me_2)S(PO_3)WQ** peptide is 13% folded by glycine and 26% folded by Hα shifting. Again the discrepancy between fraction folded values for this peptide is likely due to the effect of the phosphoserine in close proximity to Gly 7 as previously discussed. Using estimated fraction folded from the Hα calculation this hairpin is destabilized by 0.2 Kcal/mol with both modifications present. It is important to note that all of the energies of stablization or destabilization for the **KSWQ** peptide system were calculated using the Hα calculation of fraction folded because this uses several residues to determine the extent of folding rather than just one. However in this peptide system there is a relatively large discrepancy in fraction folded on a per residue basis resulting in a high degree of error in ΔG of folding values. Assuming that the values are accurate this peptide is more destabilized by phosphorylation than previously discussed **WQKS** system. It seems that dimethylated lysine in **KSWQ** has a lesser effect on the overall stability as when compared to the **WQKS** as well.

Table 4.2 Fraction folded and ΔG of folding for β-hairpin peptides. Values calculated from data obtained at 20 °C, 50 mM potassium phosphate-*d2*, pD 4.0 (uncorrected), referenced to DSS.

Peptide	Fraction Folded (Gly Splitting)[a]	Fraction Folded (Hα)[b]	ΔG Folding (kcal/mol)	ΔΔG (KSWQ**(x)-KSWQ)**
KSWQ	0.33 (±0.01)	0.34 (±0.07)	0.4 (±0.2)	
KS(PO_3)WQ	0.00 (±0.01)	0.10 (±0.07)	0.9 (±0.2)	0.5(±0.2)
K(Me_2)SWQ	0.49 (±0.01)	0.50 (±0.07)	0.0 (±0.2)	- 0.4 (±0.2)
K(Me_2)S(PO_3)WQ	0.13 (±0.01)	0.26 (±0.08)	0.6 (±0.2)	0.2 (±0.2)

(a) Error determined by chemical shift accuracy on NMR spectrometer. (b) Average of the Hα values from Val3, Val5, Orn8, and Ile10. The standard deviation is in parentheses.

To assess if **KSWQ** peptide could be enzymatically phosphorylated by a kinase, the unmodified **KSWQ** was incubated with catalytic subunit of Protein Kinase A (PKA) from bovine heart. After 24 hours all of **KSWQ** peptide was completely converted to **KS(PO3)WQ** and confirmed by mass spectrometry.

The **KSWQ** design yielded a more stable β-hairpin in the unmodified state than **WQKS** but it was still relatively low and large discrepancies in the determination of fraction folded were observed for all hairpin peptides in this series. For these reasons, no further studies were conducted on this system. Yet this design gave some evidence that phosphorylation towards the turn results in a larger destabilization of hairpin formation. It was also shown that this peptide sequence can be enzymatically phosphorylated by PKA which was encouraging for future designs that could potentially be used as sensors.

iii. WWKS System.

The next design sequence studied for a potential tunable peptide that relies on phosphorylation of serine for destabilization of structure and methylation of lysine for stabilization was the **WWKS** system (Figure 4.4). This sequence is based on the **Trppocket**

sequence discussed in Chapter 3[23] where the leucine residue at position 11 is replaced with serine or phosphoserine. From previous studies on the **Trppocket** hairpin system it is expected that the **WWKS** system will be well folded with a highly favorable interaction between Lys 9 and the cross strand tryptophan cleft at positions 2 and 4. Also a methylated lysine at position 9 should be more stable than an unmethylated counterpart. However, we did not know if phosphorylation at Ser 11 would be sufficient enough to cause a desired global destabilization of hairpin formation. The phosphoserine is positioned towards the termini of the hairpin, as well as being oriented on the outside of the stabilizing side chain-side chain cluster which may only result in a local of alteration at positions 11 and 12.

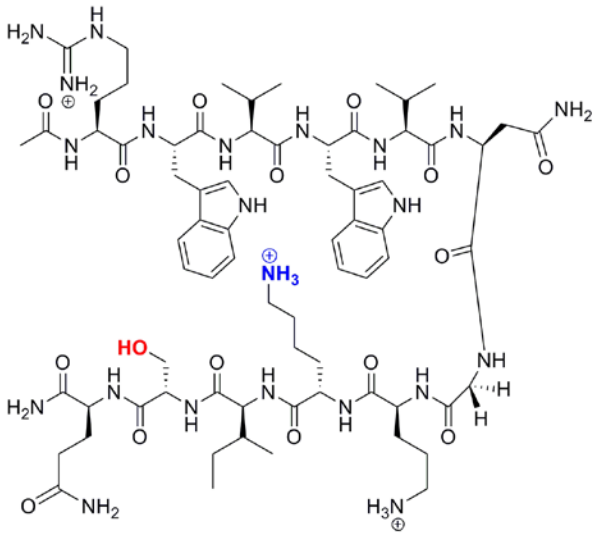

Figure 4.4 Schematic representation of **WWKS** series of peptides. The ammonium group of Lysine at position 2 in blue is dimethylated in **WWK(Me_2)S** and **WWK(Me_2)S(PO_3)** peptides. The hydroxyl group of serine at position 4 in red is phosphorylated in **WWKS(PO_3)** and **WWK(Me2)S(PO_3)** peptides.

Since there was a potential that phosphorylated **WWKS** hairpin would not be destabilized, only the unmodified **WWKS, WWKS(PO_3)** and **cyclic WWKS** were

[23] Riemen, A. J.; Waters, M. L. *Biochemistry* **2009**, *48*, 1525-1531.

synthesized and characterized by NMR. Analysis of Hα chemical shifts compared to random coil controls indicated that the unmodified **WWKS** peptide forms a well folded β-hairpin peptide (Figure 4.5). A large degree of downfield shifting from random coil was observed for the residues composing of the β-sheet was observed with exception of residues 9 and 11 which were upfield shifted, as is seen in the Trppocket peptide and is caused by electronic shielding of the cross-strand tryptophans. Analysis of Hα chemical shifts for the phosphorylated **WWKS(PO_3)** also revealed a well folded hairpin. The Hα shifting observed was very similar to the Hα shifting in the unmodified **WWKS** peptide with exception of residue 11 which was downfield shifted.

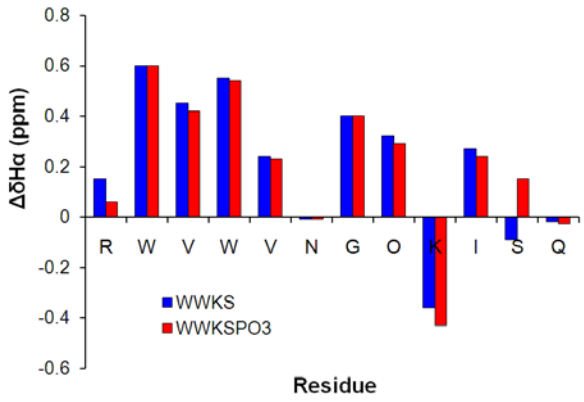

Figure 4.5 Hα chemical shift differences from random coil controls. The Gly bars reflect the Hα separation in the hairpin. Conditions: 293 K, 50 mM potassium phosphate in pD 4.0 buffer (uncorrected), referenced to DSS.

Quantification of the fraction folded for both **WWKS** and **WWKS(PO_3)** was calculated using the methods discussed in the experimental (Table 4.3). This confirmed that a moderately high degree of folding was occurring in both peptides and that there was little global alteration in hairpin structure with incorporation of phosphoserine at position 11. Both peptides are within error of each other in the 70% folded regime. There was no alteration in

the degree of glycine splitting indicating that the turn region was not affected by phosphorylation towards the terminus in this hairpin design.

Table 4.3 Fraction folded and ΔG of folding for β-hairpin peptides. Values calculated from data obtained at 20 °C, 50 mM potassium phosphate-*d2*, pD 4.0 (uncorrected), referenced to DSS.

Peptide	Fraction Folded (Gly Splitting)[a]	Fraction Folded (Hα)[b]
WWKS	0.72 (±0.01)	0.77 (±0.08)
WWKS(PO_3)	0.72 (±0.01)	0.71 (±0.08)

Indeed it was apparent that phosphoserine did little to alter the structure of this well folded system. Thus, no further studies were conducted using this sequence because the criteria for unfolding by phosphorylation were not met. Even through this sequence did not meet the desired goals, important design elements where elucidated. In particular, the incorporation of a tryptophan cleft on the NHB face of the hairpin was highly stabilizing which resulted in a moderately well folded unmodified sequence.

C. Trpswitch (KSWW) Studies.

i. Design.

The **Trpswitch** β-hairpin peptide was based on previously discussed β-hairpin systems.[23] A schematic representation is given in Figure 4.6. The lysine at position 2 is located on the NHB face of the β-hairpin cross strand from a tryptophan pocket motif found to be highly stabilizing in previously discussed trppocket peptide[23], however now the tryptophan pocket is oriented on the C-terminal chain of the β-hairpin as opposed to the N-terminal chain. Di-methylated lysine is known to have a more favorable interaction with the tryptophan cleft in the Trp Pocket peptides[23] so it is expected that the incorporation of dimethyl lysine at position 2 will increase overall folding. The serine at position 4 on the NHB face, is located

cross-strand from tryptophan 9 is not expected to have any unfavorable interactions until it is phosphorylated causing a disruption in the β-hairpin structure as seen in previously discussed β-hairpin systems.[20] This interaction should be highly destabilizing because it occurs close to the nucleating turn sequence. Essentially we have combined the favorable design elements from the **KSWQ** with **WWKS** to create the desired switch system. Extensive characterization was performed on the **Trpswitch** series because it met the desired criteria we sought.

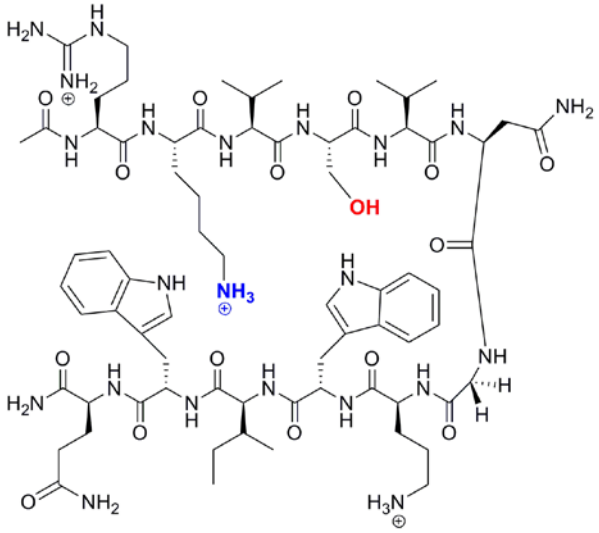

Figure 4.6 Schematic representation of **Trpswitch** series of peptides. The ammonium group of Lysine at position 2 in blue is dimethylated in **Trpswitch(Me_2)** and **Trpswitch(Me_2PO_3)** peptides. The hydroxyl group of serine at position 4 in red is phosphorylated in **Trpswitch(PO_3)** and **Trpswitch(Me_2PO_3)** peptides.

ii. Trpswitch Peptide structure studies.

Structural studies were preformed on **Trpswitch** peptide and its modified variants using NMR spectroscopy and circular dichroism (CD). As previously discussed, downfield chemical shifts of the Hα from random coil values in the peptide backbone are indicative of β-hairpin structure and can be used to determine the extent of folding. [22,24,25,26] A downfield

[24] Syud, F. A.; Stanger, H. E.; Gellman, S. H. *J Am Chem Soc* **2001**, *123*, 8667-8677.

shift of ≥ 0.1 of at least 3 consecutive residues from random coil value indicate β-sheet structure (Figure 4.7a).[22] The peptides **Trpswitch**, **Trpswitch(Me_2)** and **Trpswitch(Me_2PO_3)** all exhibit downfield shifting of at least 0.1 ppm for residues designed to form β-sheet with exception to serine 4 and valine 5 which are upfield shifted due to electronic shielding from cross strand indole rings of the tryptophan at position 9. This is similar to what was seen in the **KSWQ** system. The peptide **Trpswitch(PO_3)** appears to be unstructured with little difference from random coil values. The extent of these peptides folding into a β-hairpin structure was quantified using two methods describe in the experimental section involving the splitting difference observed from the diastereotopic glycine Hα in the turn and the extent of Hα shifting per residue compared to 100% folded cyclic control . **Trpswitch** is calculated to be approximately 65% folded in aqueous solution (Table 4.4). **Trpswitch(PO_3)** folding is negligible and is considered unstructured. Incorporation of the phosphoserine resulted in a net destabilization of at least 2.0 kcal/mol of the ΔG of folding from the unmodified **Trpswitch**. **Trpswitch(Me_2)** is calculated to be approximately 86% folded which is a 0.7 kcal/mol increase of stabilization (Table 4.4). The doubly modified peptide **Trpswitch(Me_2PO_3)** is calculated to be roughly 30% folded and is approximately a 0.9 kcal/mol decrease in stability when compared to the unmodified **Trpswitch** (Table 4.4).

---

[25] Griffiths-Jones, S. R.; Maynard, A. J.; Searle, M. S. *J Mol Biol* **1999**, *292*, 1051-69.

[26] Syud, F. A.; Espinosa, J. F.; Gellman, S. H. *J Am Chem Soc* **1999**, *121*, 11577-11578.

Table 4.4 Fraction folded and ΔG of folding for β-hairpin peptides. Values calculated from data obtained at 20 °C, 50 mM potassium phosphate-*d2*, pD 7.0 (uncorrected), referenced to DSS.

Peptide	Fraction Folded (Gly Splitting)[a]	Fraction Folded (Hα)[b]	ΔG Folding (kcal/mol)	ΔΔG (**Trpswitch(x)-Trpswitch)**
Trpswitch	0.68 (±0.01)	0.65 (±0.02)	-0.37 (±0.02)	
Trpswitch(PO_3)	0 (±0.01)	0.05 (±0.07)	1.7 (±1.0)	2.07 (±1.0)
Trpswitch(Me_2)	0.89 (±0.01)	0.86 (±0.08)	-1.11 (±0.08)	-0.73 (±0.08)
Trpswitch(Me_2PO_3)	0.43 (±0.01)	0.30 (±0.08)	0.5 (±0.2)	0.87 (±0.2)

(a) Error determined by chemical shift accuracy on NMR spectrometer. (b) Average of the Hα values from Val3, Val5, Orn8, and Ile10. The standard deviation is in parentheses.

The use of CD was also employed to confirm β-sheet structure of these peptides (Figure 4.7b). β-sheet structure is characterized by a minima between 210-215 nm while random coil structure is characterized by a minima around 198 nm. The spectra of **Trpswitch** and **Trpswitch(Me_2)** have large minima at 215 nm with **Trpswitch(Me_2)** having the larger of the two, which correlates well with the NMR data, confirming that theses are well folded β-hairpins. **Trpswitch(PO_3)** has a large minima at 198 nm which is expected since this peptide appears to be unfolded by NMR. The CD spectrum of **Trpswitch(Me_2PO_3)** appears as a mixture between unfolded and β-sheet structure with a minima around 198 nm and a shoulder at 215 nm which is consistent with the NMR data estimating that this peptide is only 30% folded.

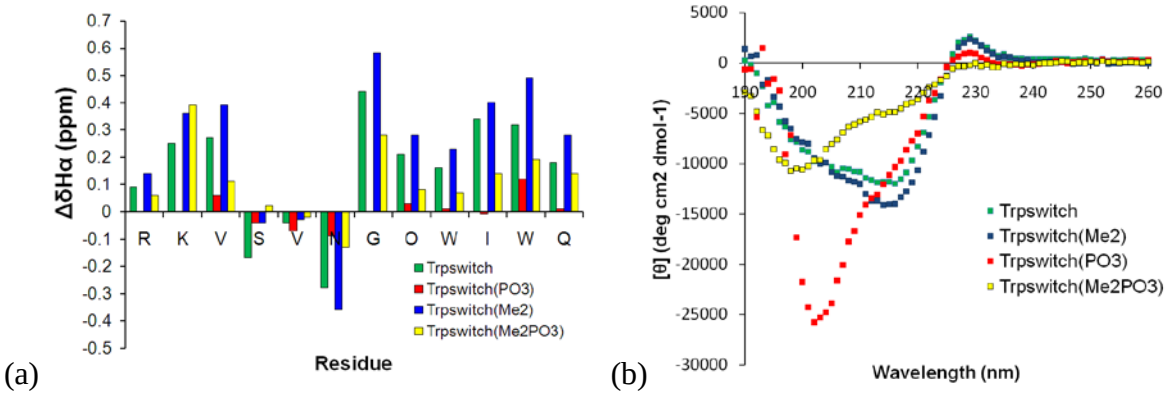

Figure 4.7 (a) Hα chemical shift differences from random coil controls. The Gly bars reflect the Hα separation in the hairpin. Conditions: 293 K, 50 mM potassium phosphate in pD 7.0 buffer (uncorrected), referenced to DSS. (**b)** Circular dichroism spectra comparison of Trpswitch peptides at 298 K in 10 mM sodium phosphate pH 7.0 buffer.

iii. Methylation of Lysine results in increased β-hairpin stability.

The unmodified **Trpswitch** peptide is moderately folded allowing for its stability to be increased or decreased upon modification. Incorporation of dimethylated lysine results in a more stable β-hairpin as was seen in the similar Trp pocket peptide.[23] In nature, an aromatic cage motif is observed in the crystal structures of methylated lysine recognition domains and many of these domains have been shown to be specific for di, or trimethylated lysine while having negligible binding affinity to unmodified lysine.[27] Increase in β-hairpin stability in the **Trpswitch(Me$_2$)** peptide is due to more favorable interaction of the dimethyl ammonium group with the two cross strand tryptophan indole rings. This is observed in NMR by the upfield shifting of the dimethyl lysine side chain from random coil values (Figure 4.8). Upfield shifting of the lysine side chain is the result of these hydrogens being electronically shielded by π-clouds of indole rings in the cross strand tryptophans. Thus, the more upfield shifting observed indicates increased interaction of the lysine side chain with the tryptophan

[27] (a) Adams-Cioaba, M. A.; Min, J. R. *Biochem Cell Biol* **2009**, *87*, 93-105. (b) Taverna, S. D.; Li, H.; Ruthenburg, A. J.; Allis, C. D.; Patel, D. J. *Nat Struct Mol Biol* **2007**, *14*, 1025-1040.

pocket. Comparison of the extent of side chain residue upfield shifting between **Trpswitch** and **Trpswitch(Me$_2$)** of lysine 2 also shows an interesting trend where in **Trpswitch** the delta and the epsilon methylene hydrogens experience approximately the same amount of upfield shifting and the gamma methylene experiences little upfield shifting whereas **Trpswitch(Me$_2$)** shows a progressive increase in upfield shifting of the methylene hydrogens from the gamma to epsilon position. This difference in upfield shifting along the lysine side chain suggests that lysine and dimethylated lysine are interacting differently with the cross-strand tryptophans. **Trpswitch(Me$_2$PO$_3$)** also exhibits some upfield shifting of dimethylated lysine but to a much lesser extent compared to **Trpswitch** and **Trpswitch(Me$_2$)** which suggests that this lysine is interacting to some extent with the tryptophans retaining some β-hairpin-like structure, correlating with Hα shift and CD data. The lysine in **Trpswitch(PO$_3$)** has some slight upfield shifting of its side chain protons which suggests that the peptide may rarely sample a conformation where lysine can interact with the tryptophans even though the extent of β-hairpin formation is estimated to be zero.

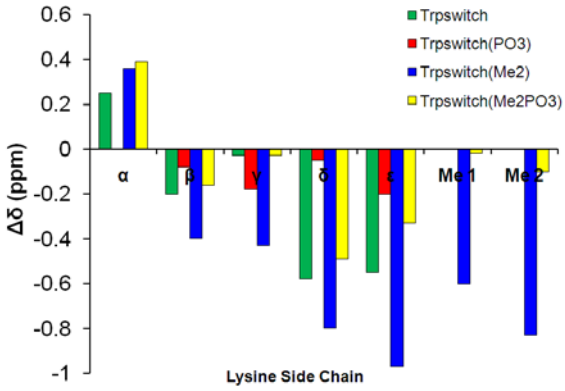

Figure 4.8 Lysine 2 side chain chemical shift from random coil values. Conditions: 20 °C, 50 mM potassium phosphate-*d2*, pD 7.0 (uncorrected), referenced to DSS.

NOESY NMR experiments were also preformed on the more stable **Trpswitch** and **Trpswitch(Me$_2$)** peptides to further confirm β-hairpin formation and specific side chain

interactions (Figure 4.9). **Trpswitch** has cross strand NOEs between tryptophan at position 9 and lysine 2 as well as serine 4. It appears that tryptophan 11 has little contact with lysine 2 or the nature of this interaction is highly dynamic thus resulting in no observed long range NOEs. **Trpswitch(Me_2)** has more cross strand interactions between the lysine side chain and the two tryptophans suggesting a more rigid and stable structure β-hairpin than the unmethylated **Trpswitch**. Some of the cross strand NOEs observed for tryptophan 9 and lysine 2 are different between **Trpswitch** and **Trpswitch(Me_2)** which suggests that the tryptophans are adopting different conformations in the two peptides which is supported by lysine upfield shifting data.

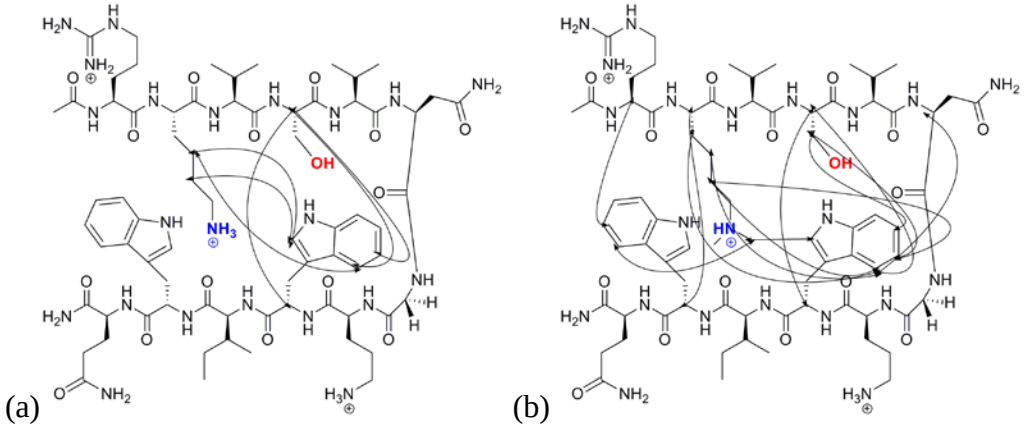

Figure 4.9 NOEs of cross strand residues on the NHB face in (a) **Trpswitch**, (b) **Trpswitch(Me_2)**.

Thermal denaturations were performed on the well folded peptides **Trpswitch** and **Trpswitch(Me_2)** to obtain thermodynamic parameters for folding to gain insight to the driving forces involved in β-hairpin stabilization. Peptide unfolding was monitored by NMR (Figure 4.10) using the extent of glycine splitting to determine fraction folded as described in the experimental section. The data was fit to extract the ΔH°, ΔS°, and ΔCp° of folding using the method reported by Searle (eq 4 experimental) (Table 4.5).[28] **Trpswitch(Me_2)** has a

[28] Maynard, A. J.; Sharman, G. J.; Searle, M. S. *J Am Chem Soc* **1998**, *120*, 1996-2007.

larger enthalpic component than the unmodified **Trpswitch** and a relatively similar entropic penalty for folding. The increased enthalpy of folding for **Trpswitch(Me_2)** can be explained by a stronger cation-π interaction between the tryptophan cleft and the dimethyl lysine as opposed to unmethylated lysine. A Cation-π interaction of the positively charged lysine and methylated lysine packing against the π-clouds of tryptophans has been shown to be a major stabilizing force in many β-hairpins.[17,18,19,29] In these previously reported systems methylation of lysine results in the change of driving force for folding from more enthalpic to more entropic due to more favorable hydrophobic packing of the methyl groups with the tryptophan along with distributing the cationic charge on the methyl groups allowing for increased number favorable conformations. However this is not what is observed in **Trpswitch** system. The cation-pi interaction is stronger with dimethyl lysine in **Trpswitch(Me_2)** which is indicated by the more favorable ΔH° of folding and extent of upfield shifting of the dimethylated lysine side chains. This discrepancy may be due to the positioning of the tryptophan cleft and the lysine, where in the trppocket system[23] the tryptophan cleft is located on the N-terminal strand of the hairpin and the lysine is close to the more ordered turn region. The lysine and the tryptophans may not adopt an optimal cation-pi interaction in **Trpswitch** until it is methylated thus promoting a more stable β-hairpin conformation**.** This hypothesis is supported by the NOE data for **Trpswitch** where the lysine has very few contacts with tryptophan 9 that suggest lysine is highly dynamic and thus a large entropic penalty is observed in the more stable **Trpswitch(Me_2)** which is ordering this side chain. A negative heat capacity, ΔCp°, of folding is an indication that

[29] Hughes, R. M.; Kiehna, S. E.; Waters, M. L. *Biopolymers* **2005**, *80*, 497-497.

hydrophobic clustering is occurring in the folded β-hairpin[30] which is observed for both **Trpswitch** and **Trpswitch(Me$_2$)**.

Table 4.5 Thermodynamic Parameters for Folding at 298 K for **Trpswitch** and **Trpswitch(Me$_2$)** peptides. Conditions: 50 mM sodium acetate-d_4, pH 4.0 (uncorrected), referenced to DSS. Error obtained through thermal data fitting of equation 4 (experimental).

Peptide	ΔH° kcal/mol	ΔS° cal/mol K	ΔCp° cal/mol K
Trpswitch	-6.88 (±0.8)	-22 (±0.2)	-55 (±9)
Trpswitch(Me$_2$)	-8.1 (±0.1)	-23.9 (±0.4)	-60 (±11)

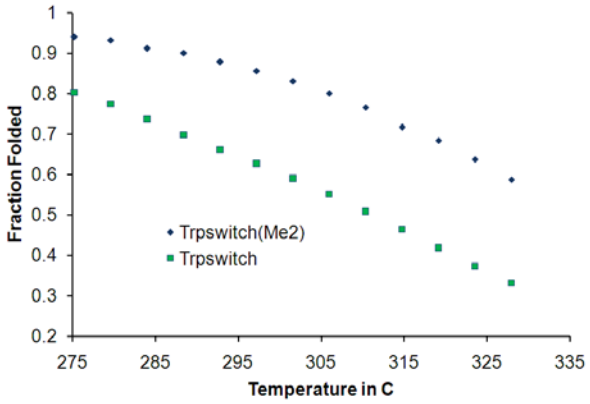

Figure 4.10 Thermal Denaturation of **Trpswitch[**green] and **Trpswitch(Me2)[**blue]**.** Values calculated from data obtained in 50 mM sodium acetate-d_4, pH 4.0 (uncorrected), referenced to DSS. Fraction folded was calculated from extent of Gly splitting.

iv. Destablization of Trpswitch by Phosphoserine.

There have been reported peptide systems that observe a loss in secondary structure or local conformation due to phosphorylation of key residues. [20,31,32,33,34] Disruption of α-

[30] Prabhu, N. V.; Sharp, K. A. *Annu Rev Phys Chem* **2005**, *56*, 521-48.

[31] Szilak, L.; Moitra, J.; Krylov, D.; Vinson, C. *Nat Struct Biol* **1997**, *4*, 112-4.

[32] Garcia-Alai, M. M.; Gallo, M.; Salame, M.; Wetzler, D. E.; McBride, A. A.; Paci, M.; Cicero, D. O.; de Prat-Gay, G. *Structure* **2006**, *14*, 309-319.

helical peptides has been observed when residues on the interior of the helix are phosphorylated.[31,33,34] Peptide studies on the PEST sequence in the E2 protein from the papillomavirus have shown that serine phosphorylation of this region destabilize intrinsic α-helical and poly-proline II structure.[32] The destabilization that occurs when serine 4 is phosphorylated in **Trpswitch(PO_3)** and **Trpswitch(Me_2PO_3)** is primarily the result of unfavorable cross-strand anion-pi interaction as was reported in similar β-hairpin systems.[20] The negatively charged phosphate is repulsed by the electron rich indole ring of the cross strand tryptophan that results in the disruption of the β-hairpin formation. As was observed in previously discussed phosphorylated hairpins in Chapter 2[20] the β-hairpin structure is retained by **Trpswitch(PO_3)** and **Trpswitch(Me_2PO_3)** in lower pH where the phosphate group is protonated thus reducing its electronegativity (Figure 4.11 and Table 4.). Since the extent of folding is not completely regained at pH 1.2 where the phosphate group is neutrally charged, phosphoserine could also be prohibiting more stable hairpin structure through steric clash of the sidechains or poorer β-sheet propensity.

---

[33] Tokmakov, A. A.; Sato, K. I.; Fukami, Y. *Biochem Biophys Res Commun* **1997**, *236*, 243-7.

[34] Andrew, C. D.; Warwicker, J.; Jones, G. R.; Doig, A. J. *Biochemistry* **2002**, *41*, 1897-1905.

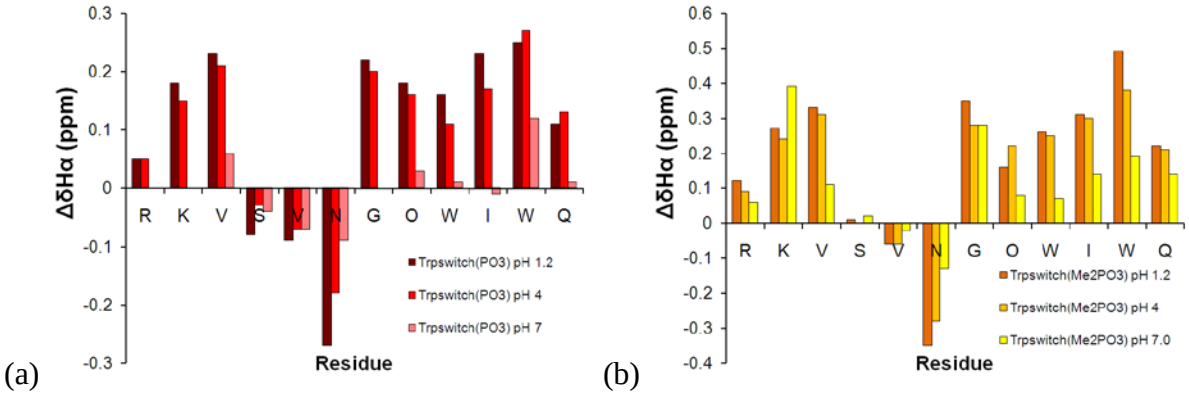

Figure 4.11 Hα chemical shift differences from random coil controls in varying pD for (a) **Trpswitch(PO3)** and (b) **Trpswitch(Me2PO3)**.The Gly bars reflect the Hα separation in the hairpin. At pD 7.0 the phosphate group has a 2- charge, while at pD 4.0 it has 1- charge and a neutral charge at pD 1.2. All NMR data obtained at 20°C.

Table 4.6 Fraction folded of phosphorylated **Trpswitch** analogs. Fraction folded determined from Val 3, Gly 7, Orn 8, and Ile 10 Hα chemical shift data as described in experimental. Error calculated from standard deviation of average residue fraction folded calculations.

	Fraction Folded		
Peptide	pH 1.2	pH 4.0	pH 7.0
Trpswitch(PO_3)	0.51 (±0.07)	0.44 (±0.10)	0.05 (±0.07)
Trpswitch(Me_2PO_3)	0.60 (±0.12)	0.60 (±0.13)	0.30 (±0.08)

v. Enzymatic phosphorylation of Trpswitch.

To assess if the Trpswitch peptide could be enzymatically phosphorylated by a kinase, **Trpswitch** and **Trpswitch(Me_2)** were incubated with catalytic subunit of Protein Kinase A (PKA) from bovine heart. After 24 hours all of **Trpswitch** peptide was completely converted to **Trpswitch(PO_3)** confirmed by mass spectrometry. **Trpswitch(Me_2)** was also phosphorylated to **Trpswitch(Me_2PO_3)** but still contained some unphosphorylated peptide after 24 hours. The slower phosphorylation of **Trpswitch(Me_2)** is speculated to be due to either the incorporation of the dimethyl lysine or the increased β-hairpin stability or a

combination of both. The dimethyllysine may not be the optimal residue for substrate recognition of PKA thus causing a decrease in the rate of phosphorylation. The β-hairpin conformation may also prevent proper binding to PKA and the **Trpswitch** must therefore unfold to be phosphorylated which happens less frequently in the more stable **Trpswitch(Me$_2$)**. A crystal structure of PKA bound to a peptide substrate that cannot be phosphorylated due a mutation of serine to an alanine shows an extend structure in the active site of the enzyme (Figure 4.12), providing evidence that unfolding of the β-hairpin is required for phosphorylation.[35] Thus, not only does methylation stabilize the folded state, it also acts as an inhibitor to phosphorylation, thereby maintaining the folded or "on" state. The ability for **Trpswitch** to be enzymatically phosphorylated is promising for future *de novo* designed β-hairpin peptides, where their structure can be controlled *in vivo*.

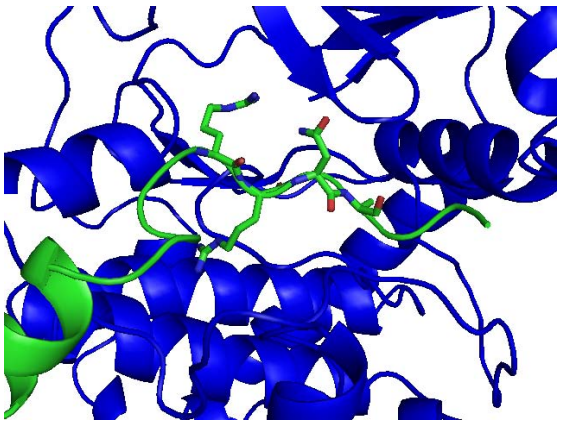

Figure 4.12 Peptide substrate bound to porcine PKA active site (pdb: 2GFC). Peptide substrate contains recognition sequence RRNA in green and PKA enzyme is represented in blue.

[35] Bossemeyer, D.; Engh, R. A.; Kinzel, V.; Ponstingl, H.; Huber, R. *EMBO J* **1993**, *12*, 849-859.

D. Conclusion.

Using an iterative design processes we have designed a moderately folded β-hairpin peptide, that's stability can be tuned based on the type of post-translational modification present. As is seen in HP1-histone 3 interaction, methylation of a key lysine residue results in a favorable cation-pi interaction that promotes a more stable structure in **Trpswitch**. The hairpin structure can be destabilized upon the incorporation phosphoserine which is similar to lose of binding of HP 1 to Histone 3 when a specific serine residue is phosphorylated. By using post-translational modification, it is feasible to design sensor systems to study biological systems that use these modifications. Through proper design, small structured peptide systems can also be used to explore the effects of post-translational modification in more complex naturally occurring systems. The **Trpswitch** peptide lends itself as a starting point to design more complicated peptide systems that rely on post-translation modification to tune structure resulting in a lose or gain of function.

E. Experimental.

i. Synthesis and Purification of peptides.

Peptides were synthesized by automated solid phase peptide synthesis on an Applied Biosystems Pioneer Peptide Synthesizer using Fmoc protected amino acids on a PEG-PAL-PS resin. Fmoc-[N]-protected and Benzl-[O]-protected phosphoserine, and dimethylated Fmoc-protected lysine were purchased from AnaSpec. Activation of amino acids was performed with HBTU, HOBT in the presence of DIPEA in DMF. Peptide deprotection was carried out in 2% DBU, 2% piperidine in DMF for approximately 10 min. Extended cycles (75 min) were used for each amino acid coupling step. All control peptides where acetylated at the N-terminus with 5% acetic anhydride, 6% lutidine in DMF for 30 min. Cleavage of the peptide from the resin was performed in 95:2.5:2.5 Trifluoroacetic acid (TFA): Ethanedithiol

or Triisopropylsilane (TIPS): water for 3 h. Ethanedithiol was used as a scavenger in for sulfur containing peptides. TFA was evaporated and cleavage products were precipitated with cold ether. The peptide was extracted into water and lyophilized. It was then purified by reverse phase HPLC, using a Vydac C-18 semipreparative column and a gradient of 0 to 100% B over 40 minutes, where solvent A was 95:5 water:acetonitrile, 0.1% TFA and solvent B was 95:5 actonitrile:water, 0.1% TFA. After purification the peptide was lyophilized to powder and identified with ESI-TOF mass spectroscopy.

ii. Cyclization of peptides.

Cyclic control peptides were cyclized by oxidizing the cysteine residues at the ends of the peptide via stirring in a 10 mM phosphate buffer (pH 7.5) in 1% DMSO solution for 9 to 12 hours. The solution was lyophilized to a powder and purified with HPLC using the method described above.

iii. CD Spectroscopy.

CD spectroscopy was performed on an Aviv 62DS Circular Dichroism Spectrophotometer. Spectra were collected from 260 nm to 185 nm at 25°C, 1 sec scanning.

iv. NMR Spectroscopy.

NMR samples were made to a concentration of 1 mM in D_2O buffered to pD 4.0 (uncorrected) with 50 mM NaOAc-d3, 24 mM AcOH-d4, 0.5 mM DSS, or pD 7.0 (uncorrected) with 50 mM $KPOD_4$, 0.5 mM DSS. Samples were analyzed on a Varian Inova 600-MHz instrument. One dimensional spectra were collected by using 32-K data points and between 8 to 128 scans using 1.5 sec presaturation. Two dimensional total correlation spectroscopy (TOCSY), nuclear Overhauser spectroscopy (NOESY) experiments were

carried out using the pulse sequences from the chempack software. Scans in the TOCSY experiments were taken 16 to 32 in the first dimension and 64 to 128 in the second dimension. Scans in the NOESY experiments were taken 32 to 64 in the first dimension and 128 to 512 in the second dimension with mixing times of 200 to 500 msec. All spectra were analyzed using standard window functions (sinbell and Gaussian with shifting). Presaturation was used to suppress the water resonance. Assignments were made by using standard methods as described by Wüthrich.[36] All experiments were run at 293 K except for thermal melt experiments.

Table 4.7 NOEs observed in Peptides **Trpswitch ,** and **Trpswitch(Me_2)** at 298K.

Trpswitch				Trpswitch(Me2)			
Residue	**Proton**	**Residue**	**Proton**	**Residue**	**Proton**	**Residue**	**Proton**
Lys 2	γ	Trp 9	Ar 2	Arg 1	α	Trp 11	Ar 5
Lys 2	δ	Trp 9	Ar 2	Lys 2	α	Trp 11	α
Lys 2	γ	Trp 9	Ar 4	Lys 2	β	Trp 11	α
Ser 4	α	Trp 9	α	Lys 2	γ	Trp 9	Ar 4
Ser 4	α	Trp 9	Ar 4	Lys 2	δ	Trp 9	Ar 4
Ser 4	α	Trp 9	Ar 5	Lys 2	δ	Trp 9	Ar 5
				Lys 2	CH3	Trp 9	Ar 2
				Lys 2	CH3	Trp 11	Ar 4
				Ser 4	α	Trp 9	α
				Ser 4	β	Trp 9	Ar 5
				Ser 4	β	Trp 9	Ar 6
				Trp 9	Ar 4	Asn 6	α

v. Determination of fraction folded.

To determine the unfolded chemical shifts, 7-mers were synthesized as unstructured controls and cyclic peptides were synthesized for fully folded. The chemical shifts for residues in the strand and one turn residue were obtained from each 7-mer peptide. The

[36] Wüthrich, K. *NMR of Proteins and Nucleic Acids*; Wiley: New York, 1986.

chemical shifts of the fully folded state were taken from the cyclic peptides. The fraction folded on a per residue bases was determined from Equation 1.

$$\text{Fraction Folded} = [\delta obs - \delta 0]/[\ \delta 100 - \delta 0], \qquad [1]$$

where δobs is the observed Hα chemical shift, δ100 is the Hα chemical shift of the cyclic peptides, and δ0 is the Hα chemical shift of the unfolded 7-mers. The overall fraction folded for the entire peptide was obtained by averaging the fraction folded of resides Val 3, Lys 8, and Ile 10. These residues are in hydrogen bonded positions have been shown to be the most reliable in determining fraction folded.[26] The overall fraction fold was also determined using the extent of Hα glycine splitting observed in the turn residue Gly 7 given in Equation 2.

$$\text{Fraction Folded} = [\Delta\delta_{\text{Gly Obs}}]/[\ \Delta\delta_{\text{Gly 100}}], \qquad [2]$$

where $\Delta\delta_{\text{Gly Obs}}$ is the difference in the glycine Hα chemical shifts of the observed, and $\Delta\delta_{\text{Gly 100}}$ is the difference in the glycine Hα chemical shifts of the cyclic peptides.

The ΔG of folding at 298 K for the **Trpswitch** peptides was calculated using Equation 3 where *f* is the fraction folded.

$$\Delta G = -RT \ln (f/(1-f)), \quad [3]$$

vi. Determination of thermodynamic parameters.

Variable temperature NMR was used in order to determine the thermodynamic parameters of the peptide folding. A temperature range of 275 to 351 K was explored in five-degree increments using a Varian Inova 600-MHz spectrometer. Temperature calibration was performed with ethylene glycol and methanol standards by using standard macros in Varian

software. The change in glycine chemical shift difference was followed with temperature. The fraction folded of the peptide was plotted against temperature, and the curve was fitted by using the following Equation 4[28]:

$$\text{Fraction folded} = (\exp[x / RT])/ (1 + \exp[x / RT]) \quad [4]$$

Where

$$x = (T[\Delta S_{298}^\circ + \Delta Cp^\circ \ln\{T / 298\}] - [\Delta H_{298}^\circ + \Delta Cp^\circ\{T-298\}])$$

Table 4.8 Temperature Dependence of the Fraction Folded from Glycine Chemical Shift Data for the Trpswitch and Trpswitch(Me_2)**.**

Trpswitch:		Trpswitch(Me_2):	
Temp (K)	Fraction folded	Temp (K)	Fraction folded
275.25	0.802	275.25	0.942
279.64	0.774	279.64	0.933
284.04	0.737	284.04	0.912
288.43	0.698	288.43	0.901
292.83	0.661	292.83	0.879
297.22	0.627	297.22	0.856
301.62	0.590	301.62	0.831
306.01	0.551	306.01	0.801
310.41	0.508	310.41	0.766
314.80	0.464	314.80	0.717
319.20	0.418	319.20	0.685
323.59	0.373	323.59	0.638
327.99	0.330	327.99	0.588

vii. Enzymatic Phosphorylation of Trpswitch.

The peptides **Trpswitch** and **Trpswitch(Me_2)** were enzymatically phosphorylated with Protein Kinase A Catalytic Subunit from bovine heart purchased from Sigma Aldrich. Lyophilized Protein Kinase A was reconstituted in PKA buffer (10 mM magnesium chloride, 6 mg/ml dithiothreitol, 50 mM potassium phosphate buffer at pH 6.9) and allowed to sit for 10 mins before adding substrate. Peptide substrate (100 μM) was reacted with 1mM adenosine triphosphate and 100 units PKA in PKA buffer at 30°C for 24 h in a total volume of 1 ml . 1 unit is defined as the transfer of 1.0 pmol of phosphate from γ-[^{32}P]-ATP to partially dephosphorylated casein per min at pH 6.5 at 30°C according to Sigma Aldrich. Extent of phosphorylation of peptides was determined by LC-MS.

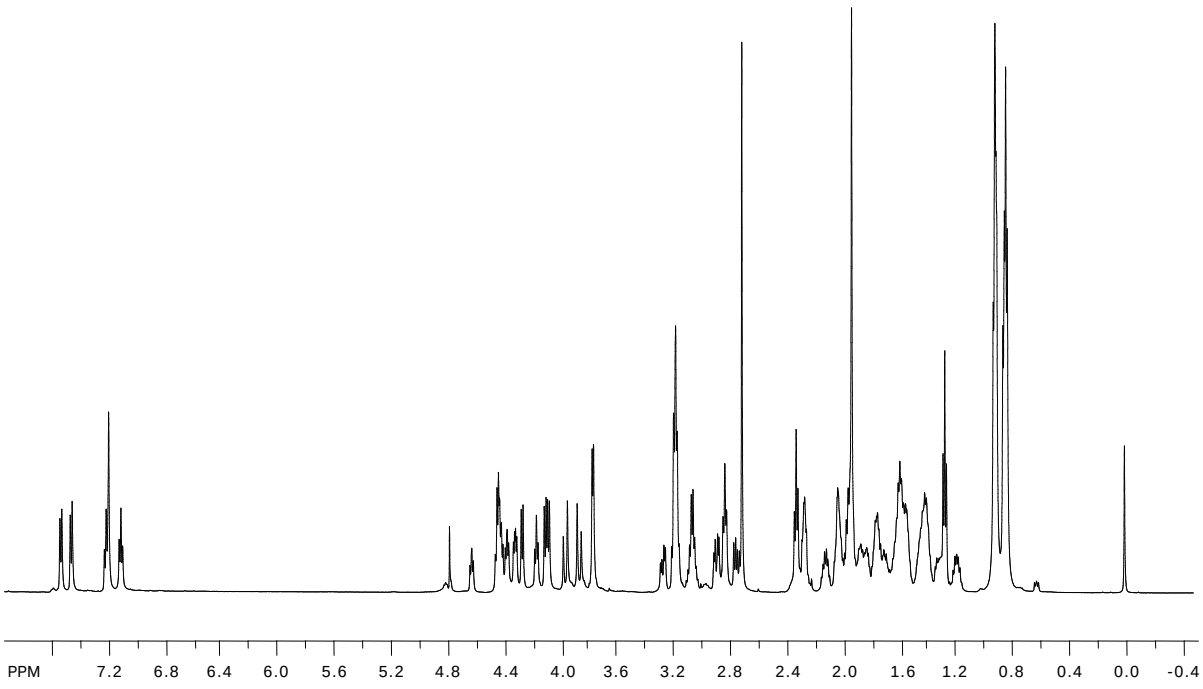

Figure 4.13 ^{1}HNMR of Peptide **WQKS:** Ac-Cys-Arg-Trp-Val-Gln-Val-Asn-Gly-Arg-Lys-Ile-Ser-Gln-Cys-NH2

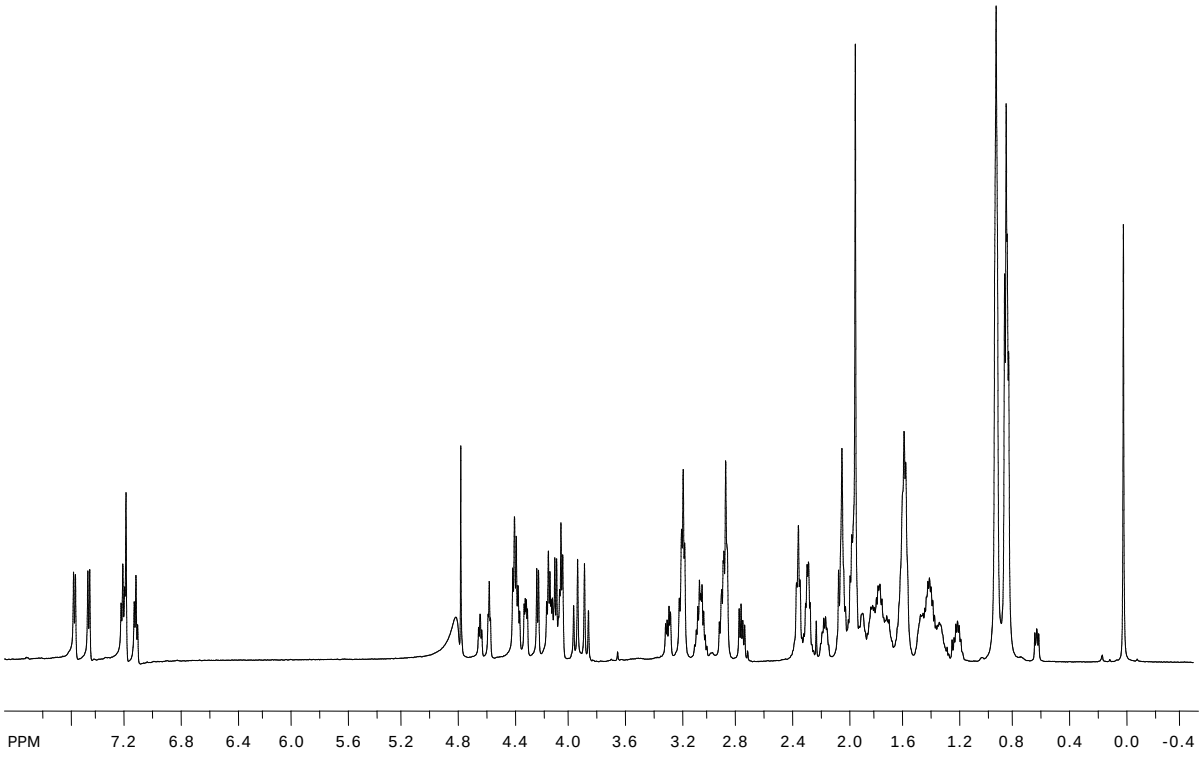

Figure 4.14 ^{1}HNMR of Peptide **WQKS(PO_3):** Ac-Arg-Trp-Val-Gln-Val-Asn-Gly-Arg-Lys-Ile-Ser(PO_3)-Gln-NH2

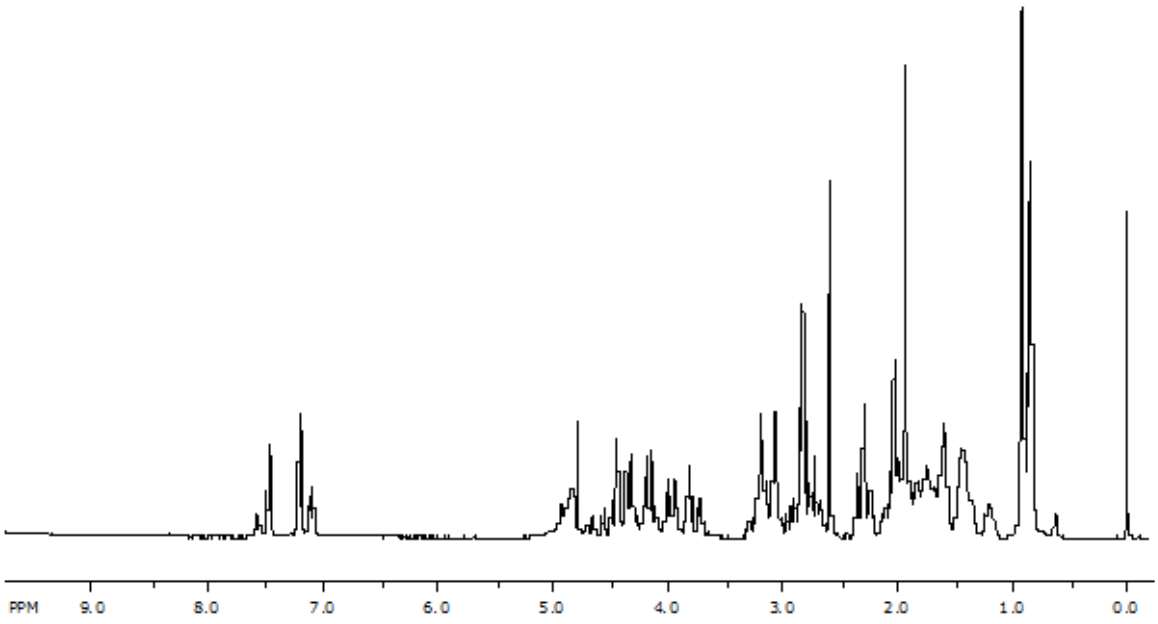

Figure 4.15 ^{1}HNMR of Peptide **WQK(Me$_2$)S:** Ac-Arg-Trp-Val-Gln-Val-Asn-Gly-Arg-Lys-Ile-Ser-Gln-NH2

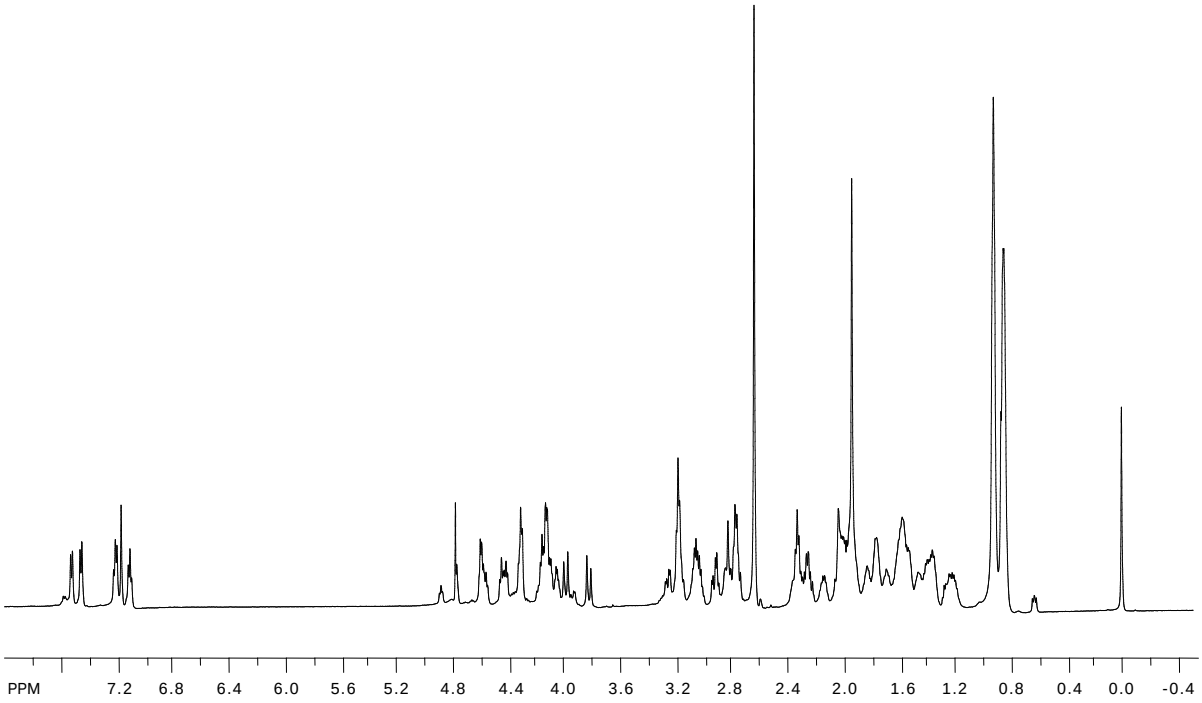

Figure 4.16 ^{1}HNMR of Peptide **WQK(Me_2)S(PO_3):** Ac-Arg-Trp-Val-Gln-Val-Asn-Gly-Arg-Lys-Ile-Ser-Gln-NH2

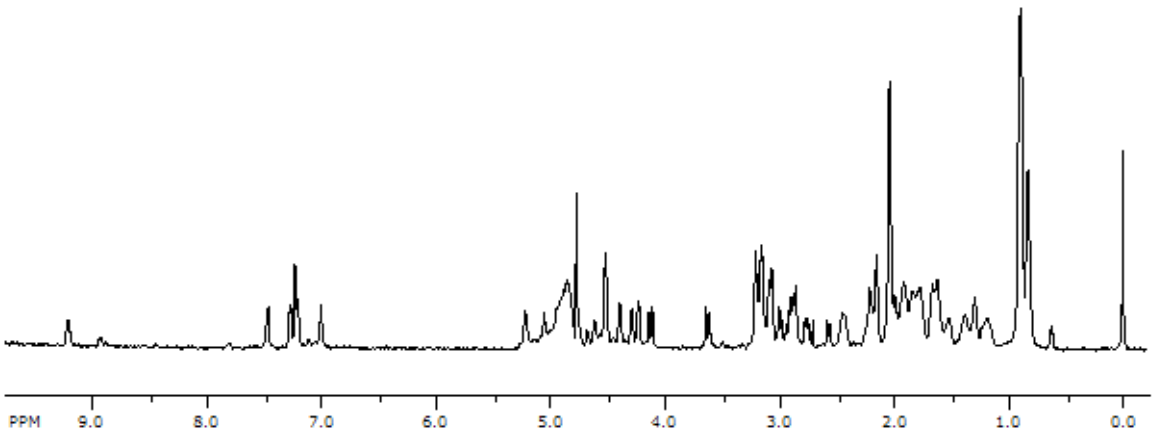

Figure 4.17 ^{1}HNMR of Peptide **cyclic WQKL:** Ac-Cys-Arg-Trp-Val-Gln-Val-Asn-Gly-Arg-Lys-Ile-Ser-Gln-Cys-NH2

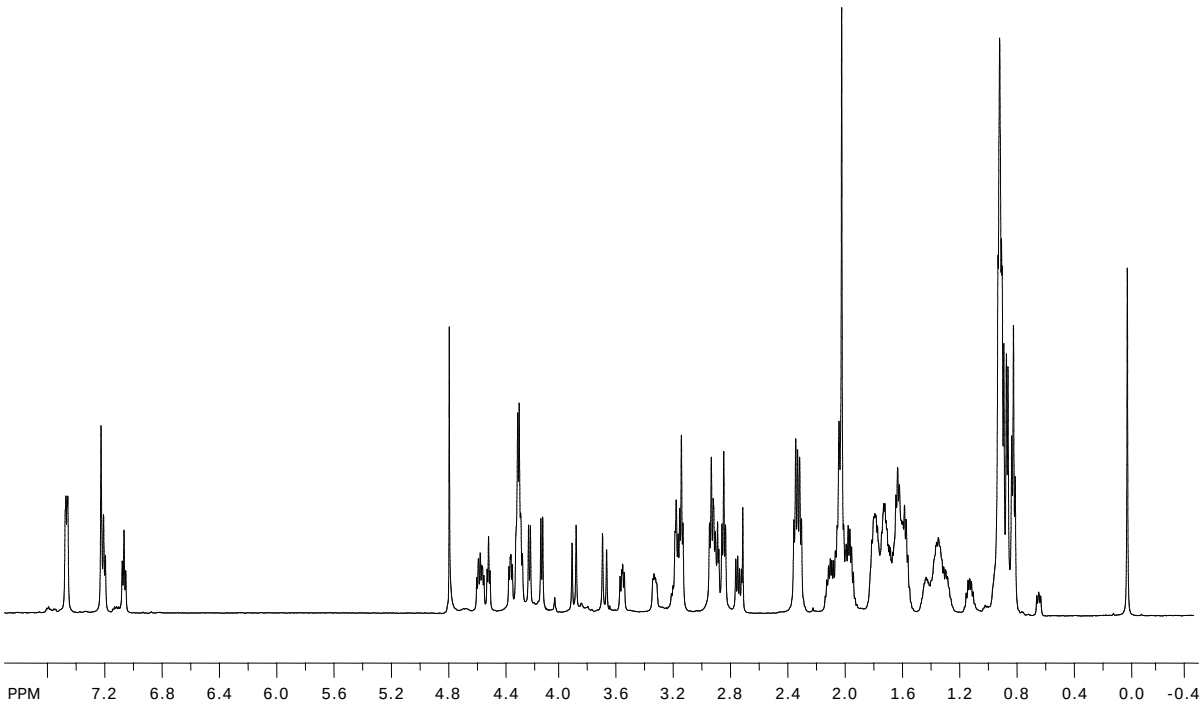

Figure 4.18 [1]HNMR of Peptide **KSWQ:** Ac-Arg-Lys-Val-Ser-Val-Asn-Gly-Lys-Trp-Ile-Gln-Gln-NH2

Table 4.9 Proton Chemical Shift Assignments for Peptide **KSWQ.**

Residue	α	β	γ	δ	ε
R	4.3	1.7	1.68	3.15	
K	4.6	1.7	1.4	1.77	2.84
V	4.31	2.01	0.88		
S	4.51	3.34/3.57			
V	4.13	2.03	0.91		
N	4.58	2.74			
G	3.91/3.69				
K	4.36	1.66	1.3	1.66	2.93
W	4.8	3.17			
I	4.21	1.79	1.12	0.85	
Q	4.31	1.99	2.32		
Q	4.31	1.99	2.32		

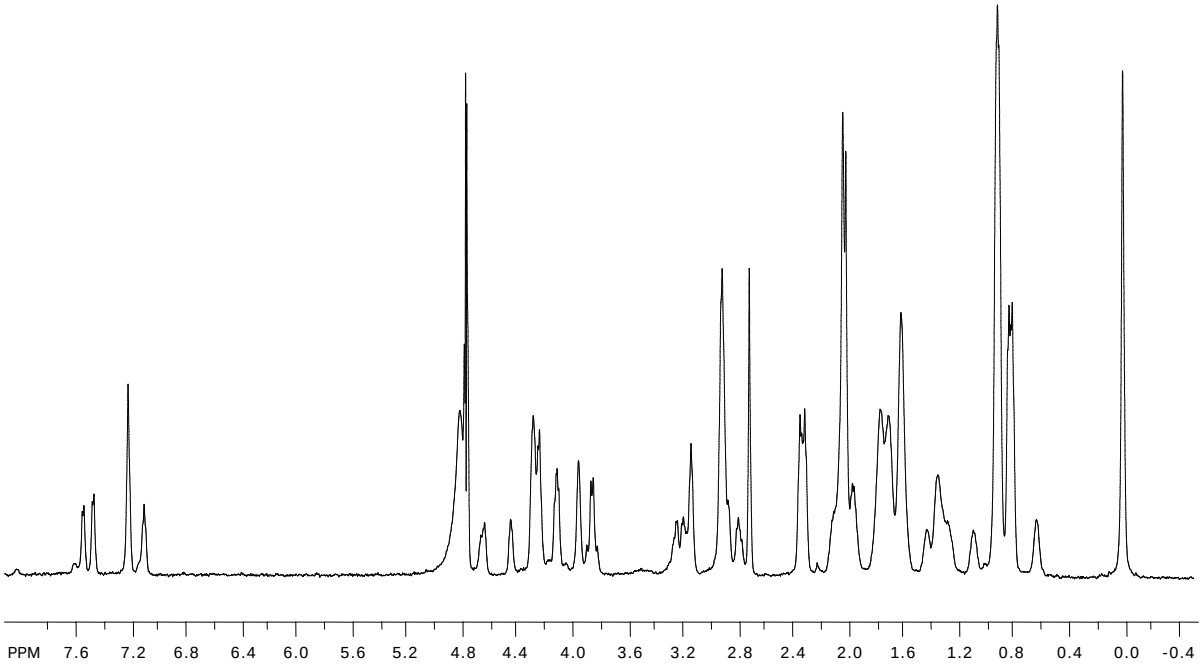

Figure 4.19 ^{1}HNMR of Peptide **KS(PO$_3$)WQ:** Ac-Arg-Lys-Val-Ser(PO$_3$)-Val-Asn-Gly-Lys-Trp-Ile-Gln-Gln-NH2

Table 4.10 Proton Chemical Shift Assignments for Peptide **KS(PO$_3$)WQ.**

Residue	α	β	γ	δ	ε
R	4.26	1.73	1.6	3.13	
K	4.44	1.69	1.39		2.9
V	4.24	1.94	0.89		
S-PO3	4.63	3.96			
V	4.1	2.04	0.89		
N	4.66	2.8			
G	3.85				
K	4.32	1.67	1.31		2.91
W	4.77	3.2			
I	4.13	1.75	1.34	0.84	
Q	4.28	1.98	2.33		
Q	4.24	1.98	2.3		

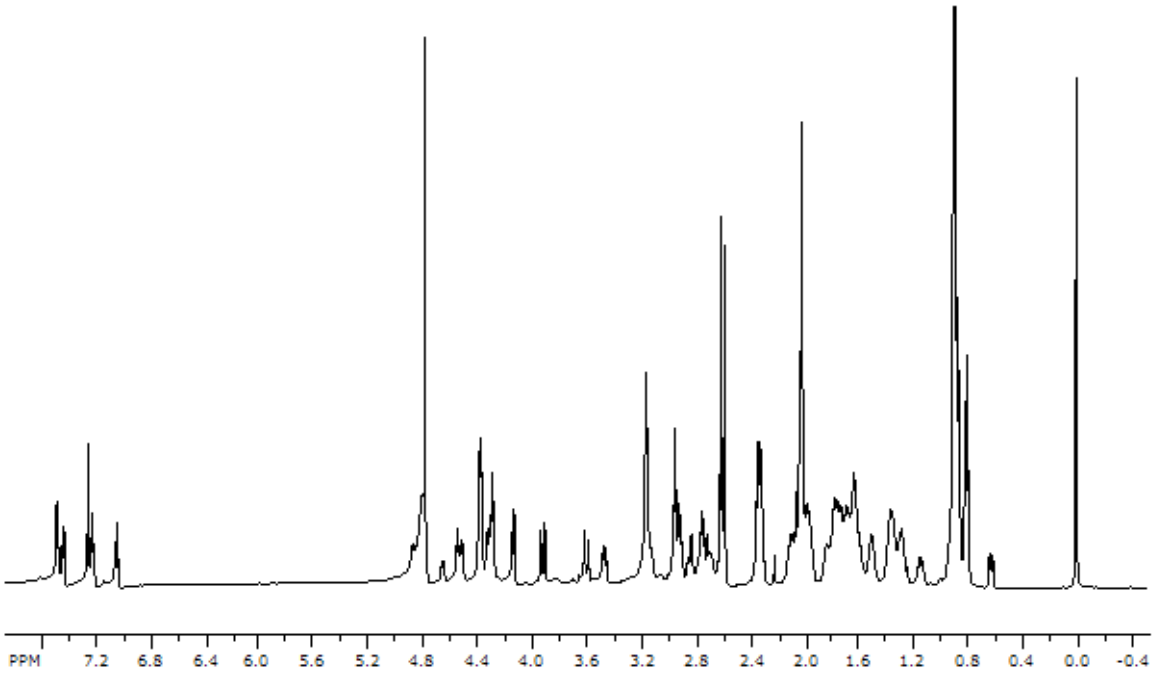

Figure 4.20 ^{1}HNMR of Peptide **K(Me$_2$)SWQ:** Ac-Arg-Lys(Me$_2$)-Val-Ser-Val-Asn-Gly-Lys-Trp-Ile-Gln-Gln-NH2

Table 4.11 Proton Chemical Shift Assignments for Peptide **K(Me$_2$)SWQ.**

Residue	α	β	γ	δ	ε
R	4.32	1.76	1.62	3.17	
K(Me2)	4.67	1.7	1.36	1.52	2.77
V	4.39	2.01	0.9		
S	4.56	3.50/3.14			
V	4.16	2	0.9		
N	4.53	2.93/2.75			
G	3.94/3.62				
K	4.4	1.72	1.33	1.65	2.96
W	4.9	3.17			
I	4.3	1.84	1.39/1.15	0.87	
Q	4.39	1.99	2.32		
Q	4.34	1.97	2.35		

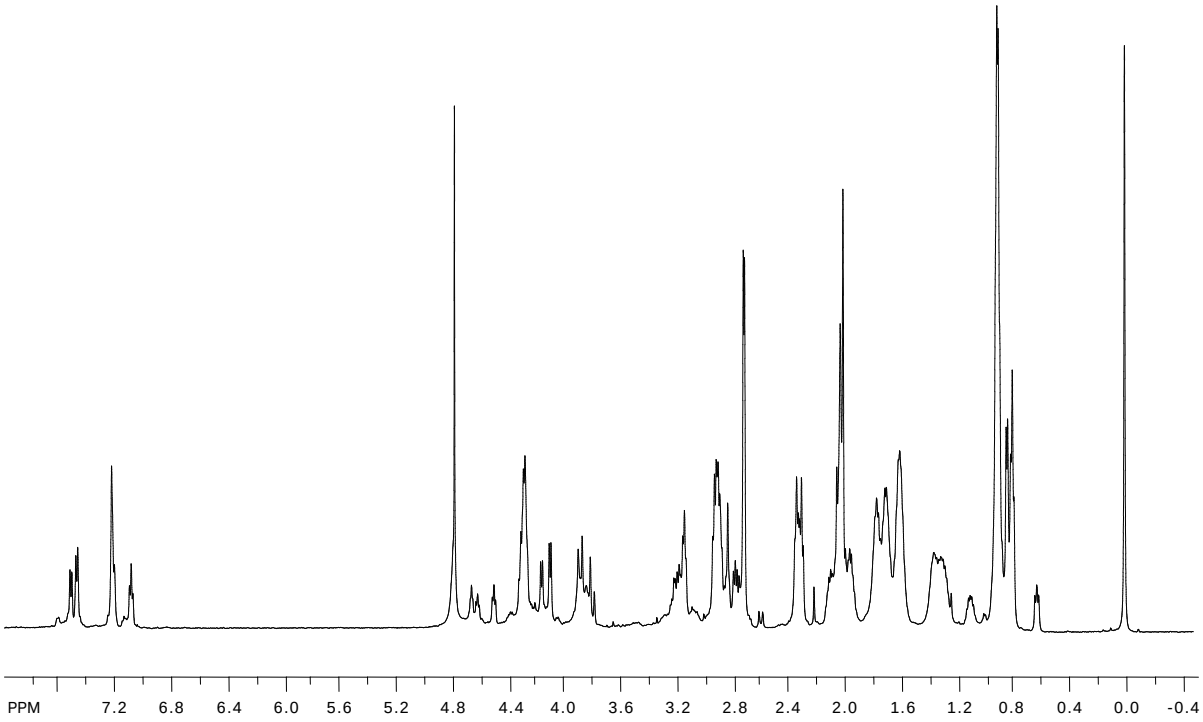

Figure 4.21 [1]HNMR of Peptide **K(Me$_2$)S(PO$_3$)WQ:** Ac-Arg-Lys(Me$_2$)-Val-Ser(PO$_3$)-Val-Asn-Gly-Lys-Trp-Ile-Gln-Gln-NH2

Table 4.12 Proton Chemical Shift Assignments for Peptide **K(Me$_2$)S(PO$_3$)WQ.**

Residue	α	β	γ	δ	ε
R	4.29	1.74	1.62	3.14	
Kme2	4.34	1.71	1.31	1.63	2.92
V	4.29	2.04	0.91		
SOPO3	4.69	3.86			
V	4.11	2.04	0.92		
N	4.63	2.84,2.78			
G	3.89,3.83				
K	4.52	1.73	1.35	1.69	2.92
			H2 7.21, H4 7.53, H5 7.10, H6 7.24, H7		
W	4.84	3.18		7.49	
I	4.18	1.79		0.85	
Q	4.29	1.98	2.33		
Q	4.29	1.98	2.33		

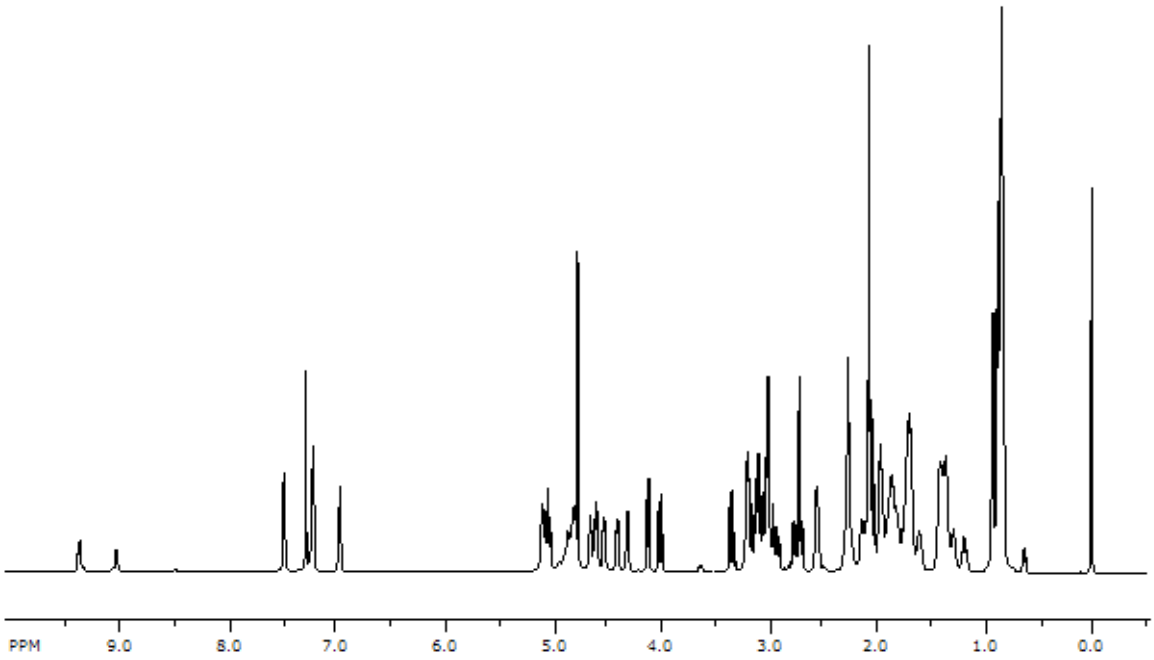

Figure 4.22 [1]HNMR of Peptide **cyclic KSWQ:** Ac-Cys-Arg-Lys-Val-Ser-Val-Asn-Gly-Lys-Trp-Ile-Gln-Gln-Cys-NH2

Table 4.13 Proton Chemical Shift Assignments for Peptide **cyclic KSWQ.**

Residue	α	β	γ	δ	ε
C					
R	4.6	1.84	1.6	3.2	
K	5.11	1.7	1.32	1.4	2.56
V	4.61	1.97	0.85		
S	5.05	3.10/2.95			
V	4.13	1.85	0.84		
N	4.32	3.04/2.70			
G	3.99/3.34				
K	4.52	1.7	1.38		3
W	5.04	3.03			
I	4.64	1.92	1.36	1.18	0.92
Q	4.64	2.1	2.25		
Q	4.86	1.97	2.25		
C					

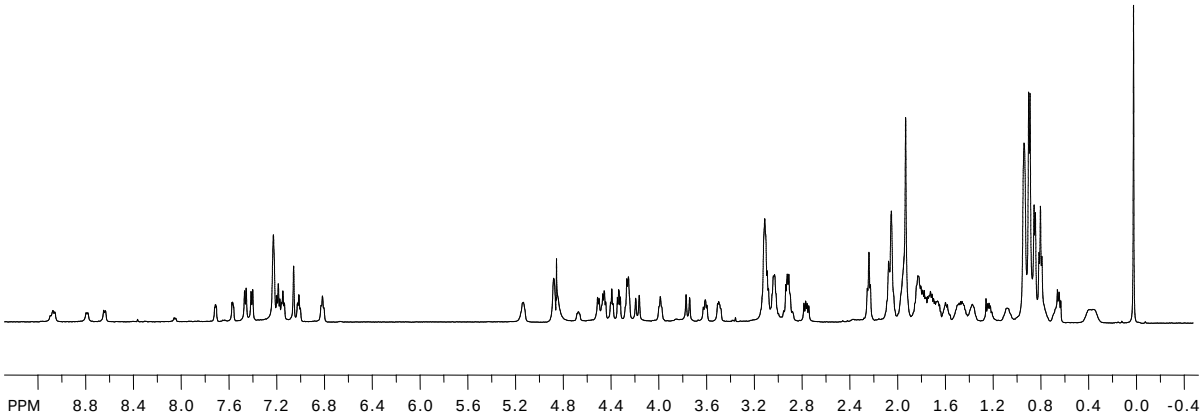

Figure 4.23 [1]HNMR of Peptide **WWKS:** Ac-Arg-Trp-Val-Trp-Val-Asn-Gly-Lys-Orn-Ile-Ser-Gln-NH2

Table 4.14 Proton Chemical Shift Assignments for Peptide **WWKS.**

Residue	α	β	γ	δ	ε
R	4.24	1.59	1.45	3.09	
W	5.11	2.91			
V	4.45	2.05	0.85		
W	5.12	3.1			
V	4.24	1.92	0.91		
N	4.45	2.74,3.06			
G	4.15,3.75				
O	4.65	1.8	1.76	3.01	
K	3.99	1.08	0.67	0.37	1.98
I	4.48	1.9	N/A	0.87	
S	4.38	3.57,3.50			
Q	4.31	1.8	2.02,2.22		

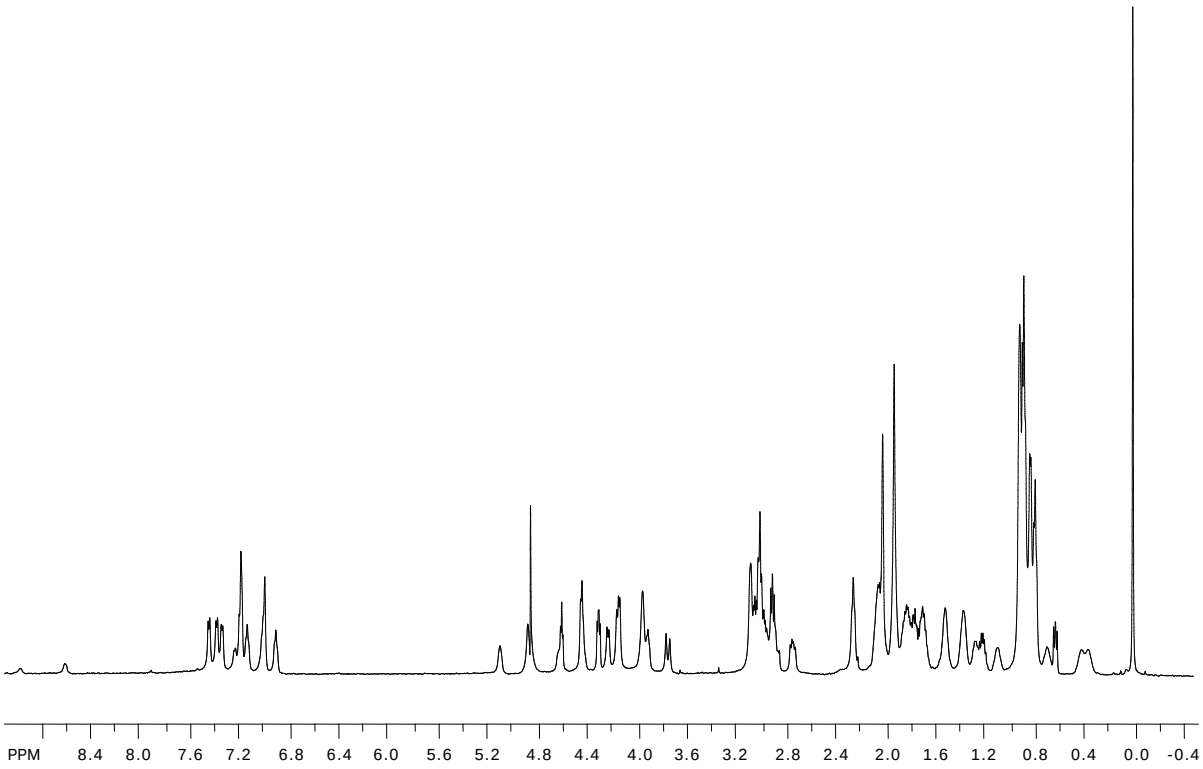

Figure 4.24 [1]HNMR of Peptide **WWKS(PO_3):** Ac-Arg-Trp-Val-Trp-Val-Asn-Gly-Lys-Orn-Ile-Ser(PO_3)-Gln-NH2

Table 4.15 Proton Chemical Shift Assignments for Peptide **WWKS(PO_3).**

Residue	α	β	γ	δ	ε
R	4.15	1.51	1.27	3	
W	5.11	3.08			
V	4.42	2.04	0.84		
W	5.11	2.9			
V	4.23	1.94	0.9		
N	4.45	2.74,3.07			
G	4.15,3.75				
O	4.62	1.81	1.7	3	
K	3.92	1.1	0.84	0.69, 0.39	
I	4.45	1.92	1.2	0.89	
S-PO3	4.62	3.95			
Q	4.3	1.85	2.06,2.25		

Table 4.16 Proton Chemical Shift Assignments for Peptide **cyclic WWKS.**

Residue	α	β	γ	δ	ε
C	4.98	2.49,2.83			
R	4.51	1.78	1.64,1.51	3.15	
W	5.16	3.07			
V	4.63	2.07	0.83		
W	4.92	2.91,3.07			
V	4.29	1.91	0.92		
N	4.39	2.75,3.08			
G	4.25,3.70				
O	4.7	1.8	1.77	3.03	
K	4.06	1.05	0.88,0.50	0.34,0.19	1.96
I	4.6				
S	4.29	2.85,3.18			
Q	4.54	1.79	2.01,2.19		
C	5.24	2.99,2.69			

Table 4.17 Proton Chemical Shift Assignments for Peptide **Trpswitch.**

Residue	α	β	γ	δ	ε
R	4.35	1.7	1.54	3.13	
K	4.63	1.57	1.43	1.29,1.08	2.45
V	4.44	1.97	0.84		
S	4.34	3.12			
V	4.13	1.94	0.88		
N	4.44	2.98	2.73		
G	3.94,3.50				
O	4.46	1.8	1.66	2.99	
W	4.94	3.05	H2 H4 7.15, H5 7.04, H6 7.22, H7 7.40		
I	4.5	1.87		0.88	
W	4.8	3.18	H2 H4 7.28,H5 7.01, H6 7.22 H7 7.48		
Q	4.33	2.02	2.19		

Table 4.18 Proton Chemical Shift Assignments for Peptide **Trpswitch(PO_3)** at pH 7**.**

Residue	α	β	γ	δ	ε
R	4.28	1.71	1.58	3.1	
K	4.38	1.69	1.28	1.61	2.8
V	4.22	2.11	0.89		
S	4.6	3.93			
V	4.09	2.05	0.91		
N	4.66	2.83			
G	3.82				
O	4.28	1.71	1.58	2.93	
W	4.79	3.06	H2 7.22, H4 7.53, H5 7.13, H6 7.17, H7 7.48		
I	4.15	1.7	1.26,1.01	4.15	
W	4.6	3.17	H2 7.22, H4 7.53, H5 7.13, H6 7.17, H7 7.48		
Q	4.16	1.78	2.1		

Table 4.19 Proton Chemical Shift Assignments for Peptide **Trpswitch(PO_3)** at pH 4**.**

Residue	α	β	γ	δ	ε
R	4.33	1.73	1.55	3.1	
K	4.53	1.57	1.52	1.17	2.62
V	4.37	1.97	0.86		
SPO3	4.61	3.77,3.59			
V	4.09	2	0.9		
N	4.57	2.92,2.78			
G	3.94, 3.74				
O	4.41	1.72	1.68	2.97	
W	4.89	3.05	H2 7.23, H4 7.64, H5 7.10, H6 7.16, 7.55		
I	4.33	1.8		0.84	
W	4.75	3.19	H2 7.23, H4 7.49,H5 7.05,H6 7.23, H7 7.41		
Q	4.28	1.82	2.18		

Table 4.20 Proton Chemical Shift Assignments for Peptide **Trpswitch(PO_3)** at pH 1.2.

Residue	α	β	γ	δ	ε
R	4.33	1.67	1.51	3.09	
K	4.56	1.58	1.45	1.33, 1.09	2.56
V	4.39	1.94	0.82		
SPO3	4.56	3.66, 3.29			
V	4.07	1.93	0.86		
N	4.48	2.92, 2.72			
G	3.92,				
O	4.43	1.71	1.64	2.96	
W	4.94	3.02, 2.96		H2 7.22 H4 7.48 H5 7.06, H6 7.16 H7 7.40	
I	4.39	1.72		0.88	
W	4.73	3.16		H2 7.22, H4 7.46, H5 6.99, H6 7.22, H7 7.31	
Q	4.26	1.8	1.98,		

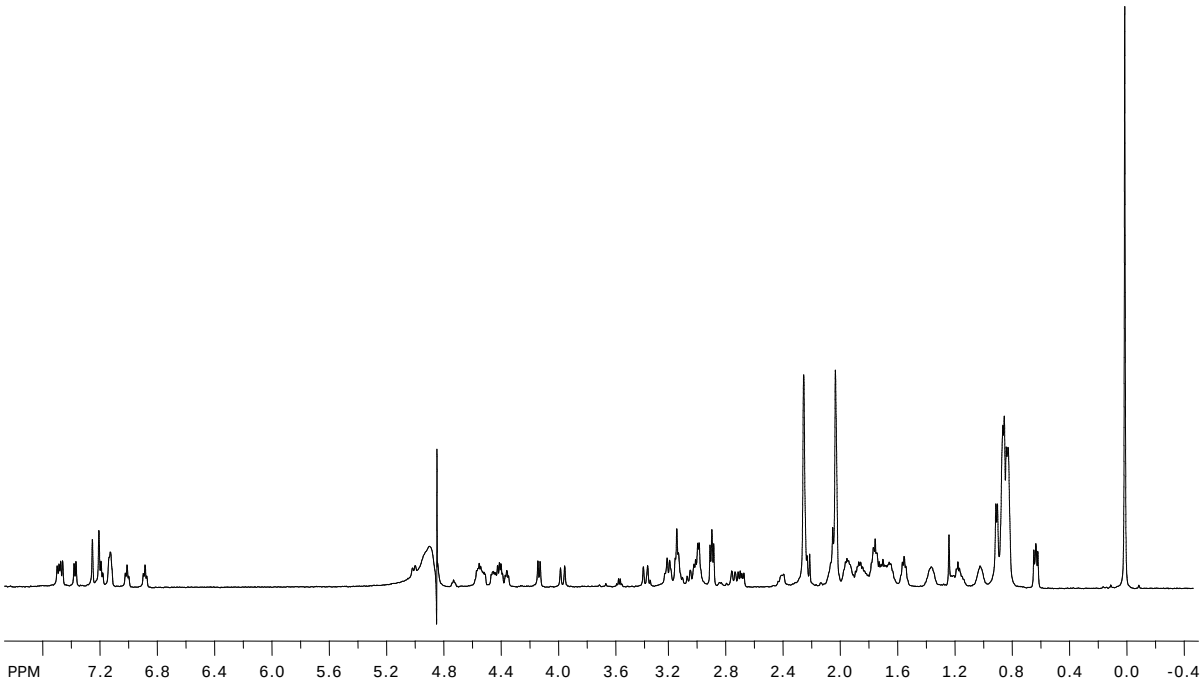

Figure 4.25 ^{1}HNMR of Peptide **Trpswitch(Me$_2$):** Ac-Arg-Lys(Me$_2$)-Val-Ser-Val-Asn-Gly-Trp-Ile-Trp-Gln-NH2

Table 4.21 Proton Chemical Shift Assignments for Peptide **Trpswitch(Me$_2$).**

Residue	α	β	γ	δ	ε
R	4.4	1.73	1.57	3.16	
Kme2	4.74	1.37	1.21,1.03	0.86	2.03, Kme2 = 2.27, 2.04
V	4.56	1.95	0.84		
S	4.47	3.23,2.42			
V	4.14	1.87	0.86		
N	4.36	2.70,3.02			
G	3.97,3.39				
O	4.53	1.77	1.69		
W	5.01	3.08,2.77	H2 7.27, H4 7.21, H5 6.91, H6 7.17, H7 7.50		
I	4.56	1.94	1.17	0.9	
W	4.97	3.18	H2 7.13, H4 7.39, H5 7.04, H6 7.13, H7 7.51		
Q	4.43	1.87	2.26,2.07		

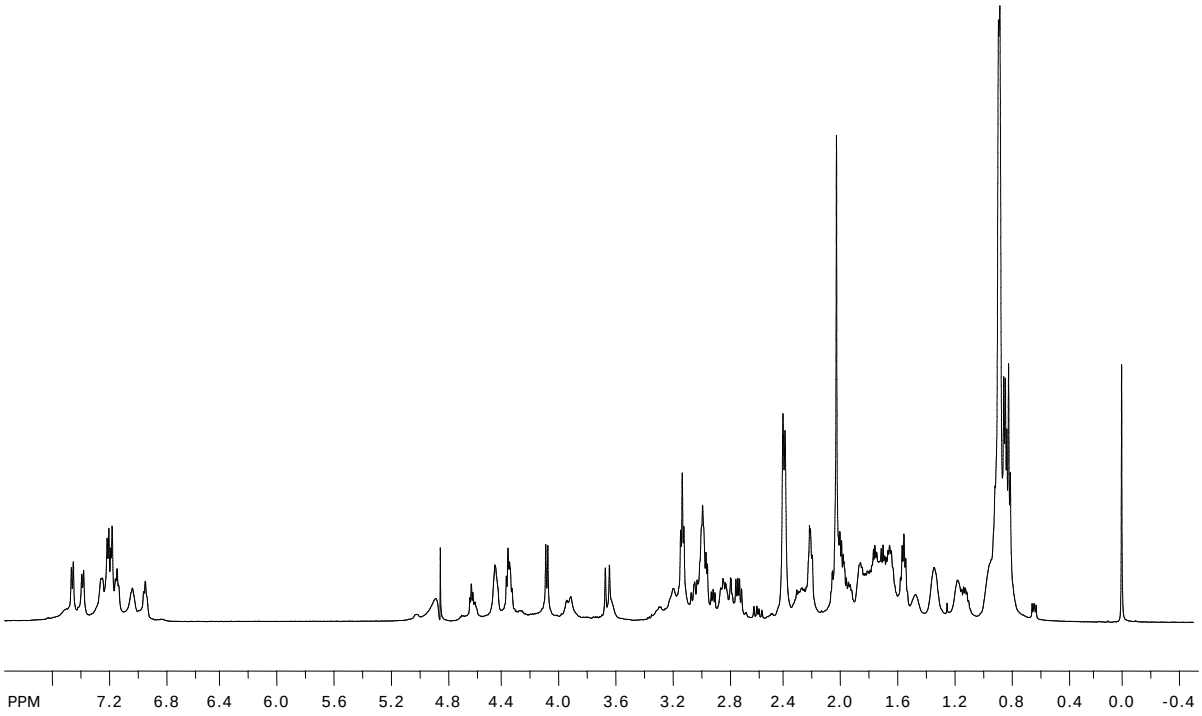

Figure 4.26 ^{1}HNMR of Peptide **Trpswitch(Me_2PO_3):** Ac-Arg-Lys(Me_2)-Val-Ser(PO_3)-Val-Asn-Gly-Trp-Ile-Trp-Gln-NH2

Table 4.22 Proton Chemical Shift Assignments for Peptide **Trpswitch(Me_2PO_3) at pH 7.**

Residue	α	β	γ	δ	ε
R	4.37	1.72	1.56	3.13	
Kme2	4.62	1.48	1.36	0.95	2.28, Kme2 = 2.77, 2.85
V	4.47	1.99	0.87		
SOPO3	4.64	3.31,3.64			
V	4.1	1.95	0.89		
N	4.47	2.98,2.73			
G	3.95,3.67				
O	4.47	1.74	1.66	3.01	
W	5.03	2.85,3.03			ND
I	4.46	1.87	1.31,1.11	0.83	
W	4.86	3.18			ND
Q	4.36	1.84	2.02,2.22		

Table 4.23 Proton Chemical Shift Assignments for Peptide **Trpswitch(Me_2PO_3)** at pH 4.

Residue	α	β	γ	δ	ε
R	4.37	1.72	1.56	3.13	
Kme2	4.62	1.48	1.36	1.19	2.28
V	4.47	1.99	0.87		
SOPO3	4.64	3.31,3.64			
V	4.1	1.95	0.89		
N	4.47	2.73,2.98			
G	3.95,3.67				
O	4.47	1.74	1.66	3.01	
W	5.03	3.03,2.85		ND	
I	4.46	1.87	1.11, 1.31	0.83	
W	4.86	3.18		ND	
Q	4.36	1.84	2.02,2.22		

Table 4.24 Proton Chemical Shift Assignments for Peptide **Trpswitch(Me_2PO_3)** at pH 1.2.

Residue	α	β	γ	δ	ε
R	4.4	1.77	1.55	3.17	
Kme2	4.65	1.45	1.3	1.13, 0.92	2.2
V	4.49	1.99	0.85		
SOPO3	4.65	3.03, 3.55			
V	4.1	1.89	0.85		
N	4.4	2.70,2.99			
G	3.97, 3.62				
O	4.41	1.68	1.34	2.99	
W	5.04	3.03	H2 7.23 H4 7.41 H5 7.04 H6 7.14 H7 7.51		
I	4.47	1.87		0.86	
W	4.97	3.15	H2 7.23 H4 7.47 H5 6.92, H6 7.20 H7 7.47		
Q	4.37	1.86	2.05, 2.23		

Table 4.25 Proton Chemical Shift Assignments for Peptide **Ac-RKVSVNG.**

Residue	α	β	γ	δ	ε
R	4.26	1.76	1.66	3.2	
K	4.38	1.77	1.46	1.66	3
V	4.17	2.09	0.94		
S	4.51	3.85			
V	4.17	2.09	0.94		
N	4.72	2.84/2.78			
G	3.91				

Table 4.26 Proton Chemical Shift Assignments for Peptide **Ac-RKVS(PO_3)VNG.**

Residue	α	β	γ	δ	ε
R	4.28	1.77	1.67	3.2	
K	4.38	1.8	1.45	1.71	3
V	4.16	2.1	0.95		
SOPO3	4.64	4.12			
V	4.16	2.1	0.95		
N	4.75	2.86/2.82			
G	3.91				

Table 4.27 Proton Chemical Shift Assignments for Peptide **Ac-NGOWIWQ.**

Residue	α	β	γ	δ	ε
N	4.66	2.66,2.77			
G	3.79				
O	4.25	1.69	1.56	2.91	
W	4.78	3.08	H2 7.24, H4 7.61, H5 7.06, H6 7.24, H7 7.37		
I	4.16	1.71	1.29,1.03	0.78	
W	4.48	3.05,3.15	H2 7.24, H4 7.61, H5 7.17, H6 7.24, H7 7.45		
Q	4.15	1.75	2.10,2.06		

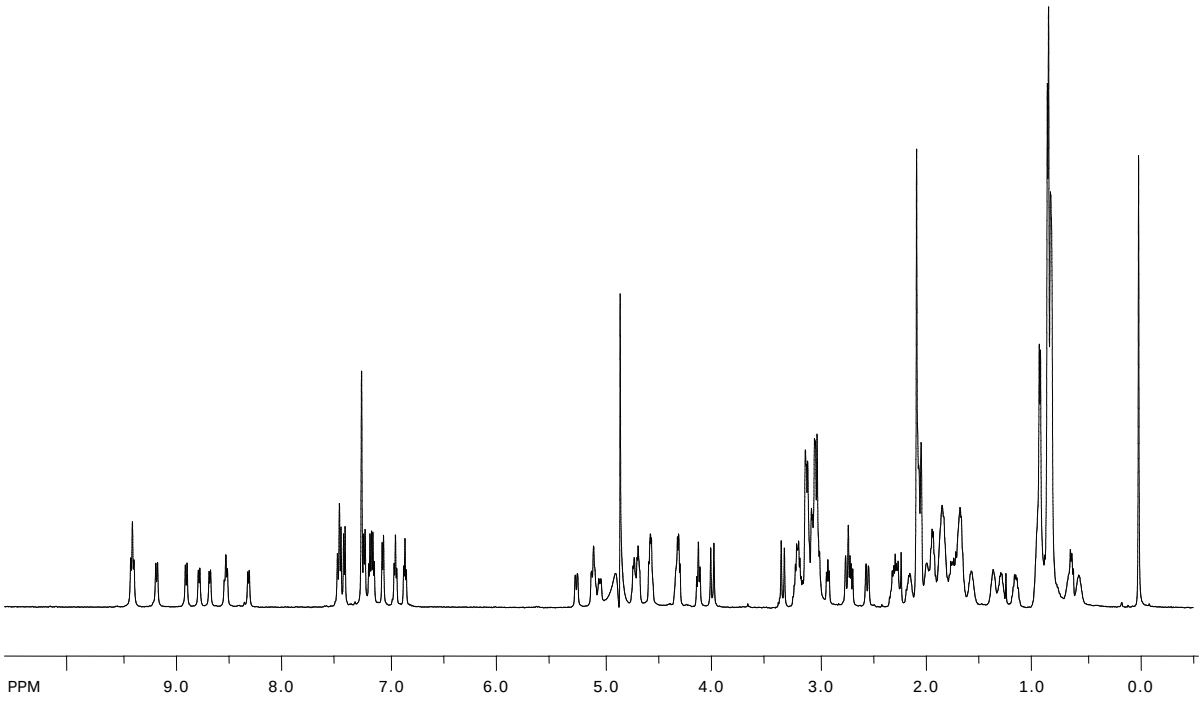

Figure 4.27 [1]HNMR of Peptide **cyclic Trpswitch:** Ac-Arg-Lys(Me_2)-Val-Ser(PO_3)-Val-Asn-Gly-Trp-Ile-Trp-Gln-NH2

Table 4.28 Proton Chemical Shift Assignments for Peptide **cyclic Trpswitch.**

Residue	α	β	γ	δ	ε
C	5.04	2.73,3.04			
R	4.73	1.84	1.59	3.21	
K	4.69	1.29	0.94	0.65	2.07
V	4.58	1.84	0.85		
S	4.33	2.05			
V	4.13	1.83	0.83		
N	4.31	3.07,2.69			
G	3.99,3.34				
O	4.57	1.82	1.68	3.02	
W	5.12	3.05	H2 7.24 , H4 7.15 , H5 6.92, H6 7.24, H7 7.39		
I	4.69	1.99	1.37,1.14	0.9	
W	5.1	3.11	H2 7.24, H4 7.15, H5 6.83, H6 7.02, H7 7.45		
Q	4.73	1.94	2.24		
C	5.27	2.54,3.07			

CHAPTER V

INVESTIGATION OF THE N-TERMINAL UBIQUITIN β-HAIRPIN

(Reproduced, in part with permission from Riemen**,** A.J.; Waters M.L., *Biopolymers.* **2008,** *90*, 394-398.)

A. Stabilization by terminal hydrophobic cluster

i. Background and significance

As discussed in chapter 1, understanding the factors necessary to form minimal structural elements in proteins and peptides is essential for de novo protein design and development of peptide model systems to measure particular interactions. Over the past decade there has been extensive research on determining what factors stabilize the formation of β-hairpins in aqueous solution. It has been shown that the turn sequence can strongly promote β-hairpins formation with a specific strand register.[1] Cross strand interactions have been shown to be a significant contributor to hairpin stability along with β-sheet propensity of the residues incorporated.[1] Hydrophobic clusters of side chains have been used as a major stabilizing interaction for designed β-hairpins.[2] It has been shown that these hydrophobic clusters are more stabilizing when positioned closer to the turn, however there is evidence that terminal residues that appear frayed by NMR can also contribute to overall stability of the hairpin.[2,3,4]

---

[1] Searle, M. S. *J Chem Soc, Perkin Trans 2* **2001**, 1011-1020.

[2] Espinosa, J. F.; Munoz, V.; Gellman, S. H. *J Mol Biol* **2001**, *306*, 397-402.

[3] Kiehna, S. E.; Waters, M. L. *Protein Sci* **2003**, *12*, 2657-2667.

In this section, we discuss the first significantly stabilizing non-aromatic hydrophobic cluster located at the termini of the naturally occurring excised N-terminal β-hairpin of ubiquitin.[5] The excised native N-terminal β-hairpin of ubiquitin modestly folds[6] in aqueous solution and has been implicated as a nucleation site for folding of ubiquitin.[7] Thus, this hairpin sequence has been used as model system to better understand the factors that contribute to β-hairpin stability and the effects on ubiquitin folding by modifying this nucleation site.[8] However only residues in the turn segment and neighboring regions have been modified and studied, leaving the terminal residues' significance unexplored.

---

[4] Espinosa, J. F.; Gellman, S. H. *Angew Chem Int Ed* **2000**, *39*, 2330-2333.

[5] Riemen, A. J.; Waters, M. L. *Biopolymers* **2008**, *90*, 394-398.

[6] Maynard, A. J.; Sharman, G. J.; Searle, M. S. *J Am Chem Soc* **1998**, *120*, 1996-2007.

[7] (a) Zerella, R.; Evans, P. A.; Ionides, J. M. C.; Packman, L. C.; Trotter, B. W.; Mackay, J. P.; Williams, D. H. *Protein Sci* **1999**, *8*, 1320-1331. (b) Harding, M. M.; Williams, D. H.; Woolfson, D. N. *Biochemistry* **1991**, *30*, 3120-3128. (c) Jourdan, M.; Searle, M. S. *Biochemistry* **2000**, *39*, 12355-12364.

[8] (a) Jourdan, M.; Searle, M. S. *Biochemistry* **2001**, *40*, 10317-10325. (b) Platt, G. W.; Simpson, S. A.; Layfield, R.; Searle, M. S. *Biochemistry* **2003**, *42*, 13762-13771. (c) Searle, M. S.; Platt, G. W.; Bofill, R.; Simpson, S. A.; Ciani, B. *Angew Chem Int Ed* **2004**, *43*, 1991-1994. (d) Bofill, R.; Simpson, E. R.; Platt, G. W.; Crespo, M. D.; Searle, M. S. *J Mol Biol* **2005**, *349*, 205-221. (e) Simpson, E. R.; Meldrum, J. K.; Searle, M. S. *Biochemistry* **2006**, *45*, 4220-4230.

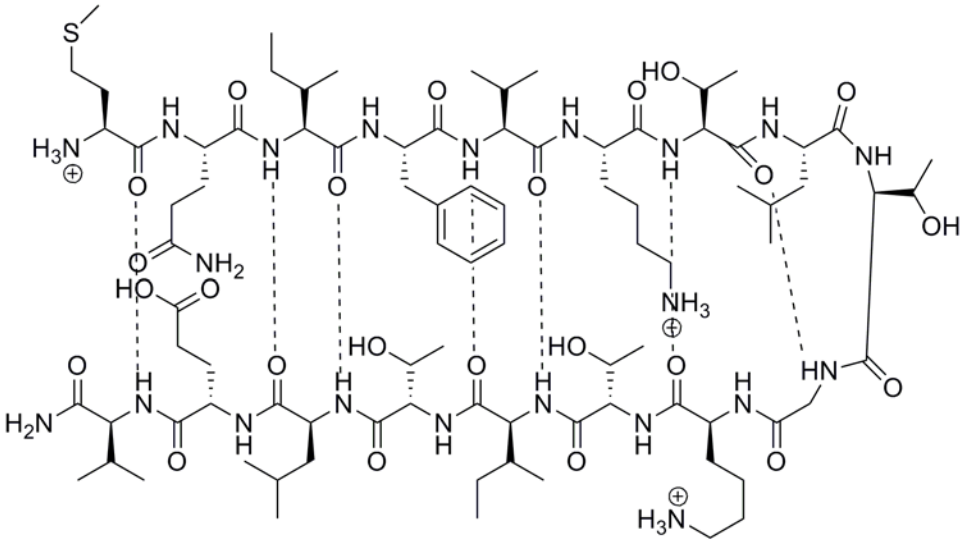

(a)

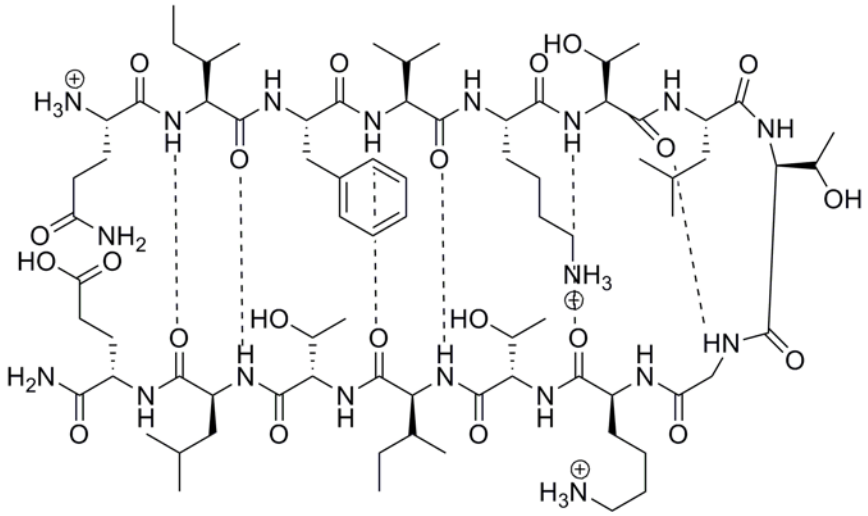

(b)

(c) **Ub(1-10)**: Ac-Met-Gln-Ile-Phe-Val-Lys-Thr-Leu-Thr-Gly-NH_2
Ub(8-17): Ac-Leu-Thr-Gly-Lys-Thr-Ile-Thr-Leu-Glu-Val-NH_2

Figure 5.1 Schematic diagrams of the β-hairpin peptides derived from the N-terminal hairpin of ubiquitin. **(A)** the native 17mer of ubiquitin, **UbN**, and **(B)** the 15-residue peptide **UbD** in which residues 1 and 17 have been deleted. Interstrand hydrogen bonding and relative orientation of the side chains are indicated through dashed lines. **(C)** Sequences for the control peptides **Ub(1-10)** and **Ub(8-17)** used to determine the random coil chemical shifts.

ii. Results.

To investigate the importance on β-hairpin stability of the terminal residues of the native 17 residue N-terminal hairpin of ubiquitin (**UbN**), (Figure 5.1A) a terminal deletion mutant (**UbD**) was synthesized and studied by NMR (Figure 5.1B). Random coil chemical shifts

were determined from peptide**s Ub(1-10)** and **Ub(8-17)** consisting of only residues 1 through 10 and residues 8 to 17 of the native ubiquitin β-hairpin, respectively. As discussed in previous chapters, downfield chemical shifting of backbone hydrogens in peptides relative to random coil values is indicative of β-hairpin structure.[9] A comparison of the downfield shifting of the carbon α-hydrogens (Hα) of **UbD** and **UbN** relative to random coil shifts is given in Figure 5.2. A downfield chemical shift of $\geq$ 0.1 is accepted as showing β-sheet structure and most of the Hα of the native ubiquitin's residues exhibit this extent of shifting.[10] The **UbD** peptide however shows very few residues with downfield shifting $\geq$ 0.1 ppm, except for isoleucine 13 which is 0.2 ppm downfield shifted. The terminal residues glutamine and glutamic acid are upfield shift from random coil in the **UbD** peptide which is an indication of fraying at the ends of the hairpin. Fraying of terminal residues is commonly observed in other β-hairpin peptides.[2,3,11] The decrease in the extent of downfield shifting of Hα along the entire peptide is evidence that the hairpin stability decreases upon removal of the N-terminal methionine and C-terminal valine.

[9] Sharman, G. J.; Griffiths-Jones, S. R.; Jourdan, M.; Searle, M. S. *J Am Chem Soc* **2001**, *123*, 12318-12324.

[10] Wishart, D. S.; Sykes, B. D.; Richards, F. M. *J Mol Biol* **1991**, *222*, 311-333.

[11] (a) Blanco, F. J.; Rivas, G.; Serrano, L. *Nat Struct Biol* **1994**, *1*, 584-590. (b) Cochran, A. G.; Skelton, N. J.; Starovasnik, M. A. *Proc Nat Acad Sci U.S.A.* **2001**, *98*, 5578-5583. (c) Tatko, C. D.; Waters, M. L. *Protein Sci* **2003**, *12*, 2443-2452. (d) Tatko, C. D.; Waters, M. L. *J Am Chem Soc* **2004**, *126*, 2028-2034. (e) Hughes, R. M.; Waters, M. L. *J Am Chem Soc* **2005**, *127*, 6518-9. (f) Hughes, R. M.; Waters, M. L. *J Am Chem Soc* **2006**, *128*, 12735-12742.

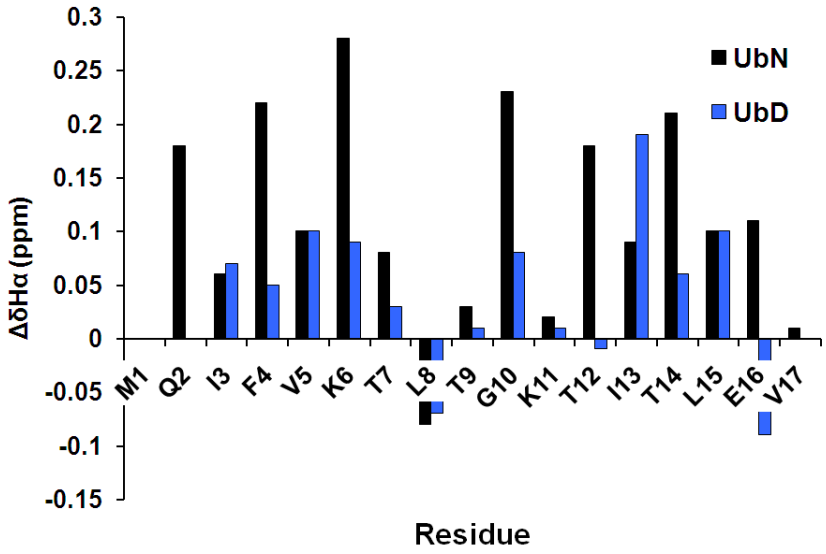

Figure 5.2 Hα chemical shift differences: **UbN** (black bars) and **UbD** (blue bars) from random coil peptides **Ub(1-10)** and **Ub(8-17)**. The Gly bars reflect the Hα separation in the hairpin. Conditions: 298 K, 50 mM sodium acetate-d_4, pH 4.0 (uncorrected), referenced to DSS.

The chemical shift of the backbone amide hydrogens from random coil control values were also compared between the two peptides (Figure 5.3). Greater downfield shifting is typically seen for the hydrogen bonded amide protons in the peptide backbone of the sheet portion of β-hairpins while non-hydrogen sites show a lesser change. Turn regions of β-hairpins generally exhibit upfield shifting of the back bone amide protons. The backbone amides of both **UbN** and **UbD** exhibit downfield shifting in the appropriate hydrogen bonding pattern is seen in the native peptide (positions I3, V5, T7, I13, L15, and V17) but to a lesser extent in **UbD**, indicating that **UbD** is folding in the proper register but is forming a less stable hairpin than **UbN**.

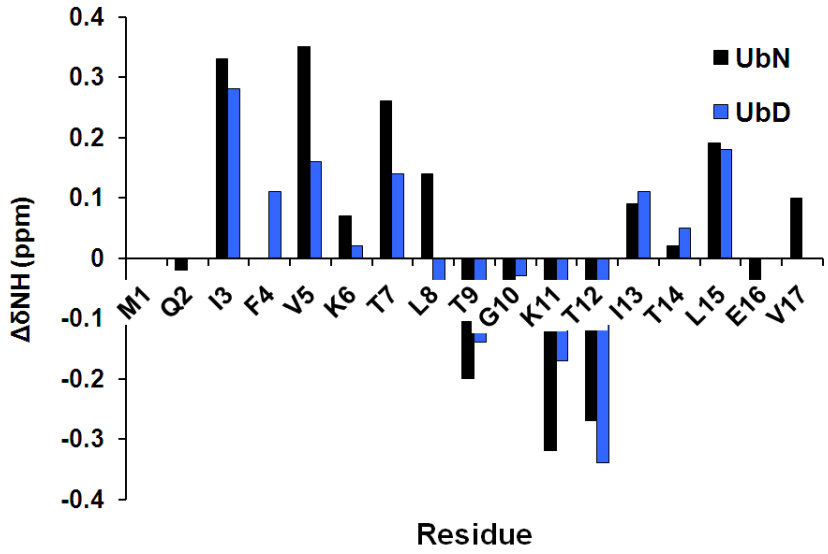

Figure 5.3 Backbone amide chemical shift differences of **UbN** (black bars) and **UbD** (blue bars) relative to random coil peptides **Ub(1-10) and Ub(8-17)**. Conditions: 298 K, 50 mM sodium acetate-d_4, pH 4.0 (uncorrected), referenced to DSS.

NOESY experiments were preformed on the **UbD** peptide to give further evidence that the peptide was forming a β-hairpin hairpin similar to the native hairpin. A weak NOE was observed between the γ-methyl group of Thr 14 and hydrogens 3 and 5 of phenyl ring of Phe 4. The NOE interactions observed between these residues indicates β-hairpin formation with the same register as seen in the native β-hairpin previously reported by Zerella.[7a] However, no other non-ambiguous NOEs were observed between cross strand residues. This is due to peak overlap of side chain residues, low stability of the hairpin, and more dynamic nature of the **UbD** peptide.

The extent of folding to a β-hairpin by **UbD** peptide was quantified using two methods and compared to the native β-hairpin. The first method utilizes the extent of Hα downfield shifting relative to random coil and the fully folded state (Experimental Section). The second method utilizes the extent of the distereotopic glycine Hα splitting located in the turn of the hairpin relative to glycine Hα splitting observed in a fully folded control (Experimental

Section). The NMR chemical shifts of residues 1-17 from the full ubiquitin protein was used as the fully folded state and peptides **Ub(1-10)** and **UB(8-17)** were used as random coil controls for appropriate hairpin segments.[12] Both methods give an overall folding for the native β-hairpin of about 20%, which is in agreement with the value reported by Zerella.[7a] Overall folding of **UbD** peptide was an estimated 10% by both methods showing a destablization in folding by approximately 0.7 kcal/mol relative to the native β-hairpin.

Since these peptides have low β-hairpin stability in aqueous solution, co-solvent experiments were performed with aqueous methanol to characterize the extent of destabilization upon deletion of the terminal residues. Addition of methanol has been shown to increase the folding population of the native β-hairpin.[7a] CD methanol titrations of **UbN** and **UbD** were preformed to determine the optimal methanol concentration for maximum β-hairpin formation of these peptides (Figure 5.4). At 30% methanol, **UbN** has reached the maximum β-hairpin formation induced by methanol, while at 40% methanol **UbD** still appears to be mostly random coil. Although addition of methanol has little effect on the CD spectrum of **UbD,** increased β-hairpin population was observed by downfield shifting of CαH in both **UbN** and **UbD** upon the addition of methanol (Figure 5.4). CD spectra interperations of β-hairpins have been shown to be ambiguous, and may not accurately reflect β-hairpin folding populations and in some cases appear as random coil.[13] Strong NOE's were observed for **UbD** between Hα of Phe4 and Thr14 confirming that hairpin was forming in same strand register as the native hairpin. Based on the Hα downfield shifting and Gly splitting, the overall fraction folded of **UbD** in 40% methanol is estimated to be 50% while **UbN** is

[12] Weber, P. L.; Brown, S. C.; Mueller, L. *Biochemistry* **1987**, *26*, 7282-7290.

[13] Lacroix, E.; Kortemme, T.; de la Paz, M. L.; Serrano, L. *Curr Opin Struct Biol* **1999**, *9*, 487-493.

approximately 80% folded at 30% methanol. Deletion of the terminal residues destabilizes the hairpin approximately 0.7 kcal/mol in the presence of co-solvent, which agrees with the extent of destabilization observed in aqueous solution.

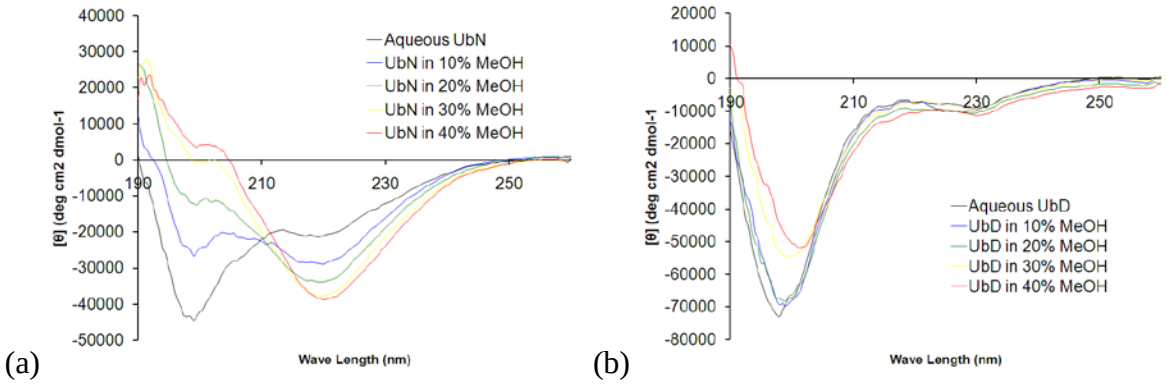

Figure 5.4 CD spectra of (a) **UbN** and (b) **UbD** in 0, 10, 20, 30, and 40% methanol. Conditions: 10mM sodium phosphate buffer pH 7.0 at 298 K with varying amounts of methanol cosolvant.

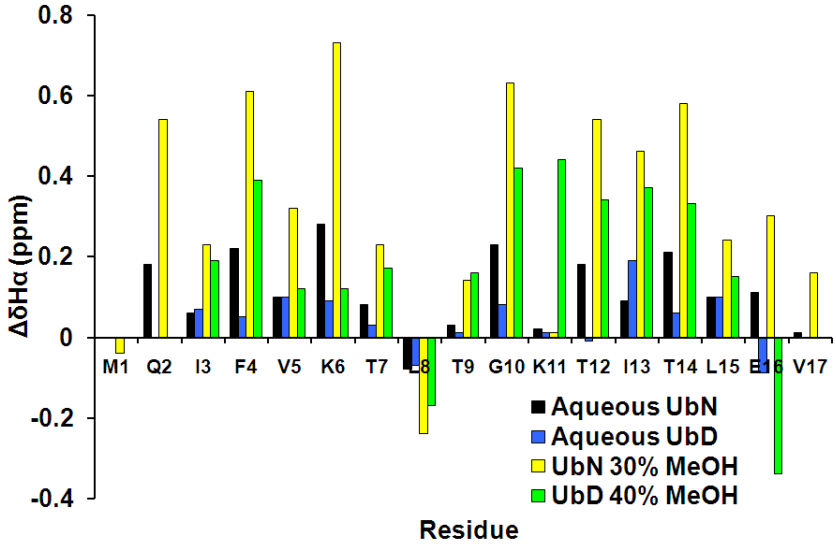

Figure 5.5 Hα chemical shift differences increase upon addition of methanol: **UbN** in pH 4 buffer (black bars), **UbD** in pH 4 buffer (blue bars), **UbN** in 30% methanol (green bars), **UbD** in 40% methanol (yellow bars). The Gly bars reflect the Hα separation in the hairpin.

iii. Discussion

The terminal residues Met 1 and Val 17 of the N-terminal ubiquitin hairpin surprisingly add a significant amount of structural stability. Residues Met 1, Val 17, and Ile 3 make a

hydrophobic cluster in the crystal structure of ubiquitin (Figure 5.6).[14] We postulate that enhanced stability from these residues is the result of the formation of a hydrophobic cap at the end of the hairpin that helps to prevent the terminal residues from fraying. Indeed, NMR data demonstrates that the deletion of Met1 and Val17 results in an upfield shift of Gln2 and Glu16, indicating that these residues are considerably more frayed in the absence of the hydrophobic cluster.

In the context of the protein, Bamezai and coworkers have shown that Met1 contributes at least 3.4 kcal/mol to the stability of native conformation of ubiquitin, as compared to a loss of 0.7 kcal/mol upon deletion of Met1 and Val17 in the isolated hairpin.[15] Thus, Met1 appears to be an important residue both in terms of stabilizing the N-terminal hairpin of ubiquitin and the overall protein stability of ubiquitin, suggesting that it may play a key role in the nucleation of folding.

There is evidence that hydrophobic residues at the termini of de novo designed β-hairpins can provide some stability. Espinosa and coworkers saw that as they moved a hydrophobic cluster found in GB1 C-terminal β-hairpin away from the nucleating turn sequence that the hairpin structure propagated further, however the overall stability of the hairpin was decreased compared to shorter hairpins.[4] Kiehna also saw incorporation of phenylalanine cross strand pair at the termini of a de novo design β-hairpin added stability over Lysine-Glutamic acid cross strand pair or no cross strand pair.[3] The aromatic cross strand pair of phenylalanines was reported to add about -0.3 kcal/mol to the stability of that particular β-

[14] Vijaykumar, S.; Bugg, C. E.; Cook, W. J. *J Mol Biol* **1987**, *194*, 531-544.

[15] Bamezai, S.; Banez, M. A. T.; Breslow, E. *Biochemistry* **1990**, *29*, 5389-5396.

hairpin system.[3] It appears that nature has used a similar hydrophobic capping strategy in the N-terminal β-hairpin of ubiquitin to help increase the stability of a fairly long hairpin.

Figure 5.6 Terminal residues of N-terminal hairpin of ubiquitin (pdb code: 1ubq). The hydrophobic cluster between Met1, Ile13 and Val17 is shown in green. These residues are packed into the core of the protein.[14]

iv. Conclusion.

These studies provide evidence that the terminal hydrophobic cluster in a naturally occurring β-hairpin from ubiquitin significantly enhances the stability of the hairpin in aqueous solution. As this hairpin has been proposed to nucleate folding of the protein and since these residues make tertiary contacts within the native protein, this hydrophobic cluster may play a key role in the nucleation of protein folding. Moreover, these results suggest a general strategy for increasing the stability of designed β-hairpin systems by creating a cap for the hairpin, similar to capping strategies used in α-helices.

B. Incorporation of Cation-π interactions.

i. Introduction.

As mentioned in the previous section, extensive research has been conducted on the N-Terminal β-hairpin of ubiquitin. These studies have elucidated the importance of the turn sequence in enforcement of proper strand register in β-hairpin formation[16] and the implications of a stabilizing this hairpin on the ubiquitin folding pathway [8b,d]. However aforementioned studies dealt with stabilizing the N-terminal ubiquitin hairpin through turn optimization. Thus no extensive studies utilizing stabilizing side chain-side chain cross strand

[16] Searle, M. S.; Williams, D. H.; Packman, L. C. *Nat Struct Biol* **1995**, *2*, 999-1006.

interactions have been conducted on this hairpin. We sought to investigate the effects of incorporation of a stabilizing cation-π interaction on the N-terminal ubiquitin hairpin and to determine the implications on the overall ubiquitin folding pathway through incorporation of a redesigned hairpin. Not only will these studies further our understanding of β-hairpin design, but also help in delineating the complex concert of interactions responsible for protein folding.

ii. System Design.

To investigate the effects of incorporation of a cation-π interaction in the N-terminal hairpin of ubiquitin (residues 1-17) and its effect on overall Ubiquitin folding we redesigned the non hydrogen bonded residues (NHB) residues of this hairpin (Figure 5.7). The NHB residues were altered from the native sequence because geometries for side chain-side chain cross-strand interactions at these positions are more favorable and well studied.[11b-c,17] Also, the NHB residues side chains are located on the solvent exposed exterior of native ubiquitin protein, thus it is believed that mutating these residues will not disrupt the contacts to the interior of the full protein for future folding studies. The cross strand pair, residues 2 and 16, was mutated from Gln and Glu to Arg and Gln respectively to increase the net positive charge on the peptide to 2+ to help increase solubility and reduce aggregation. Residues 4 and 12 were mutated to Trp and Lys or trimethylated Lys for a favorable cross strand cation-π interaction similar to other β-hairpins previously discussed (Chapter 3, Chapter 4).[11c,e,18] Additionally residues 6 and 14 were mutated to Gln and Leu respectively to help induce a more stable β-hairpin as was previously used in hairpin designs (Chapter 4).[18] The Leu at

[17] Syud, F. A.; Stanger, H. E.; Gellman, S. H. *J Am Chem Soc* **2001**, *123*, 8667-77.

[18] Hughes, R. M.; Benshoff, M. L.; Waters, M. L. *Chem Eur J* **2007**, *13*, 5753-5764.

position 14 should have favorable hydrophobic contacts with the cross strand Trp. These mutations should induce a more stable hairpin than the modestly folded native sequence (20%) in aqueous solution.

(a)

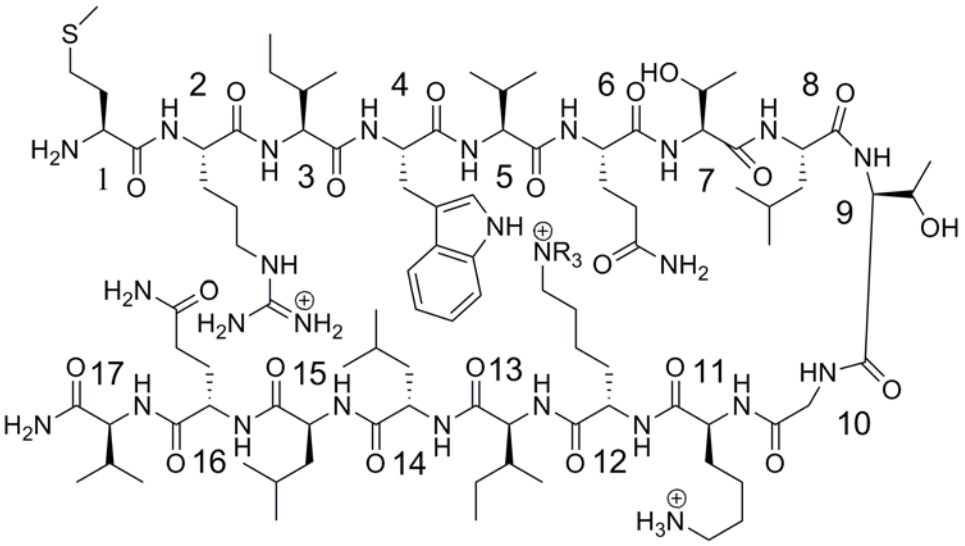

(b) **ubWQKL(1-10)**: Ac-Met-Arg-Ile-Trp-Val-Gln-Thr-Leu-Thr-Gly-NH_2
ubWQKL(8-17): Ac-Leu-Thr-Gly-Lys-Lys-Ile-Leu-Leu-Gln-Val-NH_2

Figure 5.7 Schematic diagrams of the proposed β-hairpin structure formed by **ubWQKL** (R=H) and **ubWQKme3L** (R=Me). Sequences for the control peptides **ubWQKL(1-10)** and **ubWQKL(8-17)** used to determine the random coil chemical shifts.

iii. Results and Discussion.

The peptide **ubWQKL** was synthesized with some difficultly by solid phase peptide synthesis. It became apparent that this particular sequence required multiple coupling cycles towards the end of the synthesis, particular during the last three residues (Ile 3, Arg 2 and Met 1). Even with multiple coupling cycles there were still many impurities observed during purification. This peptide was characterized by NMR, however the leucine residues could not be assigned unambiguously. Nonetheless, we were still able to measure the chemical shift difference of the Hα from random coil control peptides with the exception of residues 8, 14, and 15 (Figure 5.8). Downfield shifting of ≥ 0.1 ppm was observed for a majority of the

residues indicating some β-sheet formation, albeit not to a much larger extent than what was observed for the native sequence discussed in section A and in some cases less than what was observed in the native sequence (positions 5, 6, 11, 12, 13, 15).

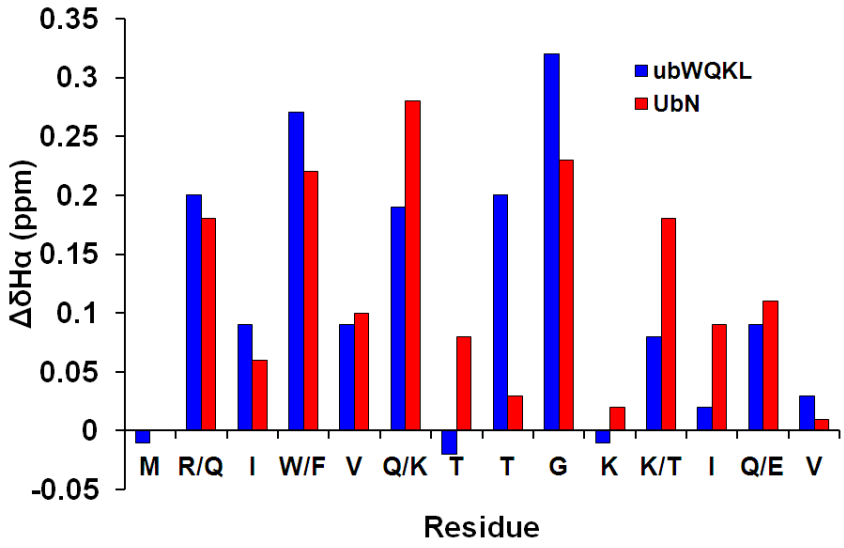

Figure 5.8 Hα chemical shift difference of **ubWQKL** and **UbN** from random coil peptides. The Gly bars reflect the Hα separation in the hairpin. Conditions: 298 K, 50 mM sodium acetate-d_4, pH 4.0 (uncorrected), referenced to DSS.

The peptide **ubWQKme3L** was synthesized with a trimethylated lysine at position 12 to see if this peptide had an increased favorable interaction with the diagonally cross-strand tryptophan similar to what was previously reported in *de novo* designed β-hairpins.[11e,18] This peptide was also difficult to synthesize compounded by the extra synthetic step of methylating Lys 12. Several rounds of HPLC purification were required to obtain pure product. NMR characterization was also difficult for this peptide system with many residues whose chemical shifts could not be unambiguously assigned; hence no Hα chemical shift from random coil control analysis was performed.

The fraction folded for **ubWQKL** and **ubWQKme3L** was estimated using the extent of glycine splitting observed in residue 10 as described in the experimental section (Table 5.1).

Due to the difficulty of synthesis and potential unintended oxidation of Met1 no fully folded cyclic control using disulfide link terminal cysteine residues were successfully synthesized. Thus, the glycine splitting observed in the native protein[12] was used as a fully folded control in estimating the fraction folded for these peptides. Analysis of the fraction folded calculation for **ubWQKL** revealed that this peptide was around 44% folded which is approximately a 20% fold increase over the native sequence. The **ubWQKme3L** was estimated to be 58% folded based on Gly splitting which is an increase over both the native and **ubWQKL** peptides. Calculation of fraction folded could not be determined by the Hα shift method due to the lack of applicable fully folded control. In this regard, the fraction folded calculated from gly splitting of these peptides gives qualitative information at best about the **ubWQKL** system.

Table 5.1 Fraction folded calculation for **ubWQKL** and **ubWQKme3L** peptides using Gly 10 splitting.

Peptide	Glycine splitting	ΔGlycine splitting	Fraction Folded[a]
WQKL	3.81, 4.13	0.32	0.44
WQKme3L	3.77, 4.19	0.42	0.58

(a) Fraction folded was calculated using the Gly splitting observed in the ubiquitin protein as a fully folded control.[12]

Redesign of the side chain-side chain interactions for the N-terminal β-hairpin of ubiquitin proved to be more challenging than originally anticipated. Nonetheless, the mutations introduced into this system appeared to have some of the desired effects on hairpin stability. The **ubWQKL** peptide was estimated to be more folded than the native sequence which was predicted based on design principles from previously described systems with a similar NHB site sequence (Chapter 4).[18] Methylation of Lys 12 in the **ubWQKme3L** peptide also appears to follow the observed increase in stability for previously described systems (Chapter 4).[11e,18] However, there is not enough data to conclusively determine if this

increase in stability is due to an increased interaction with the cross strand tryptophan in the **ubWQKme3L** peptide. Regardless of the synthetic hurdles in the ubiquitin sequence, it is still important to understand the consequences of redesigning a naturally occurring system. The studies on the **ubWQKL** system provide some promising results for future redesign of this system that can be incorporated into the native protein to gain further insights into protein folding.

C. Experimental Section

i. Synthesis and purification of peptides.

Peptides were synthesized by automated solid phase peptide synthesis on an Applied Biosystmes Pioneer Peptide Synthesizer using Fmoc protected amino acids on a PEG-PAL-PS resin. Activation of amino acids was performed with HBTU, HOBT in the presence of DIPEA in DMF. Deprotections were carried out in 2% DBU, 2% piperdine in DMF for approximately 10 minutes. Extended cycles (75 min) were used for each amino acid coupling step. All control peptides were acetylated at the N-terminus with 5% acetic anhydride, 6% lutidine in DMF for 30 min. Cleavage of the peptide from the resin was performed in 95:2.5:2.5 Trifluoracetic acid (TFA): Ethanedithiol or Triisopropylsilane (TIPS): water for 3 h. Ethanedithiol was used as a scavenger in for sulfur containing peptides. TFA was evaporated and cleavage products were precipitated with cold ether. The peptide was extracted into water and lyophilized. It was then purified by reverse phase HPLC, using a Vydac C-18 semipreparative column and a gradient of 0 to 100% B over 40 minutes, where solvent A was 95:5 water:acetonitrile, 0.1% TFA and solvent B was 95:5 actonitrile:water, 0.1% TFA. After purification the peptide was lyophilized to powder and identified with ESI-TOF mass spectroscopy.

ii. Methylation of dimethyl lysine.

The **ubWQKme3L** peptide was synthesized with a dimethyl lysine at position 12 and then methylated to trimethyl lysine on resin by reacting with 8 µl 1,3,4,6,7,8-Hexahydro-1-methyl-2H-pyrimide [1,2-9-] pyrimidine and 62 µl brought up to 5 ml in DMF. Reaction mixture was agitated by nitrogen bubbling under a vented septum for 5 h. Resin was washed with DMF 3x and then washed with 3x dichloromethane.

iii. NMR Spectroscopy.

NMR samples were made to a concentration of 1 mM in D_2O buffered to pD 4.0 (uncorrected) with 50 mM NaOAc-d3, 24 mM AcOH-d4, 0.5 mM DSS. Samples were analyzed on a Varian Inova 600-MHz instrument. One dimensional spectra were collected by using 32-K data points and between 8 to 128 scans using 1.5 second presaturation. Two dimensional total correlation spectroscopy (TOCSY) and nuclear overhauser spectroscopy (NOESY) experiments were carried out using the pulse sequences from the chempack software. Scans in the TOCSY experiments were taken 16 to 32 in the first dimension and 64 to 128 in the second dimension. Scans in the NOESY experiments were taken 32 to 64 in the first dimension and 128 to 512 in the second dimension with mixing times of 200 to 500 msec. All spectra were analyzed using standard window functions (sinbell and Gaussian with shifting). Presaturation was used to suppress the water resonance. Assignments were made by using standard methods as described by Wüthrich.[19] All experiments were run at 298 K.

iv. Determination of fraction folded.

[19] Wüthrich, K. *NMR of Proteins and Nucleic Acids*; Wiley: New York, 1986.

To determine the unfolded chemical shifts, 10-mers were synthesized. The chemical shifts for residues in the strand and one turn residue were obtained from each 10-mer peptide. The chemical shifts of the fully folded state were taken from the previously published NMR characterization of ubiquitin protein.[12] The fraction folded on a per residue bases was determined from equation 1.

$$\text{Fraction Folded} = [\delta\text{obs} - \delta 0]/[\,\delta 100 - \delta 0], \qquad [1]$$

where δobs is the observed Hα chemical shift, δ100 is the Hα chemical shift of the native ubiquitin protein, and δ0 is the Hα chemical shift of the unfolded 10-mers. The overall fraction folded for the entire peptide was obtained by averaging the fraction folded for all of the residues except for the terminal residues, Ile 3, and the turn residues Leu 8, Thr 9, Gly 10, and Lys 11. The terminal residues were omitted due to fraying and Ile3 gave anomalous folding which was also observed by Zerella.[7a] The overall fraction fold was also determined using the extent of Hα glycine splitting observed in the turn residue Gly 10 given in equation 2.

$$\text{Fraction Folded} = [\Delta\delta_{\text{Gly Obs}}]/[\,\Delta\delta_{\text{Gly 100}}], \qquad [2]$$

where $\Delta\delta_{\text{Gly Obs}}$ is the difference in the glycine Hα chemical shifts of the observed, and $\Delta\delta_{\text{Gly 100}}$ is the difference in the glycine Hα chemical shifts of the native ubiquitin protein.

v. CD Spectroscopy.

CD spectroscopy was performed on an Applied photophysics Pistar -180 Circular Dichroism spectrophotometer at 298 K. Peptides were dissolved in phosphate buffer of pH 7.5 and the appropriate amount of methanol was titrated in for each concentration. Spectra were collected from 260 nm to 185nm with 1 s scanning every 0.2 nm.

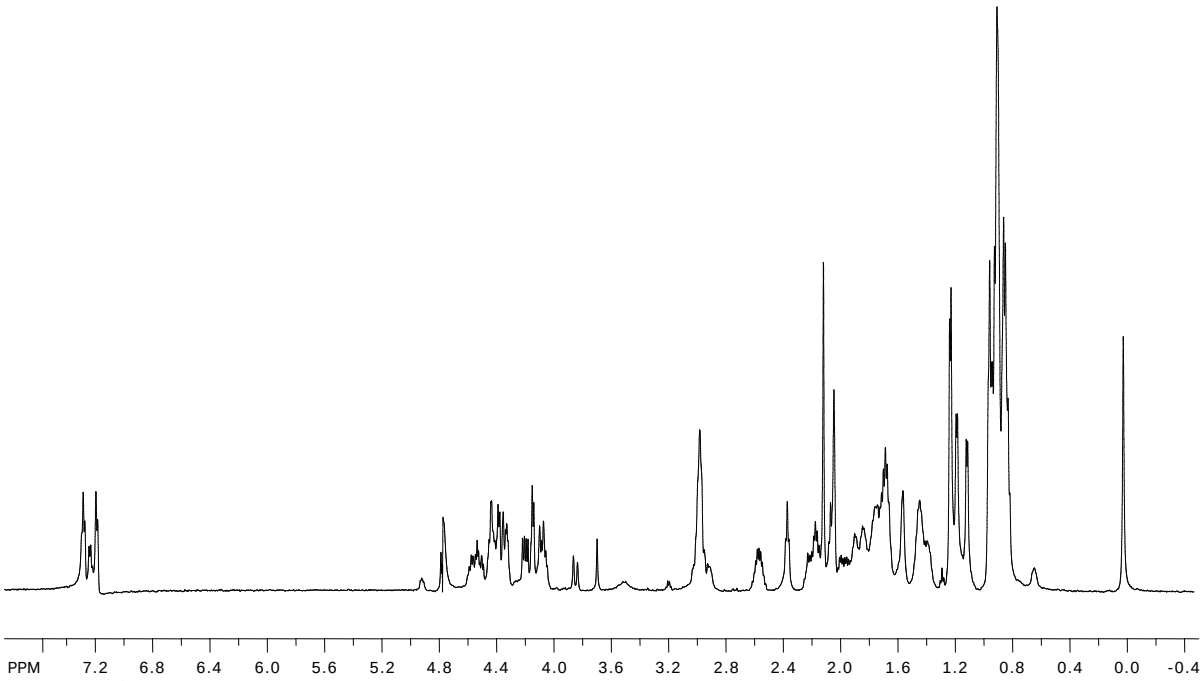

Figure 5.9 ^{1}HNMR of Peptide **UbN:** NH2-Met-Gln-Ile-Phe-Val-Lys-Thr-Leu-Thr-Gly-Lys-Thr-Ile-Thr-Leu-Glu-Val-NH2

Table 5.2 Proton Chemical Shift Assignments for Peptide **UbN.**

Residue	α	β	γ	δ	ε	Amide
M	4.13	2.13	2.53			
Q	4.53	1.85	2.14			8.72
I	4.18	1.96	0.85			8.6
F	4.9	2.91	H2,6 7.22	H3,5 7.25	H4 7.31	8.44
V	4.13	2.01,1.76	0.9			8.44
K	4.58	1.71	1.43	1.71	2.97	8.44
T	4.41	4.15	1.19			8.37
L	4.36	nd	nd	0.86		8.56
T	4.34	4.16	1.19			7.96
G	4.07, 3.84					8.25
K	4.4	nd	nd	nd	2.95	7.93
T	4.56	4.06	1.15			8.37
I	4.19	1.75	1.34	0.85		8.39
T	4.52	4.04	1.08			8.27
L	4.42	nd	nd	0.85		8.49
E	4.49	1.95	2.34			8.31
V	4.09	2.01	0.91			8.25

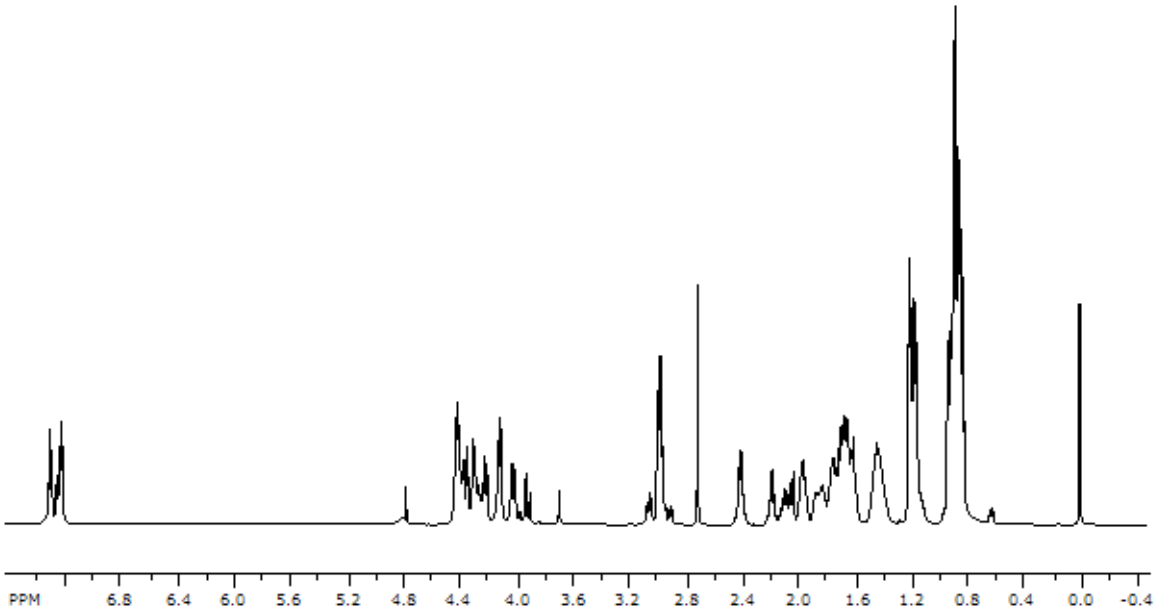

Figure 5.10 ^{1}HNMR of Peptide **UbD:** NH-Gln-Ile-Phe-Val-Lys-Thr-Leu-Thr-Gly-Lys-Thr-Ile-Thr-Leu-Glu-NH2

Table 5.3 Proton Chemical Shift Assignments for Peptide **UbD.**

Residue	α	β	γ	δ	ε	Amide
Q	4.01	1.98	2.13			
I	4.19	1.75	nd	0.86		8.55
F	4.73	2.93	H2,6 7.24	H3,5 7.26	H4 7.32	8.55
V	4.13	1.95	0.86			8.25
K	4.39	1.77	1.41	1.66	2.96	8.39
T	4.36	4.23	1.18			8.25
L	4.37	1.62	nd	0.86		8.34
T	4.32	4.22	1.18			8.02
G	3.99, 3.91					8.34
K	4.39	1.77	1.41	1.66	2.96	8.08
T	4.37	4.1	1.14			8.3
I	4.29	1.84	1.43	0.86		8.41
T	4.37	4.1	1.14			8.3
L	4.42	1.65	nd	0.9		8.48
E	4.29	1.94	2.39			8.34

Table 5.4 Proton Chemical Shift Assignments for Peptide **Ub(1-10).**

Residue	α	β	γ	δ	ε	Amide
M	4.13	2.14	2.54			
Q	4.35	1.9	2.17			8.74
I	4.12	1.74	1.12	0.8		8.27
F	4.68	2.96	H2,6 7.24	H3,5 7.27	H4 7.31	8.44
V	4.03	1.95	0.88			8.09
K	4.3	1.78	1.42	1.73	2.98	8.37
T	4.33	4.22	1.19			8.11
L	4.44	1.63	nd	0.88		8.42
T	4.31	4.2	1.19			8.16
G	3.94, 3.87					8.37

Table 5.5 Proton Chemical Shift Assignments for Peptide **Ub(8-17).**

Residue	α	β	γ	δ	ε	Amide
L	4.23	1.86	0.87			
T	4.31	4.12	1.15			8.52
G	3.97, 3.95					8.52
K	4.38	1.72	1.42	1.72	2.96	8.25
T	4.38	4.15	1.15			8.64
I	4.1	1.72	nd	0.85		8.3
T	4.31	4.12	1.15			8.25
L	4.32	1.59	nd	0.89		8.3
E	4.38	1.99	2.38			8.37
V	4.08	2.04	0.92			8.15

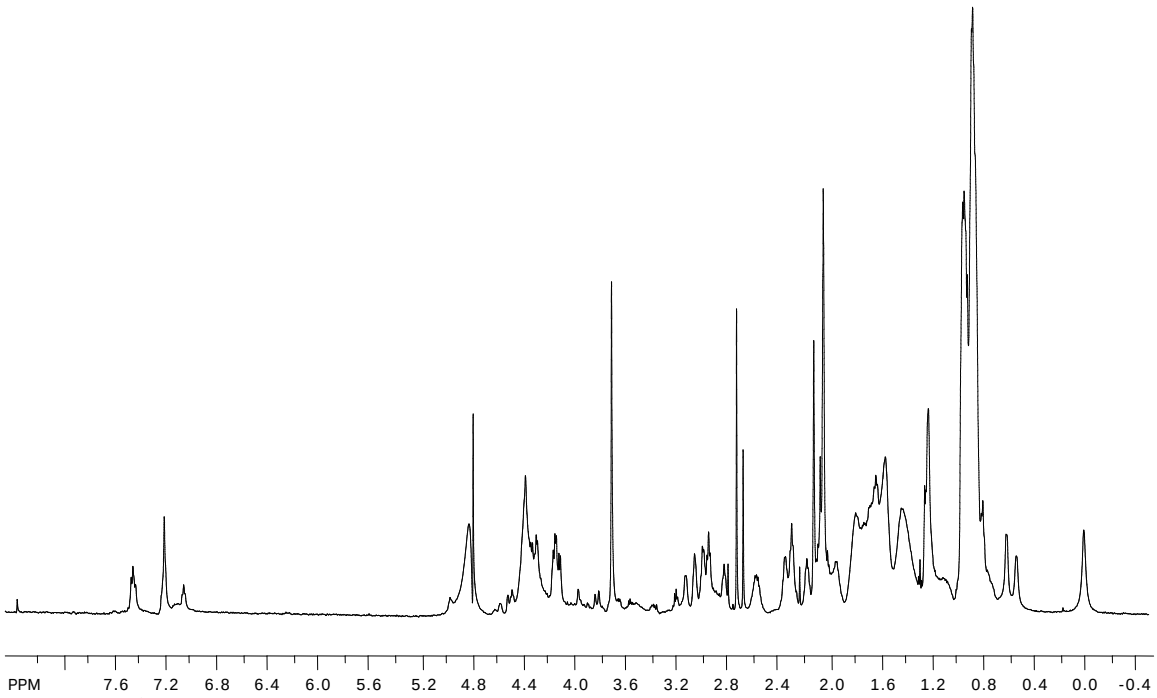

Figure 5.11 ^{1}HNMR of Peptide **ubWQKL:** NH-Met-Arg-Ile-Trp-Val-Gln-Thr-Leu-Thr-Gly-Lys-Lys-Ile-Leu-Leu-Gln-Val-NH2.

Table 5.6 Proton Chemical Shift Assignments for Peptide **ubWQKL.**

Residue	α	β	γ	δ	ε
M	4.13	2.16	2.55		
R	4.55	1.62	1.54	3.03	
I	4.27	2.06	1.72,1.38	0.86	
W	4.96	3.1			
V	4.1	2.04	0.93		
Q	4.38	1.96	2.31		
T	4.34	4.23	1.2		
L	nd	nd	nd		
T	4.56	nd	1.23		
G	4.13, 3.81				
K	4.29	nd	nd	nd	2.96
K	4.38	nd	nd	nd	2.95
L	nd	nd	nd		
L	nd	nd	nd		
I	4.12	1.82	nd	0.88	
Q	4.46	2.03	2.27		
V	4.12	2.07			

Table 5.7 Proton Chemical Shift Assignments for Peptide **ubWQKL(1-10).**

Residue	α	β	γ	δ	ε
M	4.14	2.16	2.56		
R	4.35	1.64	1.47	3.04	
I	4.18	1.94	0.85		
W	4.69	3.2			
V	4.01	1.88	0.84		
Q	4.19	1.97	2.29		
T	4.36	4.24	1.19		
L	4.44	1.64	nd	0.89	
T	4.36	4.19	1.17		
G	3.91				

Table 5.8 Proton Chemical Shift Assignments for Peptide **ubWQKL(8-17).**

Residue	α	β	γ	δ	ε
L	4.38	1.59	0.88		
T	4.34	4.28	1.19		
G	3.96				
K	4.3	1.7	1.39	nd	2.96
K	4.3	1.7	1.39	nd	2.96
I	4.1	1.82	1.45	0.86	
L	4.34	1.59	nd	0.87	
L	4.34	1.59	nd	0.87	
Q	4.37	1.97	2.33		
V	4.09	2.06	0.93		

CHAPTER VI

DESIGN AND STUDY OF TERTIARY INTERACTIONS BETWEEN β-HAIRPIN AND α-HELIX

A. Introduction.

As discussed in Chapter 1, advancement in protein design allows for a better understanding of structure function relationships in proteins and the development of useful novel proteins. Over the past few years many mini-proteins have been developed that fold into a variety of tertiary structures.[1] Since helical systems have been studied for over 30 years and are well understood, design rules are available to create tertiary interactions that will form α-helical coiled coil dimers, trimers, and tetramers.[2,3] The study of β-sheet interactions has increased over the past decade and has led to the design of β-sandwich proteins.[4] However design of peptides that have hairpin-helix interactions is not as well understood as helix-helix and hairpin-hairpin interactions. The structural motif of α helicies packing against β-sheets is very common in proteins (Figure 6.1). Additionally, this same

---

[1] Imperiali, B.; Ottesen, J. J. *J Pept Res* **1999**, *54*, 177-184.

[2] Micklatcher, C.; Chmielewski, J. *Curr Opin Chem Biol* **1999**, *3*, 724-729.

[3] Hill, R. B.; Raleigh, D. P.; Lombardi, A.; Degrado, W. F. *Acc Chem Res* **2000**, *33*, 745-754.

[4] (a)Quinn, T. P.; Tweedy, N. B.; Williams, R. W.; Richardson, J. S.; Richardson, D. C. *Proc Nat Acad Sci U. S.A.* **1994**, *91*, 8747-8751.(b) Lim, A.; Saderholm, M. J.; Makhov, A. M.; Kroll, M.; Yan, Y. B.; Perera, L.; Griffith, J. D.; Erickson, B. W. *Protein Sci* **1998**, *7*, 1545-1554. (c) Kraemer-Pecore, C. M.; Lecomte, J. T. J.; Desjarlais, J. R. *Protein Sci* **2003**, *12*, 2194-2205. (d) Ilyina, E.; Roongta, V.; Mayo, K. H. *Biochemistry* **1997**, *36*, 5245-5250.

configuration is seen in protein-protein recognition events where an α-helix in one protein domain will bind to a β-sheet surface in another. One important example of this is the binding of p53 with MDM2 (Figure 6.1d).[5] Currently there are a few *de novo* designed mini protein with involving α-helix packing against a β-sheet such as the ββα design based on the zinc finger domain.[6] Another *de novo* mini-protein was developed using computational simulations that contains a β-hairpin interacting with an α-helix.[7] However, there is not a set of well defined, general, design principles that exist for hairpin-helix tertiary interaction as there are for α-helical coiled coil systems.

[5] Yin, H.; Lee, G. I.; Park, H. S.; Payne, G. A.; Rodriguez, J. M.; Sebti, S. M.; Hamilton, A. D. *Angew Chem Int Ed* **2005**, *44*, 2704-2707.

[6] Struthers, M. D.; Cheng, R. P.; Imperiali, B. *J Am Chem Soc* **1996**, *118*, 3073-3081.

[7] Dahiyat, B. I.; Mayo, S. L. *Science* **1997**, *278*, 82-87.

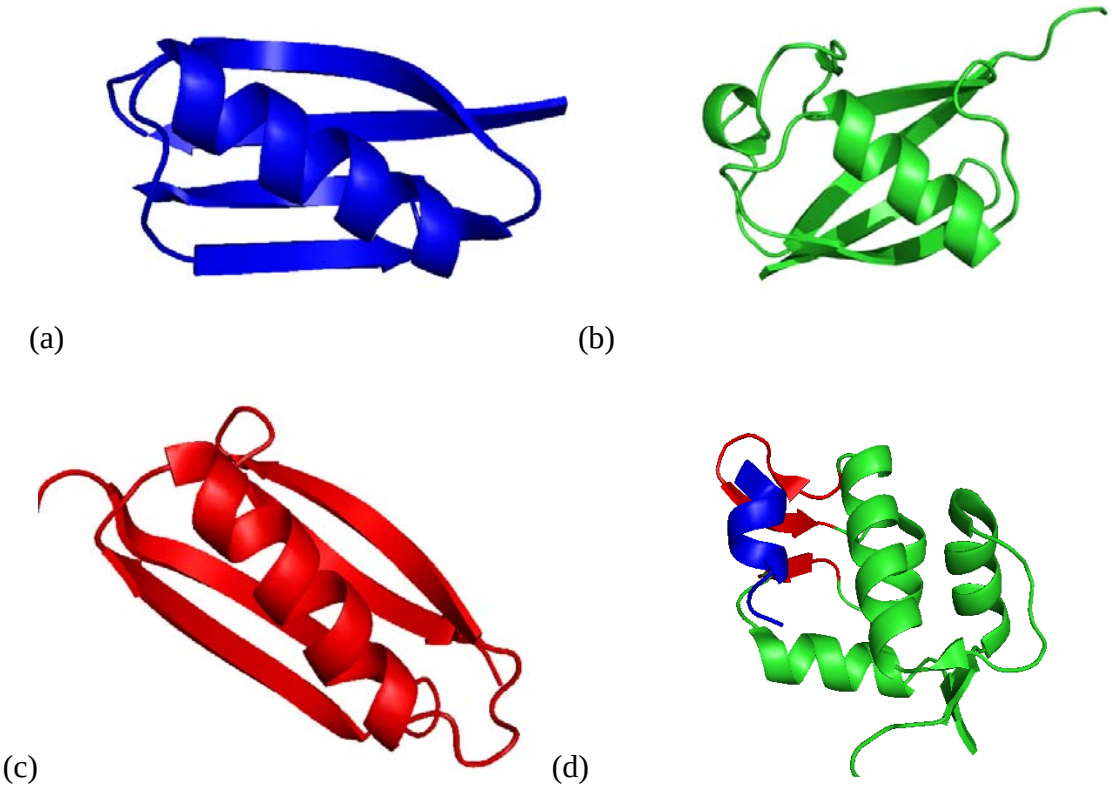

Figure 6.1 Examples of α-helix-β-sheet motif in proteins (a) B1 domain of streptococcal protein G (pdb code: 3GB1), (b) Ubiquitin (pdb code: 1UBQ), and (c) B1 domain of protein L (pdb code: 2ptl). (d) Helical peptide from the tumor suppressor protein p53 (blue) bound to its inhibitor(green) where the interacting β-sheet portion is in red.

The goal of this project is to determine the key factors that dictate tertiary interactions between α-helices and β-hairpins. To this end the hairpin-helix interactions of protein GB1 will initially be used as a template to study the requirements necessary for tertiary contacts. Streptococcal protein GB1 is a small 56 residue protein that consists of a β-hairpin α-helix β-hairpin motif in which the two hairpins pack against the α-helix (Figure 6.1a). This system has been thoroughly studied making it ideal for investigating hairpin-helix interactions. The C-terminal β-hairpin (**Hairpin 1)** is known to fold autonomously in water[8] with a fraction

[8] Blanco, F. J.; Rivas, G.; Serrano, L. *Nat Struct Biol* **1994**, *1*, 584-590.

folded of 40% and is indicated as the nucleation site for GB1 folding [9] making this β-hairpin a logical candidate for manipulation of hairpin-helix interactions.

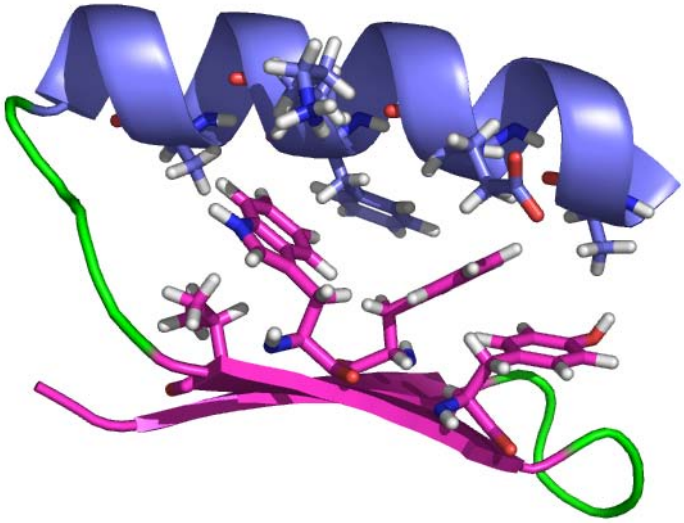

Figure 6.2 GB1 domain [pdb code: 3GB1] showing side chain interactions between the α-helix (blue) and the C-terimnal β-hairpin 2(purple).

B. Helix 2 – Hairpin 2 Studies.

i. Design.

To determine if it is feasible to observe a binding event between the α-helix and the C-terminal β-hairpin of GB1 intermolecularly, two peptides were designed after their respective domain fragments. Since it is unlikely that the native sequence fragments will bind effectively in the absence of the full protein sequence we sought to preorder the secondary structures of these peptides while keeping observed side chain-side chain contacts intact. Figure 6.2 highlights the side chains that are observed in the tertiary interaction between the helix and C-terminal hairpin as seen in the crystal structure of GB1.

[9] Kobayashi, N.; Honda, S.; Yoshii, H.; Uedaira, H.; Munekata, E. *FEBS Lett* **1995**, *370*, 282-282.

The native C-terminal hairpin fragment was redesigned by replacing the native DDATKT loop with the hairpin stabilizing VpGK(p = d-proline) turn[10] and referred to as **Hairpin 2** (Table 6.1). The VpGK turn sequence is know to adopt a favorable type II' which is highly stabilizing in β-hairpins[11] which should produce a more stable hairpin over the native peptide.

Using the AGIDIR program developed by Serrano and coworkers that estimates the α-helicity of a given peptide sequence under specific conditions[12], we determined that the excised α-helix sequence of the native GB1 referred to as **Helix 1** was likely to have no helical structure in aqueous solution (Table 6.1). Thus, the sequence was redesigned to have a higher percentage of helix formation in aqueous solution to give the **Helix 2** peptide (Table 6.2). All the residues that are implicated in tertiary interactions with the C-terminal hairpin in GB1 were maintained in the **Helix 2** peptide while all other residues with low α-helix propensity were mutated to alanine which has highest α-helix propensity of all natural amino acids. Additional alanine repeats were added to the C-terminus of the peptide to help induce helix formation, while lysine residues were incorporated to maintain water solubility of the peptide. A helix cap sequence of acelyated Asp was incorporated to the N-terminus to help induce helix formation as well.[2] Tyr with a Gly spacer was incorporated at the C-terminus as a spectroscopic tag to allow for UV determination of concentration of the peptide in solution. The AGIDIR program predicts that the **Helix 2** sequence will be 32% folded under the conditions used for CD (10 mM sodium phosphate, pH 7.5, 298 K).

---

[10] Stanger, H. E.; Gellman, S. H. *J Am Chem Soc* **1998**, *120*, 4236-4237.

[11] Haque, T. S.; Gellman, S. H. *J Am Chem Soc* **1997**, *119*, 2303-2304.

[12] Munoz, V.; Serrano, L. *Biopolymers* **1997**, *41*, 495-509.

Table 6.1 Synthesized peptides based on GB1 Protein. Colored residues are found in native GB1 where blue residues are residues that make interactions between the α helix and β hairpin in C-terminal portion GB1 as seen in the NMR structure[11] and red residues are favorable for α-helix formation. The percent helicity is indicated in parenthesis next to the helix sequences and was calculated using AGIDIR[12].

Peptide	Sequence
Helix 1	Ac-AATAEKVFKQYAND-NH_2 (2%)
Helix 2	Ac-DAAAAAEKAFKAAAKAAAAKAAAAGY-NH_2 (32%)
Helix 3	Ac-YGDAAAAKKAAAAAAAEKAFKAAAAGGGC-NH_2 (47%)
Helix 4 Native	Ac-YGDAAAAKKAAAAATAEKVFKQYANC-NH_2 (17%)
Helix 4	Ac-YGDAAAAKKAAAAAAAEKAFKAAAAC-NH_2 (53%)
Hairpin 1	Ac-GEWTYDDATKTFTVTE-COOH
Hairpin 2	Ac-GEWTYVpGKFTVTE-NH_2
Hairpin 3	Ac-CGEWTYVpGKFTVTE-NH_2
Hairpin 4	Ac-CGRWTYVpGKFTKTQ-NH_2
Hairpin 5	Ac-CGVDGEWTYVpGKFTVTE-NH2

ii. Results and Discussion.

(a) Analysis of Helix peptides. To confirm that the native α-helix sequence was indeed poorly folded, **Helix 1** was synthesized and analyzed by CD at 298 K using 100 μM **Helix 1**. The spectrum indicated that the peptide was unstructured with a minimum at 198 nm (Figure 6.3). Previous work done by Blanco and Serrano[13] shows that a peptide consisting of residues 21-40 of GB1 is unstructured by CD, which is consistent with the predicted AGADIR[12] value of 2% helicity and the observation that **Helix 1** is unstructured.

[13] Blanco, F. J.; Serrano, L. *Eur J Biochem* **1995**, *230*, 634-649.

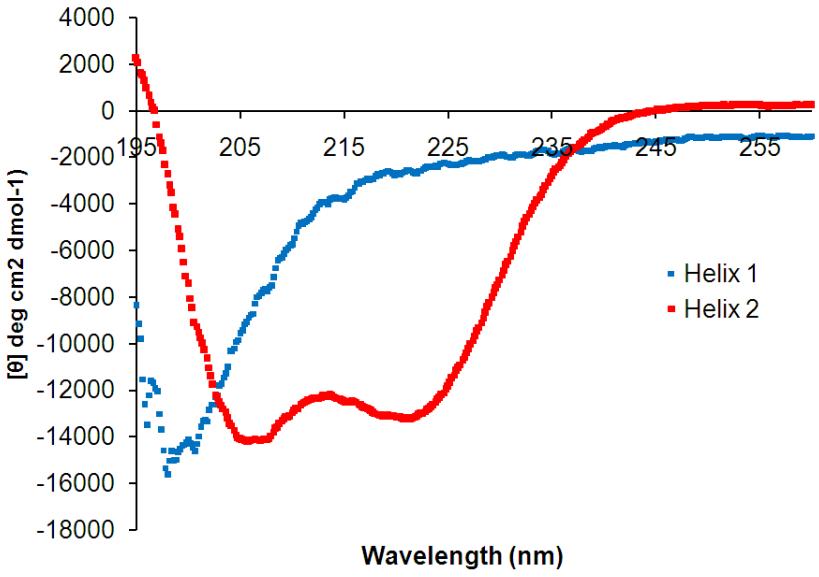

Figure 6.3 CD spectrum of **Helix 1** (blue) and **Helix 2** (red) peptide, Conditions: 10mM phosphate buffer, pH 7.5, 298 K.

The designed **Helix 2** was synthesized and characterized by CD to identify secondary structure formation. The CD spectrum of 39.4 μM **Helix 2** revealed minima at 205 nm and 222 nm indicating α helix structure (Figure 6.3). The percent helicity was calculated for this peptide to be 33% using the method described in the experimental section which correlates well with the 32% helicity predicted by AGADIR. Thus, the design methodology for **Helix 2** resulted in a more structured α-helix than the native GB1 α-helix fragment **Helix 1**.

(b) Analysis of Hairpin 2. The C-terminal β-hairpin with the modified VpGK turn, **Hairpin 2,** was synthesized and characterized by NMR and CD. For complete NMR characterization a cyclic fully folded control **cyclic Hairpin 2** was synthesized with the sequence Ac-CEWTYVpGKFTVTC-NH_2. Cyclization was achieved by a disulfide bond between cysteine residues at the N and C-termini of the peptide. Unfolded control peptides consisting of either the N-terminal arm (**Hairpin 2 control 1)** or residues 7-14 or the C-terminal arm (**Hairpin 2 control 2)** were used to obtain random coil chemical shifts. As discussed in Chapter 1, downfield shifting of ≥ 0.1 ppm of the Hα protons along the peptide

backbone relative to unfolded values indicates a β-sheet conformation.[14] Analysis of the Hα shifting indicated β-sheet formation with downfield shifting ≥ 0.1 ppm for most residues (Figure 6.4). The residues Val 10 and Phe 12 are upfield shifted due to electronic shielding effects of the cross strand aromatic residues, while d-Pro 7 is upfield shifted due to its presence in the turn. Upfield shifting observed at Glu-14 is indicative of typical fraying observed in β-hairpin peptides.

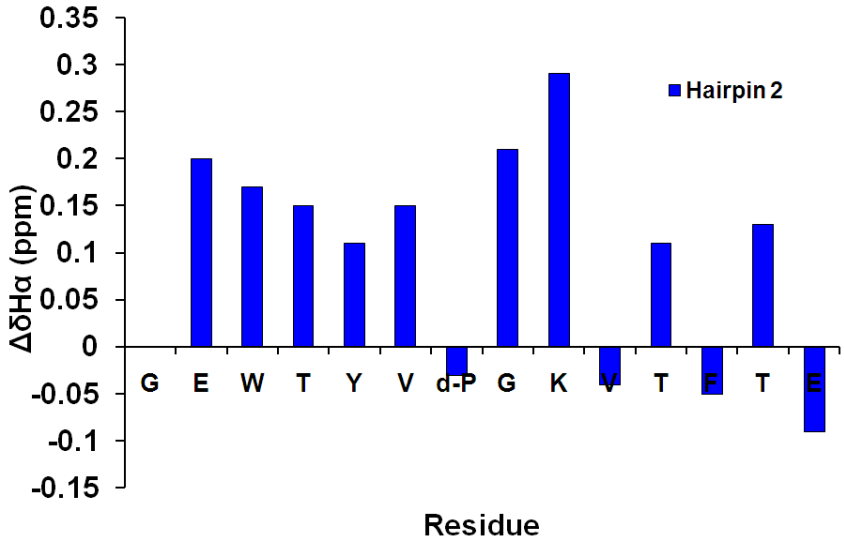

Figure 6.4 Hα chemical shift difference of **Hairpin 2** from random coil peptides. The Gly bars reflect the Hα separation in the hairpin. Conditions: 298 K, 50 mM sodium acetate-d_4, pH 4.0 (uncorrected), referenced to DSS.

CD analysis also confirmed β-sheet formation where 42.0 μM of **Hairpin 2** appears to have some unstructured character with a minimum at 198 nm but also has some β sheet character with a minimum at 210 nm (Figure 6.5).

The extent of folding to a β-hairpin by **Hairpin 2** was quantified from the NMR data using two methods described in Chapter 1 and the Experimental Section. Both Hα shifting method and glycine splitting method showed that **Hairpin 2** was approximately 60% folded.

[14] Sharman, G. J.; Griffiths-Jones, S. R.; Jourdan, M.; Searle, M. S. *J Am Chem Soc* **2001**, *123*, 12318-12324.

This is a 20% increase in stability over the natural **Hairpin 1** (40% folded) peptide described by Blanco *et. al*.[8] Thus, incorporation of the Type II' VpGK turn resulted in a more stable β-hairpin sequence as predicted.

(c) Evidence of intramolecular interaction between Helix 2 and Hairpin 2. To ascertain if preordered **Helix 2** and **Hairpin 2** peptides interact with each other, a CD spectrum of a solution containing 39.4 μM **Helix 2** and 42.0 μM **Hairpin 2** was obtained. Since CD signals are additive, any difference in the spectra of the mixed hairpin-helix solution relative to the additive signal of the two peptides will indicate intermolecular interactions. Comparison of the spectrum of the mixture of the two peptides to the spectrum calculated from the addition of individual signals of the separate 39.4 μM **Helix 2** and 42.0 μM **Hairpin 2** solutions (Figure 6.5) shows an increased helical signal for the mixture of **Helix 2** and **Hairpin 2** relative to the sum of the individual peptides.

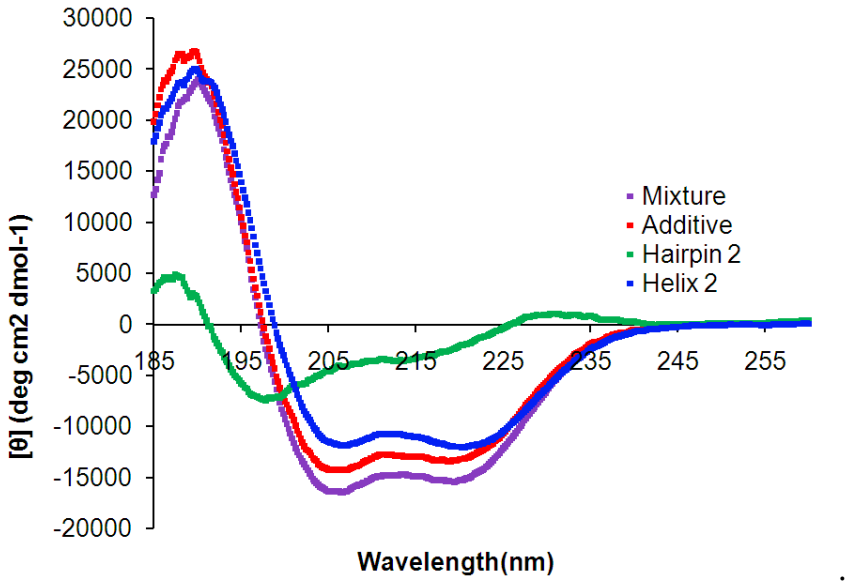

Figure 6.5 CD comparison of **Helix 2** (Blue) and **Hairpin 2**(green), mixture of **helix2** and **hairpin2** (purple) to Additive signals of **Helix 2** and **Hairpin 2** (red). Conditions: 10mM phosphate, pH 7.5, 298K**.**

The CD spectral data suggests that **Hairpin 2** is binding to **Helix 2** and is inducing further α helical folding within **Helix 2.** Kobayashi *et al*.[9] have shown that the C-terminal β-hairpin fragment will induce GB1 structure to a fragment peptide containing the rest of the protein, but they also have shown that no structure was induced when the C-terminal β-hairpin fragment was mixed with the α-helical fragment of GB1. Hence, increasing the stability of both secondary structures appears to produce a more favorable tertiary interaction.

We attempted to determine a binding constant between these two peptides through monitoring change in helicity of the peptide mixture by CD. A fixed concentration of **Helix 2 (**50 μM) was mixed with increasing concentrations of **Hairpin 2 (**0-170 μM)**.** However, no appreciable change beyond error was observed with increasing concentrations of **Hairpin 2**, therefore we sought other methodologies to study redesigned helix-hairpin interactions.

C. Disulfide Exchange Studies with Helix – Hairpin peptides.

Since intermolecular binding events between our previously discussed Helix-Hairpin system are likely very weak, an alternative approach was adopted to determine if our designed systems where interacting favorably. A covalently linked disulfide exchange strategy was utilized which takes advantage of oxidative disulfide linkage between two cysteine residues on separate peptides. This strategy has been used to determine favorable tertiary interaction in coiled-coil α-helical peptides.[15] Allowing the reaction of equal concentrations of helix peptide and hairpin peptide to reach equilibrium should result in the formation of three distinct species (Figure 6.6); heterodimer of helix linked to hairpin,

[15] Oakley, M. G.; Kim, P. S. *Biochemistry* **1998**, *37*, 12603-12610.

homodimer of helix linked to helix, and a homodimer hairpin linked to hairpin. If the peptides do not have any favorable interactions between each other or themselves the reaction should yield a product ratio of 1:2:1 for hairpin homo dimer, helix-hairpin hetero dimer, and helix homo dimer, respectively. However a deviation from the random product ratio would indicate some favorable interaction between species is occurring. Therefore a statically significant increase in heterodimer formation over homodimeric species would suggest that there is a favorable interaction between hairpin and the helix, warranting further investigation. The disulfide exchange methodology is amenable for library screens making it an attractive method for determining favorable tertiary interactions between a helix-hairpin interface.

Figure 6.6 Schematic representation of disulfide exchange reaction between Helix and Hairpin.

i. Helix3-Hairpin3 Studies.

Peptides **Helix 3** and **Hairpin 3 (Table 6.1)** were designed with cysteines on the end of each sequence to allow for covalent linkage under oxidative conditions between the C-terminal β-hairpin and the α-helix similar to the native GB1 protein. The **Helix 3** peptide was redesigned from **Helix 2** to allow for covalent linkage that was a closer mimic of the natural GB1 sequence. Thus, the linking cysteine residue was positioned at the C-terminus of the peptide with a three Gly spacer representing the same number of residues consisting of the loop sequence that connects the helix to the C-terminal hairpin in GB1. The helix stabilizing

alanine lysine repeats were also positioned near the N-terminus along with the spectroscopic tyrosine tag to maintain helix formation.

A disulfide exchange reaction was carried out to determine if the designed **Helix 3** and **Hairpin 3** had favorable interactions to form a non-statistical ratio of heterodimers over homodimers at equilibrium. Three solutions were prepared, one consisting of 25 μM **Helix3,** another of 25 μM **Hairpin 3**, and one containing both 25 μM **Helix3** and 25 μM **Haipin3.** All solutions were prepared in 10mM sodium phosphate buffer at pH 8 and open to air to allow for air oxidation. The disulfide exchanged was followed by analytical HPLC for all three solutions. After 7 days all the solutions had reached equilibrium. (Figure 6.7) Peak area integration at 280 nm and 214 nm was used to determine the concentration of each species at equilibrium and a ratio of 1:2:1 was found for homodimer of **Helix 3,** heterodimer **Helix 3-Hairpin 3**, and homodimer **Hairpin 3** respectivily.

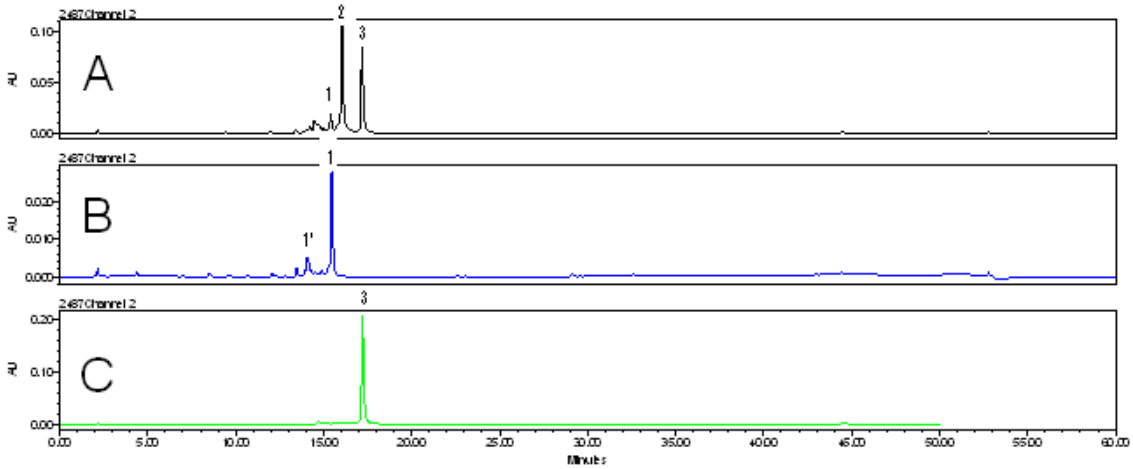

Figure 6.7 Analytical HPLC traces for disulfide exchange reaction for **Helix 3-Hairpin 3** at 280 nm. Trace **A** is disulfide exchange between **Helix 3** and **Hairpin 3** at equilibrium. Peak 1 is the homodimer of **Helix 3**, peak 2 is the heterodimer of **Helix 3-Hairpin 3,** and peak 3 is the homodimer of **Hairpin 3**. Trace **B** is the disulfide exchange for **Helix 3** control solution at equilibrium. Peak 1' is the monomer of **Helix 3** and peak 1 is the homodimer of **Helix 3**. Trace **C** is the disulfide exchange for **Hairpin 3** control solution at equilibrium. Peak 3 is the homodimer of **Hairpin 3.** Note: the extinction coefficient at 280 nm for the **Hairpin 3** homodimer is 1.7 times greater than heterodimer.

ii. Helix3-Hairpin4 Studies.

Since the ratio found for heterodimer formation suggested no interaction between helix and hairpin between competing species and alternative hairpin design was used to disfavor homodimer formation of the hairpin species. **Hairpin 4** contains mutations of Glu to Arg at position 3 and Val to Lys at position 13 to create net positive charges on each face of the hairpin to disfavor aggregation and homodimer formation (Table 6.1). Although we changed Val residue at the interface between the helix and the hairpin in GB1 we reasoned that this Val was primarily interacting with cross strand tryptophan within the hairpin and would have minimal effects on tertiary interaction. A disulfide exchange reaction was performed using 100 μM **Helix3** and 100 μM **Hairpin4** and monitored using analytical HPLC. However after 7 days no visible peaks were seen indicating precipitation of the peptides in solution. Thus we sought to increase the rate of equilibration before precipitation could occur.

To increase the rate of dimer formation in the disulfide exchange reaction the concentration of peptide species was increased to 250 μM. The disulfide exchanged was conducted at the higher concentration and after 4 days all the solutions had reached equilibrium (Figure 6.8). Peak area integration at 280 nm and 214 nm revealed a ratio of 1:2:1 for homodimer of **Helix 3,** heterodimer **Helix 3-Hairpin 4**, and homodimer **Hairpin 4** respectively.

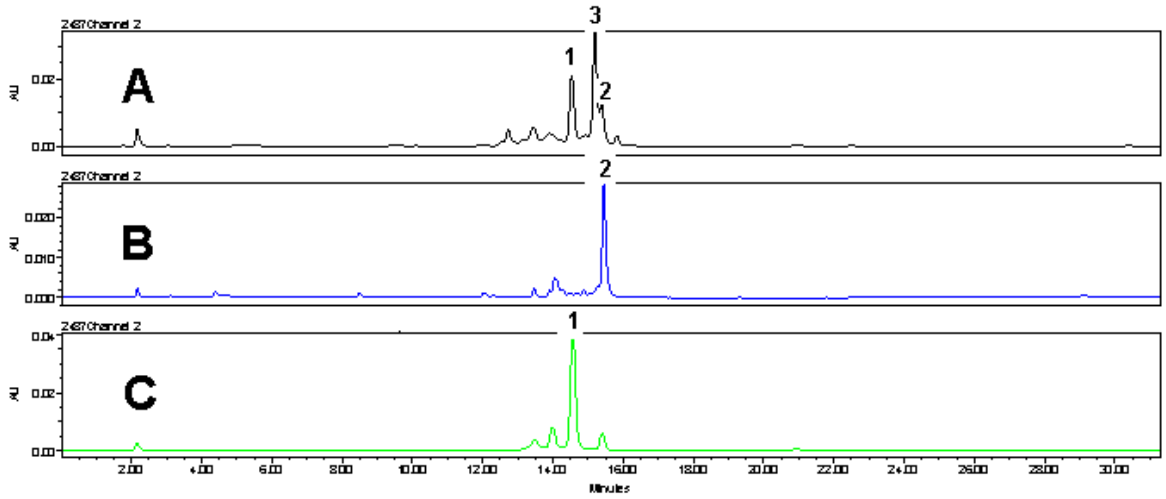

Figure 6.8 Analytical HPLC traces for disulfide exchange reaction for **Helix 3-Hairpin 4** at 280 nm. Trace **A** is disulfide exchange between **Helix 3** and **Hairpin 4** at equilibrium. Peak 1 is the homodimer of **Hairpin 4**, peak 2 is the homodimer of **Helix 3** and peak 3 is the heterodimer of **Helix 3-Hairpin 4**. Trace **B** is the disulfide exchange for **Hairpin 4** control solution at equilibrium. Trace **C** is the disulfide exchange for **Helix 3** control solution at equilibrium.

iii. Helix4 and Helix4 native - Hairpin 5 Studies.

Since the ratio found for heterodimer formation showed no evidence for favorable helix-hairpin interactions for the previously discussed systems, we hypothesized that the turn sequence residues that connect the helix and the hairpin in the native protein may be important for proper positioning of the secondary structures to interact with each other. The

native turn sequence residues were reintroduced on **Hairpin 5** and the GGGC residues were removed on the helix to give **Helix 4** and **Helix 4 native** (Table 6.1). **Helix 4 native** was designed as a control to see if in fact all of helix residues in GB1 are necessary for tertiary interaction with C-terminal hairpin. Disulfide exchange reactions were performed using 200 μM **Helix 4** mixed with 200 μM **Hairpin 5,** and 200 μM **Helix 4 native** mixed with 200 μM **Hairpin 5** which were again monitored using analytical HPLC. However, noisy analytical traces were obtained for both experiments with multiple peaks observed, many of which were overlapping and broadened, making peak identification and quantification impossible. We reasoned that this was likely due to peptide insolubility at pH 8 so the disulfide reaction was redesigned to use 5% DMSO as an oxidizing agent and lower the pH of the solution to 7.5. The DMSO method was expected to be quicker than air induced oxidation method with less likelihood of peptide precipitation.

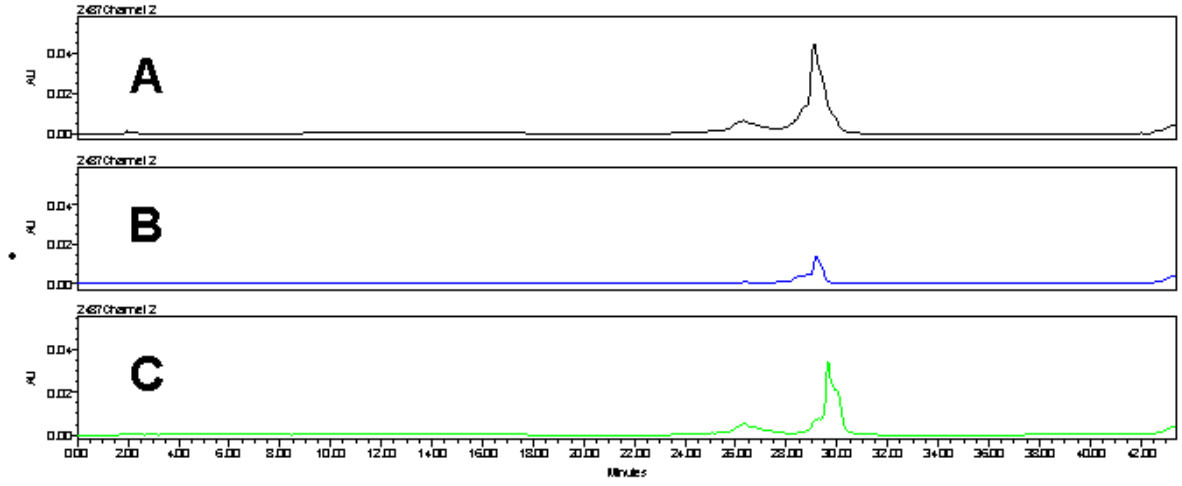

Figure 6.9 Analytical HPLC traces for disulfide exchange reaction using 5% DMSO for **Helix 4 native-Hairpin 5** at 280 nm. Trace **A** is disulfide exchange between **Helix 4 native** and **Hairpin 5** at equilibrium. Trace **B** is the disulfide exchange for **Helix 4 native** control solution at equilibrium. Trace **C** is the disulfide exchange for **Hairpin 5** control solution at equilibrium.

Disulfide exchange reaction using DMSO was preformed for 100 μM **Helix 4** mixed with 100 μM **Hairpin 5** and for 100 μM **Helix 4 native** mixed with 100 μM **Hairpin 5.** After 5 days the reactions had reached equilibrium but again the HPLC traces still showed some peak broadening and overlap and the presence of impurities that add to difficulty of obtaining accurate quantification of the species present. (Figure 6.9 and 6.10) Better separation methods and alternative oxidation conditions will be required to obtain clean HPLC traces so that the product formation ratio can be accurately determined.

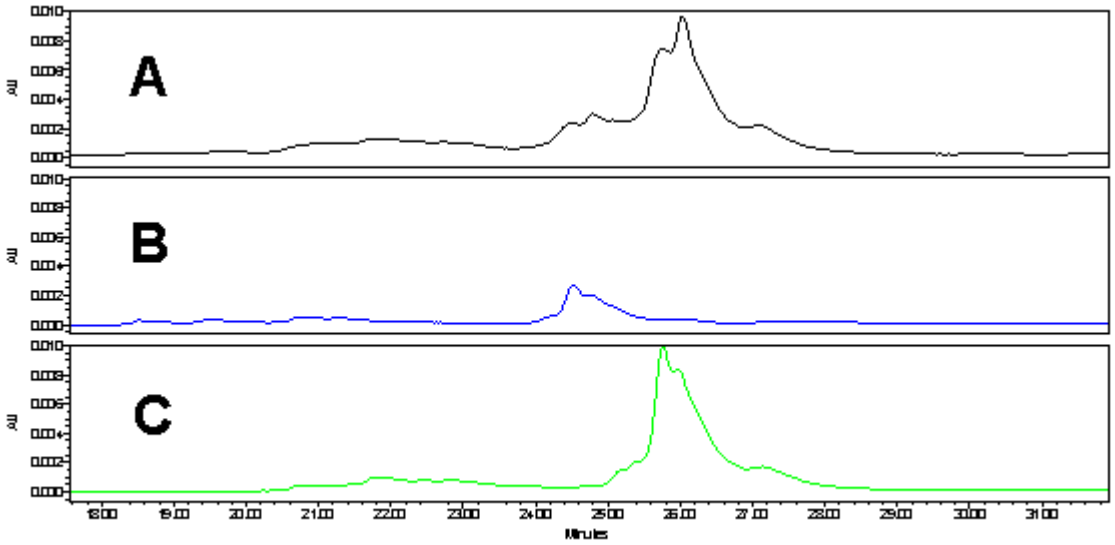

Figure 6.10 Analytical HPLC traces for disulfide exchange reaction using 5% DMSO for **Helix 4-Hairpin 5** at 280 nm. Trace **A** is disulfide exchange between **Helix 4** and **Hairpin 5** at equilibrium.Trace **B** is the disulfide exchange for **Helix 4** control solution at equilibrium. Trace **C** is the disulfide exchange for **Hairpin 5** control solution at equilibrium.

D. Future Work

Although the studies discussed in the previous section did not yield any definitive results regarding tertiary interactions between an α-helix and a β-sheet, the disulfide exchange method seems to be the most promising route for initial screening. Adjustment of experimental conditions and redesign of helix and hairpin monomers will be required in

future experiments, but the wealth of information obtained will be worth the effort. The design principles elucidated from these kinds of experiments will open up new strategies for disruption of protein-protein interactions. This could potentially lead to novel drugs, as well as allow scientists to study complex biological pathways mediated through protein-protein binding events.

E. Experimental.

i. Synthesis and purification of peptides.

Peptides were synthesized by automated solid phase peptide synthesis on an Applied Biosystems Pioneer Peptide Synthesizer using Fmoc protected amino acids on a PEG-PAL-PS resin. Activation of amino acids was performed with HBTU, HOBT in the presence of DIPEA in DMF. Deprotections were carried out in 2% DBU, 2% piperdine in DMF for approximately 10 minutes. Extended cycles (75 min) were used for each amino acid coupling step. All peptides where acetylated at the N-terminus with 5% acetic anhydride, 6% lutidine in DMF for 30 min. Cleavage of the peptide from the resin was performed in 95:2.5:2.5 Trifluoracetic acid (TFA): Ethanedithiol or Triisopropylsilane (TIPS): water for 3 hours. Ethanedithiol was used as a scavenger for sulfur containing peptides. TFA was evaporated and cleavage products were precipitated with cold ether. The peptide was extracted into water and lyophilized. It was then purified by reverse phase HPLC, using a Vydac C-18 semipreparative column and a gradient of 0 to 100% B over 40 minutes, where solvent A was 95:5 water:acetonitrile, 0.1% TFA and solvent B was 95:5 actonitrile:water, 0.1% TFA. After purification the peptide was lyophilized to powder and identified with ESI-TOF mass spectroscopy.

ii. Cyclization of Cyclic peptides. Cyclic control peptides were cyclized by oxidizing the cysteine residues at the ends of the peptide by stirring in a 10 mM phosphate buffer (pH 7.5) in 1% DMSO solution for 9 to 12 hours. The solution was lyophilized to a powder and purified with HPLC using previously described method.

iii. CD Spectroscopy.

CD spectroscopy was performed on an Applied photophysics Pistar-180 Circular Dichroism spectrophotometer at 298.15 K. Spectra were collected from 260nm to185nm with every 0.2 nm per 1 s scanning. The molar ellipticity [θ] is given in units of degrees centimeter^2 decimole^{-1}. Peptide solutions were dissolved in 10mM phosphate buffer of pH 7.5.

iv. Calculation of percentage helicity for Helix 1 and Helix 2 using CD.

The percentage helicity was calculated for Helix 1 and Helix 2 using the following equation:

Equation 1. Fraction helix = $([\theta]_{222,obs} - ([\theta]_{222,0})/ ([\theta]_{222,100} - ([\theta]_{222,0})$

where $[\theta]_{222,obs}$ is the observed mean residue ellipticity at 222 nm. Values used for 0% and 100% helicity,$[\theta]_{222,0}$ and $[\theta]_{222,100,}$ were +640 deg cm^2 and –40000(1-2.5/*n*), respectively, where *n* is the number of residue units.[16]

v. Disulfide Exchange Reactions.

Disulfide exchange reactions where prepared in 10mM sodium phosphate buffer at pH 8 phosphate buffer at either pH 8.0 or pH 7.5 with 5% DMSO depending on the experiment. Concentrations of peptide were calculated by measuring the UV absorption at 280 nm in the presences of 5 M GdnHCl where the extinction coefficients of **Helix 3** and **Helix 4** peptides

[16] Butterfield, S. M.; Patel, P. R.; Waters, M. L. *J Am Chem Soc* **2002**, *124*, 9751-9755.

are 1400 $M^{-1}cm^{-1}$; helix 4 native is 2680 $M^{-1}cm^{-1}$, and the hairpin peptides are 7090 $M^{-1}cm^{-1}$. The reactions were monitored by reverse phase analytical HPLC, using a Atlantis dC-18 analytical column and a gradient of 0 to 50% B over 40 minutes, where solvent A was 95:5 water:acetonitrile, 0.1% TFA and solvent B was 95:5 actonitrile:water, 0.1% TFA.

vi. NMR Spectroscopy.

NMR samples were made to a concentration of 1 mM in D_2O buffered to pD 4.0 (uncorrected) with 50 mM NaOAc-d3, 24 mM AcOH-d4, 0.5 mM DSS. Samples were analyzed on a Varian Inova 600-MHz instrument. One dimensional spectra were collected by using 32-K data points and between 8 to 128 scans using 1.5 second presaturation. Two dimensional total correlation spectroscopy (TOCSY) and nuclear overhauser spectroscopy (NOESY) experiments were carried out using the pulse sequences from the chempack software. Scans in the TOCSY experiments were taken 16 to 32 in the first dimension and 64 to 128 in the second dimension. Scans in the NOESY experiments were taken 32 to 64 in the first dimension and 128 to 512 in the second dimension with mixing times of 200 to 500 msec. All spectra were analyzed using standard window functions (sinbell and Gaussian with shifting). Presaturation was used to suppress the water resonance. Assignments were made by using standard methods as described by Wüthrich.[17] All experiments were run at 298.15 K.

vii. Determination of fraction folded.

To determine the unfolded chemical shifts, **Hairpin 2 control 1** and **control 2** were synthesized as unstructured controls and the cyclic peptide **cyclic Hairpin 2** was synthesized

[17] Wüthrich, K. *NMR of Proteins and Nucleic Acids*; Wiley: New York, 1986.

for fully folded. The chemical shifts for residues in the strand and one turn residue were obtained from each **Hairpin 2 controls**. The chemical shifts of the fully folded state were taken from the **cyclic Hairpin 2** peptide. The fraction folded on a per residue bases was determined from Equation 2.

$$\text{Fraction Folded} = [\delta\text{obs} - \delta 0]/[\,\delta 100 - \delta 0], \qquad [2]$$

where δobs is the observed Hα chemical shift, δ100 is the Hα chemical shift of the cyclic peptides, and δ0 is the Hα chemical shift of the unfolded **Control** peptides. The overall fraction folded for the entire peptide was obtained by averaging the fraction folded of residues Glu2, Thr 4, Val 6, Lys 9, Thr 11, and Thr 13. These residues are in hydrogen bonded positions have been shown to be the most reliable in determining fraction folded.[18] The overall fraction fold was also determined using the extent of Hα glycine splitting observed in the turn residue Gly 7 given in Equation 3.

$$\text{Fraction Folded} = [\Delta\delta_{\text{Gly Obs}}]/[\,\Delta\delta_{\text{Gly 100}}], \qquad [3]$$

where $\Delta\delta_{\text{Gly Obs}}$ is the difference in the glycine Hα chemical shifts of the observed, and $\Delta\delta_{\text{Gly 100}}$ is the difference in the glycine Hα chemical shifts of the cyclic peptides.

[18] Syud, F. A.; Espinosa, J. F.; Gellman, S. H. *J Am Chem Soc* **1999**, *121*, 11577-11578.

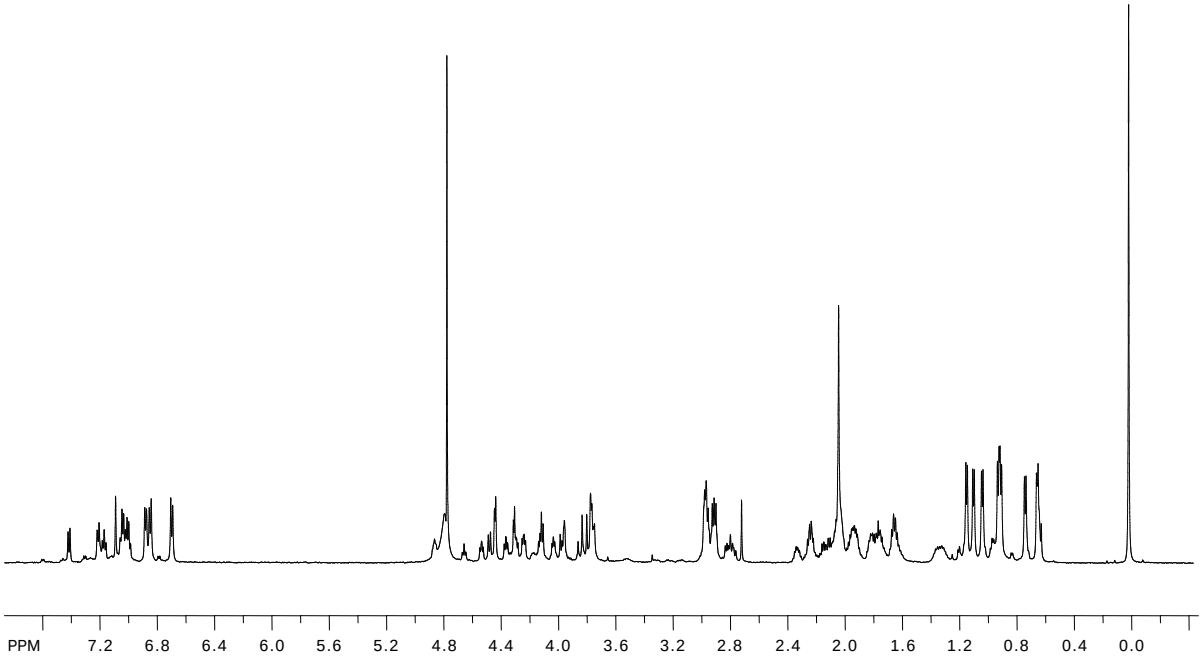

Figure 6.11 [1]HNMR of Peptide **Hairpin 2:** Ac-Gly-Glu-Trp-Thr-Tyr-Val-dPro-Gly-Lys-Phe-Thr-Val-Thr-Glu-NH2

Table 6.2 Proton Chemical Shift Assignments for Peptide **Hairpin 2.**

Residue	α	β	γ	δ	ε
G	3.77				
E	4.37	1.82	2.13		
W	4.88	2.81,2.96	nd	nd	nd
T	4.31	4.14	1.13		
Y	4.68	2.87	nd	nd	nd
V	4.48	2.01	0.91		
d-P	4.36	2.32	2.01	3.77	
G	3.98, 3.77				
K	4.53	1.72	1.33	1.72	2.96
V	4.12	1.62	0.68		
T	4.44	4.03	1.03		
F	4.68	2.87	nd	nd	nd
T	4.44	3.95	1.08		
E	4.24	1.94	2.23		

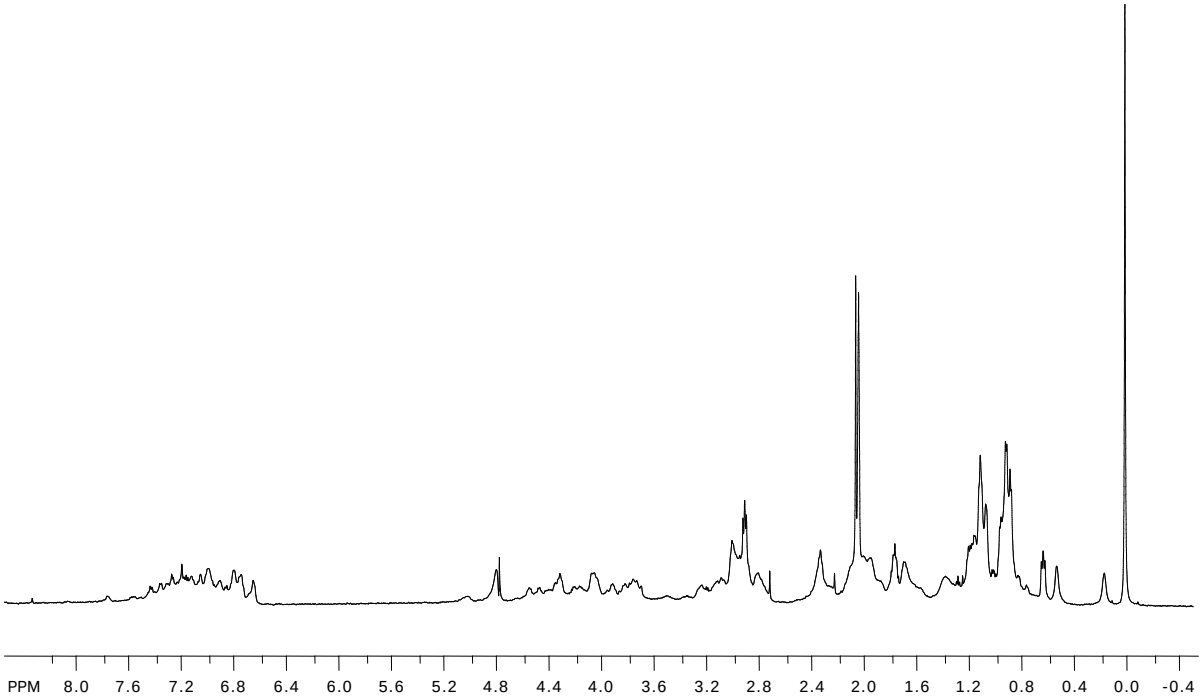

Figure 6.12 ^{1}HNMR of Peptide **cyclic Hairpin 2:** Ac-Cys-Glu-Trp-Thr-Tyr-Val-dPro-Gly-Lys-Phe-Thr-Val-Thr-Cys-NH2

Table 6.3 Proton Chemical Shift Assignments for Peptide **cyclic Hairpin 2.**

Residue	α	β	γ	δ	ε
C	4.82	3.05			
E	4.54	1.94	2.28		
W	5.03	2.79	nd	nd	nd
T	4.4	4.15	1.15		
Y	4.63	2.99			
V	4.44	1.94	0.89		
d-P	4.33	2.3	2	3.76, 3.77	
G	4.01, 3.70				
K	4.67	1.81	1.36	1.74	2.97
V	4.43	1.16	0.13,0.49		
T	4.65	4.05	1.07		
F	4.67	2.95	nd	nd	nd
T	4.54	3.91	1.02		
C	4.52	3.02			

Table 6.4 Proton Chemical Shift Assignments for Peptide **Hairpin 2 control 1.**

Residue	α	β	γ	δ	ε
G	3.77				
E	4.17	1.8	2.17		
W	4.71	3.2			
T	4.16	3.98	0.96		
Y	4.57	2.79	H2,6 7.04	H3,5 6.85	
V	4.33	2.02	0.91		
d-P	4.39	2.23	1.96	3.64, 3.70	
G	3.85				

Table 6.5 Proton Chemical Shift Assignments for Peptide **Hairpin 2 control 2.**

Residue	α	β	γ	δ	ε
d-P	4.37	2.26	1.99	3.65	
G	3.87				
K	4.24	1.64	1.27	1.63	2.91
V	4.16	2.08	0.95		
T	4.33	4.15	1.19		
F	4.73	3.04	H2,6 7.24	H3,5 7.34	H4 7.30
T	4.31	4.09	1.14		
E	4.33	1.96	2.4		

REFERENCES

Adams-Cioaba, M.A., Min, J.R., 2009. Structure and function of histone methylation binding proteins. Biochemistry and Cell Biology-Biochimie Et Biologie Cellulaire 87, 93-105.

Ali, M.H., Taylor, C.M., Grigoryan, G., Allen, K.N., Imperiali, B., Keating, A.E., 2005. Design of a heterospecific, tetrameric, 21-residue miniprotein with mixed alpha/beta structure. Structure 13, 225-234.

Ambroggio, X.I., Kuhlman, B., 2006. Design of protein conformational switches. Current Opinion in Structual Biology 16, 525-530.

Andrew, C.D., Warwicker, J., Jones, G.R., Doig, A.J., 2002. Effect of phosphorylation on alpha-helix stability as a function of position. Biochemistry 41, 1897-1905.

Balakrishnan, S., Zondlo, N.J., 2006. Design of a protein kinase-inducible domain. Journal of the American Chemical Society 128, 5590-5591.

Bamezai, S., Banez, M.A.T., Breslow, E., 1990. Structural and Functional-Changes Associated with Modification of the Ubiquitin Methionine. Biochemistry 29, 5389-5396.

Bannister, A.J., Zegerman, P., Partridge, J.F., Miska, E.A., Thomas, J.O., Allshire, R.C., Kouzarides, T., 2001. Selective recognition of methylated lysine 9 on histone H3 by the HP1 chromo domain. Nature 410, 120-124.

Bielska, A.A., Zondlo, N.J., 2006. Hyperphosphorylation of tau induces local polyproline II helix. Biochemistry 45, 5527-5537.

Blanco, F.J., Jimenez, M.A., Herranz, J., Rico, M., Santoro, J., Nieto, J.L., 1993. Nmr Evidence of a Short Linear Peptide That Folds into a Beta-Hairpin in Aqueous-Solution. Journal of the American Chemical Society 115, 5887-5888.

Blanco, F.J., Rivas, G., Serrano, L., 1994. A Short Linear Peptide That Folds into a Native Stable Beta-Hairpin in Aqueous-Solution. Nature Structural Biology 1, 584-590.

Blanco, F.J., Serrano, L., 1995. Folding of Protein-G B1 Domain Studied by the Conformational Characterization of Fragments Comprising Its Secondary Structure Elements. European Journal of Biochemistry 230, 634-649.

Bofill, R., Simpson, E.R., Platt, G.W., Crespo, M.D., Searle, M.S., 2005. Extending the folding nucleus of ubiquitin with an independently folding beta-hairpin finger: Hurdles to rapid folding arising from the stabilisation of local interactions. Journal of Molecular Biology 349, 205-221.

Bossemeyer, D., Engh, R.A., Kinzel, V., Ponstingl, H., Huber, R., 1993. Phosphotransferase and Substrate Binding Mechanism of the Camp-Dependent Protein-Kinase Catalytic Subunit from Porcine Heart as Deduced from the 2.0 Angstrom Structure of the Complex with Mn2+ Adenylyl Imidodiphosphate and Inhibitor Peptide Pki(5-24). Embo Journal 12, 849-859.

Burley, S.K., Petsko, G.A., 1986. Amino-Aromatic Interactions in Proteins. Febs Letters 203, 139-143.

Butterfield, S.M., Patel, P.R., Waters, M.L., 2002. Contribution of aromatic interactions to alpha-helix stability. Journal of the American Chemical Society 124, 9751-9755.

Camus, M.S., Dos Santos, S., Chandravarkar, A., Mandal, B., Schmid, A.W., Tuchscherer, G., Mutter, M., Lashuel, H.A., 2008. Switch-peptides: Design and characterization of controllable super-amyloid-forming host-guest peptides as tools for identifying anti-amyloid agents. ChemBioChem 9, 2104-2112.

Cochran, A.G., Skelton, N.J., Starovasnik, M.A., 2001a. Tryptophan zippers: Stable, monomeric beta-hairpins. Proceedings of the National Academy of Sciences of the United States of America 98, 5578-5583.

Cochran, A.G., Tong, R.T., Starovasnik, M.A., Park, E.J., McDowell, R.S., Theaker, J.E., Skelton, N.J., 2001. A minimal peptide scaffold for beta-turn display: Optimizing a strand position in disulfide-cyclized beta-hairpins. Journal of the American Chemical Society 123, 625-632.

Cohen, P., 2001. The role of protein phosphorylation in human health and disease - Delivered on June 30th 2001 at the FEBS Meeting in Lisbon. European Journal of Biochemistry 268, 5001-5010.

Dahiyat, B.I., Mayo, S.L., 1997. De novo protein design: Fully automated sequence selection. Science 278, 82-87.

Dai, Q.H., Tommos, C., Fuentes, E.J., Blomberg, M.R.A., Dutton, P.L., Wand, A.J., 2002. Structure of a de novo designed protein model of radical enzymes. Journal of the American Chemical Society 124, 10952-10953.

DeGrado, W.F., 1997. Proteins from scratch. Science 278, 80-81.

Devos, A.M., Ultsch, M., Kossiakoff, A.A., 1992. Human Growth-Hormone and Extracellular Domain of Its Receptor - Crystal-Structure of the Complex. Science 255, 306-312.

Errington, N., Doig, A.J., 2005. A phosphoserine-lysine salt bridge within an alpha-helical peptide, the strongest alpha-helix side-chain interaction measured to date. Biochemistry 44, 7553-7558.

Espinosa, J.F., Gellman, S.H., 2000. A designed beta-hairpin containing a natural hydrophobic cluster. Angewandte Chemie-International Edition 39, 2330-2333.

Espinosa, J.F., Munoz, V., Gellman, S.H., 2001. Interplay between hydrophobic cluster and loop propensity in beta-hairpin formation. Journal of Molecular Biology 306, 397-402.

Fischle, W., Tseng, B.S., Dormann, H.L., Ueberheide, B.M., Garcia, B.A., Shabanowitz, J., Hunt, D.F., Funabiki, H., Allis, C.D., 2005. Regulation of HP1-chromatin binding by histone H3 methylation and phosphorylation. Nature 438, 1116-1122.

Flocco, M.M., Mowbray, S.L., 1994. Planar Stacking Interactions of Arginine and Aromatic Side-Chains in Proteins. Journal of Molecular Biology 235, 709-717.

Gallivan, J.P., Dougherty, D.A., 1999. Cation-pi interactions in structural biology. Proceedings of the National Academy of Sciences of the United States of America 96, 9459-9464.

Garcia-Alai, M.M., Gallo, M., Salame, M., Wetzler, D.E., McBride, A.A., Paci, M., Cicero, D.O., de Prat-Gay, G., 2006. Molecular basis for phosphorylation-dependent, PEST-mediated protein turnover. Structure 14, 309-319.

Gellman, S.H., 1998. Minimal model systems for beta sheet secondary structure in proteins. Current Opinion in Chemical Biology 2, 717-725.

Griffiths-Jones, S.R., Maynard, A.J., Searle, M.S., 1999. Dissecting the stability of a beta-hairpin peptide that folds in water: NMR and molecular dynamics analysis of the beta-turn and beta-strand contributions to folding. Journal of Molecular Biology 292, 1051-1069.

Griffiths-Jones, S.R., Maynard, A.J., Sharman, G.J., Searle, M.S., 1998. NMR evidence for the nucleation of a beta-hairpin peptide conformation in water by an Asn-Gly type I ' beta-turn sequence. Chemical Communications, 789-790.

Haque, T.S., Gellman, S.H., 1997. Insights on beta-hairpin stability in aqueous solution from peptides with enforced type I' and type II' beta-turns. Journal of the American Chemical Society 119, 2303-2304.

Harding, M.M., Williams, D.H., Woolfson, D.N., 1991. Characterization of a Partially Denatured State of a Protein by 2-Dimensional Nmr - Reduction of the Hydrophobic Interactions in Ubiquitin. Biochemistry 30, 3120-3128.

Hill, R.B., Raleigh, D.P., Lombardi, A., Degrado, W.F., 2000. De novo design of helical bundles as models for understanding protein folding and function. Accounts of Chemical Research 33, 745-754.

Hughes, R.M., Benshoff, M.L., Waters, M.L., 2007. Effects of chain length and N-methylation on a cation-pi interaction in a beta-hairpin peptide. Chemistry-a European Journal 13, 5753-5764.

Hughes, R.M., Kiehna, S.E., Waters, M.L., 2005. Influence of posttranslational modifications on beta-hairpin stability. Biopolymers 80, 497-497.

Hughes, R.M., Waters, M.L., 2005. Influence of N-methylation on a cation-pi interaction produces a remarkably stable beta-hairpin peptide. Journal of the American Chemical Society 127, 6518-6519.

Hughes, R.M., Waters, M.L., 2006. Arginine methylation in a beta-hairpin peptide: Implications for Arg-pi interactions, Delta Cp degrees, and the cold denatured state. Journal of the American Chemical Society 128, 12735-12742.

Hughes, R.M., Wiggins, K.R., Khorasanizadeh, S., Waters, M.L., 2007. Recognition of trimethyllysine by a chromodomain is not driven by the hydrophobic effect. Proceedings of the National Academy of Sciences of the United States of America 104, 11184-11188.

Ilyina, E., Roongta, V., Mayo, K.H., 1997. NMR structure of a de novo designed, peptide 33mer with two distinct, compact beta-sheet folds. Biochemistry 36, 5245-5250.

Imperiali, B., Ottesen, J.J., 1999. Uniquely folded mini-protein motifs. Journal of Peptide Research 54, 177-184.

Jackel, C., Kast, P., Hilvert, D., 2008. Protein design by directed evolution. Annual Review of Biophysics 37, 153-173.

Jacobs, S.A., Khorasanizadeh, S., 2002. Structure of HP1 chromodomain bound to a lysine 9-methylated histone H3 tail. Science 295, 2080-2083.

Johnson, L.N., Lewis, R.J., 2001. Structural basis for control by phosphorylation. Chemical Reviews 101, 2209-2242.

Jourdan, M., Searle, M.S., 2000. Cooperative assembly of a nativelike ubiquitin structure through peptide fragment complexation: Energetics of peptide association and folding. Biochemistry 39, 12355-12364.

Jourdan, M., Searle, M.S., 2001. Insights into the stability of native and partially folded states of ubiquitin: Effects of cosolvents and denaturants on the thermodynamics of protein folding. Biochemistry 40, 10317-10325.

Kiehna, S.E., Waters, M.L., 2003. Sequence dependence of beta-hairpin structure: Comparison of a salt bridge and an aromatic interaction. Protein Science 12, 2657-2667.

Kobayashi, N., Honda, S., Yoshii, H., Uedaira, H., Munekata, E., 1995. Complement Assembly of 2 Fragments of the Streptococcal Protein-G B1 Domain in Aqueous-Solution (Vol 366, Pg 99, 1995). Febs Letters 370, 282-282.

Kouzarides, T., 2007. Chromatin modifications and their function. Cell 128, 693-705.

Kraemer-Pecore, C.M., Lecomte, J.T.J., Desjarlais, J.R., 2003. A de novo redesign of the WW domain. Protein Science 12, 2194-2205.

Kuhnle, H., Borner, H.G., 2009. Biotransformation on polymer-peptide conjugates: a versatile tool to trigger microstructure formation. Angew Chem Int Ed Engl 48, 6431-6434.

Lachner, M., O'Carroll, N., Rea, S., Mechtler, K., Jenuwein, T., 2001. Methylation of histone H3 lysine 9 creates a binding site for HP1 proteins. Nature 410, 116-120.

Lacroix, E., Kortemme, T., de la Paz, M.L., Serrano, L., 1999. The design of linear peptides that fold as monomeric beta-sheet structures. Current Opinion in Structural Biology 9, 487-493.

Lai, J.R., Huck, B.R., Weisblum, B., Gellman, S.H., 2002. Design of non-cysteine-containing antimicrobial beta-hairpins: Structure-activity relationship studies with linear protegrin-1 analogues. Biochemistry 41, 12835-12842.

Lawrence, D.S., Wang, Q., 2007. Seeing is Believing: Peptide-Based Fluorescent Sensors of Protein Tyrosine Kinase Activity. ChemBioChem 8, 373-378.

Lennartsson, A., Ekwall, K., 2009. Histone modification patterns and epigenetic codes. Biochimica Et Biophysica Acta-General Subjects 1790, 863-868.

Li, H.T., Ilin, S., Wang, W.K., Duncan, E.M., Wysocka, J., Allis, C.D., Patel, D.J., 2006. Molecular basis for site-specific read-out of histone H3K4me3 by the BPTF PHD finger of NURF. Nature 442, 91-95.

Lim, A., Saderholm, M.J., Makhov, A.M., Kroll, M., Yan, Y.B., Perera, L., Griffith, J.D., Erickson, B.W., 1998. Engineering of betabellin-15D: A 64 residue beta sheet protein that forms long narrow multimeric fibrils. Protein Science 7, 1545-1554.

Low, C., Homeyer, N., Weininger, U., Sticht, H., Balbach, J., 2009. Conformational Switch upon Phosphorylation: Human CDK Inhibitor p19(INK4d) between the Native and Partially Folded State. Acs Chemical Biology 4, 53-63.

Martin, C., Zhang, Y., 2005. The diverse functions of histone lysine methylation. Nature Reviews Molecular Cell Biology 6, 838-849.

Maynard, A.J., Sharman, G.J., Searle, M.S., 1998. Origin of beta-hairpin stability in solution: Structural and thermodynamic analysis of the folding of model peptide supports hydrophobic stabilization in water. Journal of the American Chemical Society 120, 1996-2007.

Micklatcher, C., Chmielewski, J., 1999. Helical peptide and protein design. Current Opinion in Chemical Biology 3, 724-729.

Mimna, R., Camus, M.S., Schmid, A., Tuchscherer, G., Lashuel, H.A., Mutter, M., 2007. Disruption of amyloid-derived peptide assemblies through the controlled induction of a beta-sheet to alpha-helix transformation: application of the switch concept. Angewandte Chemie-International Edition 46, 2681-2684.

Mitchell, J.B.O., Nandi, C.L., Mcdonald, I.K., Thornton, J.M., Price, S.L., 1994. Amino/Aromatic Interactions in Proteins - Is the Evidence Stacked against Hydrogen-Bonding. Journal of Molecular Biology 239, 315-331.

Munoz, V., Serrano, L., 1997. Development of the multiple sequence approximation within the AGADIR model of alpha-helix formation: Comparison with Zimm-Bragg and Lifson-Roig formalisms. Biopolymers 41, 495-509.

Nakayam, J., Rice, J.C., Strahl, B.D., Allis, C.D., Grewal, S.I.S., 2001. Role of histone H3 lysine 9 methylation in epigenetic control of heterochromatin assembly. Science 292, 110-113.

Nielsen, S.J., Schneider, R., Bauer, U.M., Bannister, A.J., Morrison, A., O'Carroll, D., Firestein, R., Cleary, M., Jenuwein, T., Herrera, R.E., Kouzarides, T., 2001. Rb targets histone H3 methylation and HP1 to promoters. Nature 412, 561-565.

Oakley, M.G., Kim, P.S., 1998. A buried polar interaction can direct the relative orientation of helices in a coiled coil. Biochemistry 37, 12603-12610.

Pagel, K., Koksch, B., 2008. Following polypeptide folding and assembly with conformational switches. Current Opinion in Chemical Biology 12, 730-739.

Peedicayil, J., 2007. The role of epigenetics in mental disorders. Indian Journal of Medical Research 126, 105-111.

Platt, G.W., Simpson, S.A., Layfield, R., Searle, M.S., 2003. Stability and folding kinetics of a ubiquitin mutant with a strong propensity for nonnative beta-hairpin conformation in the unfolded state. Biochemistry 42, 13762-13771.

Pochan, D.J., Schneider, J.P., Kretsinger, J., Ozbas, B., Rajagopal, K., Haines, L., 2003. Thermally reversible hydrogels via intramolecular folding and consequent self-assembly of a de Novo designed peptide. Journal of the American Chemical Society 125, 11802-11803.

Prabhu, N.V., Sharp, K.A., 2005. Heat capacity in proteins. Annual Review Physical Chemistry 56, 521-548.

Quinn, T.P., Tweedy, N.B., Williams, R.W., Richardson, J.S., Richardson, D.C., 1994. Betadoublet - De-Novo Design, Synthesis, and Characterization of a Beta-Sandwich Protein. Proceedings of the National Academy of Sciences of the United States of America 91, 8747-8751.

Ralph, S.A., Scherf, A., 2005. The epigenetic control of antigenic variation in Plasmodium falciparum. Current Opinion in Microbiology 8, 434-440.

Ramirez-Alvarado, M., Kortemme, T., Blanco, F.J., Serrano, L., 1999. beta-hairpin and beta-sheet formation in designed linear peptides. Bioorganic & Medicinal Chemistry 7, 93-103.

RamirezAlvarado, M., Blanco, F.J., Serrano, L., 1996. De novo design and structural analysis of a model beta-hairpin peptide system. Nature Structural Biology 3, 604-612.

Riemen, A.J., Waters, M.L., 2008. Stabilization of the N-terminal beta-hairpin of ubiquitin by a terminal hydrophobic cluster. Biopolymers 90, 394-398.

Riemen, A.J., Waters, M.L., 2009. Controlling Peptide Folding with Repulsive Interactions between Phosphorylated Amino Acids and Tryptophan. Journal of the American Chemical Society 131, 14081-14087.

Riemen, A.J., Waters, M.L., 2009. Design of Highly Stabilized beta-Hairpin Peptides through Cation-pi Interactions of Lysine and N-Methyllysine with an Aromatic Pockets. Biochemistry 48, 1525-1531.

Roach, P.J., 1991. Multisite and Hierarchical Protein-Phosphorylation. Journal of Biological Chemistry 266, 14139-14142.

Schalch, T., Job, G., Noffsinger, V.J., Shanker, S., Kuscu, C., Joshua-Tor, L., Partridge, J.F., 2009. High-Affinity Binding of Chp1 Chromodomain to K9 Methylated Histone H3 Is Required to Establish Centromeric Heterochromatin. Molecular Cell 34, 36-46.

Scrutton, N.S., Raine, A.R.C., 1996. Cation-pi bonding and amino-aromatic interactions in the biomolecular recognition of substituted ammonium ligands. Biochemical Journal. 319, 1-8.

Searle, M.S., 2001. Peptide models of protein beta-sheets: design, folding and insights into stabilising weak interactions. Journal of the Chemical Society-Perkin Transactions 2, 1011-1020.

Searle, M.S., 2004. Insights into stabilizing weak interactions in designed peptide beta-hairpins. Biopolymers 76, 185-195.

Searle, M.S., Griffiths-Jones, S.R., Skinner-Smith, H., 1999. Energetics of Weak Interactions in a β-hairpin Peptide: Electrostatic and Hydrophobic Contributions to Stability from Lysine Salt Bridges. Journal of the American Chemical Society 121, 11615-11620.

Searle, M.S., Platt, G.W., Bofill, R., Simpson, S.A., Ciani, B., 2004. Incremental contribution to protein stability from a beta hairpin "finger": Limits on the stability of designed beta hairpin peptides. Angewandte Chemie-International Edition 43, 1991-1994.

Searle, M.S., Williams, D.H., Packman, L.C., 1995. A Short Linear Peptide Derived from the N-Terminal Sequence of Ubiquitin Folds into a Water-Stable Nonnative Beta-Hairpin. Nature Structural Biology 2, 999-1006.

Sela, M., Anfinsen, C.B., Harrington, W.F., 1957. The Correlation of Ribonuclease Activity with Specific Aspects of Tertiary Structure. Biochimica Et Biophysica Acta 26, 502-512.

Sharman, G.J., Griffiths-Jones, S.R., Jourdan, M., Searle, M.S., 2001. Effects of amino acid phi,psi propensities and secondary structure interactions in modulating H alpha chemical shifts in peptide and protein beta-sheet. Journal of the American Chemical Society 123, 12318-12324.

Sharman, G.J., Searle, M.S., 1997. Dissecting the effects of cooperativity on the stabilisation of a de novo designed three stranded anti-parallel beta-sheet. Chemical Communications, 1955-1956.

Sharman, G.J., Searle, M.S., 1998. Cooperative interaction between the three strands of a designed antiparallel beta-sheet. Journal of the American Chemical Society 120, 5291-5300.

Shults, M.D., Pearce, D.A., Imperiali, B., 2003. Modular and tunable chemosensor scaffold for divalent zinc. Journal of the American Chemical Society 125, 10591-10597.

Signarvic, R.S., DeGrado, W.F., 2003. De novo design of a molecular switch: Phosphorylation-dependent association of designed peptides. Journal of Molecular Biology 334, 1-12.

Simpson, E.R., Meldrum, J.K., Searle, M.S., 2006. Engineering diverse changes in beta-turn propensities in the N-terminal beta-hairpin of ubiquitin reveals significant effects on stability and kinetics but a robust folding transition state. Biochemistry 45, 4220-4230.

Skwarczynski, M., Kiso, Y., 2007. Application of the O-N intramolecular acyl migration reaction in medicinal chemistry. Current Medicinal Chemistry 14, 2813-2823.

Smith, C.K., Regan, L., 1997. Construction and design of beta-sheets. Accounts of Chemical Research 30, 153-161.

Stanger, H.E., Gellman, S.H., 1998. Rules for antiparallel beta-sheet design: D-Pro-Gly is superior to L-Asn-Gly for beta-hairpin nucleation. Journal of the American Chemical Society 120, 4236-4237.

Stotz, C.E., Borchardt, R.T., Middaugh, C.R., Siahaan, T.J., Vander Velde, D., Topp, E.M., 2004. Secondary structure of a dynamic type I' beta-hairpin peptide. Journal of Peptide Research 63, 371-382.

Strahl, B.D., Allis, C.D., 2000. The language of covalent histone modifications. Nature 403, 41-45.

Streicher, W.W., Makhatadze, G.I., 2006. Calorimetric evidence for a two-state unfolding of the beta-hairpin peptide trpzip4. Journal of the American Chemical Society 128, 30-31.

Struthers, M.D., Cheng, R.P., Imperiali, B., 1996. Economy in protein design: Evolution of a metal-independent beta beta alpha motif based on the zinc finger domains. Journal of the American Chemical Society 118, 3073-3081.

Syud, F.A., Espinosa, J.F., Gellman, S.H., 1999. NMR-based quantification of beta-sheet populations in aqueous solution through use of reference peptides for the folded and unfolded states. Journal of the American Chemical Society 121, 11577-11578.

Syud, F.A., Stanger, H.E., Gellman, S.H., 2001. Interstrand side chain--side chain interactions in a designed beta-hairpin: significance of both lateral and diagonal pairings. Journal of the American Chemical Society 123, 8667-8677.

Syud, F.A., Stanger, H.E., Gellman, S.H., 2001. Interstrand side chain-side chain interactions in a designed beta-hairpin: Significance of both lateral and diagonal pairings. Journal of the American Chemical Society 123, 8667-8677.

Szilak, L., Moitra, J., Krylov, D., Vinson, C., 1997. Phosphorylation destabilizes alpha-helices. Nature Structual Biology 4, 112-114.

Taniguchi, A., Skwarczynski, M., Sohma, Y., Okada, T., Ikeda, K., Prakash, H., Mukai, H., Hayashi, Y., Kimura, T., Hirota, S., Matsuzaki, K., Kiso, Y., 2008. Controlled Production of Amyloid beta Peptide from a Photo-Triggered, Water-Soluble Precursor "Click Peptide". ChemBioChem 9, 3055-3065.

Tatko, C.D., Waters, M.L., 2003. The geometry and efficacy of cation-pi interactions in a diagonal position of a designed beta-hairpin. Protein Science 12, 2443-2452.

Tatko, C.D., Waters, M.L., 2004. Comparison of C-H center dot center dot center dot pi and hydrophobic interactions in a beta-hairpin peptide: Impact on stability and specificity. Journal of the American Chemical Society 126, 2028-2034.

Tatko, C.D., Waters, M.L., 2004. Effect of halogenation on edge-face aromatic interactions in a beta-hairpin peptide: Enhanced affinity with Iodo-substituents. Organic Letters 6, 3969-3972.

Taverna, S.D., Li, H., Ruthenburg, A.J., Allis, C.D., Patel, D.J., 2007. How chromatin-binding modules interpret histone modifications: lessons from professional pocket pickers. Nature Structural & Molecular Biology 14, 1025-1040.

Tokmakov, A.A., Sato, K.I., Fukami, Y., 1997. Phosphorylation-sensitive secondary structure in a synthetic peptide corresponding to the activation loop of MAP kinase. Biochemical and Biophysical Research Communications 236, 243-247.

Torrado, A., Imperiali, B., 1996. New synthetic amino acids for the design and synthesis of peptide-based metal ion sensors. Journal of Organic Chemistry 61, 8940-8948.

Vijaykumar, S., Bugg, C.E., Cook, W.J., 1987. Structure of Ubiquitin Refined at 1.8 a Resolution. Journal of Molecular Biology 194, 531-544.

Waggoner, D., 2007. Mechanisms of disease: epigenesis. Seminars in Pediatric Neurology 14, 7-14.

Walkup, G.K., Imperiali, B., 1997. Fluorescent chemosensors for divalent zinc based on zinc finger domains. Enhanced oxidative stability, metal binding affinity, and structural and functional characterization. Journal of the American Chemical Society 119, 3443-3450.

Wang, Q., Cahill, S.M., Blumenstein, M., Lawrence, D.S., 2006. Self-Reporting Fluorescent Substrates of Protein Tyrosine Kinases. Journal of the American Chemical Society 128, 1808-1809.

Waters, M.L., 2004. Aromatic interactions in peptides: Impact on structure and function. Biopolymers 76, 435-445.

Weber, P.L., Brown, S.C., Mueller, L., 1987. Sequential H-1-Nmr Assignments and Secondary Structure Identification of Human Ubiquitin. Biochemistry 26, 7282-7290.

Wishart, D.S., Sykes, B.D., Richards, F.M., 1991. Relationship between Nuclear-Magnetic-Resonance Chemical-Shift and Protein Secondary Structure. Journal of Molecular Biology 222, 311-333.

Wüthrich, K., 1986. NMR of Proteins and Nucleic Acids. Wiley, New York.

Yin, H., Lee, G.I., Park, H.S., Payne, G.A., Rodriguez, J.M., Sebti, S.M., Hamilton, A.D., 2005. Terphenyl-based helical mimetics that disrupt the p53/HDM2 interaction. Angewandte Chemie-International Edition 44, 2704-2707.

Zerella, R., Evans, P.A., Ionides, J.M.C., Packman, L.C., Trotter, B.W., Mackay, J.P., Williams, D.H., 1999. Autonomous folding of a peptide corresponding to the N-terminal beta-hairpin from ubiquitin. Protein Science 8, 1320-1331.

Zhang, K., Lin, W.C., Latham, J.A., Riefler, G.M., Schumacher, J.M., Chan, C., Tatchell, K., Hawke, D.H., Kobayashi, R., Dent, S.Y.R., 2005. The set1 methyltransferase orwoses IpI1 aurora kinase functions in chromosome segregation. Cell 122, 723-734.

Zhang, Y., Reinberg, D., 2001. Genes & Development, 2343-2360.